UNCLASSIFIED

AD NUMBER

AD-503 586

CLASSIFICATION CHANGES

TO **UNCLASSIFIED**

FROM **CONFIDENTIAL**

AUTHORITY

OCA; Jun 30, 1984

19990610080

THIS PAGE IS UNCLASSIFIED

UNCLASSIFIED

AD NUMBER

AD-503 586

NEW LIMITATION CHANGE

TO

DISTRIBUTION STATEMENT: A

Approved for public release; Distribution is unlimited.

LIMITATION CODE: 1

FROM **No Prior DoD Distr Scty Cntrl St'mt Assgn'd**

AUTHORITY

AFRPL via Ltr; Feb 5, 1986

THIS PAGE IS UNCLASSIFIED

CONFIDENTIAL

AFRPL-TR-69-73

(U) CERTIFICATION TESTS OF A HYBRID PROPULSION SYSTEM FOR THE SAINT/TOWER TARGET MISSILE

AD 863 886

F. S. READ, JR.

B. R. BORNHORST

TECHNICAL REPORT AFRPL-TR-69-73

JUNE 1969

IN ADDITION TO SECURITY REQUIREMENTS WHICH MUST BE MET, THIS DOCUMENT IS SUBJECT TO SPECIAL EXPORT CONTROLS AND EACH TRANSMITTAL TO FOREIGN GOVERNMENTS OR FOREIGN NATIONALS MAY BE MADE ONLY WITH PRIOR APPROVAL OF AFRPL (RPOR/STINFO), EDWARDS CA 93523

AIR FORCE ROCKET PROPULSION LABORATORY
DIRECTORATE OF LABORATORIES
AIR FORCE SYSTEMS COMMAND
UNITED STATES AIR FORCE
EDWARDS, CALIFORNIA

DOWNGRADED AT 3 YEAR INTERVALS.
DECLASSIFIED AFTER 12 YEARS.
DOD DIR 5200.10

CONFIDENTIAL

SECURITY MARKING

The classified or limited status of this report applies to each page, unless otherwise marked.
Separate page printouts MUST be marked accordingly.

THIS DOCUMENT CONTAINS INFORMATION AFFECTING THE NATIONAL DEFENSE OF THE UNITED STATES WITHIN THE MEANING OF THE ESPIONAGE LAWS, TITLE 18, U.S.C., SECTIONS 793 AND 794. THE TRANSMISSION OR THE REVELATION OF ITS CONTENTS IN ANY MANNER TO AN UNAUTHORIZED PERSON IS PROHIBITED BY LAW.

NOTICE: When government or other drawings, specifications or other data are used for any purpose other than in connection with a definitely related government procurement operation, the U.S. Government thereby incurs no responsibility, nor any obligation whatsoever; and the fact that the Government may have formulated, furnished, or in any way supplied the said drawings, specifications, or other data is not to be regarded by implication or otherwise as in any manner licensing the holder or any other person or corporation, or conveying any rights or permission to manufacture, use or sell any patented invention that may in any way be related thereto.

[redacted] UNCLASSIFIED

NOTICES

When U. S. Government drawings, specifications, or other data are used for any purpose other than a definitely related Government procurement operation, the Government thereby incurs no responsibility nor any obligation whatsoever, and the fact that the Government may have formulated, furnished, or in any way supplied the said drawings, specifications, or other data, is not to be regarded by implication or otherwise, or in any manner licensing the holder or any other person or corporation, or conveying any rights or permission to manufacture, use, or sell any patented invention that may in any way be related thereto.

UNCLASSIFIED

[redacted]

[redacted]

UNCLASSIFIED

AFRPL-TR-69-73

(U) CERTIFICATION TESTS OF A HYBRID PROPULSION SYSTEM FOR THE SANDPIPER TARGET MISSILE

Franklin B. Mead, Jr.
Bernard R. Bornhorst

In addition to security requirements which must be met, this document is subject to special export controls and each transmittal to foreign governments or foreign nationals may be made only with prior approval of AFRPL (RPOR/STINFO), Edwards, California 93523.

DOWNGRADED AT 3 YEAR INTERVALS;
DECLASSIFIED AFTER 12 YEARS.
DOD DIR 5200.10

[redacted]

UNCLASSIFIED

This document contains information affecting the national defense of the United States within the meaning of the Espionage laws, Title 18, U.S.C., Sections 793 and 794, the transmission or revelation of which in any manner to an unauthorized person is prohibited by law.

[redacted]

FOREWORD

(U) The work described in this report was performed by personnel of the Engine Research Branch, Liquid Rocket Division, Air Force Rocket Propulsion Laboratory, as part of an interlaboratory team to demonstrate the feasibility of hybrid propulsion for the Sandpiper high-performance target missile. Mr. Franklin B. Mead, Jr., was the Project Engineer and Mr. Bernard R. Bornhorst was the Program Manager. This in-house program was conducted between August 1966 and March 1968 under Project Number 573002CRQ.

(U) This report has been reviewed and approved.

George Mushalko

GEORGE MUSHALKO, Major, USAF
Chief, Engine Research Branch
Liquid Rocket Division
Air Force Rocket Propulsion Laboratory

[redacted]

(This page is unclassified)

THIS DOCUMENT CONTAINS INFORMATION AFFECTING THE NATIONAL DEFENSE OF THE UNITED STATES WITHIN THE MEANING OF THE ESPIONAGE LAWS, TITLE 18, U.S.C., SECTIONS 793 AND 794. THE TRANSMISSION OR THE REVELATION OF ITS CONTENTS IN ANY MANNER TO AN UNAUTHORIZED PERSON IS PROHIBITED BY LAW.

ABSTRACT

(U) An in-house exploratory development program was accomplished as part of an inter-laboratory team effort to demonstrate the feasibility of hybrid propulsion for the Sandpiper high-performance target missile. The objectives of this program were to: (1) conduct "off-design" tests of a flight type (heavyweight) hybrid thrust chamber assembly (TCA); (2) conduct flight certification tests on flight-weight propulsion systems delivered under a concurrent AFRPL contract; and (3) provide propulsion system field servicing and engineering support during subsequent flight tests of the propulsion system. Thirty heavyweight TCA tests were conducted, and TCA component operating characteristics, TCA component durability, effects of metal fuel grain additives on combustion, effects of fuel grain temperature on combustion, effects of IRFNA oxidizer substitution, and TCA altitude performance were evaluated. MON-25 (75% N_2O_4/25% NO) oxidizer and 90% Plexiglas (polymethylmethacrylate)/10% magnesium metal fuel were the propulsion system propellants. Eight flight-weight propulsion systems were tested over simulated mission duty cycles after being subjected to environmental extremes of temperature (-65°F to 165°F) and humidity.

(U) Results of the heavyweight TCA tests and subsequent propulsion system flight tests are summarized. The flight certification test data are presented in detail.

UNCLASSIFIED

TABLE OF CONTENTS

UNCLASSIFIED

TABLES

ILLUSTRATIONS

SECTION I

INTRODUCTION

A. BACKGROUND

(C) Existing documentation (Reference 1) indicated that improved rocket-powered target missiles were needed to simulate the flight performance of the best aircraft a potential enemy might produce in the next decade. Maximum altitude requirements might be as high as 100,000 feet, with flight speeds up to Mach 5. To meet a variety of mission profiles with actual on-station operating times of 5 minutes or greater, an extremely flexible propulsion system with a multiple step thrust capability was required. Moreover, any propulsion system developed must be cost effective and must offer ease of handling, storage under a wide range of conditions, a minimum of checkout and maintenance and a maximum of safety and reliability. Careful review of propulsion requirements for target missile applications revealed that propulsion technology was not available to provide the thrust variation and extended burning times necessary to fulfill this wide mission performance envelope. The alternatives that solids, liquids or hybrids offered to obtain the needed propulsion technology indicated that a hybrid propulsion unit might provide a quick and inexpensive means for establishing the necessary propulsion capability. An exploratory development program was conceived to develop the required propulsion technology and demonstrate under actual flight conditions a hybrid propulsion system meeting size and performance requirements for an improved rocket-powered target missile.

(U) The development of a rocket-powered missile to demonstrate hybrid propulsion technology involved three Air Force Systems Command (AFSC) laboratories. The Air Force Armament Laboratory (AFATL) at Eglin AFB, Florida, held primary responsibility for this effort. The Air Force Flight Dynamics Laboratory (AFFDL) at Wright-Patterson AFB, Ohio, provided technical support in the areas of aerodynamics.

This document contains information affecting the national defense of the United States within the meaning of the Espionage Laws, Title 18, U.S.C., Sections 793 and 794. the transmission of which in any manner to an unauthorized person is prohibited by law.

aerothermodynamics, stability and control, and vehicle flight performance. The Air Force Rocket Propulsion Laboratory (AFRPL) at Edwards AFB, California, was in charge of propulsion system design, development and preflight checkout. Flight testing was accomplished at the Air Proving Ground Center (APGC), Eglin AFB missile range over the Gulf of Mexico, with each laboratory providing direct support.

B. OBJECTIVES AND APPROACH

(U) The primary objective of this program was to conduct flight certification tests on a number of hybrid propulsion systems delivered to the AFRPL under Contract AF 04(611)-11632 by United Technology Center (Reference 6), thereby insuring that a high degree of success could be expected with the hybrid propulsion system during Sandpiper target missile flight tests at Eglin AFB. The certification tests were conducted under conditions simulating the environment that the hybrid propulsion system would experience in flight. Hybrid rocket performance, reliability, and safety were evaluated over a wide range of altitude and temperature environments to insure that system operation met Air Force requirements. Other objectives were to develop engineering experience in hybrid propulsion at the AFRPL and to contribute to the advancement of hybrid rocketry. Major areas of investigation included the effects of metal loading in the fuel grain on regression and combustion characteristics, the effects of oxidizer/fuel (O/F) ratio, the differences between ambient and altitude performance, the effect of temperature extremes on system dynamics, and the effects of vibration on system durability.

(U) A two-phase effort was initiated to accomplish the program objectives. Phase I consisted of tests using heavyweight hardware identical to that being developed by the contractor. While the contractor was taking a "rifle bore" approach with a specific end item in mind, the AFRPL approach was to conduct "off design" tests extending overall knowledge of this propulsion system and hybrid rocketry in general, but also verifying system operation and performance. Results of these tests were related

(This page is unclassified)

THIS DOCUMENT CONTAINS INFORMATION AFFECTING THE NATIONAL DEFENSE OF THE UNITED STATES WITHIN THE MEANING OF THE ESPIONAGE LAWS, TITLE 18, U.S.C., SECTION 793 AND 794, THE TRANSMISSION OR WHICH IN ANY MANNER TO AN UNAUTHORIZED PERSON IS PROHIBITED BY LAW.

to the contractor and significantly influenced decisions on the final system design. Throughout this phase, the thrust chamber assembly (TCA) did not change. Interior components such as nozzle, mixer, and injector were modified over the course of the program as described in Section III. Phase I also served as a training program for AFRPL project personnel, allowing them to become familiar with the hybrid hardware and system operation and testing procedures critical to successful conclusion of Phase II.

(U) During Phase II, 10 flight-weight propulsion systems were delivered to the AFRPL for certification testing, and five systems were shipped to the Beech Aircraft Company for mating with airframes and subsequent shipment to Eglin AFB. The 15 propulsion systems delivered to the Air Force were identical. The 10 units delivered to the AFRPL were picked at random from the total lot to obtain a representative sampling. Using this procedure, the flight-weight design concept, rather than each individual unit, would be certified for flight. Thus, the usual concept of unit acceptance testing by hot firing was bypassed.

(U) The AFRPL was responsible for handling, maintenance and checkout of the propulsion systems during the demonstration flight tests at Eglin AFB. During this portion of Phase II, AFRPL technical personnel and equipment were available prior to each flight, and it was the responsibility of the AFRPL project engineer to verify propulsion system readiness for the flight. The specific objectives of the flight demonstration test program were to obtain in-flight rocket engine performance data, demonstrate specified cruise/time profiles, demonstrate flight programmer controlled maneuvering capabilities, evaluate aircraft/missile supersonic launch capabilities and techniques, determine missile flight control system performance during launch, climb and cruise conditions, investigate target missile maintenance and handling procedures, and determine infrared signature data from the hybrid rocket motor during flight (References 2, 3).

C. DESIGN CONCEPT

(U) From the beginning, the conceptual approach utilized for the demonstration program was based upon low cost and system simplicity. The airframe proposed to demonstrate flight feasibility employed a 180-inch-long version of the Navy AQM-37A liquid bipropellant rocket-powered target missile. With only slight modification, the Air Force was able to use operational hardware and off-the-shelf components for a large portion of the missile system.

(U) In the hybrid rocket, a liquid oxidizer reacts with a solid fuel grain. While the oxidizer flow is metered through the injector by appropriate valving and tankage (liquid management system), the fuel flow, and thus the oxidizer/fuel ratio (O/F), is controlled by transport processes and chemical reactions occurring in the solid fuel combustion chamber. In other words, the oxidizer does not automatically strip off the fuel in stoichiometric proportions to provide efficient performance. Thus, the heat, mass and momentum transfer processes, and gas-phase combustion and heterogeneous fuel decomposition reactions must be understood and described before the solid fuel regression (burning) rates can be predicted, achieved, and maintained in the hybrid rocket engine. Once understood, the hybrid rocket offers the attractive features of throttling, restart capability, unrestricted use of propellant ingredients regardless of chemical compatibility (due to the complete separation of fuel and oxidizer), system simplicity (because only one liquid must be controlled), and increased safety in manufacturing, handling and operations (again, as a result of separation of fuel and oxidizer).

(U) As shown in Figure 1, the selected hybrid missile system included a nose cone with guidance and controls, a gaseous nitrogen pressurization tank, an oxidizer tank and the solid fuel combustion chamber. To control the hybrid propulsion system, the liquid management system consisting of the nitrogen and oxidizer tanks and the appropriate lines and valves was

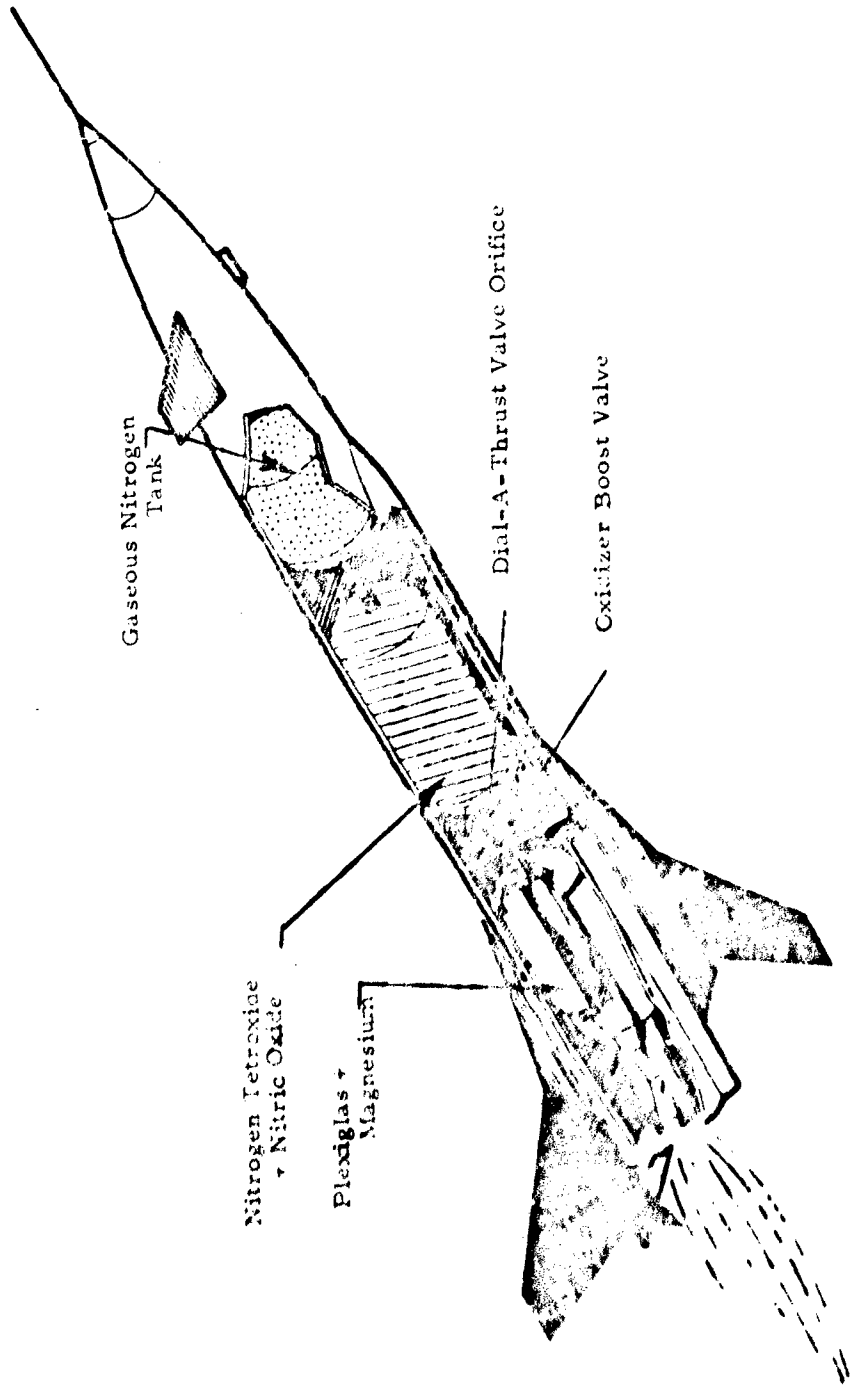

Figure 1. Hybrid Propulsion System

designed to inject a single boost flow rate through two parallel lines producing a nominal 500-lb_f boost thrust with the duration varied as required for a given mission. The sustain phase of operation was initiated by closing the main oxidizer boost valve, thus forcing the oxidizer to flow through the dial-a-thrust valve orifice which provided for variable oxidizer flow rate and was preset by mechanically adjusting the orifice prior to launch. During sustain phase, the oxidizer was aerated with gaseous nitrogen at the injector to maintain momentum and enhance atomization. The propellants utilized consisted of 10 percent powdered magnesium dispersed in 90 percent polymethylmethacrylate (Plexiglas) as the solid fuel and a mixture of 25 percent nitric oxide and 75 percent nitrogen tetroxide (MON-25) as the liquid oxidizer. The nitric oxide addition provided storability in the liquid state over a temperature range of -65°F to +165°F. The propellants were nonexplosive, nonhypergolic, and readily available at moderate cost. The thrust chamber assembly (TCA), as shown in Figure 2, consisted of a graphite nozzle assembly with a 21:1 expansion ratio, a maraging steel case, a cylindrical, single-port solid fuel grain surrounded by silica phenolic insulation, an injector designed to produce a hollow cone spray pattern and a pyrotechnic igniter. Although the airframe was 13 inches in diameter, a 10-inch-O.D. TCA was used based upon an expected future target missile diameter. The actual throat of the nozzle was pyrolytic graphite, and the rest of the nozzle was a high-density-grade graphite. The entrance to the nozzle was tapered without the plenum usually used to enhance mixing and combustion efficiency. The tapered entrance allowed smooth flow, with some loss in performance, of a protective fuel-rich boundary layer over the nozzle throat. The constriction in the fuel port was at the point of maximum regression rate where additional fuel permitted a more even burnout along the grain length.

(U) The thrust requirements for the hybrid target missile are listed in Table I. The thrust requirements reference the specified mission altitudes to delivered thrust at altitude conditions. Rating Number I was an all-boost phase mission at 50,000 ft requiring at least 60,000 lb_f-sec total

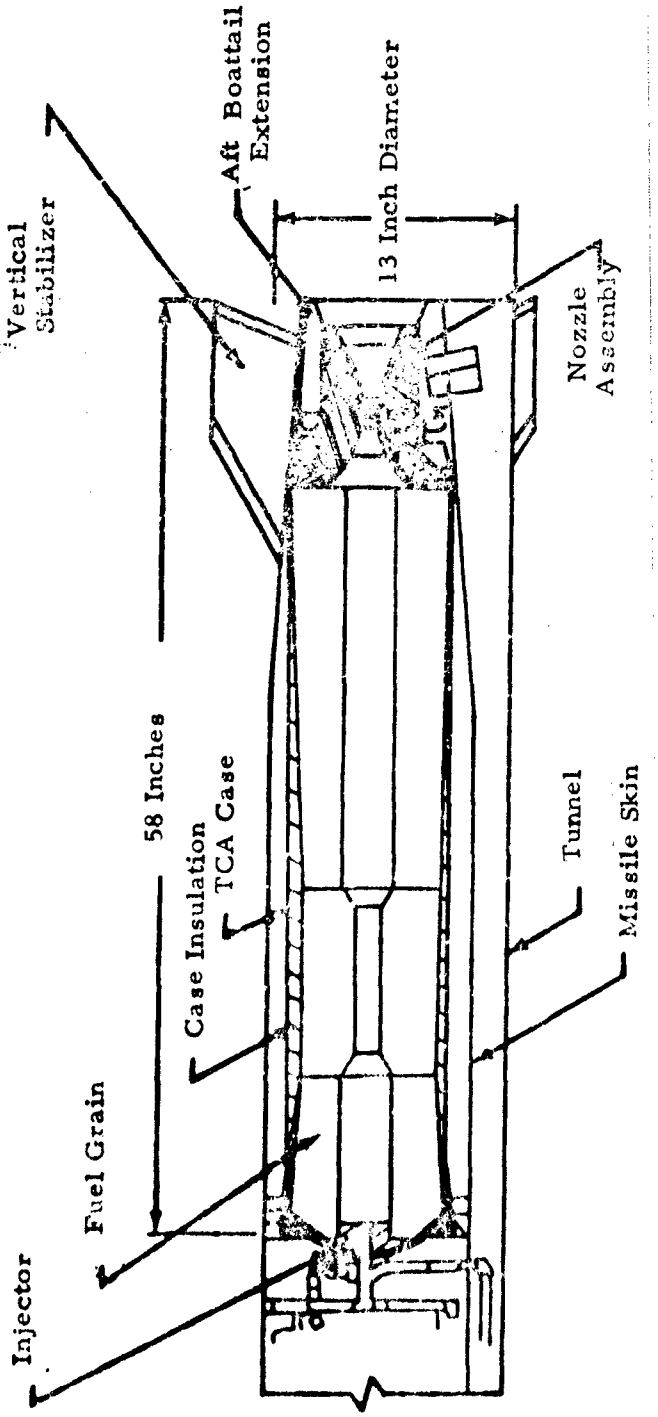

Figure 2. Thrust Chamber Assembly Installation

UNCLASSIFIED

TABLE I. ENGINE THRUST RATINGS
(AMBIENT CONDITIONS)

	RATINGS	Design Thrust Limits (lb_f) Phase Start	Design Thrust Limits (lb_f) Phase End	Minimum (lb_f-sec) Total Impulse Boost + Sustain	Nominal (sec) Duration Sustain Phase
I	50,000 ft Altitude Boost Phase	450 (min)	525 (min)	60,000	120 at min thrust
IA	50,000 ft Altitude Sustain Phase (Setting 1)	228 (min)	246 (min)	70,800	297 at min thrust
II	70,000 ft Altitude Sustain Phase (Setting 2)	134 (min)	134 (min)	71,050	(2)303 at min thrust
III	80,000 ft Altitude Sustain Phase (Setting 3)	127 (min)	127 (min)	70,000	(3)176 at min thrust
IV	90,000 ft Altitude (1) Sustain Phase (Alternate Setting)	63 (min)	64 (min)	69,500	(4)349 at min thrust

NOTES:
1. The engine controls had provisions for adjustment to this thrust level as an alternate position to Setting 1, 2, or 3.
2. Duration shall immediately follow a boost phase of 62-sec duration.
3. Duration shall immediately follow a boost phase of 93-sec duration.
4. Duration shall immediately follow a boost phase of 95-sec duration.

UNCLASSIFIED

impulse. Rating IA was a 50,000-ft mission using the first 10 sec of boost phase provided by Rating I followed by 297 sec of sustain phase with thrust matching drag at Mach 2.0. Rating Number II was a 70,000-ft mission utilizing the first 62 sec of boost phase that would be delivered in Rating I followed by 303 sec of sustain phase with a thrust level exactly matching drag at Mach 2.2. Rating Number III was an 80,000-ft mission utilizing the first 93 sec of Rating I boost phase followed by 176 sec of sustain phase with a thrust level to match drag at Mach 3.0. Rating Number IV was a 90,000-ft Mach 4 mission, applicable only to future advanced versions of the target missile because the 13-inch-diameter demonstration vehicle could not fly at this altitude and speed. Rating IV defined the minimum flow rate combustion regime for the hybrid engine. Rating I defined the maximum flow rate combustion regime, hence, an 8:1 throttling ratio was required from the hybrid TCA. The total impulse values reflect predictions for anticipated advanced versions (10-inch O.D.) of the target missile. Settings 1, 2, 3, and "Alternate" refer to positions of the dial-a-thrust valve as discussed in detail in Section II.

SECTION II

EXPERIMENTAL PROCEDURE

A. STATIC TEST PROCEDURES

1. Test Facility Design and Operation.

(U) This program was conducted at the Air Force Rocket Propulsion Laboratory altitude facility located at Test Area 1-14 (Hydro Lab), Cells A and B (Figure 3). B-Cell was the facility where liquid oxygen and propane were combusted and the exhaust used to flash water to steam for driving three two-stage ejectors located on top of the condenser. A-Cell was the hybrid engine test facility and contained the altitude test chamber, the environmental system and the oxidizer supply tank. The altitude test chamber was connected to the condenser by a diffuser. Vacuum conditions created by the steam ejector system were applied at the top of the condenser, and the engine exhaust gases passed through the diffuser to enter the bottom of the condenser where a water deluge removed the majority of particulate solid products and condensible gases.

a. Thrust Stand.

(U) The thrust stand was located in the altitude test chamber. It was designed to accommodate either the heavyweight TCA or the complete flight-weight propulsion system. Therefore, testing could be accomplished with oxidizer supplied from either the exterior supply tank or the flight-weight tankage located on the thrust stand. The thrust stand was a channel beam extension of an existing 5000 lb_f stand with a new load cell, two new alignment flexures, and two new spring flexures to support the extended thrust-bed frame.

b. Diffuser.

(U) The diffuser was a water-cooled, double-walled, straight tube with a 5-inch inside diameter. Design theory used to predict diffuser

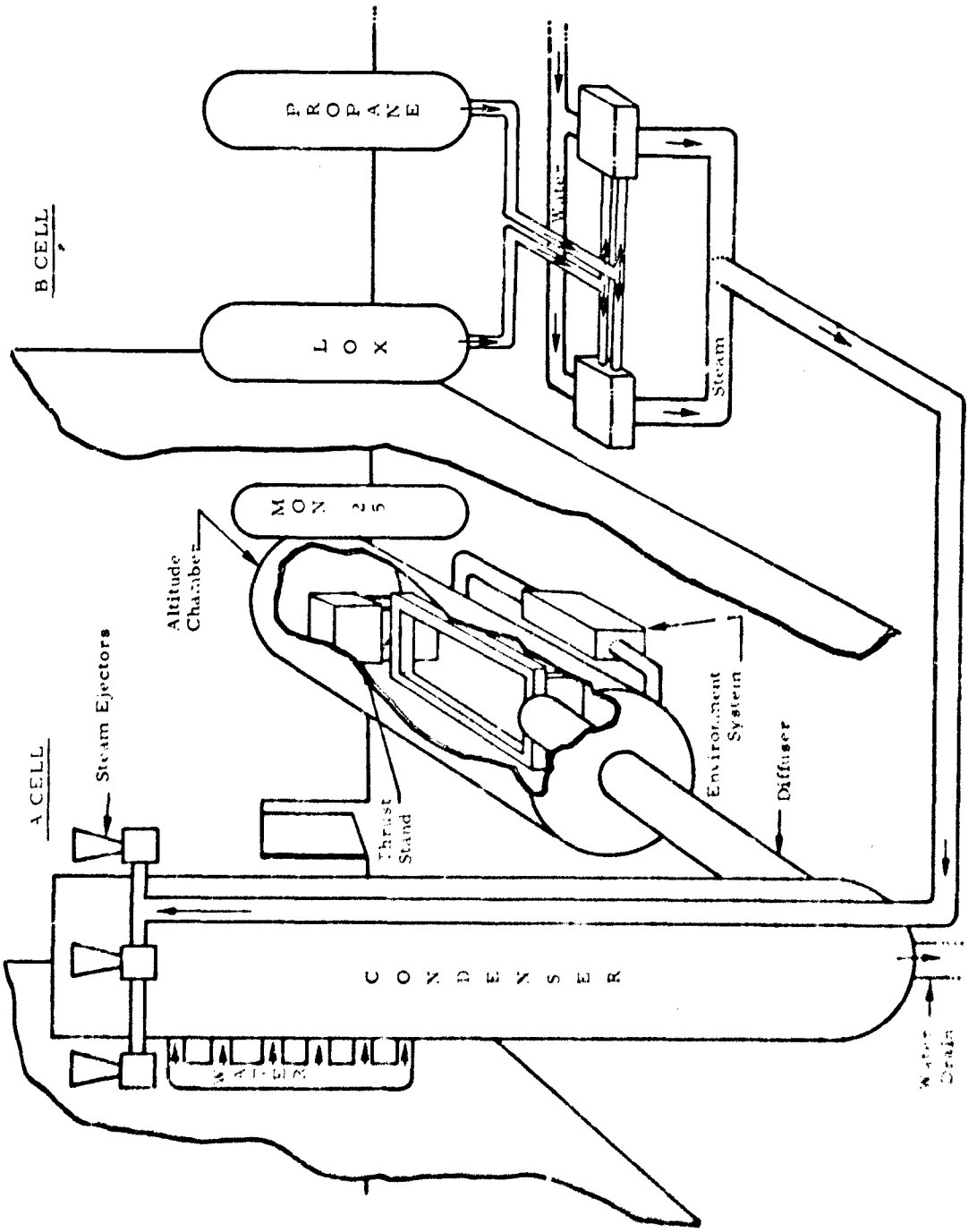

Figure 3. Test Cells A and B

performance was obtained from Reference 5. For sea-level testing, an 18-inch-diameter uncooled diffuser with a large convergent entrance was installed to collect the exhaust while still allowing observation of the exhaust plume. The ambient pressure tests were conducted with the altitude chamber door removed. This provided airflow to ingest and scrub all exhaust gases, with the altitude facility providing suction.

c. Environmental System

(U) The environmental system provided the capability of controlled temperatures from -65°F to 165°F at any desired relative humidity. Air was pumped through a closed system as the temperature-conditioning fluid. A water boiler provided steam; a dehumidifier was available to remove moisture; an electric heater was used for heating; and a liquid nitrogen heat exchanger was used for cooling. Components could act independently or in unison to provide the required conditioning environment. Operation of the environmental system was completely remote. Two insulated cocoon jackets were used to cover the entire propulsion system during system operation. Temperature levels were controlled to approximately ±1°F, and cold-conditioning time was limited by the liquid nitrogen supply. The electric heater did not impose a conditioning time limit.

d. Oxidizer System

(U) For heavyweight testing, preset variable-area cavitating venturis were used to alter oxidizer flow rates throughout the range of interest and maintain constant flow. Turbine-type flowmeters were used to measure oxidizer flow rates. A water scrubber system was used for venting the oxidizer tank and disposing of residual oxidizer in the system lines. This technique avoided the danger of toxic propellant within the close confines of the test area. The test system was designed to permit oxidizer feed to the engine either from a heavyweight storage tank or flight-weight tankage located on the thrust stand.

e. Gaseous Nitrogen System

(U) Starting altitude pressure was controllable by feeding a metered flow of gaseous nitrogen into the condenser, overloading the vacuum system, and causing an increase in pressure in the altitude test chamber. The nitrogen flow rates were controlled by three remotely operated valves of different orifice sizes acting independently or in unison with variable supply pressure (0 to 1500 psi). To effect moderate changes in altitude (10,000 ft), extremely large amounts of nitrogen were required. Normal operating times averaged 2 to 4 minutes. Once engine ignition occurred, the altitude in the test chamber was controlled mainly by diffuser operating characteristics, and the nitrogen overload system was turned off. Gaseous nitrogen was also used to aerate the oxidizer at low flow rates with a sonic orifice providing the necessary flow control.

2. Test Hardware.

a. Heavyweight TCA

(U) The thrust chamber assembly (TCA) used during Phase I, heavyweight testing, is shown in Figure 4. The heavyweight TCA consisted of a case, a forward closure, combustion chamber insulation, and igniter assembly, an injector assembly, a fuel grain assembly and a nozzle assembly. One complete TCA was initially supplied by the contractor with additional igniter and nozzle assemblies as replacements for expended hardware used during the test series. The heavyweight TCA configuration was identical to the configuration used by the contractor during his heavyweight development tests. Thus, test results and data generated at the AFRPL were useful to the contractor in his final configuration selection.

(U) The engine case was fabricated from carbon steel tubing. It was 10 inches inside diameter by 0.25 inches thick. The forward closure was fabricated from carbon steel and included the igniter and injector assemblies, the chamber pressure transducer tap, and an RTV-11 sealant tap for the fully assembled TCA. The combustion chamber insulation

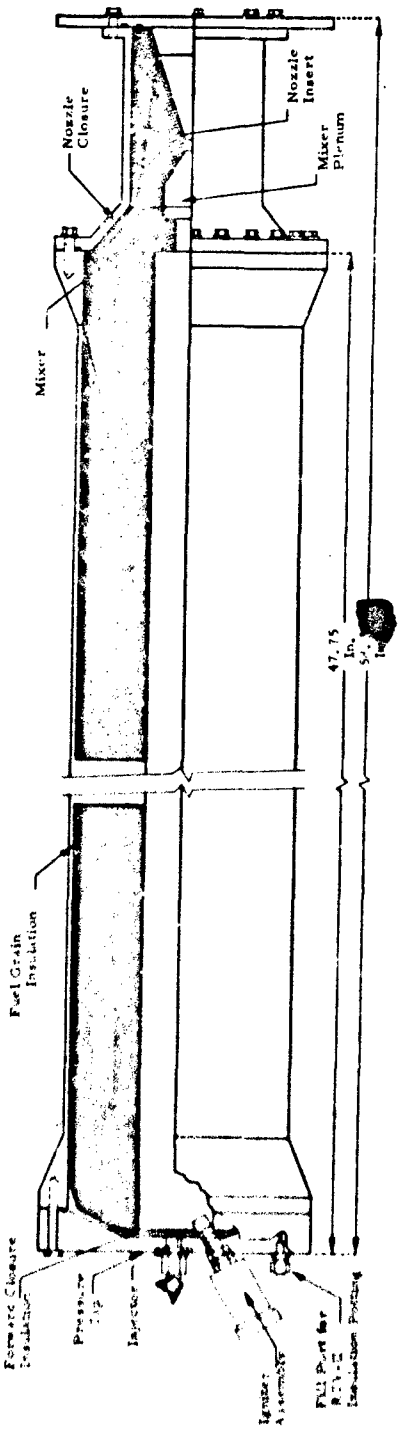

Figure 4. Heavyweight Thrust Chamber Assembly

consisted of a piece of silica phenolic bonded to the fuel grain assembly with Epon 934. This insulation was designed to protect the forward closure from the high temperatures encountered in the combustion chamber. RTV-11 was used both as an insulation surrounding the fuel grain and as a potting compound to bond the fuel grain in the case.

(U) The igniter assembly is shown in Figure 5. The igniter cartridge was a small solid charge designed by the contractor to produce high temperatures in the combustion chamber and induce a further heating effect by reaction between the solid exhaust products and the oxidizer. A standard Holex double bridge wire initiator was used to ignite the solid squib. The 304 stainless steel igniter blast tube had three exhaust channels drilled at 120° intervals to uniformly disperse the hot solid exhaust products. The igniter case was fabricated from 4130 steel, and the throat insert was high-density ATJ graphite.

b. Flight-weight Tankage

(U) The flight-weight tankage, furnished by the Beech Aircraft Company, was an integral part of the oxidizer feed system. A portion of the heavyweight tests utilized the flight-weight tankage assembly, including the nitrogen tank, the oxidizer tank, and the appropriate valving and components shown in Figures 6 and 7. The oxidizer tank held about 175 lbs of MON-25 and had a pressure rating of 930 psia. Note specifically that a combination normally closed squib valve and regulator was used to begin pressurization of the oxidizer tank. Also note the presence of a 10-micron filter in the oxidizer line. This filter was later removed. The material used for the tanks was 17-7 stainless steel.

c. Flight-weight Propulsion System

(U) The flight-weight propulsion system included the feed system assembly, initiator assembly, igniter assembly and thrust chamber assembly. The feed system assembly contained all the valving, lines and fittings required to control the nitrogen pressurant and MON-25

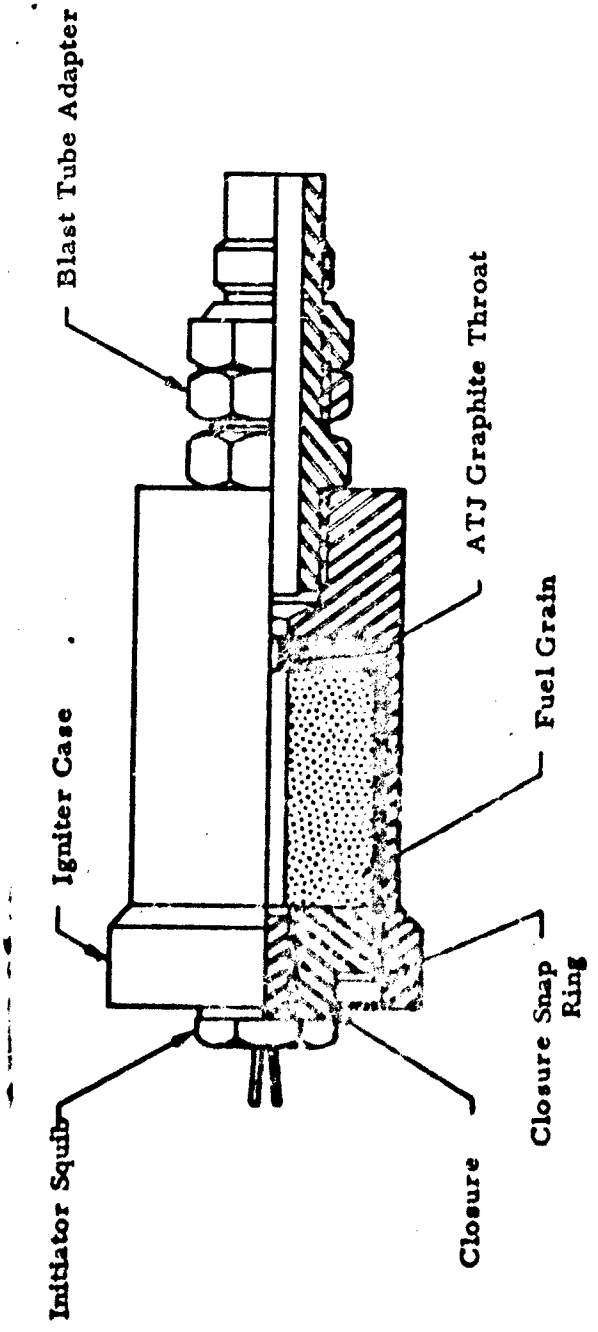

Figure 5. Igniter Assembly

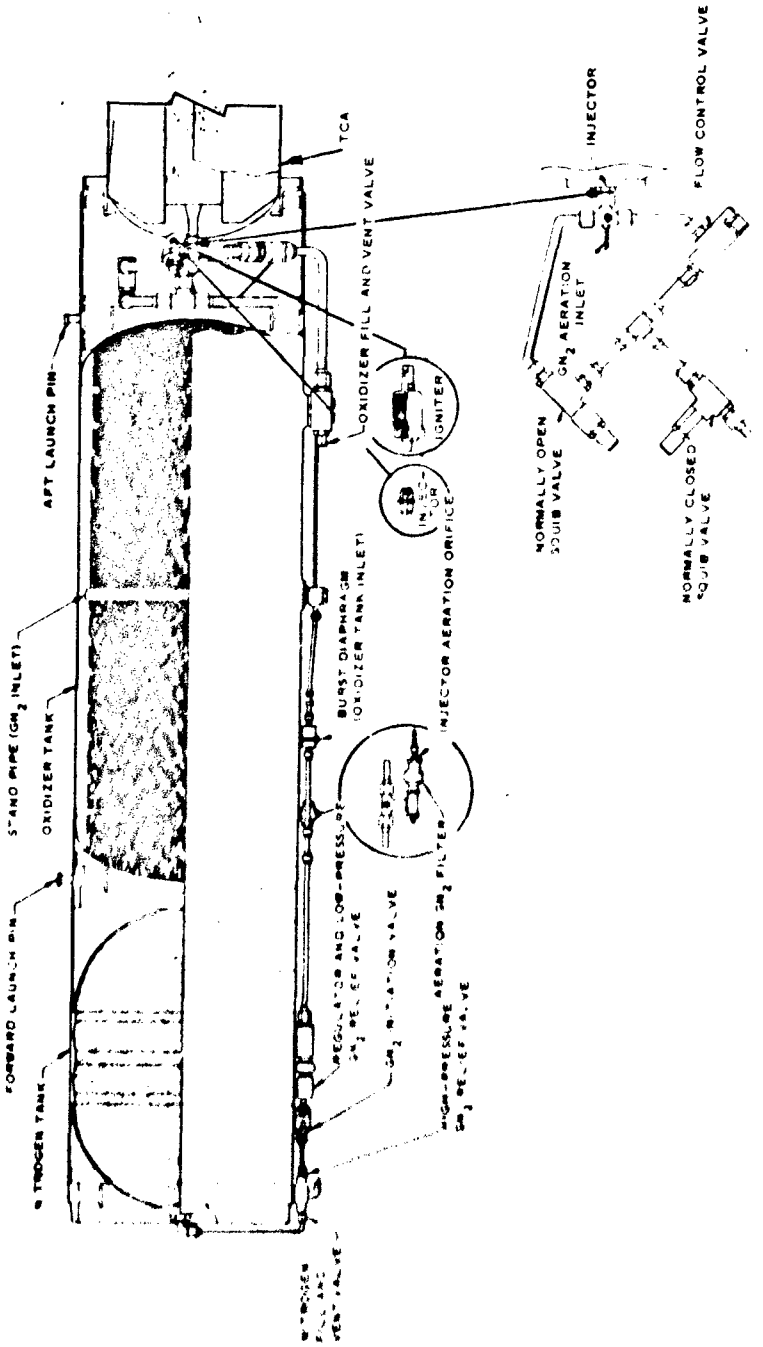

Figure 6. Oxidizer Feed System

UNCLASSIFIED

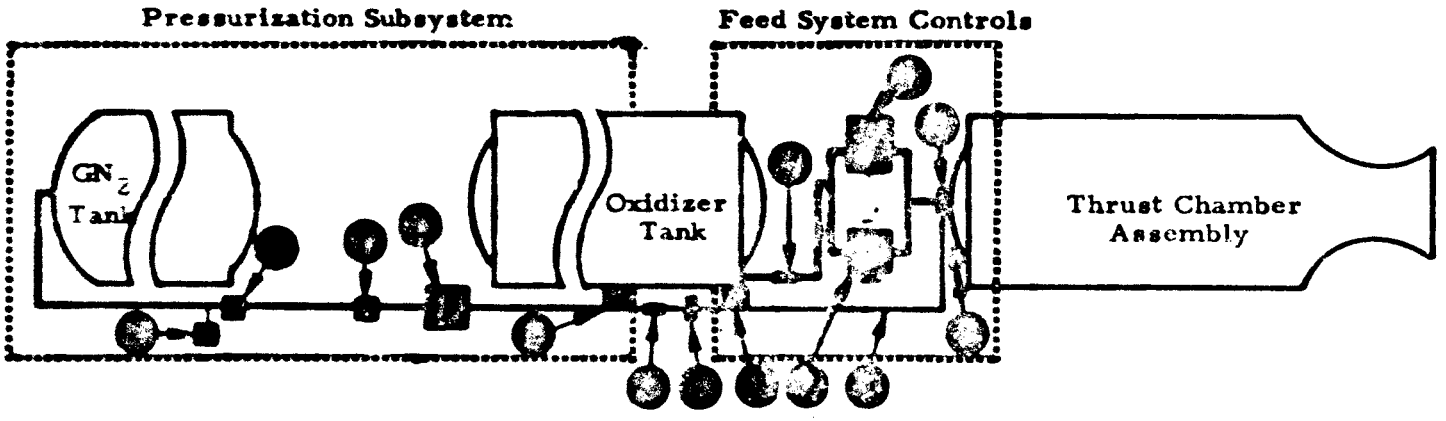

FEED SYSTEM CONTROLS

1. Normally Closed Oxidizer Start Valve
2. Boost Shutoff Valve
3. Dial-A-Thrust Orifice Valve
4. Modified Tee
5. Igniter Assembly

PRESSURIZATION SUBSYSTEM

6. Normally Closed Start Valve
7. Filter
8. Regulator
9. Burst Disk
10. Aeration Line
11. Oxidizer Fill Port
12. GN_2 Fill Valve
13. GN_2 Relief Valve
14. Aeration Orifice

Figure 7. Feed System Schematic

UNCLASSIFIED

oxidizer as shown schematically in Figure 7. All the valves used on the flight-weight system were Conax explosively operated types with Bendix dual-bridge wire initiator assemblies. These valves were off-the-shelf items meeting the environmental requirements for the system. The valves were extremely fast acting (0.002 sec or less) and lightweight (less than 1 lb_m). The nitrogen regulator used to maintain an oxidizer tank pressure of 750 psia was a refurbishable combination normally closed valve and regulator made by Pneu-Hydro Valve Corporation. A similar model is used on the Navy AQM-37A target missile. For operation on the flight-weight system, the regulator valve was always set open during installation, so that only the regulator functioned during system operation. The dial-a-thrust valve, as shown in Figure 8, was essentially a variable-orifice valve calibrated by United Technology Center (UTC) to provide oxidizer flow rates sufficient to produce desired thrust levels for the various missions. All of the 80 possible settings were not used during calibration. Flow requirements were estimated from test results, and the orifice was opened until the correct flows were obtained. The settings were then recorded and stamped on a tag attached to the valve. This inexpensive valve had wide fabrication tolerances which necessitated flow calibration of each unit. The 10-micron absolute nitrogen filter was used to prevent plugging of the 0.0135-inch-diameter aeration orifice in the aeration line. The aeration line provided nitrogen for aeration and extended into the injector via a tube through the tee connecting the boost and sustain lines. The effects of aeration on flow rates are discussed in Appendix B. The burst disk had a forward breaking pressure of 450 psia and reverse breaking pressure of 550 psia. These burst pressures were well above the maximum oxidizer vapor pressure of 270 psia (165°F).

(U) The flight-weight igniter differed from the heavyweight version only in its shorter straight-bore blast tube and one-piece welded construction. The graphite throat inserts and cartridges were shipped separately, and the igniter was loaded just prior to each test.

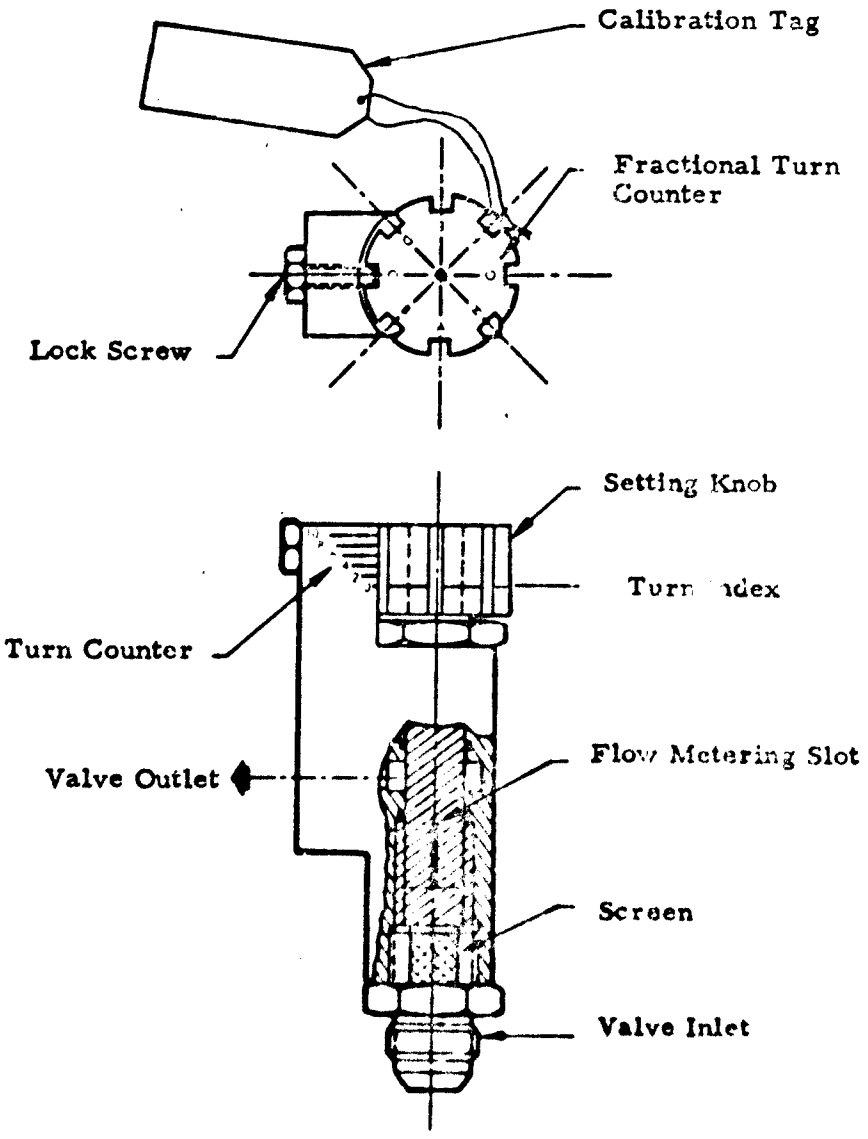

Figure 8. Dial-A-Thrust Valve

(U) The flight-weight thrust chamber assembly consisted of the splash block, forward insulation, fuel grain assembly, injector assembly, nozzle assembly and combustion chamber as shown in Figure 9. The splash block and forward insulation (Figure 10) were made from graphite phenolic and were designed to eliminate head-end recirculation effects. The splash block angle was slightly less than the injector spray angle thus allowing the oxidizer to wipe the block face. The forward insulation was thicker than the heavyweight component to decrease heat soak-through at the head end. The fuel grain was an assembly of four cylindrical billets bonded together to form a continuous fuel grain of approximately 45.7 inches in length by 9.7 inches in outside diameter. The first billet was machined to match insulation and engine case contour at the head end. A silica phenolic sleeve was placed over the outside of the fuel grain to provide additional insulation of the combustion chamber case during the terminal portion of firing. This sleeve varied in thickness, providing the greatest insulation protection in the second and third billet portion of the fuel grain where initial burnthrough of the fuel occurred most frequently. The inside diameter of the fuel grain was not uniform. The first, third, and fourth billets were a constant 3.35 inches inside port diameter. The second billet had a 2.35-inch inside diameter, tapered through 30 degrees at each end to mate evenly with billets 1 and 3. To bond the billets together, trichloroethylene was applied to the mating surfaces, softening the Plexiglas and allowing the billets to bond together.

(U) The flight-weight injector is shown in Figure 11. It produced a hollow cone spray pattern with a spinner and tapered orifice.

(U) The flight-weight nozzle assembly (see Figure 9) contained a throat insert, insert backup, exit cone, insulation, contoured throat entrance and case (aft closure). The throat insert consisted of three pyrolytic graphite washers bonded together, threaded on the outside, screwed into place and bonded on the forward surface only. Epon 901 was used exclusively as the bonding agent. The contoured throat entrance, insert

UNCLASSIFIED

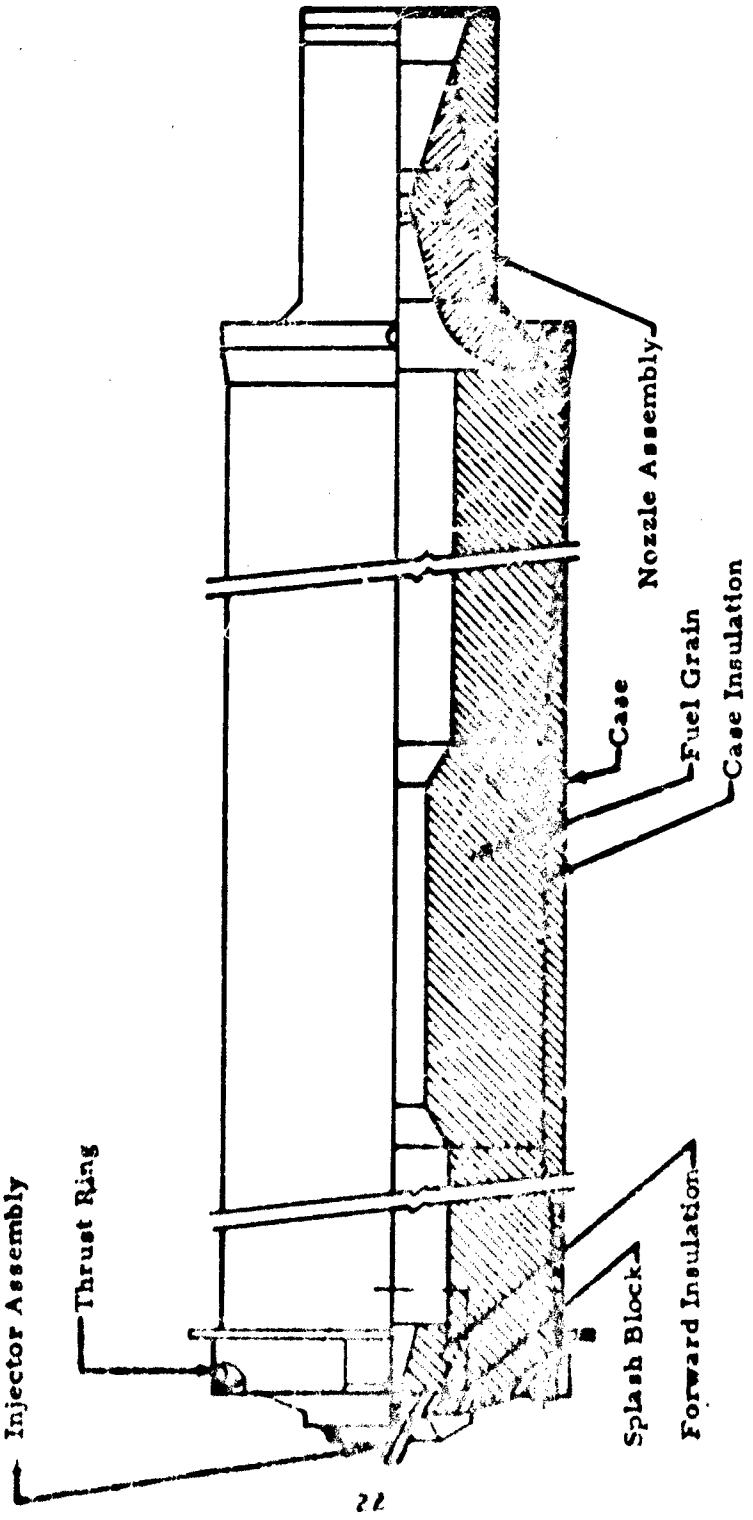

Figure 9. Flight-weight Thrust Chamber Assembly

UNCLASSIFIED

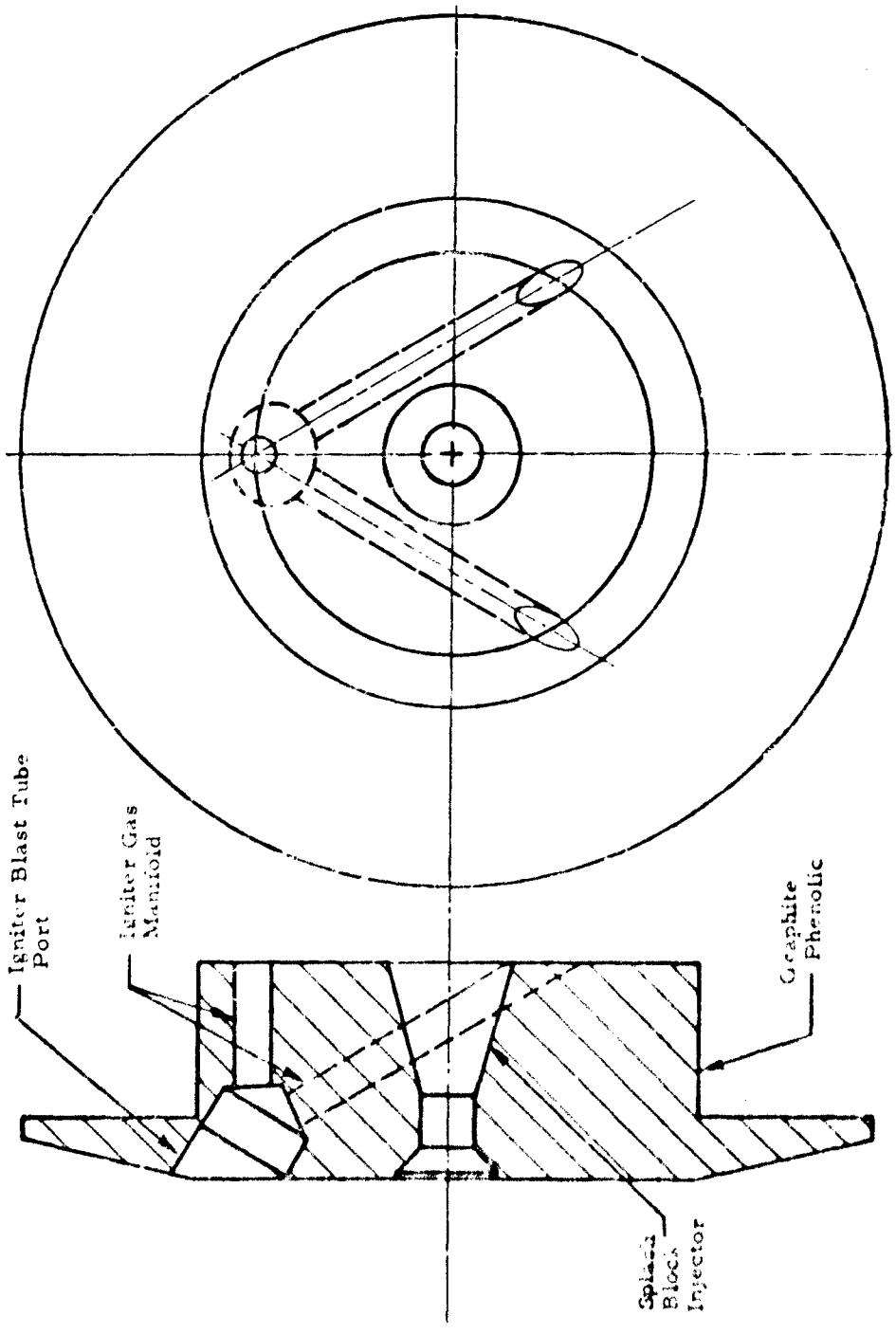

Figure 10. Forward Insulation, Igniter Manifold, and Splash Block

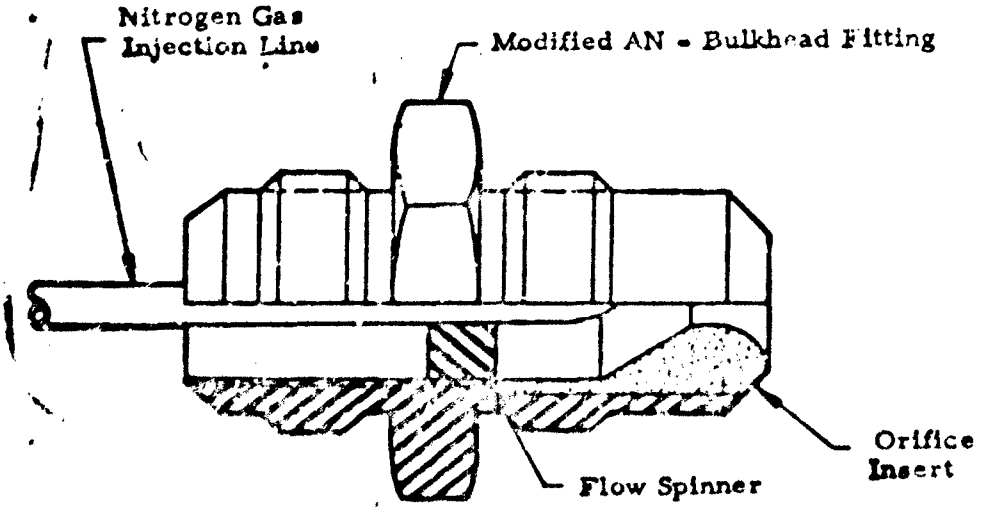

Figure 11. Flight-weight Injector

backup and exit cone were all ATJ graphite material. The contoured throat entrance allowed better utilization of fuel at the aft end of the combustion chamber and protected the nozzle throat because it did not cause high turbulence. Therefore, a fuel-rich boundary layer was formed which partially protected the throat from the oxidizer-rich central core. The nozzle exit cone consisting of graphite and silica phenolic had an expansion ratio of 21:1. The only existing joint was in the throat entrance, and it was at this point that maximum heat soak-through was predicted.

B. FLIGHT TEST PROCEDURE

1. Airframe Characteristics

(U) A half section of the Model 1069 Sandpiper hybrid target missile is shown in Figure 12. The vehicle was cylindrical with a small conduit (raceway) on the lower surface and highly swept delta wings with vertical stabilizers at the tips. Canard surfaces were used for pitch control and aileron for roll and yaw. The airframe configuration was similar to the AQM-37A and had almost identical drag and flight characteristics. The airframe was dismantled for shipment and storage by removing the nose, canards, wings and fins. Access to the equipment and controls bays was provided by removable skin panels.

2. Test Plan and Procedures

(U) The flight tests consisted of a total of six flights, three captive and three missile launches, as described in References 2 and 3. The Sandpiper missile was launched from an F-4C Phantom fighter at an altitude of approximately 49,500 ft and Mach 1.5 over the APGC Eglin Gulf test range. A Navy LAU-24/A guided missile launcher (centerline installed) and PEU-56/A firing panel were adapted for use with the Sandpiper. The launcher is a standard AQM-37A piston-operated, trapeze-type component. At launch, an ejection cartridge drove the trapeze mechanism downward and forward, enabling missile release in a level attitude. As the target left the launcher trapeze, a lanyard was pulled, activating the pressurization and ignition sequence.

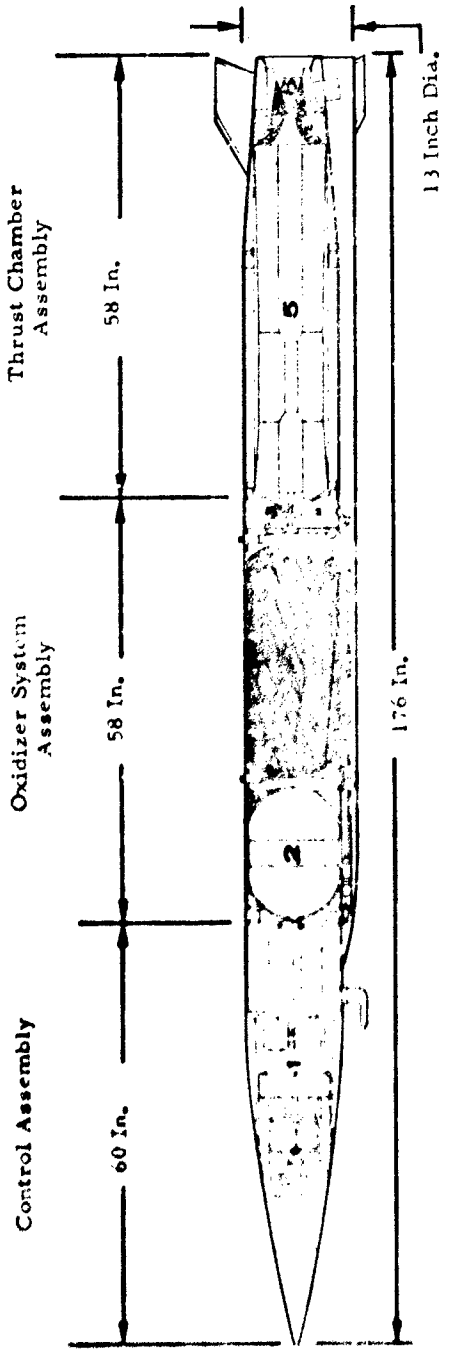

Figure 12. Hybrid Target Missile Inboard Profile

3. Assembly and Modification

(U) The target missiles were assembled at Eglin AFB before each test. The propulsion systems were shipped from UTC to the Beech Company fully loaded with oxidizer classified as an ICC class two poison. The igniter cartridges and throat inserts were shipped directly from UTC to Eglin where they were stored until final flight checkout. The Beech Company assembled each individual missile and attached the required instrumentation (Reference 3). After a complete checkout, the missile was disassembled and the various assemblies sent to Eglin where the missile was reassembled and a final check performed before flight. Following assembly at Eglin, each propulsion system was modified slightly to prevent possible vibration damage during captive and free flight. Certification vibration test results dictated that three Adele clamps be attached to the oxidizer propellant lines and rubber pads inserted between the large mass components and the tankage to provide damping action.

4. Checkout and Servicing

(U) Checkout and servicing of the Sandpiper propulsion system involved a continuity check of each squib valve (total of three), checking and loading the igniter, setting the dial-a-thrust valve and charging the nitrogen tank. A detailed procedure was developed during certification tests at the AFRPL for each of these steps (Appendix E). A special high-pressure facility was assembled specifically to pressurize the missile nitrogen tank. This system is shown schematically in Figure 13. The system contained three 2200 psig and three 6000 psig nitrogen bottles meeting MIL-P-27401 specifications. The 2200 psig bottles were used first to raise the missile nitrogen tank pressure to between 1500 psig and 1800 psig. This was accomplished by slowly filling the system in 500-psig increments with a system leak check following each incremental step. Before using the 6000-psig bottles, the missile nitrogen tank was allowed to cool and the nitrogen fill fitting was checked to insure that it still functioned properly. The fill fitting was a simple pressure sealing valve which occasionally became jammed open and had to be replaced. Since high

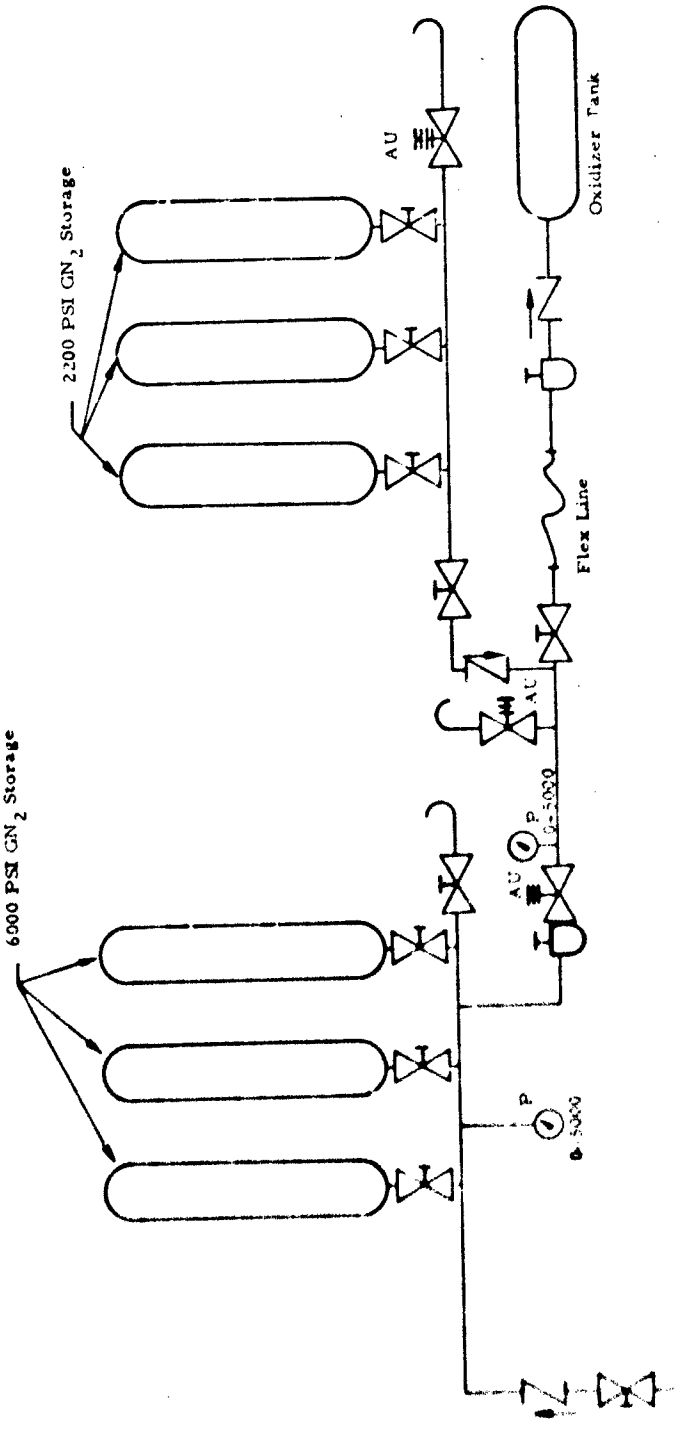

Figure 13. GN_2 Tank Pressurization Facility

pressure was available in limited quantity, the valve was always checked before using the high-pressure bottles. After these checks, the pressure was raised to 3500 psig in 500-psig increments with continuous leak checks. At 3500 psig, pressurizing was stopped and the missile system was allowed to cool to ambient temperature, since the pressurization process caused the nitrogen tank to become very hot. A voltage reading of the nitrogen pressure transducer and a pressure computation were then made to double check the nitrogen tank pressure. There was about a 100-psi difference in pressure between the nitrogen tank and the pressure gages mounted on the nitrogen servicing facility. After cooling sufficiently, the nitrogen tank was topped off to 3500 psig and the facility disconnected. The missile nitrogen tank was then fully charged. All work to this point was performed in the assembly area. Final continuity check and electrical hookup of all valves and the igniter were performed at the hot gun line just prior to mounting the missile on the launcher.

SECTION III

INSTRUMENTATION AND DATA REDUCTION

A. THRUST MEASUREMENT AND CALIBRATION

(U) Alignment of the thrust stand was accomplished by transit and level gages. Frequent mechanical calibrations maintained and verified a statistical measurement error less than ±1 percent. Appendix F details calibration tests performed during the heavyweight testing phase of the program. An end-to-end thrust calibration was performed at ambient pressure before each test with a single-beam dead-weight automatic calibrator over a range of 0 to 600 lbs_f in six steps. It was assumed that bouyancy effects were negligible between ambient and altitude pressures. Sealed load cells were initially used for thrust measurements. These load cells were supposed to be qualified for altitude testing; however calibration checks on these transducers showed that they were unsuitable. Special vented load cells were acquired and used successfully. Results of tests to evaluate the effects of abrupt changes in altitude are described in Appendix G. Ignition altitude for certification tests was set with the nitrogen loading valves. During boost-phase operation of the hybrid propulsion system, the altitude chamber was maintained at a pressure of about 0.730 psia or 67,000 ft altitude. By starting the hybrid engine at this altitude, the diffuser system did not have to pump down the altitude chamber. When the diffuser system did pump down the altitude chamber, a suction pressure on the engine developed after throttling, causing a negative thrust, and the changing pressure caused a slight error in the vented load cell. Thrust measurements were first corrected from test altitude to mission altitude by means of the pressure area term in the theoretical thrust coefficient equation. All boost thrust levels were corrected to 50,000 ft, and the sustain levels were corrected to their various mission altitudes, 50,000 ft, 70,000 ft, or 80,000 ft. Measurements made of pressure at the exhaust plane of the nozzle were then used to correct for negative thrust during transient operation. No attempt was made to correct for thrust deviations

caused by load cell adjustments to altitude. For certification tests, zero thrust was intially set at altitude. However, with the new vented load cells and using a proper time period before ignition to allow the transducer to adjust to pressure change, zero shifts were normally within noise limits of the digital data acquisition system (±3 lb_f).

B. HEAVYWEIGHT TCA

(U) Instrumentation was designed to measure hybrid engine performance, altitude test chamber characteristics, oxidizer feed system operation, diffuser performance and overall altitude facility (not discussed) operating characteristics as shown in Table II. To evaluate engine performance, measurements were made of chamber pressure, injector pressure, nozzle entrance pressure, nozzle exit pressure, thrust, oxidizer flow rate, TCA vibration levels, and TCA case temperature. Low-range instrumentation was isolated during high-pressure operation by solenoid valves actuated by the sustain control switch. Accelerometers measured vibration both axial and normal to the motor case. Thermocouples were placed on the chamber case and in the fuel grain. To control and evaluate the oxidizer feed system operation, measurements were made of oxidizer cavitating venturi entrance pressure, aeration line total pressure, oxidizer tank pressure and valve position voltage. Data reduction took the raw data recorded on magnetic tape and converted it to engineering units. L&M strip charts provided a direct readout in engineering units of parameters used to monitor and control facility operation during tests. Some engine parameters were placed on strip charts to provide instant readout of engine operation. However, strip chart data were not used in the final analysis of engine performance. The digital data acquistion system, because of its speed and accuracy, was used exclusively to calculate performance. The first step in reducing the digital data was to use the AFRPL General Data Program which, when supplied with the transducer calibration for each parameter, converted the data to engineering units. The Performance Program, which made the final calculations and printout, took samples from the General Data Program results. Normal sampling interval for

TABLE II. HEAVYWEIGHT TEST INSTRUMENTATION

Parameter	Transducer Range (high/low)
Chamber Pressure	0-1000 psig/0-100 psig
Injector Pressure	0-1000 psig/0-100 psig
Nozzle Exit Pressure	0-5 psia
Nozzle Entrance Pressure	0-750 psig/0-100 psig
Thrust	0-1000 lb_f
Oxidizer Flowrate	2.7-27 gpm/0.7-3.8 gpm
Acceleration	0-30g
TCA Case Skin Temperature	0-3000°F
Nozzle Skin Temperature	0-3000°F
Oxidizer Temperature	-26 to 150°F
OXIDIZER FEED SYSTEM	
Cavitating Venturi Pressure	0-1500 psig
Aeration Line Pressure	0-1000 psig/0-800 psig
Oxidizer Tank Pressure	0-2000 psig
Valve Position Voltage	0-28 VDC
ALTITUDE TEST CHAMBER	
Altitude Pressure	0-15 psia/0-2 psia

the digital data acquisition system was 0.003 sec. The unusual length of the tests required a special operating sequence to avoid running out of magnetic tape. During long tests, the first 10 seconds during boost, 10 seconds covering boost-to-sustain transition and the last 10 seconds of the test were sampled continuously. Other portions of the tests were sampled at 4.5-second intervals with each sampling period lasting 0.5 second. Fuel flow rates calculated from total measured TCA weight loss and nozzle throat erosion rates estimated from total change in throat diameter were averaged linearly with test time. When throttling occurred, fuel flow-rate estimates were made from previous data and the overall weight loss. Throat area was considered constant during sustain operation. Oxidizer flow rates were corrected for density changes based on temperatures measured in the oxidizer run line. Usually, oxidizer run line and oxidizer tank temperatures agreed well enough that either value could have been used.

C. FLIGHT-WEIGHT CERTIFICATION

1. Altitude Performance

(U) The certification tests verified total altitude performance of the flight-weight hybrid propulsion system. Instrumentation was limited to parameters required to measure hybrid TCA performance as shown in Table III. It was also planned to measure these same parameters during flight testing so that a comparison between certification and flight performance could be made. An attempt was made to select all instrumentation sensors as actual flight components would be mounted. To calculate TCA performance, chamber pressure, oxidizer injector pressure, thrust, and oxidizer tank pressure were measured. Thermocouples on the nozzle and engine case measured temperature as would be experienced in flight. Propulsion system functional performance was based upon data from the oxidizer pressurization system (these being nitrogen tank pressure, nitrogen regulator pressure, voltage of nitrogen start valve) and the voltages of oxidizer start valve, of the boost valve, of the oxidizer cutoff valve, and of the igniter. The cutoff valve was an added feature peculiar to the

TABLE III. FLIGHT CERTIFICATION TEST INSTRUMENTATION

Parameter	Transducer Range
Chamber Pressure	0 to 1000 psig
Injector Pressure	0 to 1000 psig
Thrust	0 to 1000 lb_f
Acceleration	0 to 30g
Nozzle Temperature	0 to 3000°F
GN_2 Tank Temperature	-300 to +160°F
Oxidizer Tank Temperature	-300 to +160°F
GN_2 Tank Pressure	0 to 4000 psig
Nozzle Exit Pressure	0 to 5 psia
GN_2 Regulator Pressure	0 to 1000 psig
TCA Case Skin Temperature	0 to 3000°F
Altitude Cell Pressure	0 to 15 psia (high)/0 to 2 psia (low)

certification test systems. This valve was installed separately by UTC only on the propulsion systems sent to the AFRPL. It provided for overboard oxidizer dump in case of emergency to avoid damaging the altitude test facility. However, this valve was never used. Thrust was measured and corrected as in the heavyweight TCA tests. Altitude chamber, diffuser and altitude facility parameters remained the same with the exception of two additional nozzle exit pressure transducers. Thrust and chamber pressure were the only performance parameters measured directly during each test. The values reported represent an average over five samples on each side of the time slice. This sampling method was not completely satisfactory. Figure 14 shows the chamber pressure printed from the complete digital data for part of a typical firing. During any time slice it

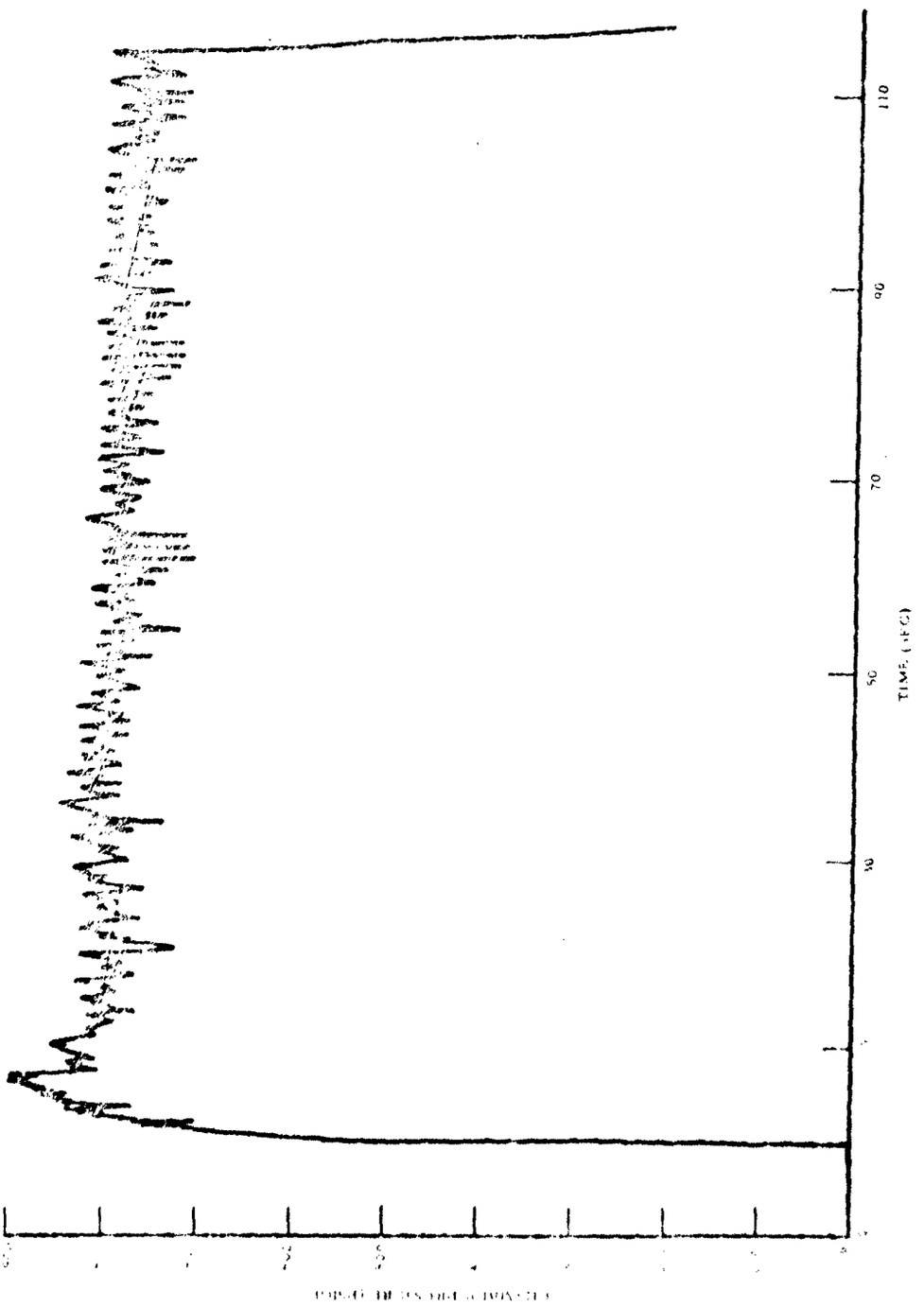

Figure 14. Typical Boost Chamber Pressure from Digital Data Acquisition System

was possible to get 10 values lying on a high or low peak. Therefore, the final performance data may be misleading if it is assumed that each number represents an accurate mean value. Actually the number may be too high or too low. Throat erosion was considered to occur only during boost phase and began after an initial period of time for the 70,000- and 80,000-ft missions. This delay time for erosion was based upon a noticeable drop in chamber pressure normally seen after 30 sec to 50 sec of run time. For the 50,000-ft missions, erosion of the throat began only after a 175-sec time delay.

2. Oxidizer and Fuel Flow Estimates

(U) Neither oxidizer nor fuel flow rates could be measured directly for use in calculating Isp and C*. Each flight-weight feed system was calibrated with water after the certification tests, and oxidizer flow rates were estimated based upon the experimental observation that the ratio of flow rate to injector pressure was constant for a given oxidizer tank pressure (see Appendix B). Using a surface mapping routine, oxidizer flows were estimated by interpolation of the water-flow data using the density ratio between water and the MON-25 oxidizer. Fuel flow rates were predicted with a theoretical hybrid combustion program using the estimated oxidizer flow rates and measured chamber pressures (see Appendix C). The oxidizer and fuel flow rates were then fed into the final Performance Program, and a complete performance analysis of each certification test was made and compared with predicted theoretical performance at the existing conditions.

3. Environmental Storage

(U) Environmental storage conditions were simulated during a number of tests. Temperatures were monitored at the air inlet and outlet to the cocoon surrounding the propulsion system and on the motor case. These parameters were recorded continuously for up to 48 hours on L&N strip charts. Sufficient time, at least 10 hours, was provided at constant temperature to allow the complete hybrid propulsion system to reach a

uniform temperature. One propulsion system was stored outside and exposed to the elements on a 24-hour basis for 2 weeks.

4. Vibration

(U) The vibration tests to verify structural integrity were conducted at the NASA Edwards AFB facility operated by JPL. These tests were used to determine detrimental effects that might be encountered during transportation, normal handling operations and launch or flight environments. Appendix D presents a summary of the results of these tests. Dummy masses simulating the flight transducers were attached to the propulsion systems before delivery to JPL.

5. Flight Test Data Reduction

(U) Data from the flight demonstration tests were recorded on magnetic tape as PDM/FM analogue data. The complete data reduction process was conducted at the AFRPL computer facility and required a modification of the then existing capability. Two separate programs to convert analogue to digital units had to be written for the SDS-190 computer system. These programs converted analogue to digital output, calibrated the data, and produced engineering units on digital tape. The digital tape was run on the IBM 7040 and printed out. This printout served as the General Data Program results. These results were distributed to all members of the program team for analysis and scrutiny.

SECTION IV

TEST RESULTS

A. HEAVYWEIGHT TCA

(U) The theoretical shifting equilibrium performance for the propellant combination MON-25/Plexiglas-10%Mg is shown in Figures 15 and 16 as a function of mixture ratio (O/F). Three chamber pressures are presented to cover the engine operating regime and provide a comparison with other known propellant combinations. The hybrid engine (TCA) operated over a chamber pressure range of 50 psia to 600 psia during heavyweight testing. The theoretical curves show the performance in both these regimes of operation. The performance at a chamber pressure of 1000 psia is presented for a standard comparison of theoretical performance expanded optimumly to sea-level altitude. The maximum specific impulse occurs at an O/F ratio of 1.75 for a chamber pressure of 1000 psia. On the high side of the optimum O/F for each pressure, the specific impulse drops off slowly. Since throttling (decreasing thrust) involves a drop in chamber pressure and a more fuel-rich shift in mixture ratio (hybrid throttling was accomplished by decreasing the oxidizer flow rate), the theoretical downward shift in optimum O/F ratio for lower chamber pressures is advantageous, and the hybrid engine may be designed to operate near maximum Isp at both high and low pressures by judicious choice of design O/F ratio at maximum thrust. The characteristic velocity in Figure 16 does not have as large a shift in optimum O/F for decreasing chamber pressure as does the specific impulse and, for O/F values below about 1.5, chamber pressure has very little effect upon characteristic velocity.

(U) Figure 17 compares the theoretical shifting Isp of MON-25 and Plexiglas loaded with 2%, 10%, and 20% by weight magnesium powder. These three combinations were tested during the heavyweight TCA effort. The effect of decreasing metal loading in the fuel grain was to shift the optimum performance O/F to higher values with a very slight maximum

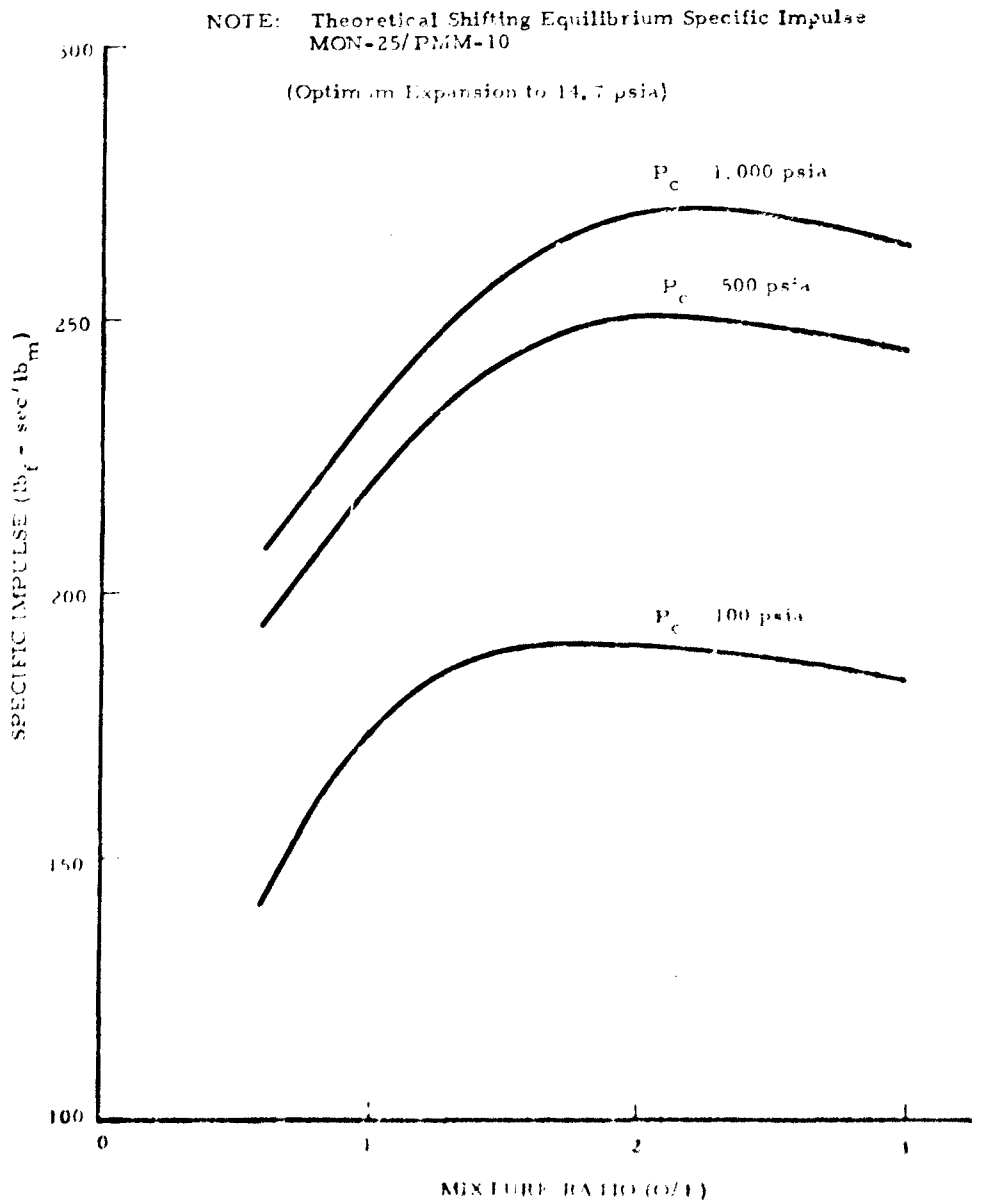

Figure 15. MON-25/PMM-10 Theoretical Isp versus O/F Ratio

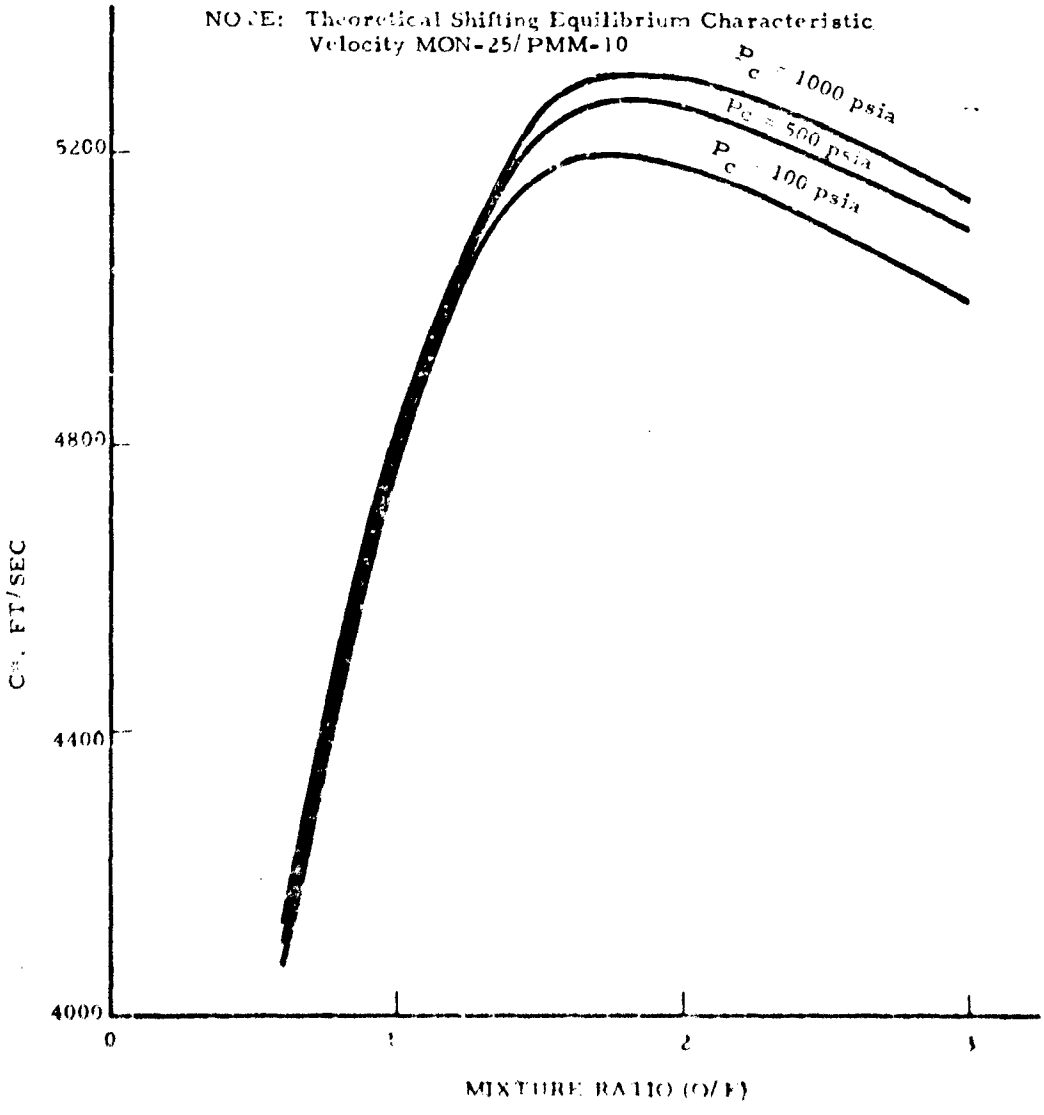

Figure 16. MON-25/PMM-10 Theoretical Characteristic Velocity versus O/F Ratio

NOTE: Theoretical Shifting Equilibrium Specific Impulse
MON-25/PMM-2, 10, 20
Chamber Pressure: 500 psi
(Optimum Expansion to 14.7 psia)

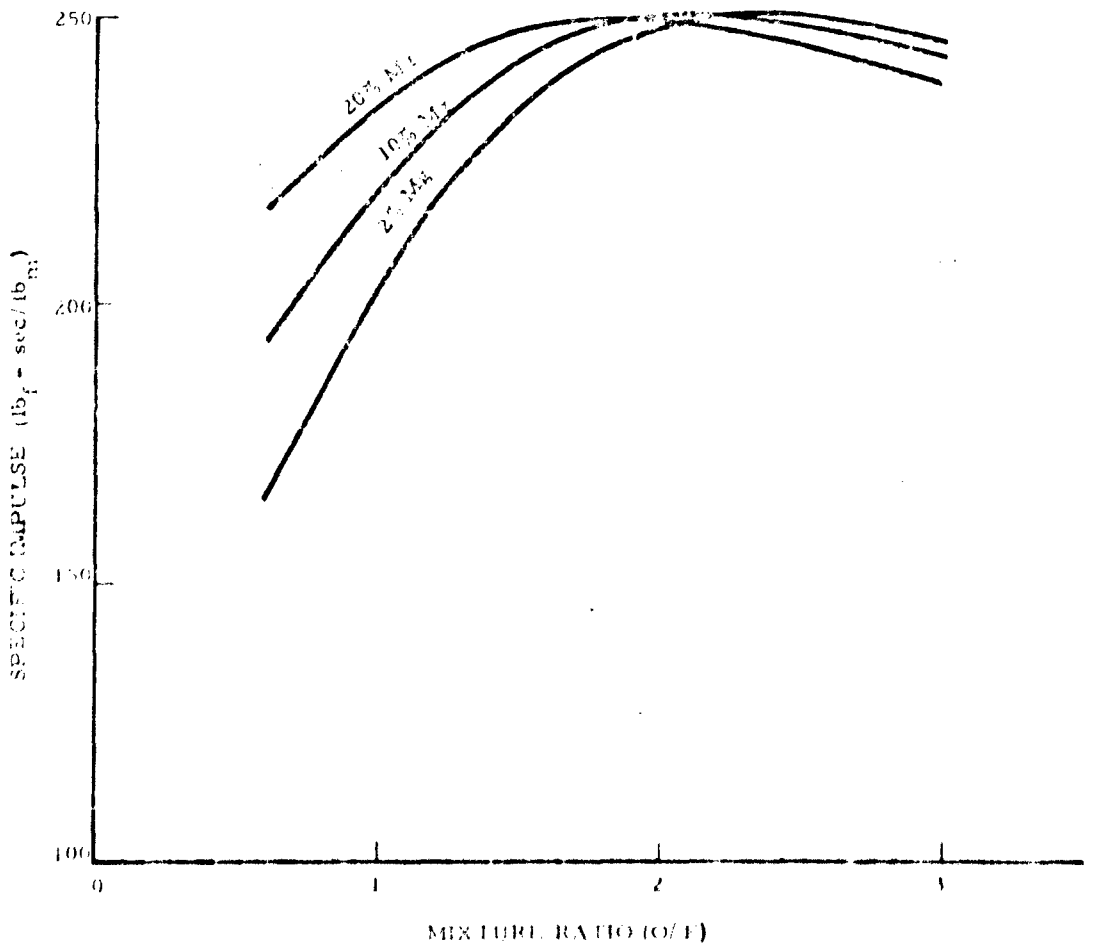

Figure 17. MON-25/PMM-2, 10, 20 Theoretical Isp versus O/F Ratio

performance increase. In the lower O/F range, the increased metal loading provides a performance advantage. Test results presented later in this section show that better combustion characteristics were obtained with lower metal loading.

(U) A summary of tests conducted during the heavyweight TCA effort is presented in Table IV. A total of 32 firings were conducted with the hybrid engine. Five of these tests were unsuccessful. During this portion of testing, the boost phase (maximum O/F, thrust and temperature) and the 90,000-ft mission phase (minimum O/F, thrust and temperature) were considered the extremes of operating conditions subject to investigation. Most of the heavyweight tests were conducted in these two regimes for this reason. After the contractor encountered difficulties in the intermediate operating regime of the 50,000-ft mission, the testing effort was altered in an attempt to furnish data that might be of assistance in contractor attempts to modify the TCA configuration to meet mission requirements. Boost-phase operation presented an extreme test of hardware durability because erosion of the graphite throat was severe in the presence of a high temperature oxidizing atmosphere, and ignition could have been difficult due to fuel grain surface flooding by excess oxidizer. In the low regime of operation, hardware durability was less of a problem, and the combustion mechanism of the solid fuel became more important here where subsurface melting and charring could severely affect hybrid rocket performance.

(U) Testing with the first fuel grain began 1 December 1966 and included the first four tests. No ignition occurred on the first test because stray voltage in the electrical circuitry caused premature firing of the igniter. The second attempt gave ignition at ambient (13.2 psia) pressure Using the diffuser system alone (no ejectors), test chamber altitude increased slowly to 15,000 ft (8.30 psia). Presumably, had the test run longer, the diffuser would have eventually dropped altitude cell pressure down close to 50,000 ft equivalent (1.74 psia) as designed. The data for

UNCLASSIFIED

TABLE IV. HEAVYWEIGHT TEST SUMMARY

Test No.	Igniter No.	Igniter Propellant Wt. (lbm)	Igniter Chamber Pressure (psia)	No. of Grain Segments	Propellant Temperature (°F)	Motor Case Pressure (psia)	Nom. Pc (psig)	Altitude Corrected Thrust (lbf)	Nominal Throat Erosion Rate (mil/sec)	Fuel Metal Loading (% by weight)	Comments
1					NO IGNITION					10	Premature Igniter Fire
2	1	1.327	54	25	AMB	50,000	435	421	2.75	10	
3	1	1.335	53	25	120°F	50,000	495	505	2.10	10	
4	1	1.327	46	25	AMB	50,000	432	444	2.21	10	
5	2				NO IGNITION (-65°F)					10	Ice in Chamber
6	2	1.498	24	25	AMB	50,000	92	72	-	10	
7	2	1.495	146	25	AMB	50,000	93	62	-	10	
8	2	1.498	73	25	AMB	50,000	93	70		10	
9	3	1.524	63	7	AMB	AMB	328	230	-	10	
10	3	1.547	63	7	AMB	AMB	678	475	0.12	10	
11	3	1.533	138	7	AMB	AMB	84	65	-	10	
12	4	1.563	63	7	AMB	AMB	480	340	0.08	2	
13	4	1.564	63	7	AMB	AMB	650	445	0.21	2	
14	4	1.565	213	7	AMB	AMB	82	68	-	2	
15	4	1.566	151	7	AMB	AMB	77	46	-	2	
16	5	1.547	54	7	AMB	AMB	575	430	0.40	20	
17	5	1.547	63	25	AMB	50K-40K	500/100	630/445	3.37	20	Nozzle Plug

UNCLASSIFIED

UNCLASSIFIED

TABLE IV. HEAVYWEIGHT TEST SUMMARY (Cont'd)

Test No.	Fuel Grain No.	Wox (lbm/sec)	Firing Duration (sec)	Nozzle Expansion Ratio	Envir. Temp (°F)	Altitude (ft MSL)	Nom. Pc (psig)	Altitude Corrected Thrust (lb_f)	Nominal Throat Erosion Rate (mil/sec)	Fuel Metal Loading (% by weight)	Comments
18	6	1.393/0.300	93.6/171.1	25	AMB.	50K/80K	490/64	560/167	2.90	10	
19	7	1.27/0.301	64/274	25	AMB.	50K/70K	490/97	510/166	0.94	10	Thrust Calib.
20	8										
21	8				NO IGNITION						Regulator Failures
22	8										
23	8	-	94.6/118.7	25	AMB.	50K/90K	494/30	586/86	1.93	10	Flight-weight System
24	9	-	55.9/113.1	25	AMB.	50K/70K	492/168	456/155	None	10	
25	10	1.250/0.461	8.4/184.4	25	AMB.	50K	483/183	447/171	None	10	
26	11	1.52/0.459	10.3/160.3	25	AMb.	50K	570/179	515/167	None	2	
27	12	1.506	96.8	25	AMB.	50K	475	650	-	20	
28	+	0.456	60.4	25	AMB.	50K	223	199	None	10	
29											
30					ALTITUDE CALIBRATION						
31	13	0.313	101.95	25	AMB.	70K	150	147	None	10	
32	14	0.310	189.77	25	AMB.	70K	133	138	None	2	
100	+	Boost	19.9/0.8	25	AMB.	-	238	221	None	10	Flight-weight System [illegible] rected Data. Combustion Extinquished During Throttle; IRFNA Oxidizer
101	+	Boost	20.1/0.9	25	AMB.	-	482	443	None	10	

+: Salvaged fuel grains

UNCLASSIFIED

the second test were corrected to 60,000 ft, for comparison with tests three and four. The third test was a firing with the heavyweight TCA conditioned to 165°F. Both tests 3 and 4 were ignited at an approximate altitude of 50,000 ft. The ignition sequence was programmed with a 200-millisecond oxidizer propellant valve opening lead before igniter fire signal.

(U) Tests 2, 3, and 4 evaluated a Spear Carbon nozzle throat insert under maximum oxidizer flow conditions. As the data show, the nozzle eroded badly. These results eliminated high-density graphite as a nozzle throat candidate, and UTC selected pyrolytic graphite after these tests. Postfire examination of the TCA after these tests revealed a number of unexpected results. Trapped in the combustion chamber were a number of large rock-like objects, small grey flakes, and fine black flakes (potato chips) as illustrated in Figure 18. Analysis of this material revealed its composition (Table V) and the fact that the rocks were hollow, containing small spheres of pure metal. These types of residue were seen throughout the testing program at the AFRPL. The quantity of each type of material seemed to depend upon the magnesium loading in the fuel grain and the oxidizer mass flux through the fuel grain port.

(U) The second fuel grain was utilized for minimum oxidizer flow rate tests to evaluate performance at low pressure in tests 5 through 8. Test number 5 was set for ignition at the minimum operational temperature of -65°F. A larger initiator with a higher heat output was used, Holex 2074, to insure ignition of the solid igniter charge at this low temperature, but ignition did not occur. A check of the hardware showed that the igniter had fired successfully and oxidizer flowed correctly into the chamber. However, there was a large amount of ice collected along the combustion chamber walls due to condensed water vapor. This ice probably prevented normal ignition because ignition occurred successfully with the warm grain in tests 6 through 8. The tests with the second fuel grain also utilized a Spear Carbon nozzle insert, and no erosion occurred. In fact, a slight decrease in nozzle area occurred due to a deposit in the throat. All of

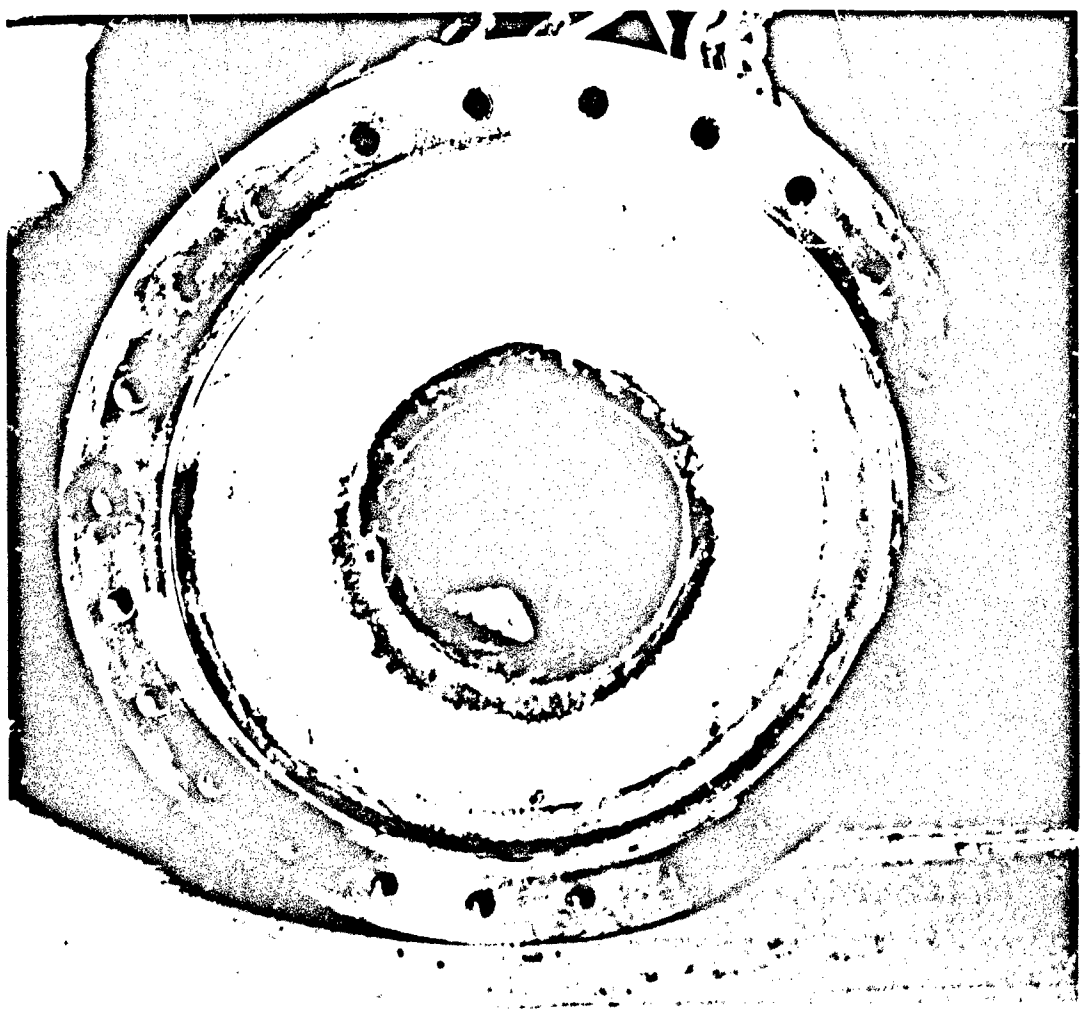

Figure 18. Fuel Debris After Tests 1 and 2, Aft End of TCA

TABLE V. CHEMICAL ANALYSIS OF FUEL DEBRIS AFTER TESTS 1 AND 2

Red Crystals	
Major:	Iron and Magnesium
Minor:	Aluminum, Silicon, Nickel, Manganese
Large Rock	
Major:	Black Material, Silver, Magnesium, Aluminum, Silicon
Minor:	Iron, Copper, Nickel, Manganese, Chromium
	The rock was broken and found to be hollow. It contained small spheres of pure metal.
Major:	Magnesium, Silver
Minor:	Aluminum
Grey Flakes	
Major:	Silver, Magnesium
Minor:	Iron, Copper, Nickel Manganese, Chromium, Aluminum Silicon
Fine Black Flakes	
Major:	Silicon, Magnesium, Aluminum
Minor:	Iron, Copper, Nickel, Chromium, Silicon

these low oxidizer flow tests produced a large amount of residue in the thrust chamber. This material, designated "potato chips," was the same type of black flakes, only larger, seen in previous testing. Figure 19 shows the chips in the combustion chamber, as seen from the aft end, after removal of the nozzle assembly following test number 7. The chips were collected and weighed. Although the chips were large volumetrically, they weighed only 13 ounces. These chips represent the accumulation from only one firing because the TCA was disassembled and the residue dumped out after each test. Presumably, this amount would be increased significantly with longer durations. Figure 20 shows the second fuel grain after tests 5 through 8. Note that burnthrough of the fuel grain occurred approximately midway down the length of the grain (forward half of the grain is on right). This picture also shows the RTV-11 insulation on the outside of the grain. It was also noted after each test that the fuel grain sagged vertically. In Figure 19, note the gap between the grain and case at the top and the rippled effect of the insulation. Evidently, the fuel grain was heated enough during firing to allow it to creep. This probably occurred after shutdown when the thermal soak-through to the case was maximum.

(U) The next eight tests, 9 through 16, were conducted at ambient pressure of 13.2 psia with a nozzle expansion of 7. A special diffuser arrangement was used for these tests, as previously described in Section II, and photographic and closed-circuit television coverage was used for observation of the exhaust plume during firings. The third fuel grain was used for tests, and very little erosion was observed. For smoother starts, oxidizer prop-valve lead time over the igniter firing was increased to 0.5 second. The first two tests, 9 and 10, resulted in a cleanly burned fuel grain like that observed in tests 2 through 4. Test 11 produced the usual potato chips.

(U) The fourth grain was loaded with 2 percent by weight magnesium, the 2 percent magnesium being just sufficient to make the Plexiglas opaque and prevent subsurface melting or other problems associated with a

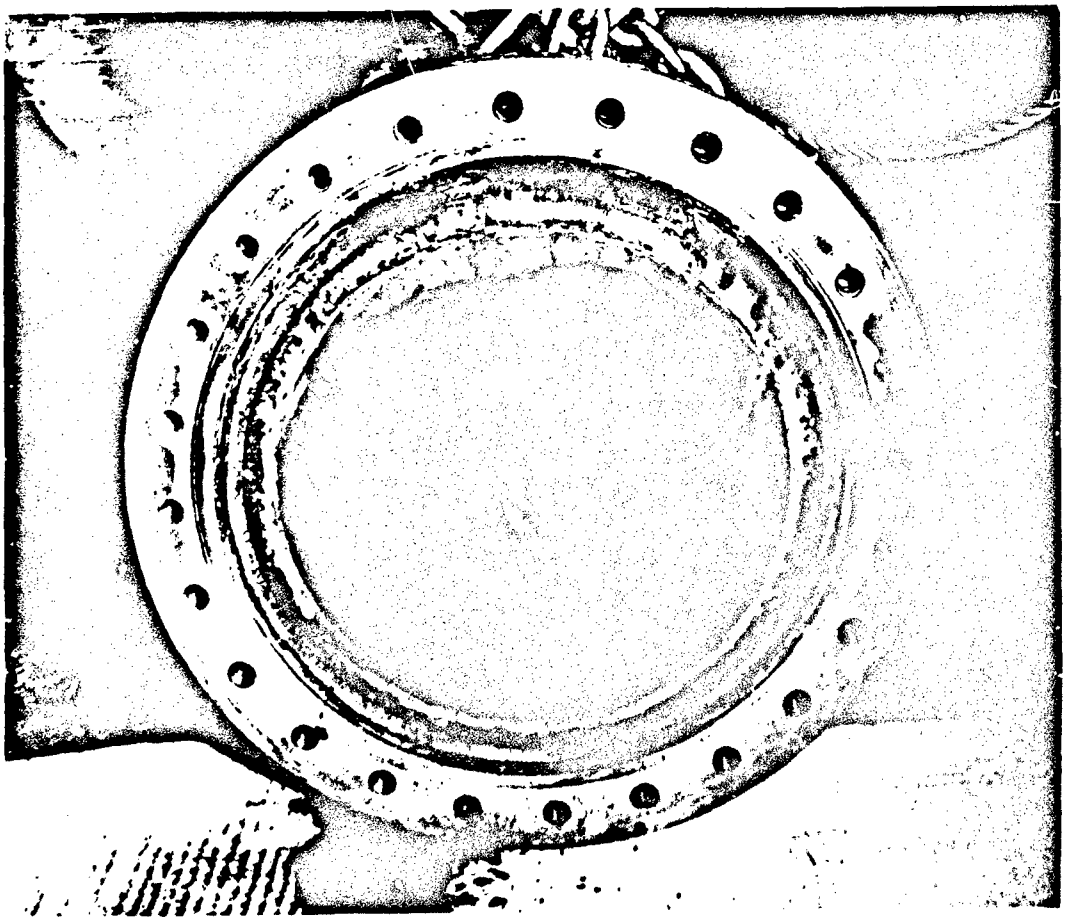

Figure 19. "Potato Chips" Debris, After Test 7, Aft End of TCA

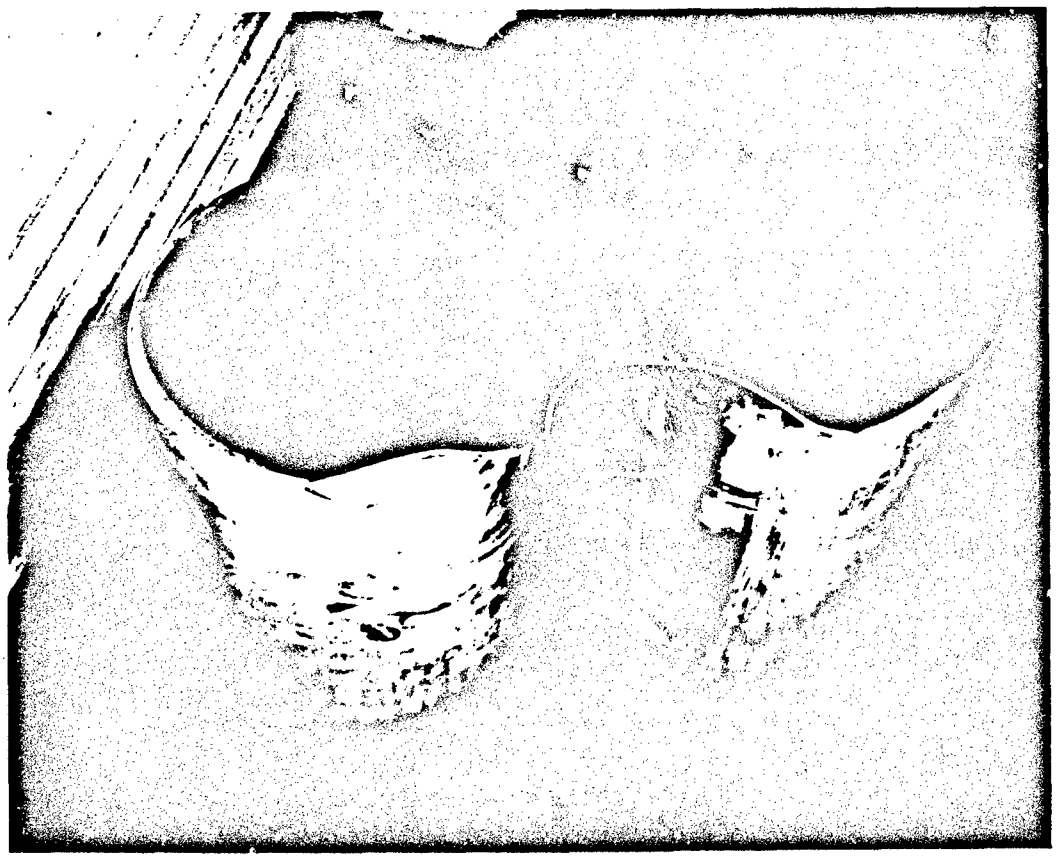

Figure 20. Fuel Grain No. 2 After Tests 5 Through 8

transparent fuel. Four tests, 12 through 15, were conducted with this grain to compare performance and combustion characteristics with the previous 10 percent magnesium loaded fuels. All tests were now being conducted with the pyrolytic graphite (PG) insert and showed considerably reduced nozzle erosion. The first 2 percent test showed a strange ripple effect on the aft end of the fuel grain after tests 12 and 13, as shown in Figure 21. Also, the fuel burned very cleanly with no residual material left in the combustion chamber. Observations of exhaust plume pictures showed a much cleaner, transparent flame than observed with the 10 percent fuel. Tests 12 and 13 also showed more rapid regression of the fuel at the head end. So rapid, in fact, that the fuel port diameter exceeded the diameter of the head end forward insulation. An asbestos ring was cut to protect the forward closure out to a larger port diameter and sufficed well for the third and fourth tests, numbers 14 and 15. The injector from test number 12, although scorched on the outside, was cleaned and found to be reusable.

(U) The fifth fuel grain containing 20 percent by weight magnesium was used for two tests, number 16 at ambient and number 17, a 50,000 to 80,000-lb-thrust duty cycle (this was the first throttling test). The combustion of the 20 percent fuel was very dirty. Observation of the exhaust plume showed a thick, heavy smoke being ejected from the engine. Also, many brightly flaming particles spiraled outward from the exhaust plume. No potato chips were observed. Instead, the grain had seemed to flow, It appeared to have oozed, as if extruded under pressure. After test 16, inspection revealed a relatively clean combustion chamber. However, after test 17, the nozzle was definitely plugged by extruding material. This plug could not be removed after the test. Note that thrust, but not duration, met requirements. This test also provided data for nozzle exit temperature effects on the heat shield. The Beech Aircraft Company designed an aluminum boattail extension surrounding the exhaust nozzle exit. Temperature measurements during a test were requested to determine whether or not insulation would be required to protect the interior of the boattail extension.

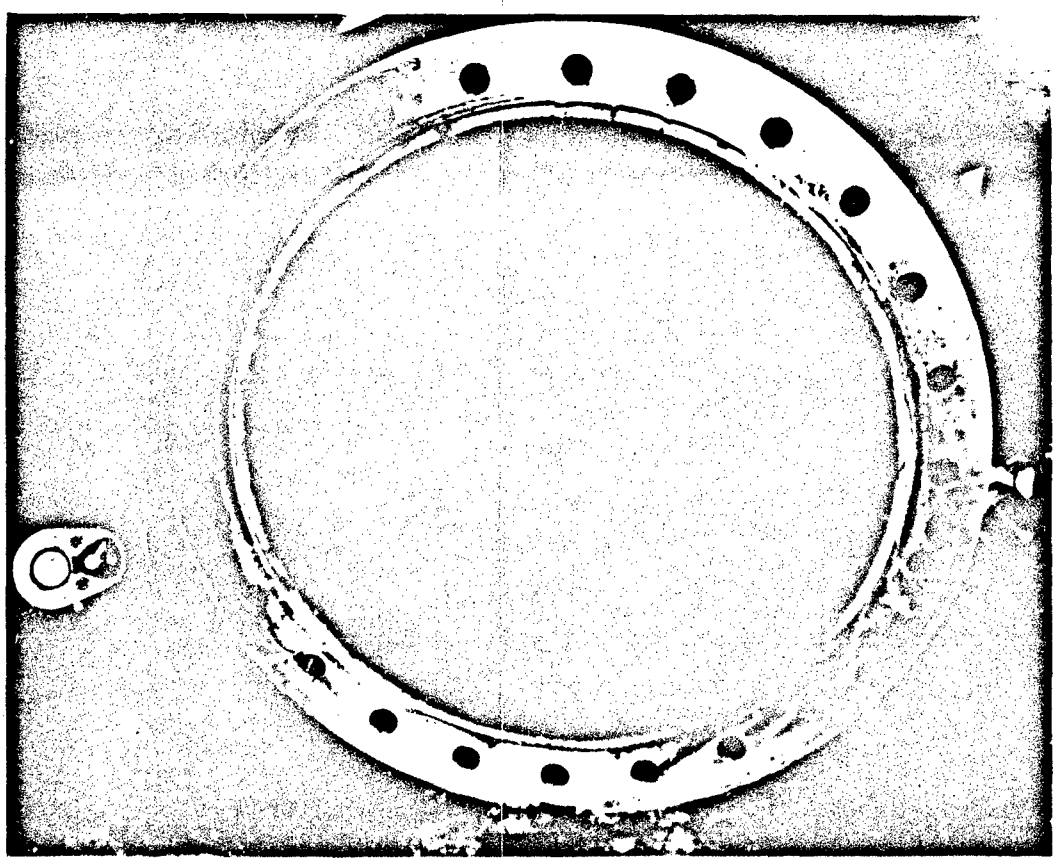

Figure 21. Fuel Surface Ripple, Aft End of TCA After Tests 12 and 13

Thermocouples were installed on a simulated boattail extension, as shown in Figure 22. The temperatures, measured during test 17, are shown in Figure 23 and resulted in the use of insulation.

(U) A comparison of the 2%, 10%, and 20% magnesium (Mg) loaded fuel behavior can be made from the first 17 tests. During high-thrust tests, the 2% fuel grain burned most cleanly but with rippled markings. Fuel grain color after firing contained a definite reddish tint. The 10% Mg fuel grain, greyish in color, burned cleanly with high oxidizer flows. The 20% Mg grain burned poorly, producing a sooty flame, ejection of ash, and extruded flow of grain material which plugged the nozzle. A comparison of thrust levels and chamber pressure for nearly identical oxidizer flow rates was impossible because of the inconsistency of the data. Even with the same fuel grain at constant oxidizer flow, the tests did not show repeatability of measured data. Inspection of the fuel grains after tests revealed that during the shutdown and cooling-off period the more volatile components of the fuel were being vaporized off in a heat penetration region near the surface. Thus, after the first test with each fuel grain, the fuel surface was chemically different at the start of the next test. A thermal analysis by UTC showed that below a regression rate of 0.004 inch/sec the thermal profile penetration rate into a pure Plexiglas was so much more rapid than the regression rate that subsurface melting and flowing of the fuel was probable.

(U) The addition of Mg metal should increase the thermal soak rate and the fuel regression rate simultaneously (Reference 4). A comparison of average-weight-loss rate for tests 13 and 10, which were run at almost identical oxidizer flow rates and after very similar previous firing histories for each grain, should reveal the average regression rate trend as a function of metal loading. This indicated a 20% increase in average regression rate for the 10% Mg grain over the 2% Mg grain. Unfortunately, no similar comparison was available for the 20% Mg fuel, but the test

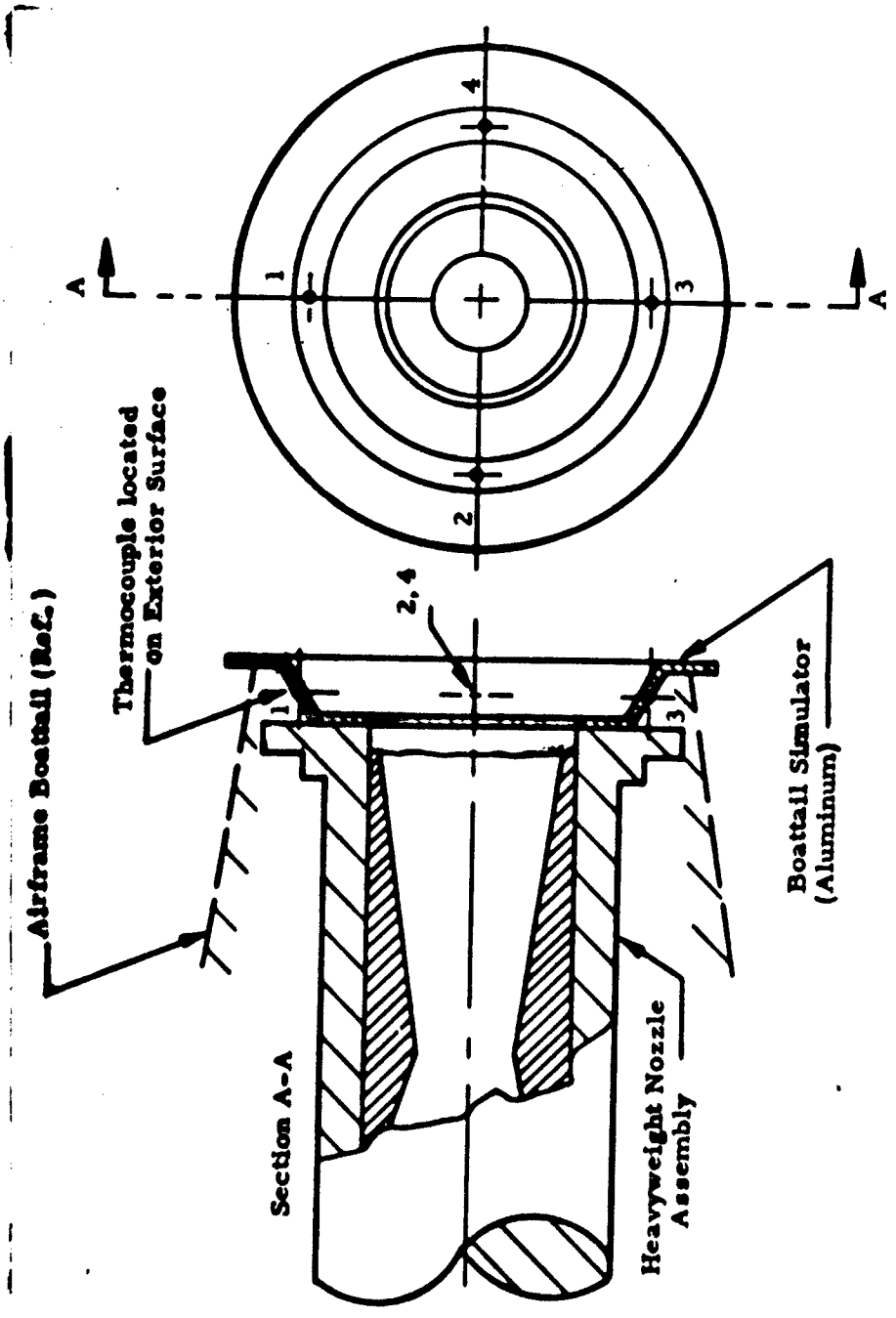

Figure 22. Simulated Boattail Extension and Thermocouple Placement

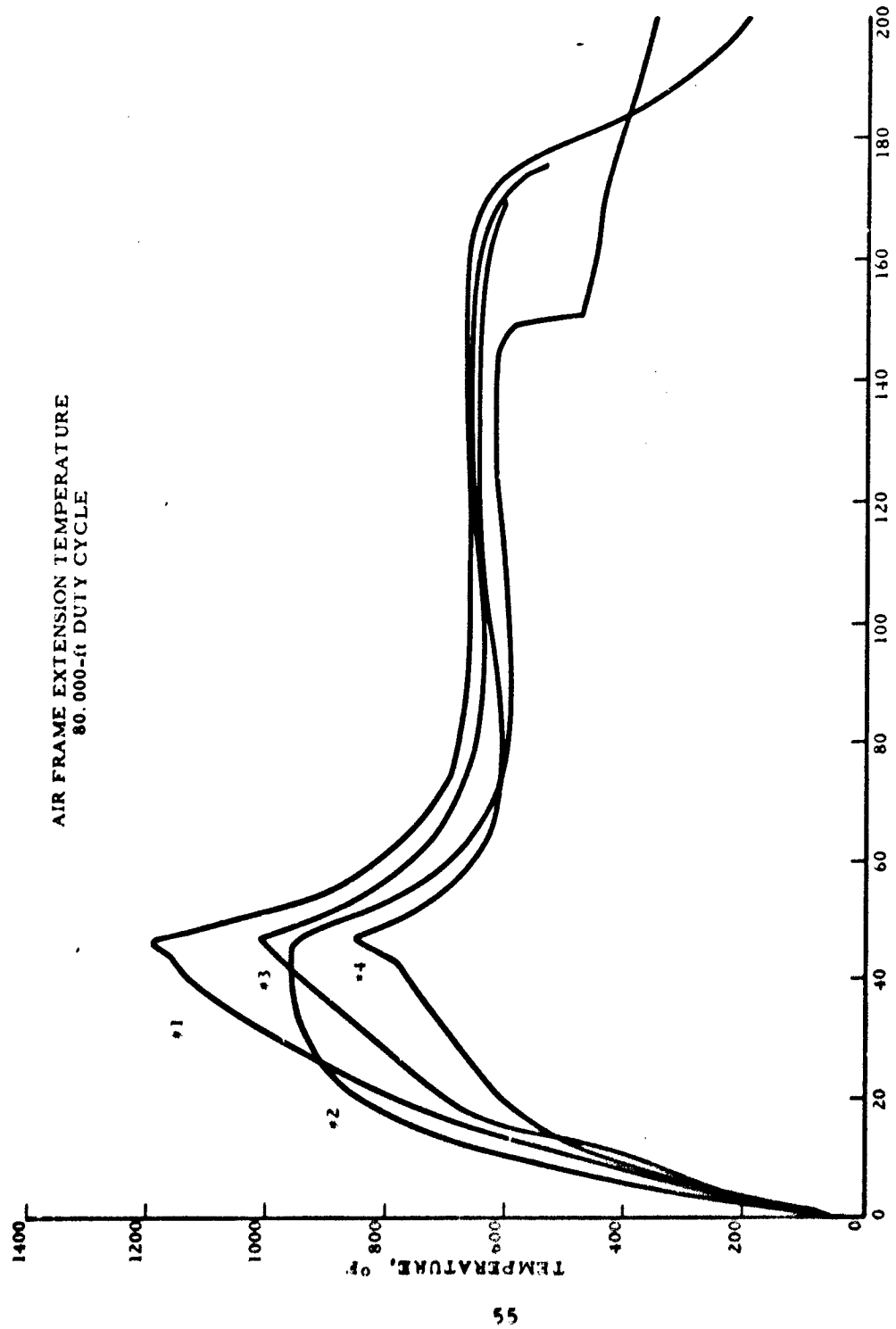

Figure 23. Simulated Boattail Extension Temperature History, Test 17

results definitely show that the thermal heat-soak rate drastically exceeded the regression rate with this fuel as evidenced by the fuel flowing observed in test 17.

(U) Test number 18 was an 80,000-ft duty cycle test with the boost thrust corrected to 50,000 feet and the sustain thrust corrected to 80,000 feet. This was the first test with boost followed by a full-length sustain. This test subjected engine hardware to actual mission conditions for the first time. The thrust levels were sufficient to have flown an actual missile for the measured duration. However, the measured nozzle erosion rate was higher than expected from previous experience with the pyrolytic insert, but extended boost operation could have caused this. It was assumed for this test that all erosion occurred during boost phase only. During this test, the heat generated at the aft end of the combustion chamber was great enough to cause the graphite mixer to break. Otherwise, the TCA components showed no unusual effects. Figure 24 shows the fuel grain and the portions where burnthough occurred (the head end is on the floor) in the first, second, and third billets.

(U) Test number 19 was similar to 18 except the shorter boost duration caused less noticeable heat effects and the sustain time was longer. This was also the first test during which thrust was calibrated at altitude (see Appendix F). Note the lower nozzle erosion rate, primarily because of lower oxidizer flow rate during boost. However, as in test 18, the fuel grain burned through in the second and third billets.

(U) At this point in the heavyweight testing, the flight-weight oxidizer feed system was mated with the heavyweight TCA in order to measure the system performance of the proposed propulsion system configuration at altitude. Although the heavyweight TCA was used, the internal configuration was identical to that proposed for flight-weight TCA used by the contractor at that time. The first three attempts (tests 20 through 22) to test with the flight-weight system gave no ignition because the combination

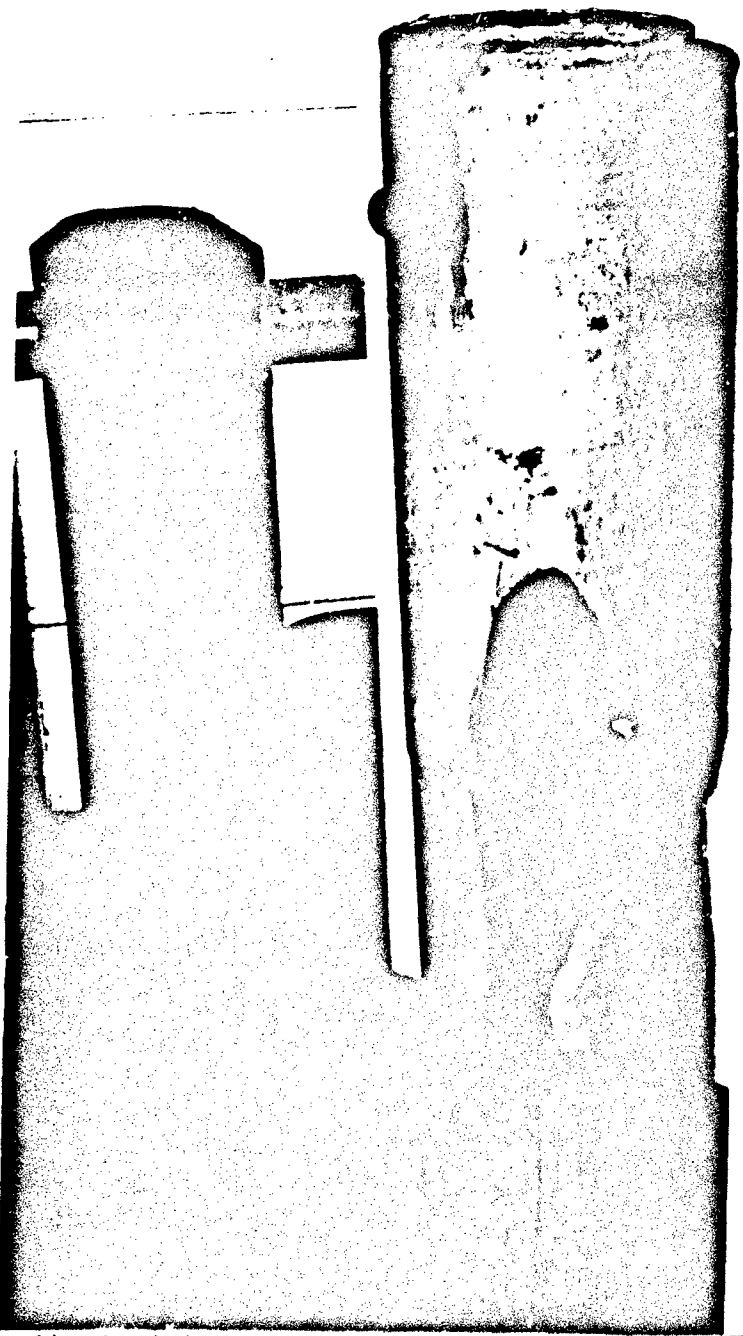

Figure 24. Fuel Grain No. 6 After Test 18, Aft End is at Top

nitrogen start valve and oxidizer tank regulator failed to function properly (see Figure 7). The ignition sequence timing was set for oxidizer start valve firing 2 seconds after nitrogen valve firing and followed by igniter fire signal 0.3 second later. Both tests 23 and 24 delivered ample thrust levels to meet program requirements, but test durations fell below minimum time limits. These tests also utilized a newly developed AFRPL injector, which improved the fuel port profile by making regression more uniform along the fuel grain length. This injector had a larger hollow cone spray angle than the previous UTC injector, and a higher oxidizer injection velocity. This injector was used exclusively in the remaining tests because of its desirable effects. Again, as in tests 18 and 19, a higher nozzle erosion rate occurred in test 24 with the longer boost time. This indicated that most nozzle erosion occurred during the 60- to 94-sec boost-phase time period.

(U) Tests 25 and 26 were an attempt to compare performance of 2% and 10% fuel grains using the facility oxidizer feed system, heavyweight TCA, and the AFRPL injector. Although the boost flow rates differed, note that the sustain thrust levels and chamber pressures were almost the same for nearly identical flow rates. The 10% fuel caused a heating effect on the forward closure insulation. This problem, along with the phenomenon of the head end grain port diameter almost exceeding the insulation diameter, occurred previously, using the AFRPL injector. Measurements consistently confirmed that the exhaust nozzle exit did not suffer erosion during any tests.

(U) Tests 28, 31, and 32 were designed to measure the insulating qualities of asbestos, graphite tape and silica phenolic as case insulation. For test 28, a fuel grain was assembled from 10% Mg fuel billets left from previous testing. It was wrapped with a 1/4-inch sleeve of asbestos and fired at a low thrust level in an attempt to get an even burnout of the fuel over a large area to better observe the effect on the insulator. Since asbestos had been used successfully at the head end, it was hoped that it

would do well around the grain. The results were comparable with the RTV-11. For tests 31 and 32, a graphite tape on 10% and 2% fuel grain was used to compare insulation qualities after fuel burnout. Of the three materials, the graphite tape was the poorest, probably because it was so easily oxidized by N_2O_4.

(U) Tests 101 and 102 were conducted with Inhibited Red Fuming Nitric Acid (IRFNA) as the oxidizer. It was anticipated at this time that this oxidizer might be substituted for MON-25 during flight testing. These two tests were conducted to compare IRFNA/PMM-10 performance with MON-25/PMM-10. The flight-weight oxidizer system was used with the heavyweight TCA. Timing for ignition sequence was as previously described. The tests were planned to be throttled duty cycles with maximum and minimum oxidizer flow rates to evaluate performance at both extremes. The dial-a-thrust valve setting was comparable with the 90,000-ft thrust level with MON-25. In both tests, the combustion process extinquished after throttling occurred. It appeared in postfire analysis that particle contaminants in the IRFNA had plugged the dial-a-thrust valve orifice. Examination of the oxidizer system and transfer lines used to fill the oxidizer tank revealed a coating of fine white powder on the inside of the liner. This powder was found to have built up around the valve orifice. The fuel grains used for these tests were rebuilt from scrap 10% fuel material, and weight loss during the tests was not measured. Burning of the fuel visually appeared similar to that observed with MON-25.

(U) Throughout the heavyweight testing phase, certain tests were conducted to evaluate various system components and their effects upon system operation. The contractor was plagued with a problem of getting the combination nitrogen start valve/regulator to function properly, and both the Beech Company and AFATL were worried about an in-line 10-micron nitrogen filter. A cold-flow test was conducted with a flight-weight Thor regulator meeting the system operational requirements to evaluate possible

performance losses due to condensation of ice on the filter. The test indicated that, with proper precautions to avoid water contamination of the system, no icing problems would result.

(U) Beginning with test 19, obtaining more accurate thrust measurements became a serious problem. The inconsistencies and lack of repeatability of engine performance indicated errors in measurement. All instrumentation was checked for accuracy, and during tests 19 and 21, thrust calibrations were conducted for the first time at ambient pressure and at altitude to evaluate dual-bridge load-cell accuracy over a large variation in pressure. The results of the calibration for tests 19 and 21 are tabulated in Table VI. These data showed deviations and lack of repeatability in thrust calibration at altitude. Laboratory checks of the load cell confirmed this and also showed that the transducer had been damaged by operation at altitude. Several different load cells had been used up to this point in time and all showed similar defects. Tests 29 and 30 furnished accurate thrust

TABLE VI. LOAD-CELL ALTITUDE CALBIRATION, TEST 19

Applied Load (lb_f)	Measured Thrust (lb_f)**		Altitude
	Bridge A	Bridge B	
600	598.6	598.7	Ambient*
600	608.3	608.3	50,000 ft (1.7 psia)
	TEST 21		
600	593.4	593.9	Ambient*
600	592.1	592.7	50,000 ft
0	-2.5	-2.8	50,000 ft

*Approximately 13.2 psia

**Ormond, Inc. Model WCL-FF-35-CD-1K-2193 load cell (Serial No. 2111)

deviation data at altitude and thrust response time to rapid changes in altitude. This was done by modifying the load cell, Transducer, Inc. Model RCL-FF34-CD-600-7309 (Serial No. 4053), used. The load cell cylinder was vented to test cell pressure by drilling a No. 31 drill (0.120 inch) hole into the load cell cylinder chamber. There was no noticeable deviation in thrust between ambient and altitude for the modified load cell. Because the venting process required a certain amount of time for adjustment to altitude, temporary deviations of thrust were experienced during transient altitude conditions, as described in Appendix F, before return to normal calibration limits. Therefore, engine ignition was started at an altitude expected to yield steady state operation, but a slight deviation in thrust due to the unbalanced pressure in the load cell immediately following throttling must be assumed.

(U) A test was run with three fuel samples to evaluate the effect of 165°F temperature soak. This test was designed to measure any change in fuel characteristics by weight loss. The samples were weighed before the test at 70°F and following 24 hours exposure to 165°F in an oven. The results show that the samples lost an average of only 3 percent of their original weight. This could have been due to vaporization of volatile substances in the Plexiglas binder. Further investigation is required to determine the complete effect of 165°F temperature soak upon the fuel.

B. FLIGHT CERTIFICATION TESTS

1. Vibration Tests

(U) The vibration tests were conducted in the JPL vibration facility at Edwards AFB, as described in Appendix D. Initially, these tests were designed to determine any detrimental effects on structural integrity that might be encountered during transportation, normal handling operation, captive flight, and launch environments, but the complete testing program was not accomplished. It was immediately obvious during checkout tests at low "g" loadings that the propulsion system would never withstand the

full "g" loading planned at the various resonance frequencies. In fact, the vibration requirements were determined to be unrealistic. It was also decided that the propulsion system would never experience such extreme conditions and that the configuration being tested was not representative of the assembled missile configuration. As a missile component, the vibration requirements should have been derived separately for the propulsion system. The main results of the vibration tests were the addition of clamps and pads to the oxidizer and nitrogen plumbing to eliminate high-frequency oscillations (buzzing). These minor modifications were very effective, and each flight-weight missile at Eglin AFB was modified similarly. Figure 25 shows the position of an additional clamp to the oxidizer line in the raceway before entering the section between the oxidizer tank and the TCA. Figure 26 shows an added clamp to the oxidizer line between the oxidizer tank and the TCA.

2. Flight Certification Firings

(U) The certification test conditions are shown in Table VII. This testing phase included two 50,000-ft duty cycles, two 70,000-ft duty cycles and four 80,000-ft duty cycles. Four 80,000-ft duty cycles were conducted because they involved longer boost phases. It was thought that this would provide more information on boost-phase performance when coupled with the 70,000-ft boost-phase data. All testing was conducted at 70°F because there were not enough tests to adequately evaluate the temperature effect, and limited analyses indicated that flight-demonstration-use temperatures would not exceed this value. However, the flight-weight propulsion system was thoroughly evaluated over a large range of storage conditions.

(U) The results of the flight certification tests are summarized in Table VIII. The tabulated data are average or mean values for two or more tests of each mission type. The duration of boost-mode operation for each mission was different than originally planned, and reflected more accurate last-minute mission analyses for the flight demonstrations. The test results indicated that delivered boost thrust and 50,000-ft mission

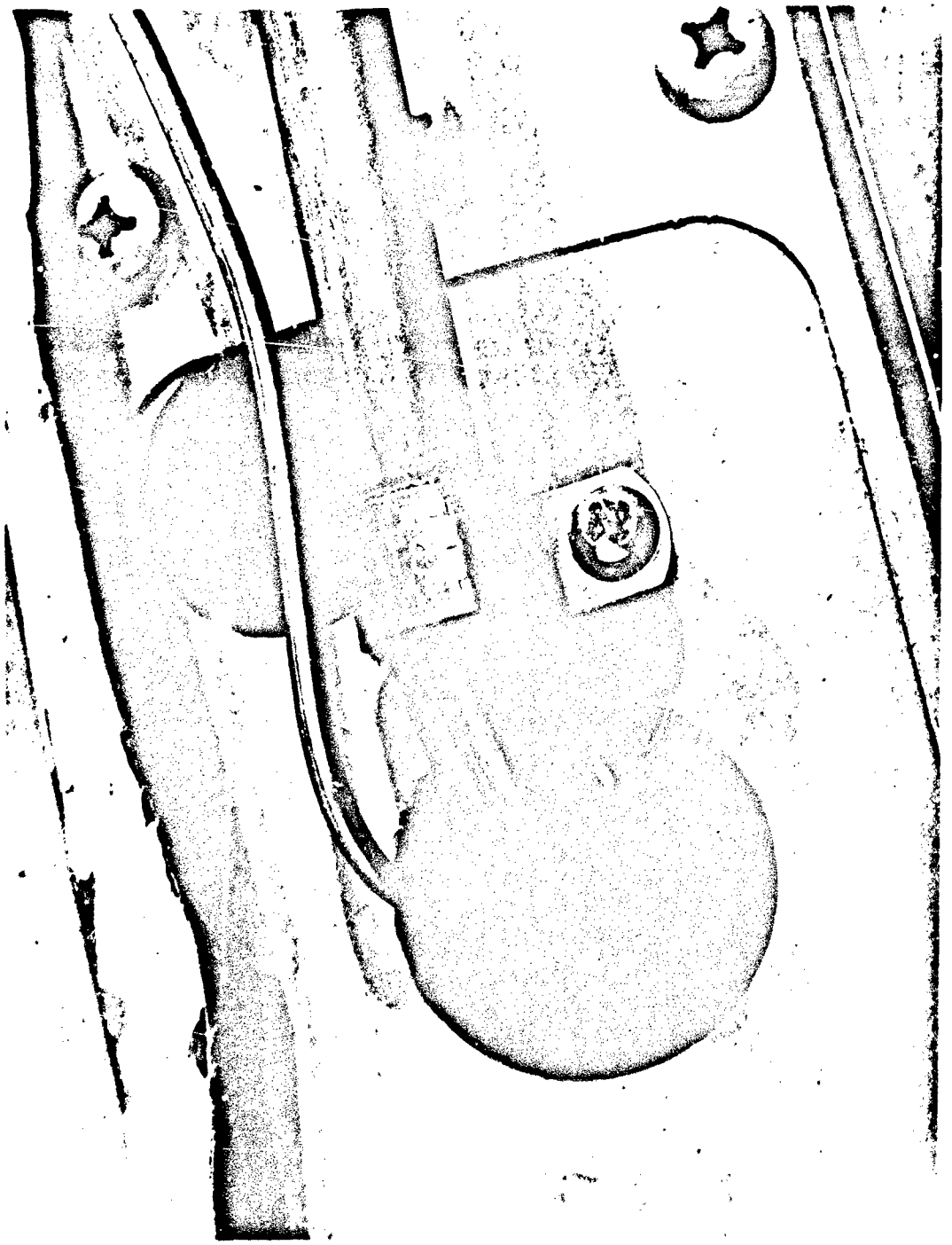

Figure 25. Antivibration Clamp, Oxidizer Line at Raceway Exit

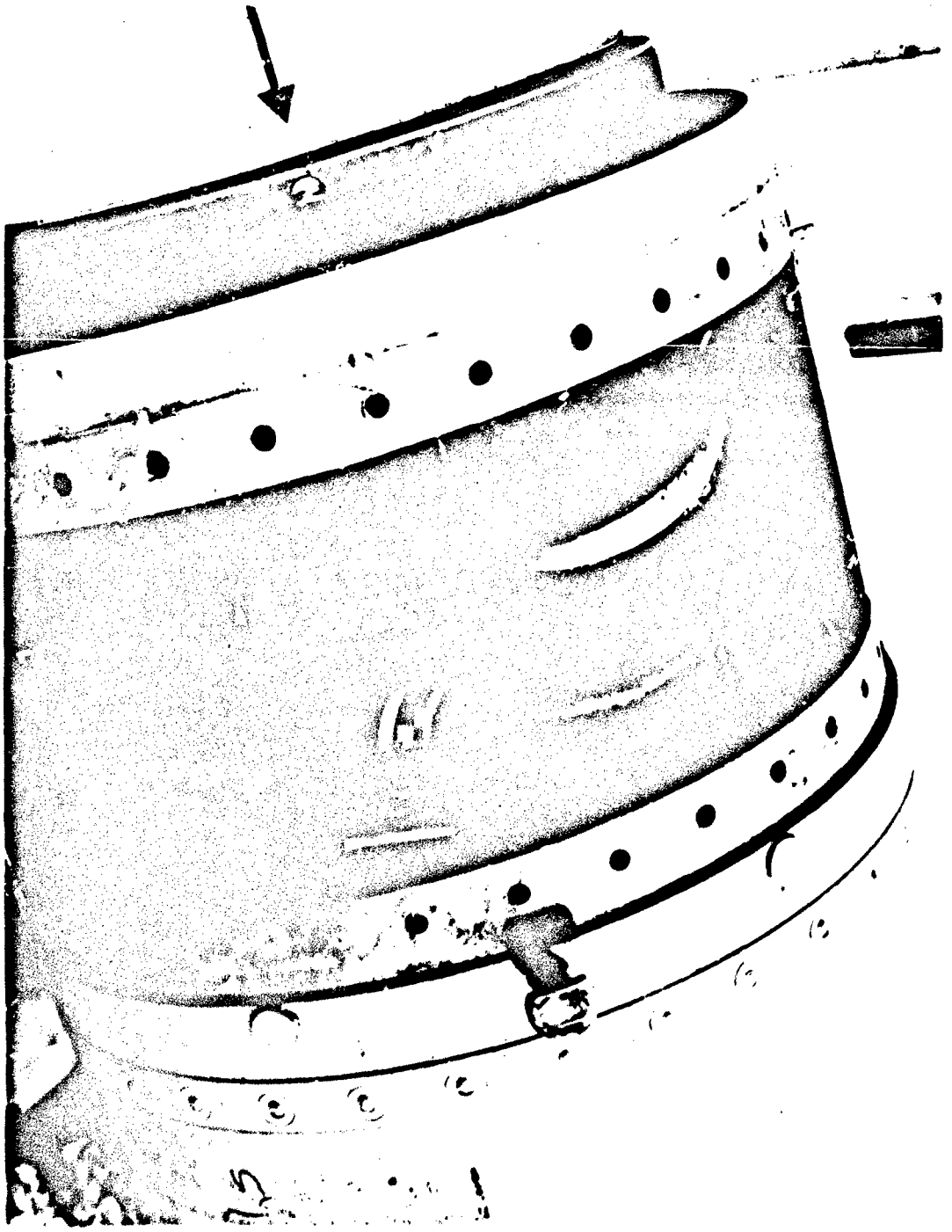

Figure 26. Antivibration Clamp, Oxidizer Line at Oxidizer Tank Bulkhead

TABLE VII. CERTIFICATION TEST CONDITIONS

Test No.	Temperature History	Simulated Duty Cycle
1F	Cycle (10 Hours at 165°F, 10 Hours at -65°F, 10 Hours at 70°F)	80,000 ft
2F	24 Hours at 70°F	80,000 ft
3F	15 Hours at 165°F and 90% Humid, 10 Hours at 70°F	70,000 ft
4F	Cycle (8 Hours at 165°F, 12 Hours at -65°F, 10 Hours at 70°F)	50,000 ft
5F	24 Hours at 70°F	70,000 ft
6F	24 Hours at 70°F	50,000 ft
7F	24 Hours at 70°F	80,000 ft
8F	24 Hours at 70°F	80,000 ft

sustain thrust levels were comparable with the UTC predictions based upon sea-level tests. However, the 70,000-ft and 80,000-ft mission sustain thrust levels were lower than anticipated by UTC, but analyses by Beech Aircraft Company predicted that the demonstration missions could still be successfully flown.

(U) The certification test data presented in the following paragraphs include engine thrust corrected for diffuser pressure differentials and corrected to mission altitude (Appendix G), chamber pressure, delivered specific impulse and specific impulse efficiency based upon corrected thrust, estimated instantaneous oxidizer flow rates (Appendix B), and predicted instantaneous fuel flow rates (Appendix C) as functions of engine burn time for each mission type.

(C) TABLE VIII. CERTIFICATION TEST PERFORMANCE SUMMARY

Duty Cycle	Average Programmed Boost Time (sec)	Average Sustain Time (sec)	**Average Nominal Boost Thrust (lb_f)	**Average Nominal Sustain Thrust (lb_f)	Average Nozzle Erosion Rate (mil/sec)	*Average Propellant Utilization (%)
50,000 ft	5	253	415	239	0.3	92%
70,000 ft	67	236	458	113	4.67	86%
80,000 ft	102	98	457	103	3.2	83%

*Based upon total propulsion system weight loss compared to initial propellant load.

**Thrust corrected to mission altitude and for nozzle base pressure effects (Appendix G).

CONFIDENTIAL

CONFIDENTIAL

a. 50,000-ft Missions (Runs 4F and 6F)

(U) Figure 27 compares the regulated oxidizer tank pressure histories for Runs 4F and 6F. Similar trends are shown, but 6F consistently ran lower in tank pressure.

(U) Run 4F: Figures 28 through 30 show the observed and estimated results for this run. The 5-sec preprogrammed boost duration barely allowed time for the propulsion system to approach full boost thrust before throttling down. The chamber pressure and thrust traces (Figure 28) indicate rising pressure and thrust due to progressive nozzle throat shrinkage from thermal soak up to 160 sec. Figure 27 indicates that oxidizer tank pressure began decaying at about 160 sec and this is reflected by dropping thrust, pressure, and oxidizer flow rate (Figure 29).

(U) Run 6F: Figures 31 through 33 depict the results of this run. Sustain chamber pressure and thrust are lower than for run 4F due to lower oxidizer tank pressure. Again, nozzle throat shrinkage drives thrust and pressure upward until about 160 sec, but in this case, oxidizer tank pressure held reasonably constant until 180 sec. The increasing thrust and decreasing pressure trends observed beyond 160 sec are due to nozzle throat erosion gradually reversing the previous decreasing throat area trend. This is evidenced by increasing oxidizer flow rates after 180 sec (Figure 32) despite decaying oxidizer tank pressure after that time. Increasing oxidizer flow rates maintain thrust through mass addition even though chamber is dropping.

(U) Run 6F was 25 sec longer than run 4F. This added duration is attributed to generally lower tank pressures and flow rates for run 6F.

UNCLASSIFIED

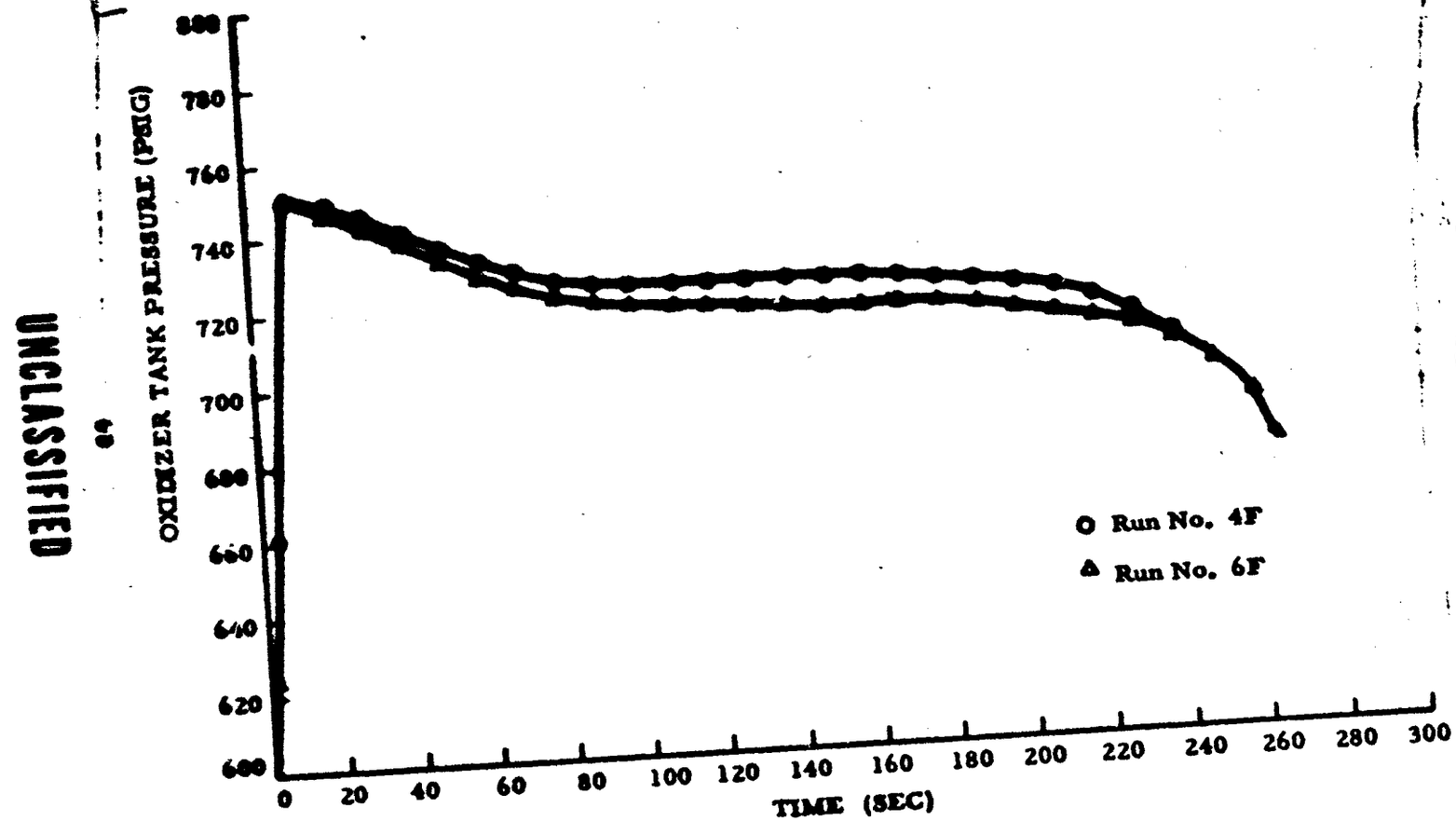

UNCLASSIFIED

Figure 27. Oxidizer Tank Pressure for 50,000-ft Missions, Runs 4F and 6F

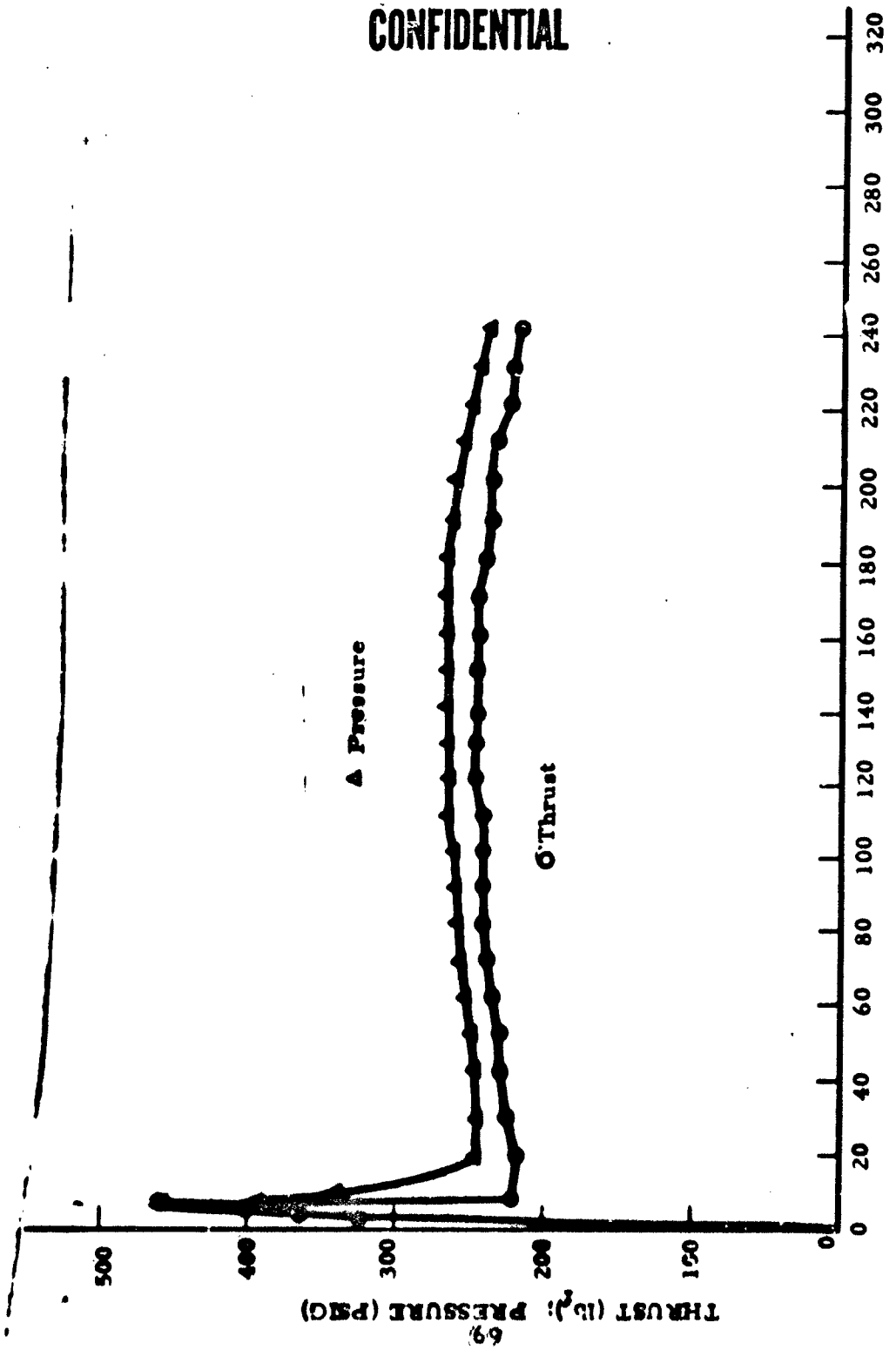

Figure 28. Thrust and Chamber Pressure versus Time, 50,000-ft Mission, Run 4F

THIS DOCUMENT CONTAINS INFORMATION AFFECTING THE NATIONAL DEFENSE OF THE UNITED STATES WITHIN THE MEANING OF THE ESPIONAGE LAWS, TITLE 18, U.S.C., SECTIONS 793 AND 794, THE TRANSMISSION OR REVELATION OF WHICH IN ANY MANNER TO AN UNAUTHORIZED PERSON IS PROHIBITED BY LAW.

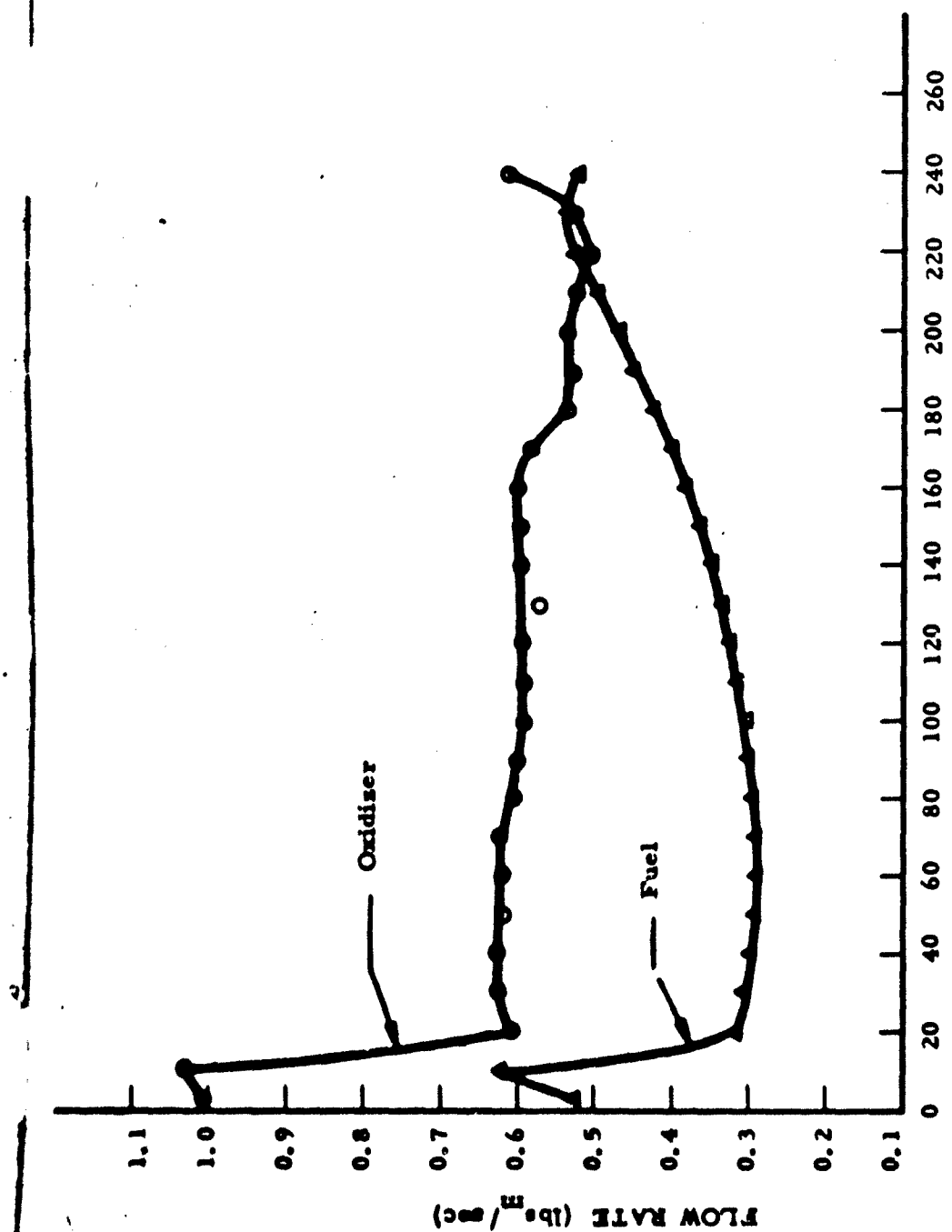

Figure 29. Oxidizer and Fuel Flow Rates; 50,000-ft Mission, Run 4F

THIS DOCUMENT CONTAINS INFORMATION AFFECTING THE NATIONAL DEFENSE OF THE UNITED STATES WITHIN THE MEANING OF THE ESPIONAGE LAWS, TITLE 18, U.S.C., SECTIONS 793 AND 794, THE TRANSMISSION OF WHICH IN ANY MANNER TO AN UNAUTHORIZED PERSON IS PROHIBITED BY LAW.

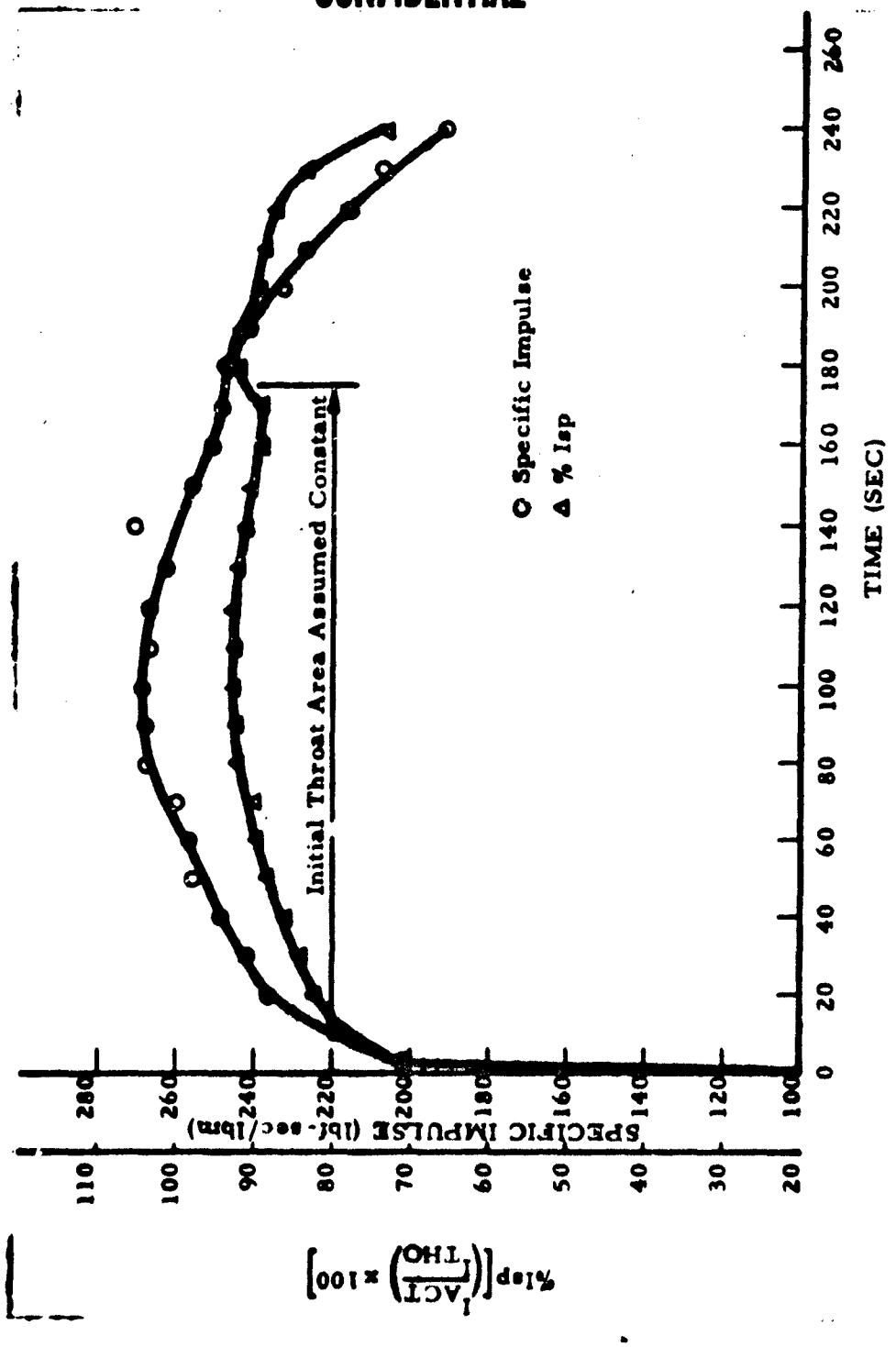

Figure 30. Isp and Isp Efficiency; 50,000-ft Mission, Run 4F

THIS DOCUMENT CONTAINS INFORMATION AFFECTING THE NATIONAL DEFENSE OF THE UNITED STATES WITHIN THE MEANING OF THE ESPIONAGE LAWS, TITLE 18, U.S.C., SECTIONS 793 AND 794, THE TRANSMISSION OR REVELATION OF WHICH IN ANY MANNER TO AN UNAUTHORIZED PERSON IS PROHIBITED BY LAW.

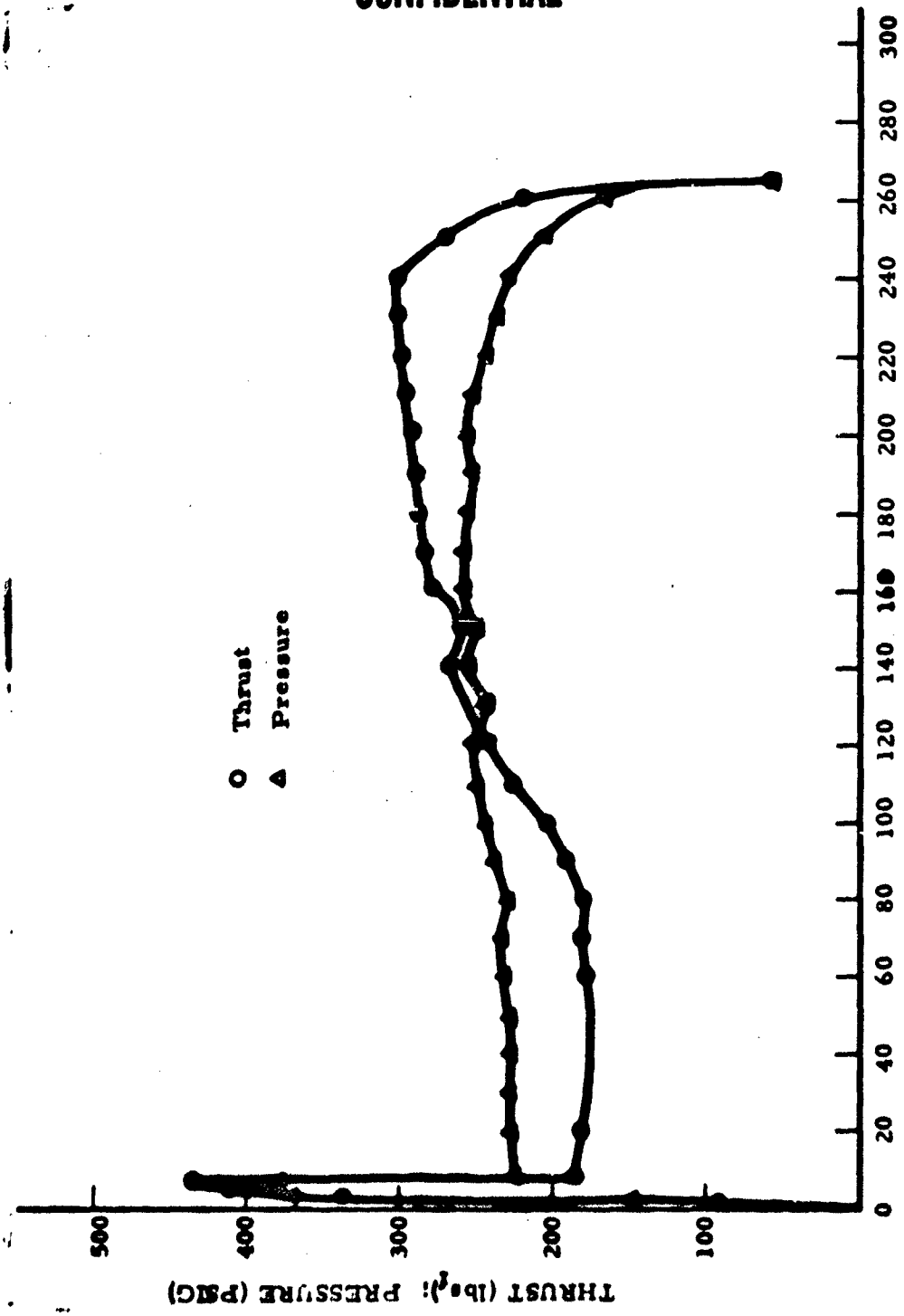

Figure 31. Thrust and Chamber Pressure versus Time; 50,000-ft Mission, Run 6F

THIS DOCUMENT CONTAINS INFORMATION AFFECTING THE NATIONAL DEFENSE OF THE UNITED STATES WITHIN THE MEANING OF THE ESPIONAGE LAWS, TITLE 18, U.S.C., SECTIONS 793 AND 794, THE TRANSMISSION OF WHICH OR THE REVELATION OF WHICH IN ANY MANNER TO AN UNAUTHORIZED PERSON IS PROHIBITED BY LAW.

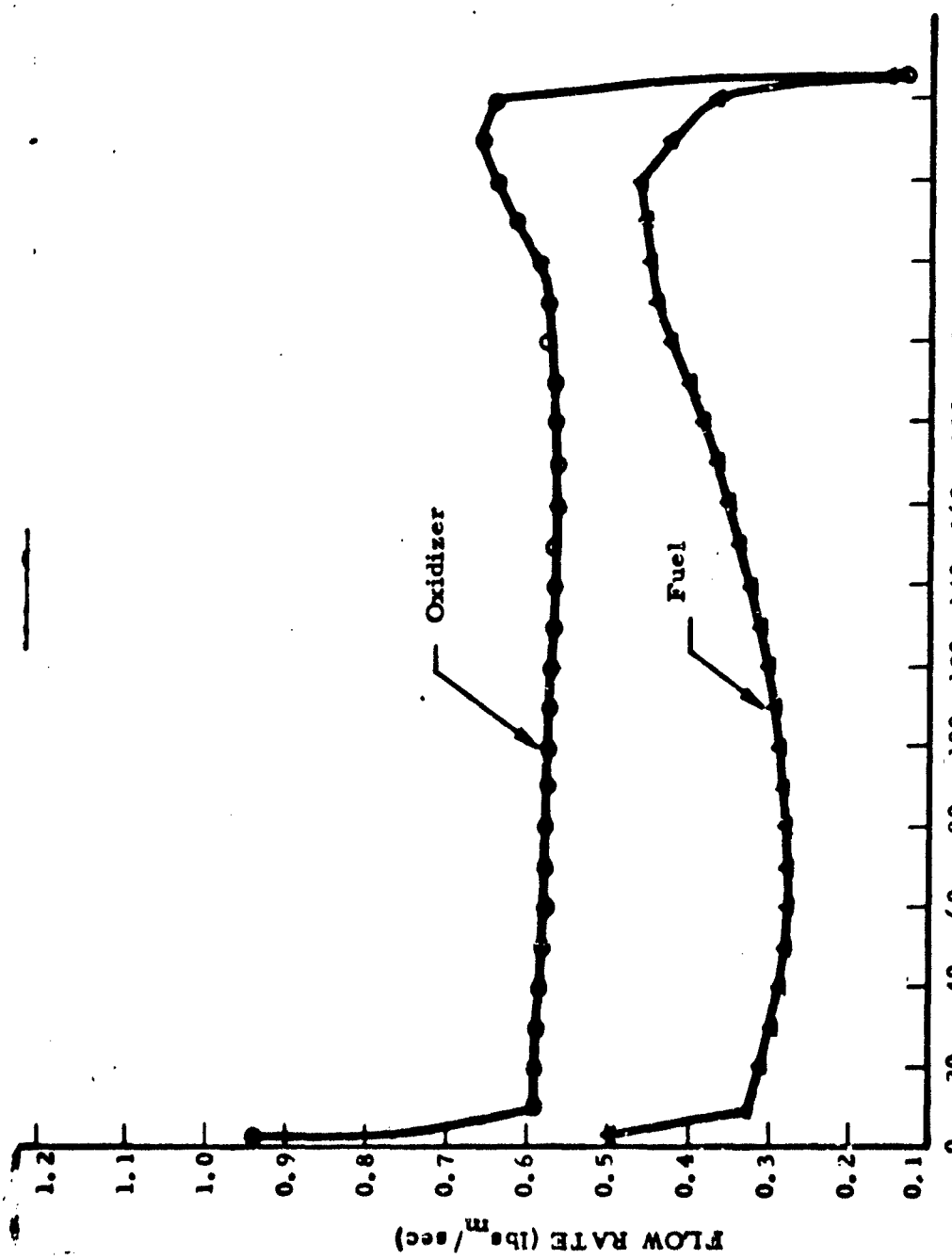

Figure 32. Oxidizer and Fuel Flow Rates; 50,000-ft Mission, Run 6F

THIS DOCUMENT CONTAINS INFORMATION AFFECTING THE NATIONAL DEFENSE OF THE UNITED STATES WITHIN THE MEANING OF THE ESPIONAGE LAWS, TITLE 18, U.S.C., SECTIONS 793 AND 794, THE TRANSMISSION OF WHICH IN ANY MANNER TO AN UNAUTHORIZED PERSON IS PROHIBITED BY LAW.

CONFIDENTIAL

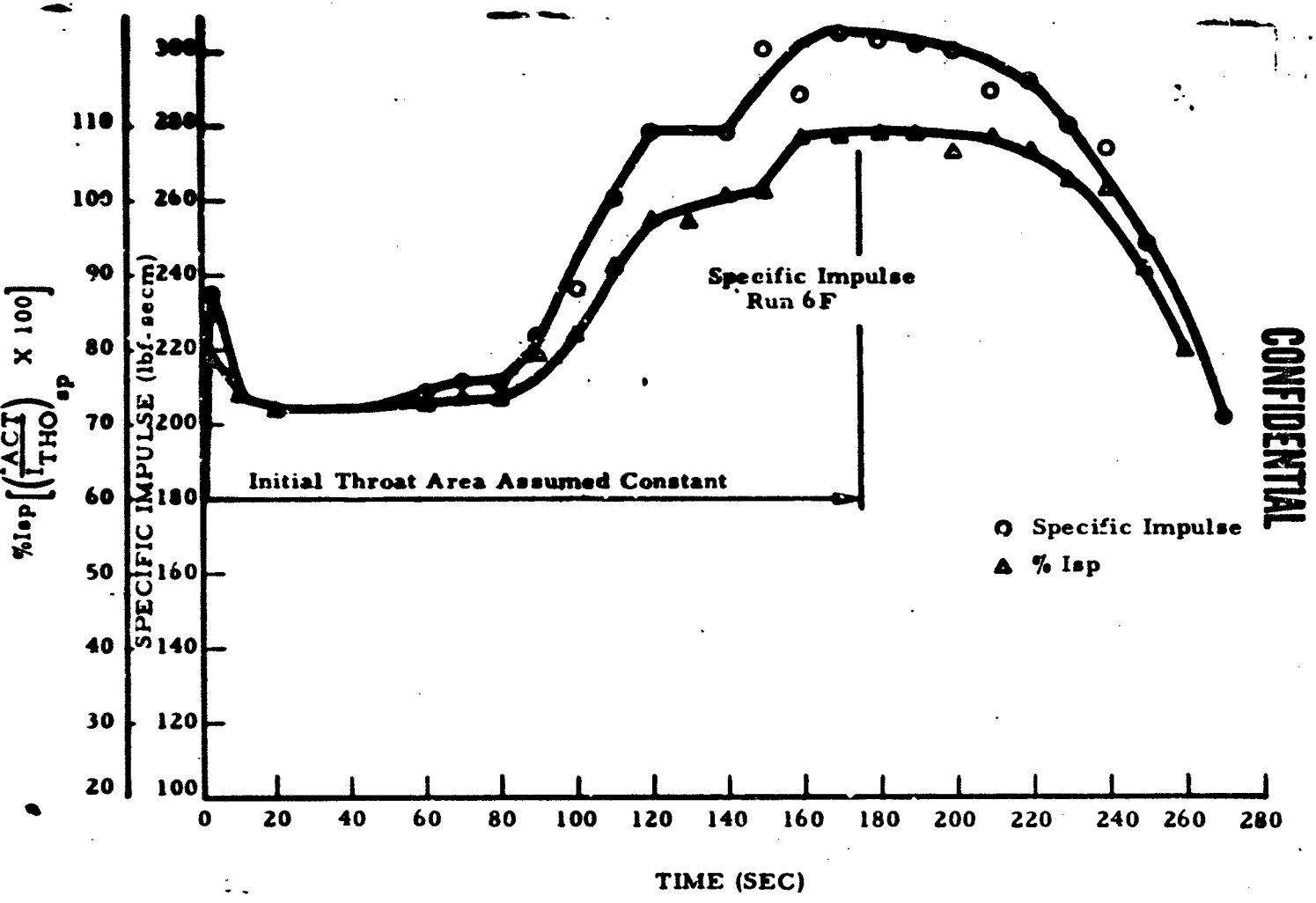

Figure 33. Isp and Isp Efficiency; 50,000-ft Mission, Run 6F

CONFIDENTIAL

b. 70,000-ft Missions (Runs 3F and 5F)

(U) Figure 34 compares the oxidizer tank pressure histories for these runs. A wide dispersion in tank pressure regulator performance can be observed. Run 3F consistently indicated 20 to 30 psi greater pressure than run 5F.

(U) Run 3F: Figures 35 through 37 show these results. The 67-sec preprogrammed boost time allows observation of boost performance characteristics from this run. No significant nozzle throat shrinkage effects are noted in boost before nozzle erosion is evidenced by dropping chamber pressure at 30 sec. Thrust is held almost constant by increased oxidizer flow despite constantly dropping chamber pressure. As seen in Figure 36, oxidizer flow rates are much more sensitive to chamber pressure in boost phase than in sustain (see Figure 32).

(U) During boost-phase operation, oxidizer flow is metered mainly by injector pressure drop, because the parallel dial-a-thrust sustain valve represents a much greater resistance path. A typical boost-phase injector pressure drop was 250 psi, and during severe nozzle erosion this rose as high as 400 psi, an increase of 60 percent. Typical water-flow pressure drops for a dial-a-thrust sustain valve are shown in Figure 38 for various mission categories. Values of about 550 psi characterize 70,000-ft missions. Further, flow rate is not very sensitive to pressure drop across the sustain valve at any setting, as shown in Figure 39. Hence, nozzle throat erosion drastically increased oxidizer flow rates during boost. High nozzle erosion rates during boost are attributed to normally high O/F ratio operation at high pressures. This is a self-aggravating situation with a blow-down type oxidizer feed system, because chamber pressure decay results in even higher O/F operation.

(U) Sustain-phase operation exhibits almost constant pressure and thrust with an indication of increasing throat erosion rate after 310 sec as evidenced by increasing thrust and oxidizer flow rate.

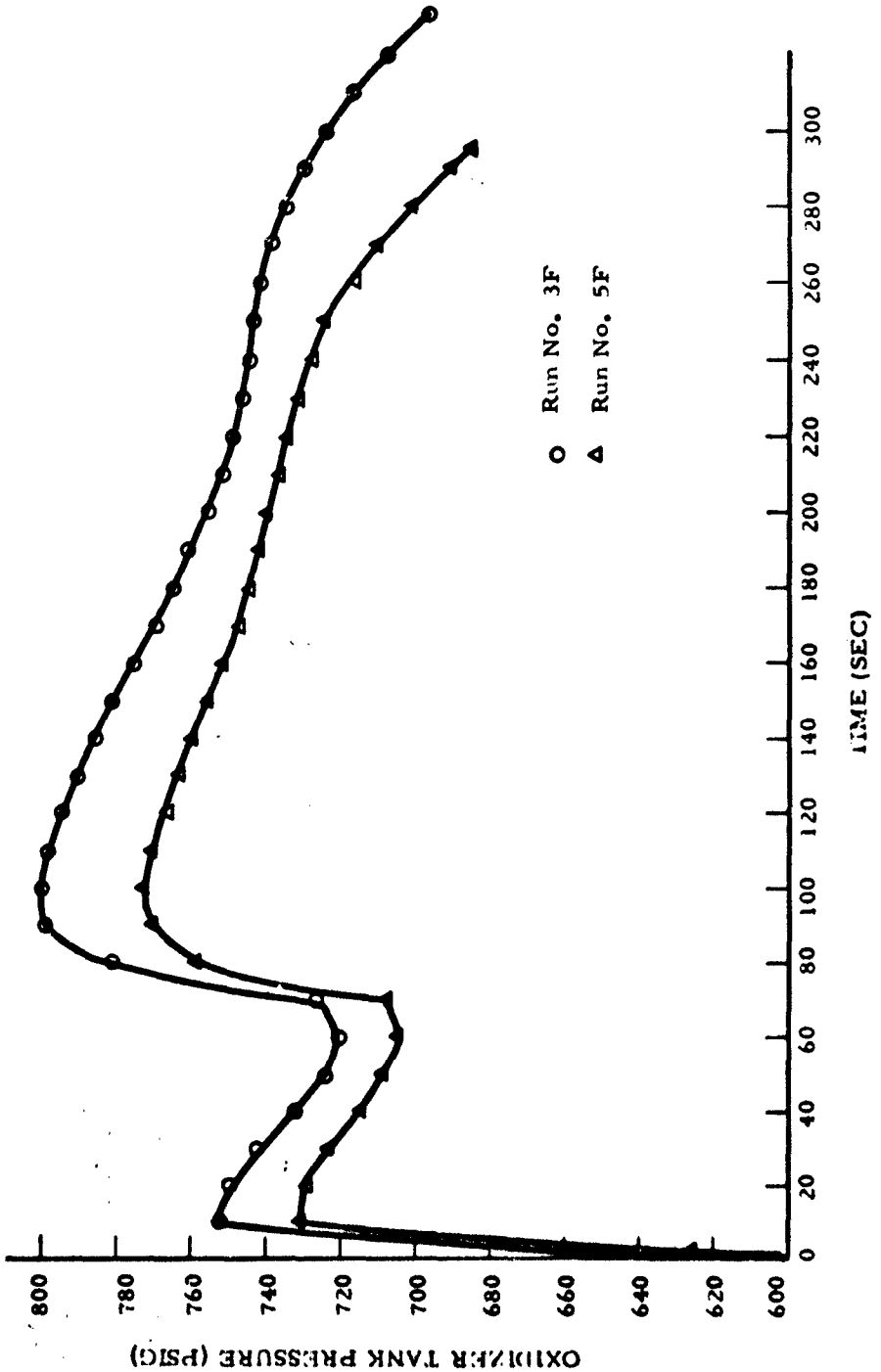

Figure 34. Oxidizer Tank Pressure for 70,000-ft Missions, Runs 3F and 5F

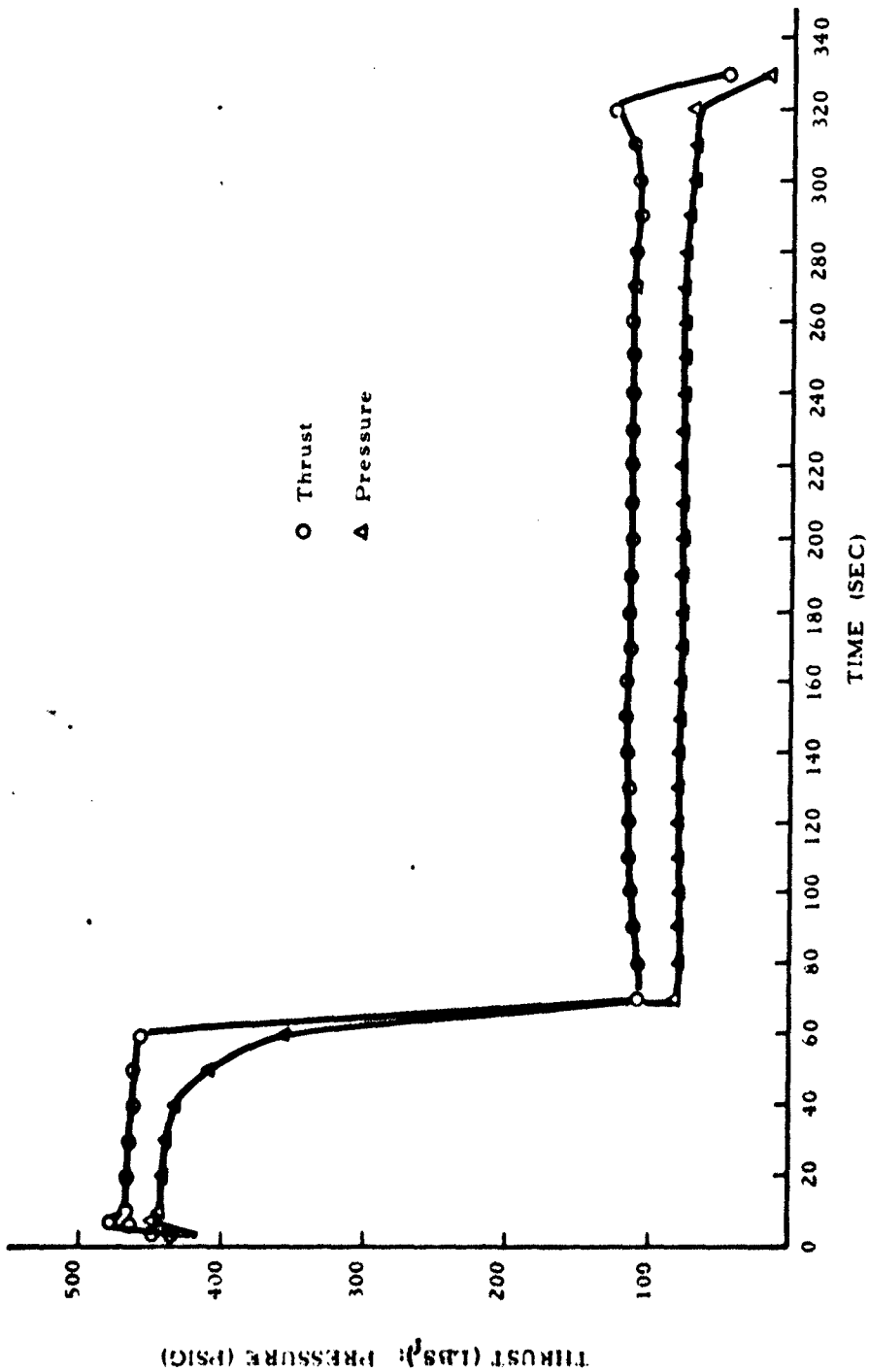

Figure 35. Thrust and Chamber Pressure versus Time for 70,000-ft Mission, Run 3F

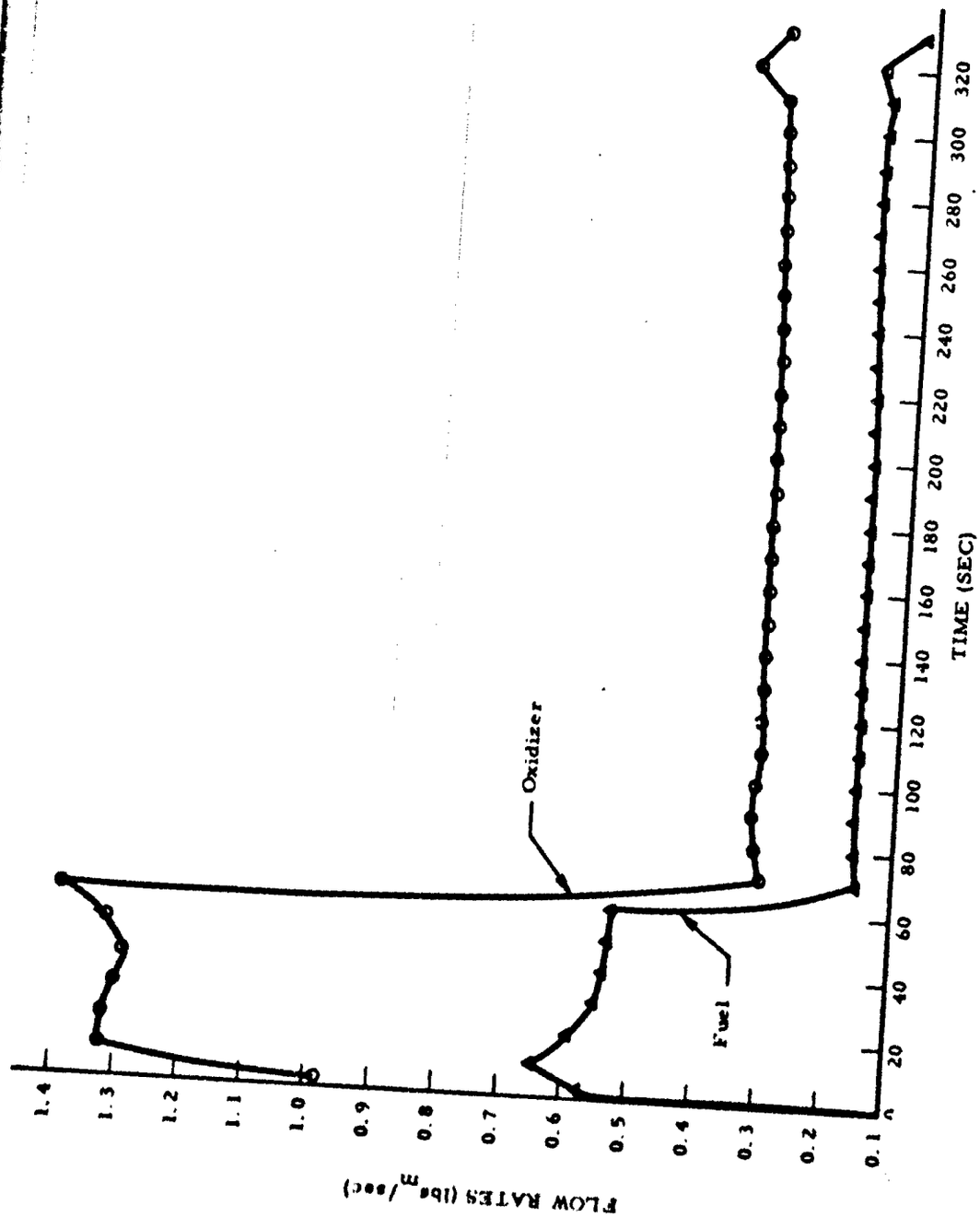

Figure 36. Oxidizer and Fuel Flow Rates; 70,000-ft Mission, Run 3F

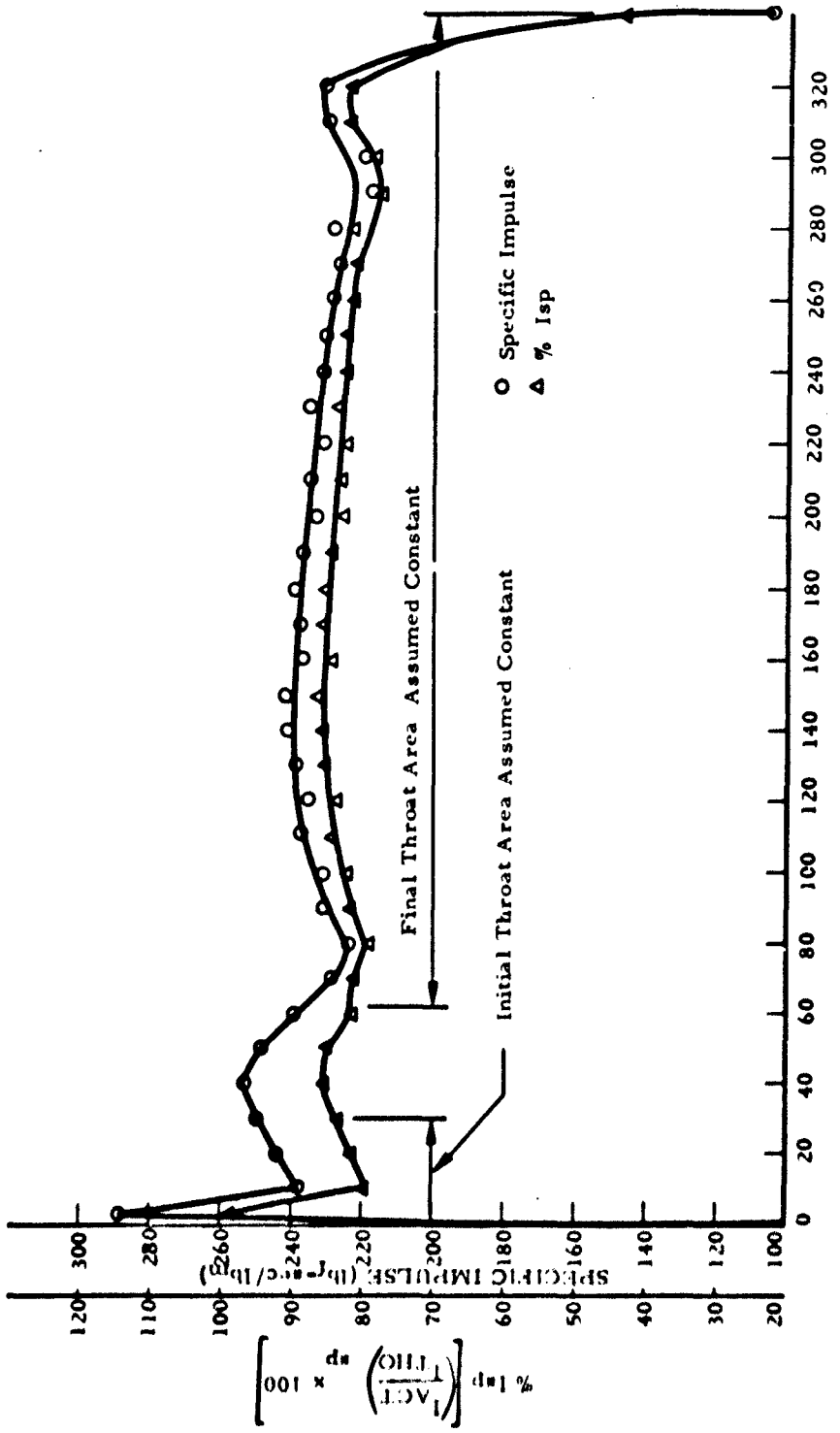

Figure 37. Isp and Isp Efficiency; 70,000-ft Mission, Run 3F

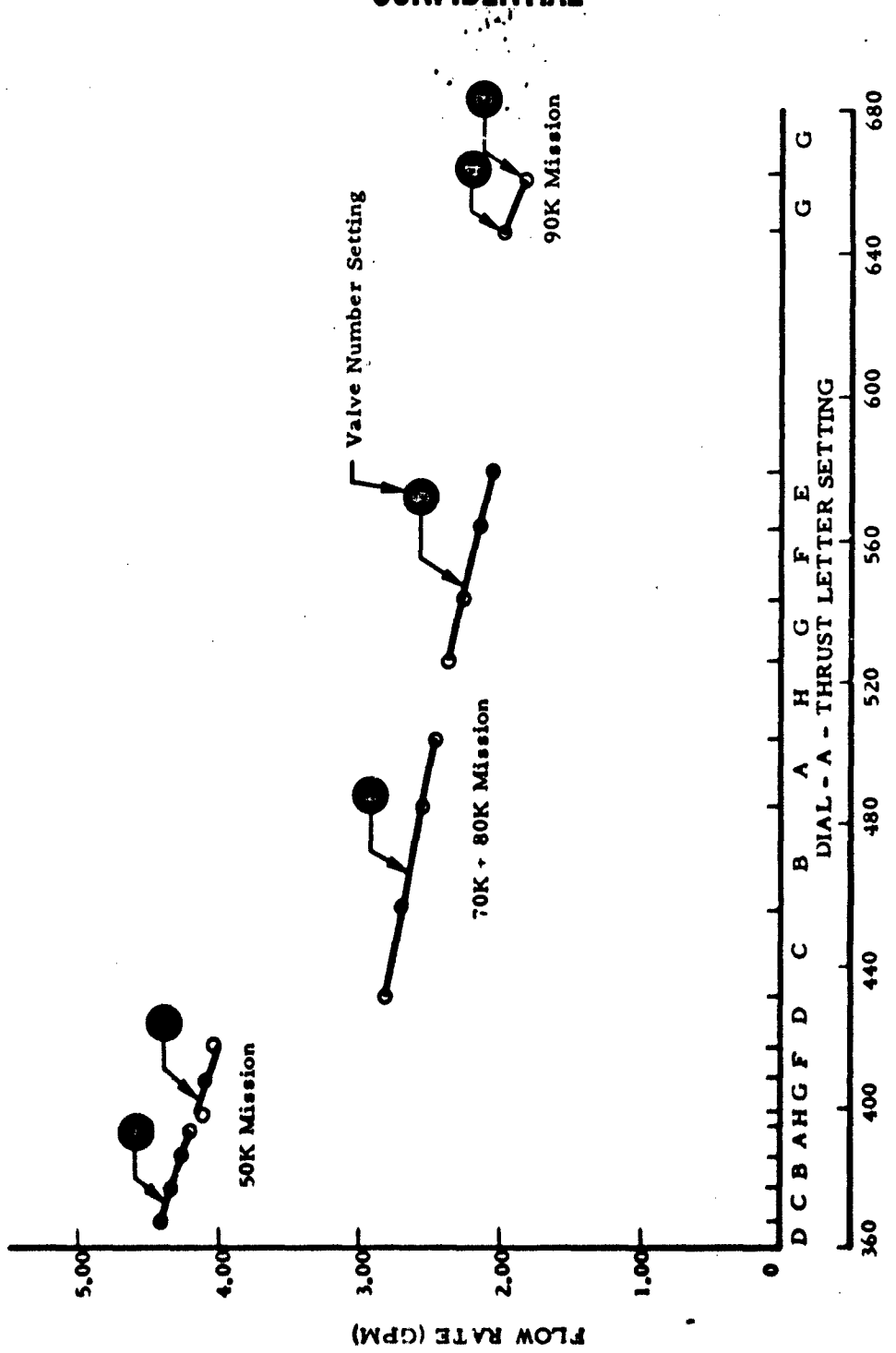

Figure 38. Typical Dial-A-Thrust Valve Flow Rate Calibration

(This page is unclassified)

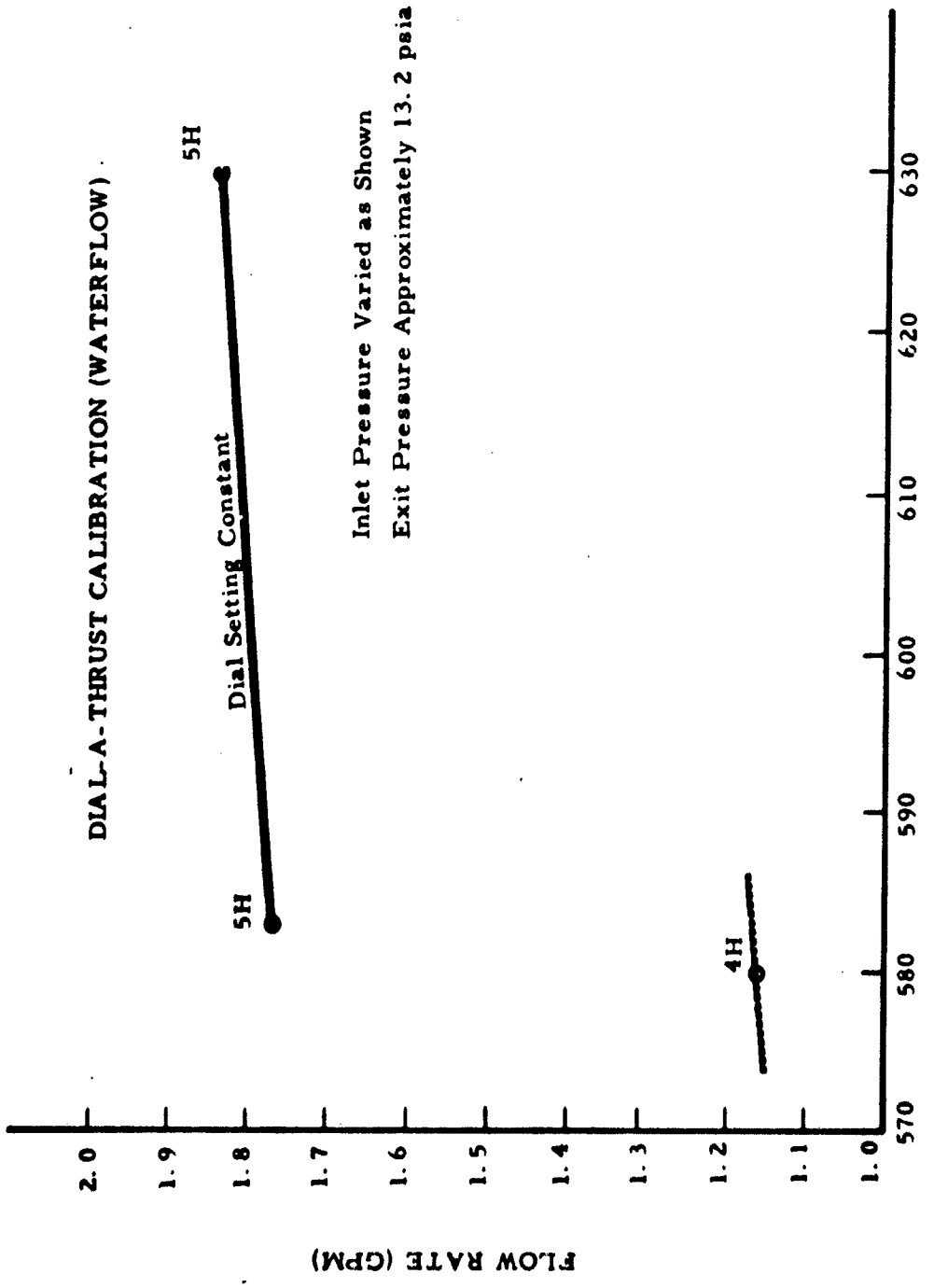

Figure 39. Typical Dial-A-Thrust Valve Sensitivity at Constant Setting

(U) Run 5F: Figures 40, 41 and 42 present these results. The lower oxidizer tank pressures observed for this run resulted in lower average O/F ratio during boost phase. However, the nozzle apparently eroded at a higher rate during boost for run 5F than for run 3F, despite the higher O/F ratios experienced in the latter case. Greater nozzle erosion in boost resulted in lower sustain chamber pressure and higher sustain oxidizer flow rates and O/F ratio for run 5F. This caused significant nozzle erosion after 180 sec as evidenced by rising oxidizer flow rates and decaying chamber pressure. Further, the higher sustain oxidizer flow rates caused oxidizer depletion 30 seconds earlier for this run. These observations identify TCA nozzle behavior as the primary factor determining resultant propulsion system performance.

c. 80,000-ft Missions (Runs 1F, 2F, 7F and 8F)

(U) Figure 43 compares the oxidizer tank pressure histories of these runs. This duty cycle exhibited the widest dispersion of tank pressure regulator performance with pressure variations up to 90 psi between tests. With the exception of run 8F, run duration appeared to vary inversely with oxidizer tank pressure.

(U) Run 1F: Figures 44 through 46 depict the results for this run. Initial tank pressure for this run was the lowest of all the 80,000-ft mission runs, and average O/F during boost was also the lowest. This apparently reduced initial nozzle erosion to the point where some throat shrinkage effects can be noted from 30 to 60 seconds with throat erosion reversing the trend thereafter (Figure 44). The oxidizer flow-rate history verifies this conclusion (Figure 45). The lower tank pressures experienced (with attendant low O/F) reduced chamber pressure decay for this run to a value lower than that experienced in either of the 70,000-ft duty cycles (runs 3F and 5F) which had boost durations 40 seconds shorter. Sustain phase exhibits almost constant pressure and thrust with some nozzle erosion indicated after about 200 seconds.

Figure 40. Thrust and Chamber Pressure versus Time; 70,000-ft Mission, Run 5F

THIS DOCUMENT CONTAINS INFORMATION AFFECTING THE NATIONAL DEFENSE OF THE UNITED STATES WITHIN THE MEANING OF THE ESPIONAGE LAWS, TITLE 18, U.S.C., SECTION 793 AND 794, THE TRANSMISSION OF WHICH IN ANY MANNER TO AN UNAUTHORIZED PERSON IS PROHIBITED BY LAW.

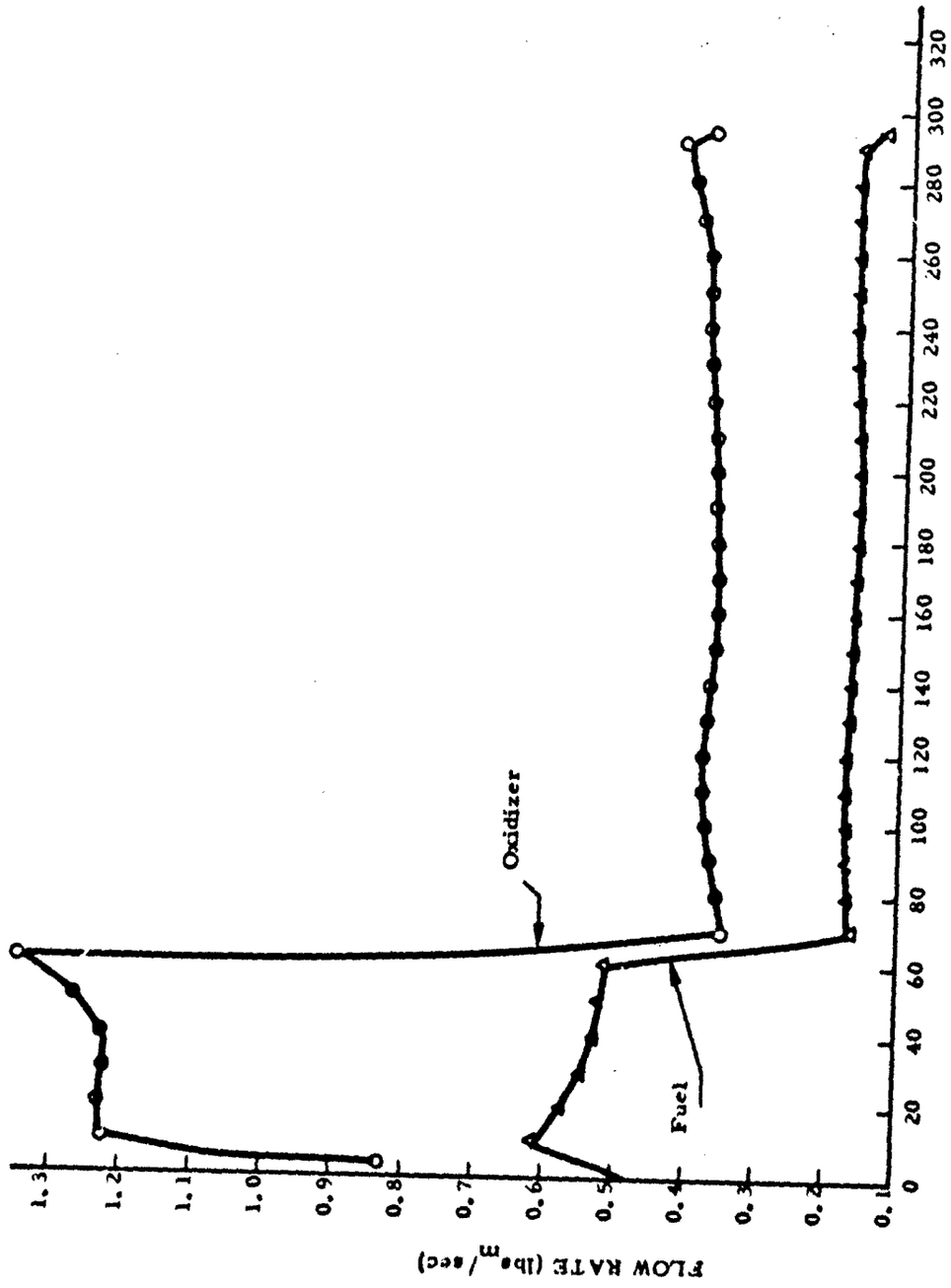

Figure 41. Oxidizer and Fuel Flow Rates; 70,000-ft Mission, Run 5F

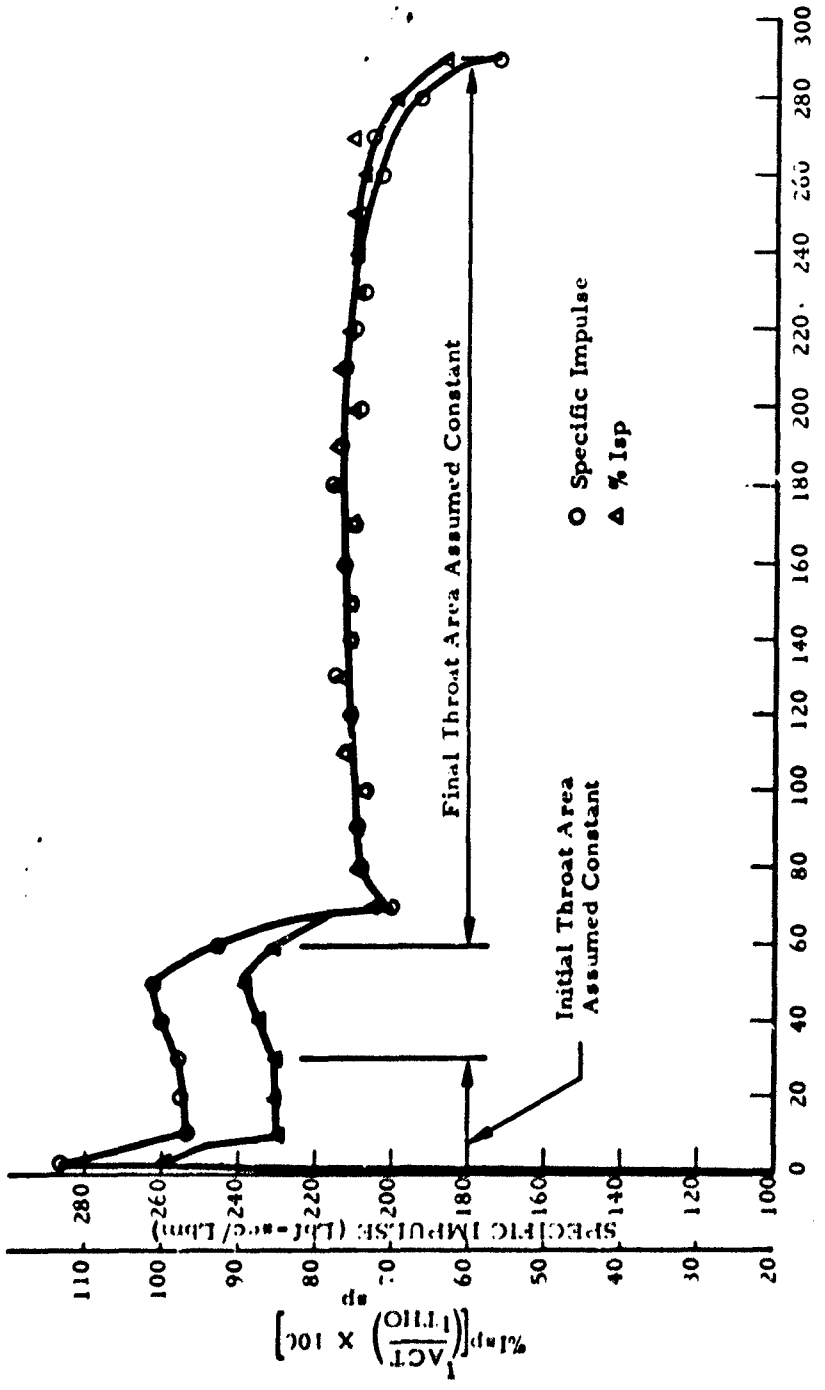

Figure 42. Isp and Isp Efficiency; 70,000-ft Mission, Run 5F

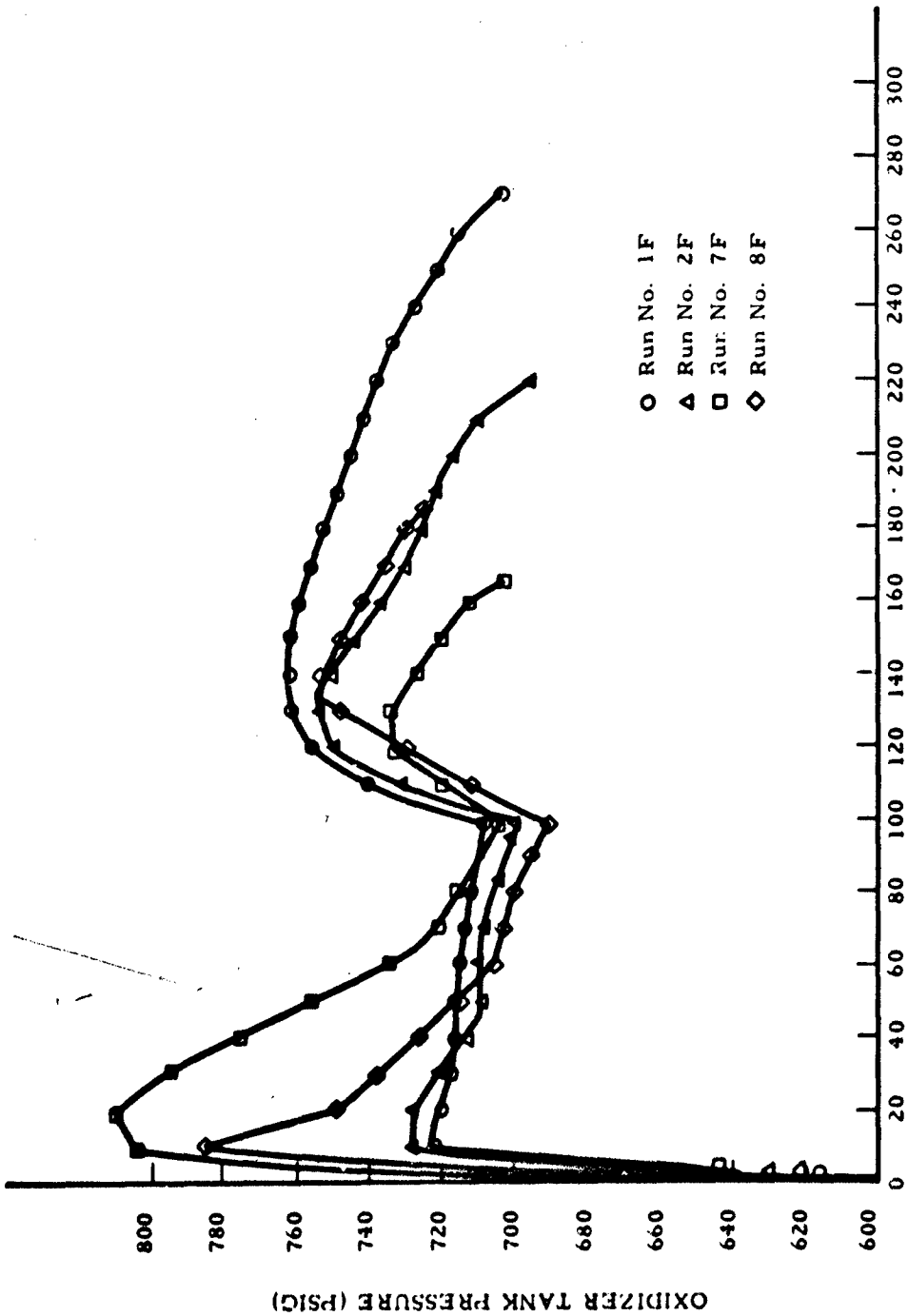

Figure 43. Oxidizer Tank Pressure for 80,000-ft Missions; Runs 1F, 2F, 7F and 8F

(This page is unclassified)

Figure 44. Thrust and Chamber Pressure versus Time; 80,000-ft Mission, Run 1F

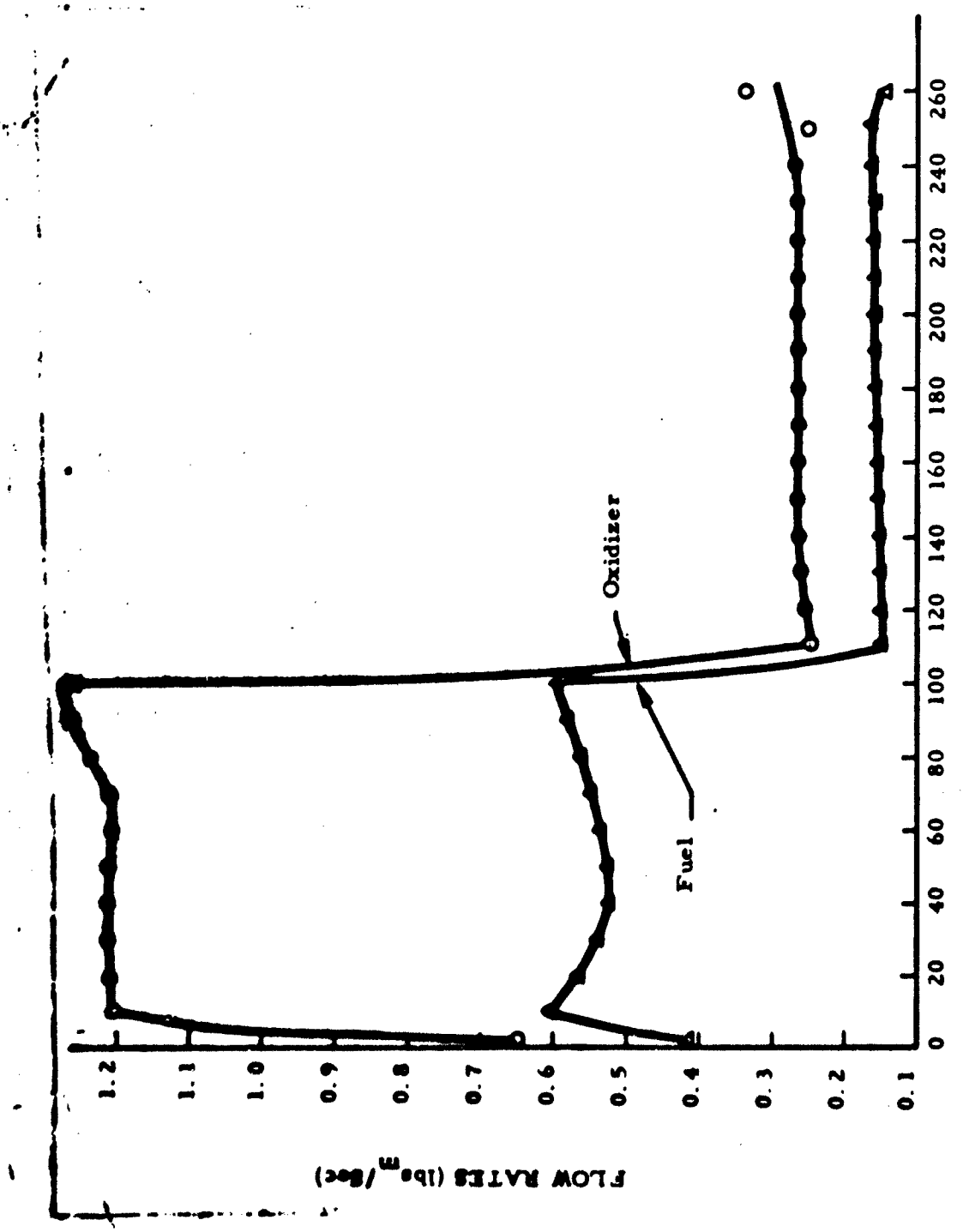

Figure 45. Oxidizer and Fuel Flow Rates; 80,000-ft Mission, Run 1F

THIS DOCUMENT CONTAINS INFORMATION AFFECTING THE NATIONAL DEFENSE OF THE UNITED STATES WITHIN THE MEANING OF THE ESPIONAGE LAWS, TITLE 18, U.S.C., SECTIONS 793 AND 794. THE TRANSMISSION OF WHICH IN ANY MANNER TO AN UNAUTHORIZED PERSON IS PROHIBITED BY LAW.

CONFIDENTIAL

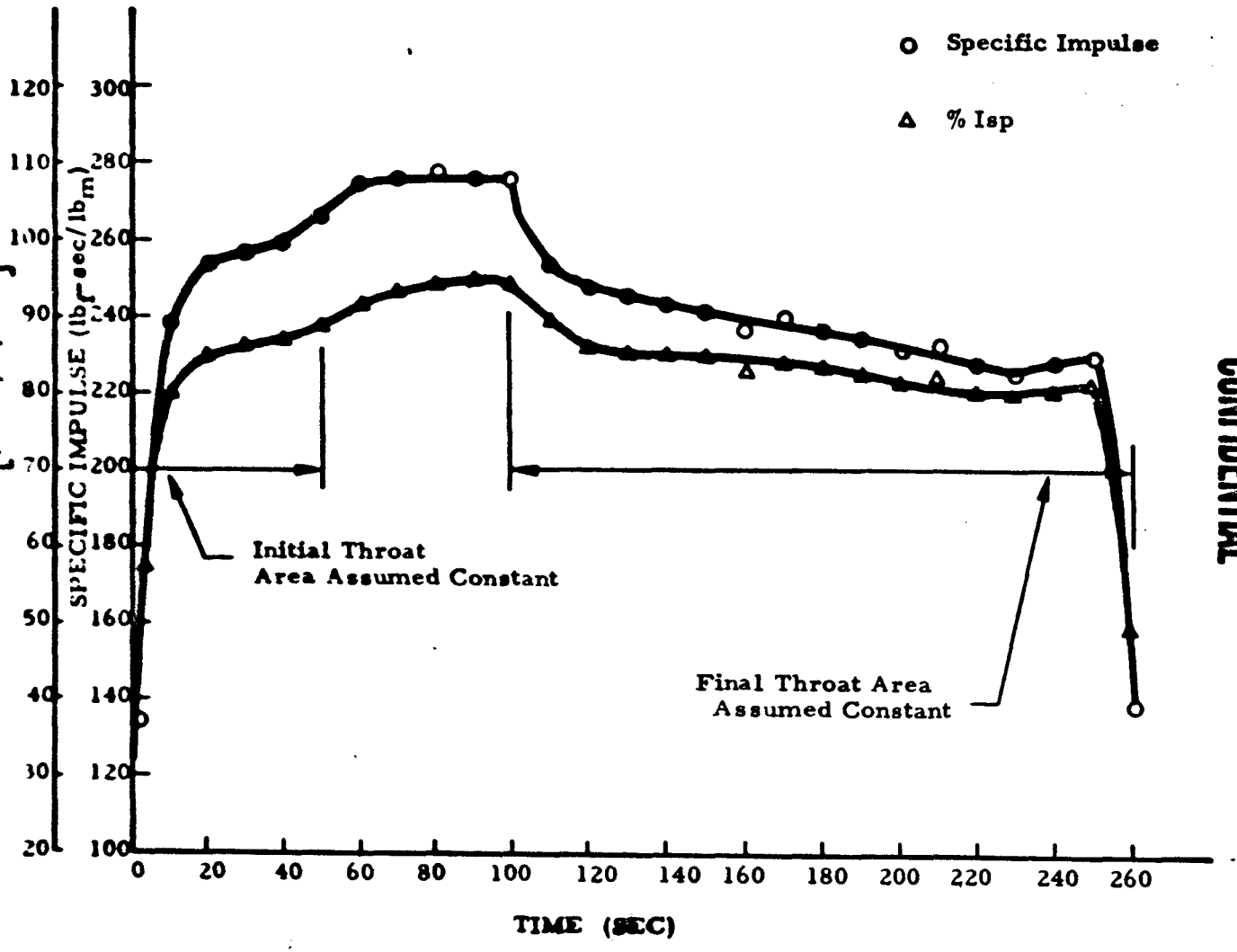

Figure 46. Isp and Isp Efficiency; 80,000-ft Mission, Run 1F

CONFIDENTIAL

(U) Run 2F: Figures 47 and 48 present the results of this test. Reliable thrust data was not obtained for this run. The chamber pressure data indicate initial pressure levels comparable with Run 1F until about 20 seconds. Initial oxidizer flow rates and attendant O/F ratio are higher than for Run 1F because of the slightly higher oxidizer tank pressure for this run. At about 20 seconds, oxidizer tank pressure began to decay to levels below that for Run 1F for the remainder of the firing. Since the oxidizer flow rates remained almost constant during boost, nozzle erosion, beginning at about 20 seconds, apparently offset the decaying tank pressure by dropping chamber pressure. Nozzle erosion was less severe than for Run 1F, however, as evidenced by slightly higher chamber pressure at the end of boost. Sustain phase indicates relatively constant pressure with some additional nozzle erosion causing a gradual rise in oxidizer flow rate. The shorter duration for this run is attributed to the higher oxidizer flow rates experienced as compared to Run 1F. The oxidizer flow rate during sustain phase for this run was high despite lower oxidizer tank pressure than for Run 1F and lower nozzle throat erosion. This occurrence could not have been due to improper dial-a-thrust valve setting, because these settings were double-checked before each test. No explanation other than malfunction or erroneous calibration of the dial-a-thrust valve has been found for this behavior.

(U) Run 7F: Figures 49 through 51 depict these results. As indicated in Figure 43, this run experienced the highest boost-phase oxidizer tank pressure of the 80,000-ft mission tests. The thrust and chamber pressure history (Figure 49) shows severe nozzle erosion starting almost immediately. This was undoubtedly caused by the high initial O/F due to high oxidizer tank pressure. Increased oxidizer flow rates maintained thrust level, but resulted in premature shutdown after only 150 sec. This run identified the oxidizer tank pressure regulator as the second most critical propulsion system component in achieving reproducible performance.

(This page is unclassified)

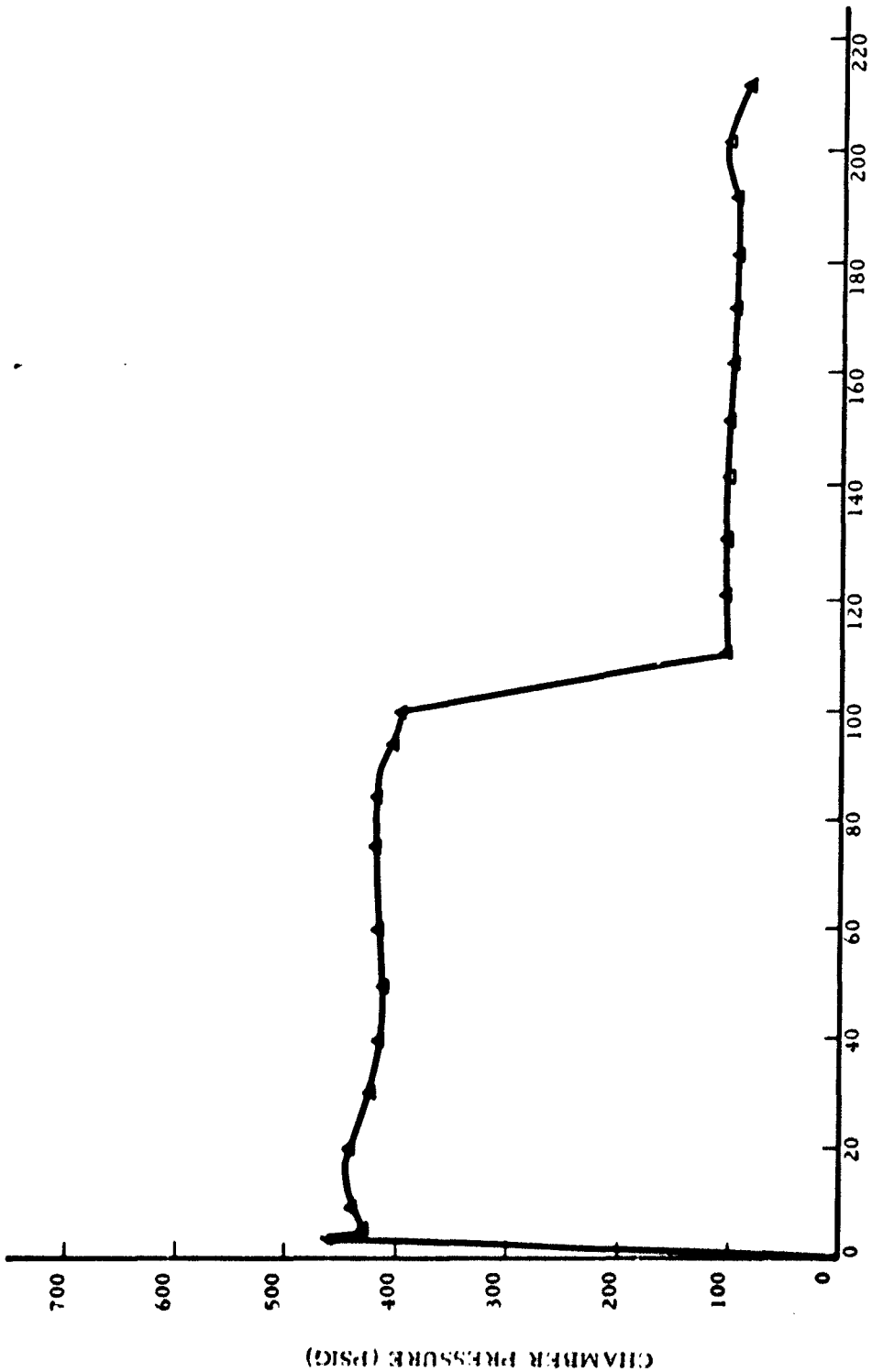

Figure 47. Chamber Pressure versus Time; 80,000-ft Mission, Run 2F

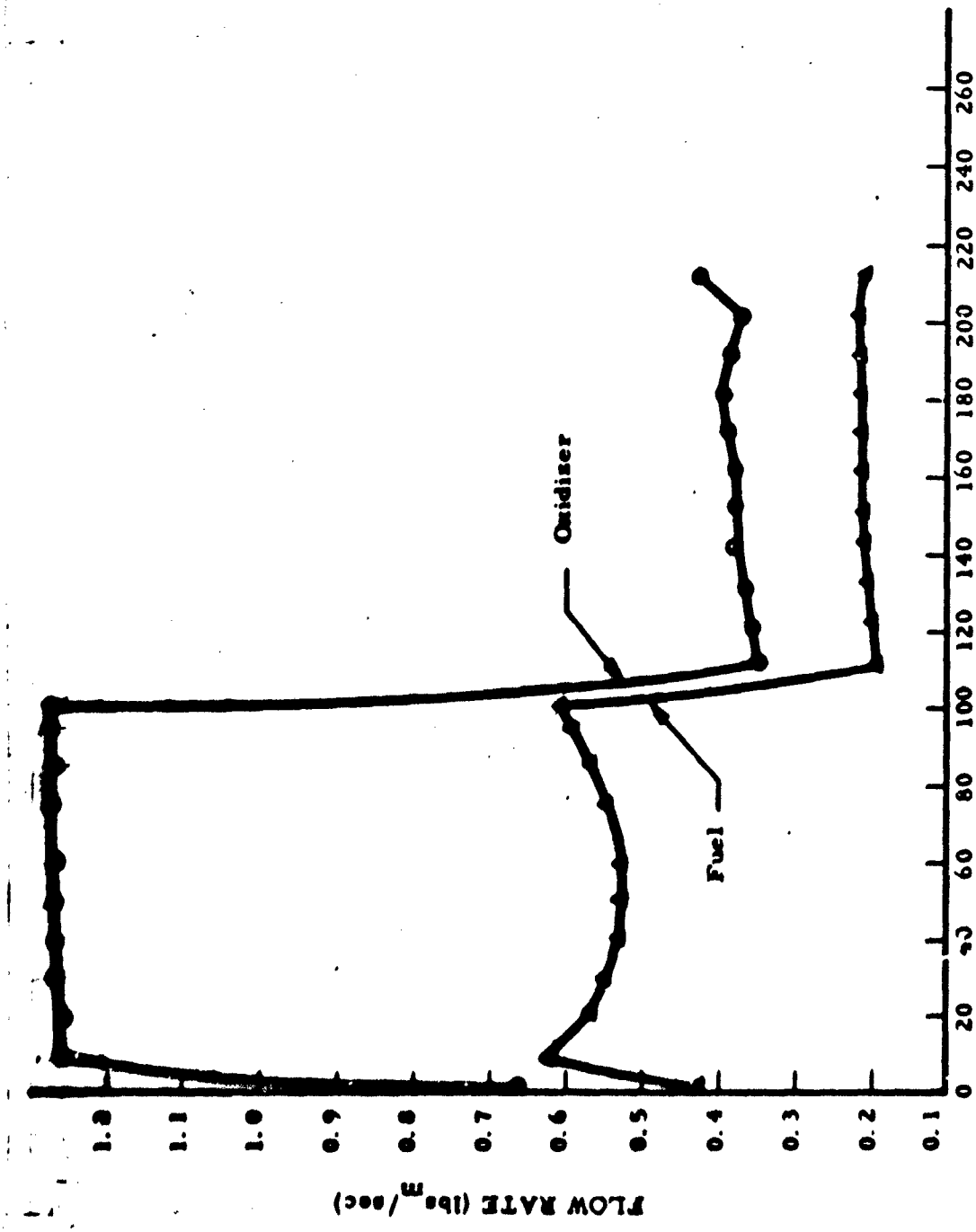

Figure 48. Oxidizer and Fuel Flow Rates; 80,000-ft Mission, Run 2F

This document contains information affecting the national defense of the United States within the meaning of the Espionage laws, Title 18, U.S.C., Section 793 and 794, the transmission of which in any manner to an unauthorized person is prohibited by law.

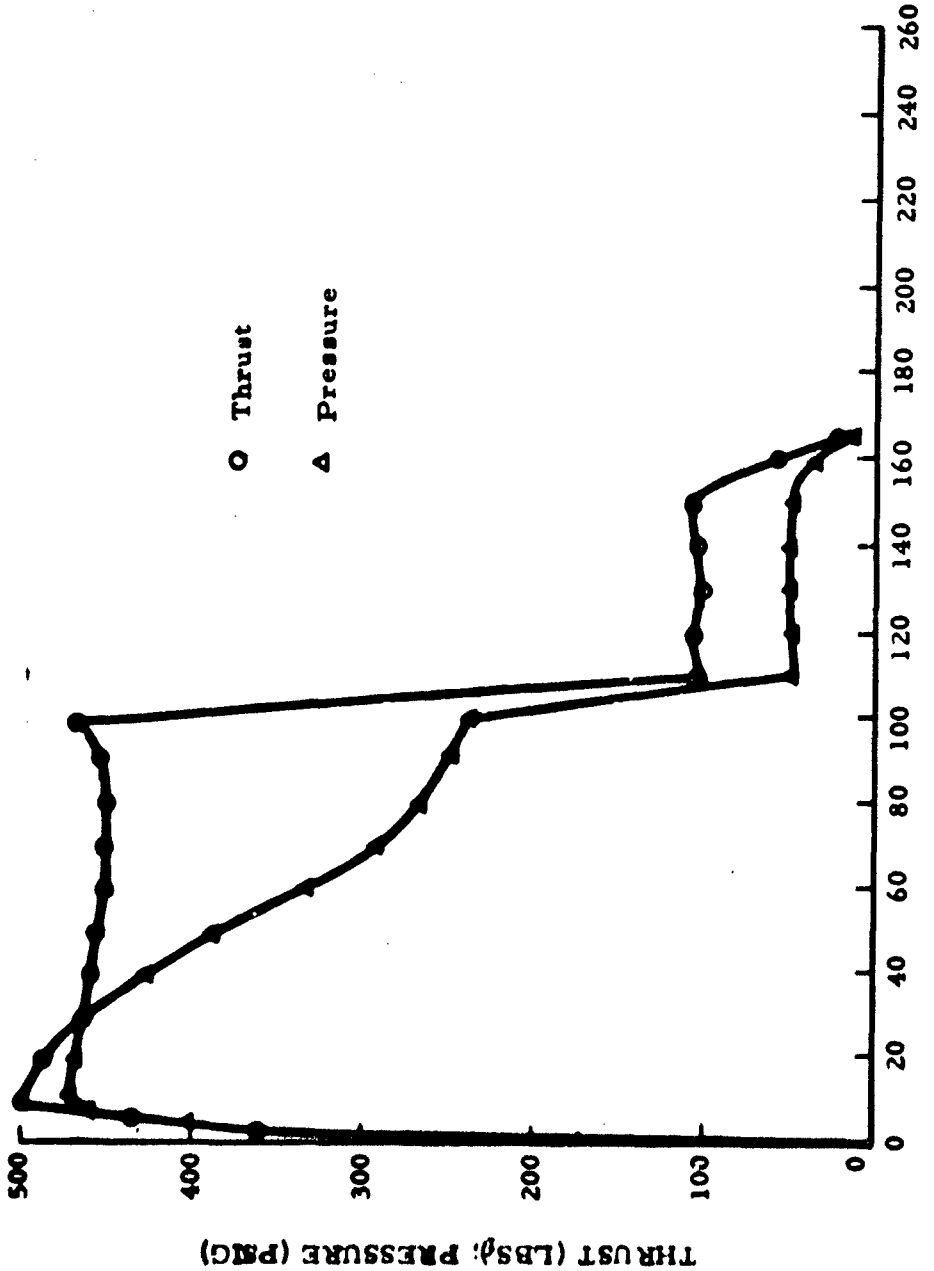

Figure 49. Thrust and Chamber Pressure versus Time; 80,000-ft Mission, Run 7F

This document contains information affecting the national defense of the United States within the meaning of the Espionage Laws, Title 18, U.S.C., Sections 793 and 794. the transmission of which in any manner to an unauthorized person is prohibited by law.

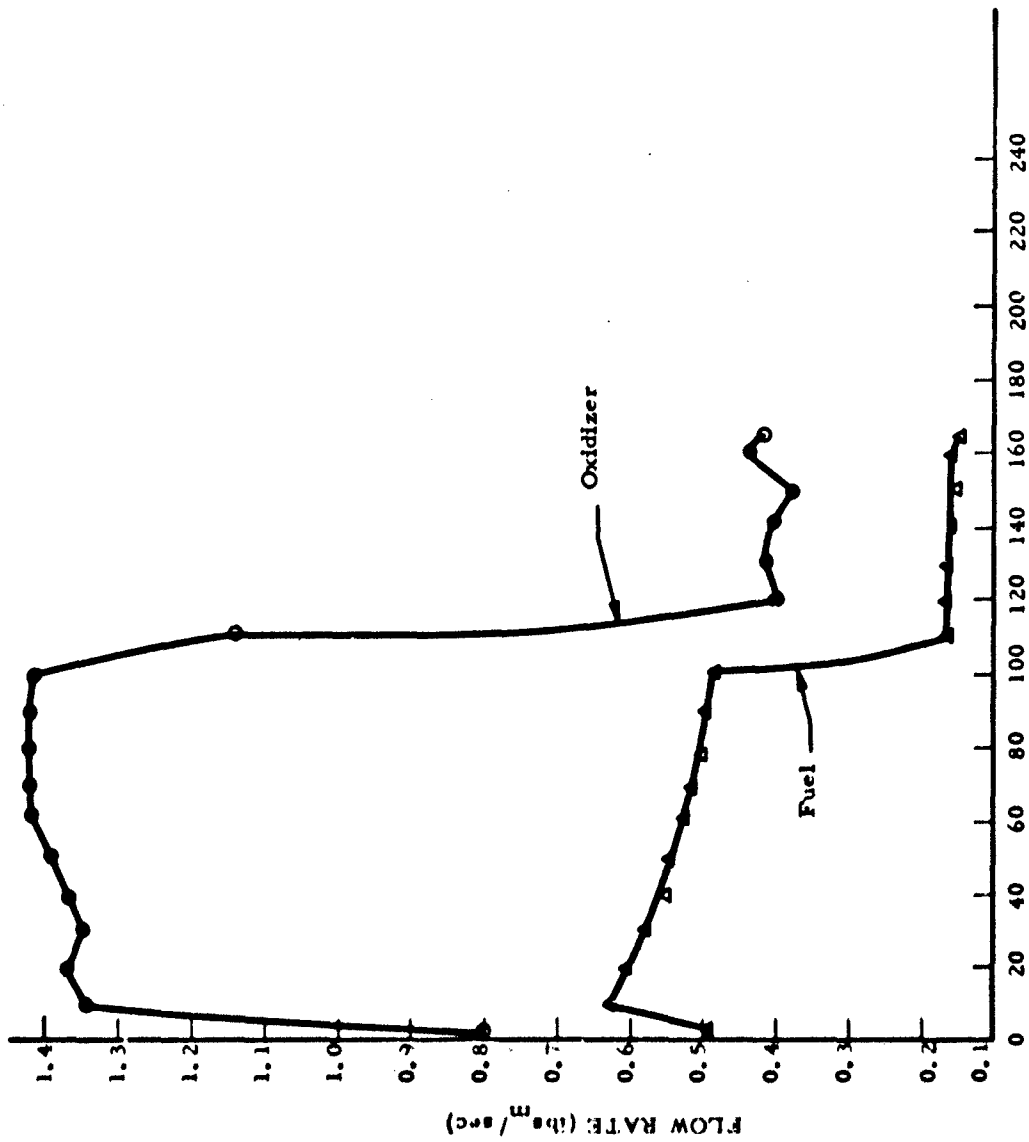

Figure 50. Oxidizer and Fuel Flow Rates; 80,000-ft Mission, Run 7F

CONFIDENTIAL

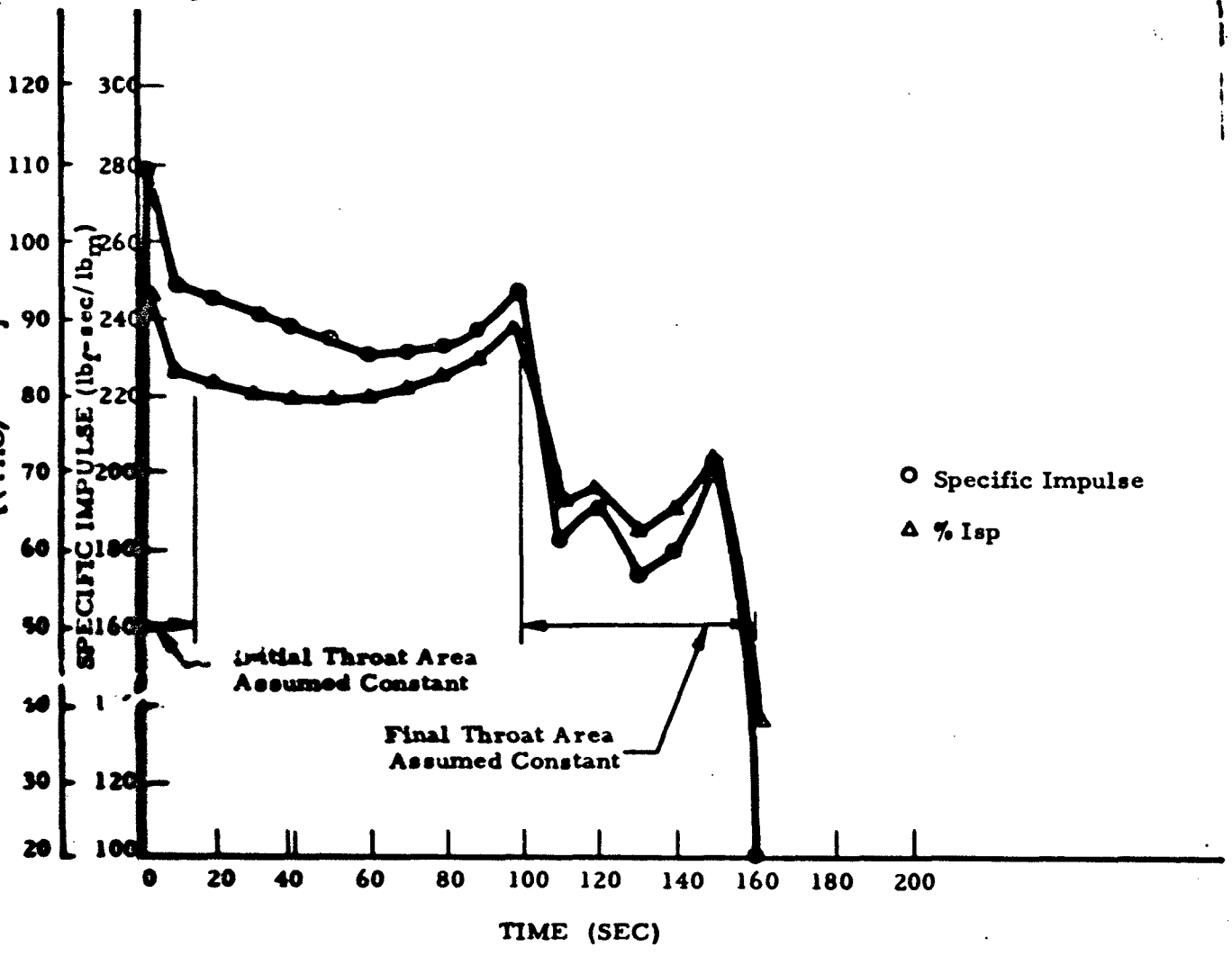

Figure 51. Isp and Isp Efficiency; 80,000-ft Mission, Run 7F

CONFIDENTIAL

(U) Run 8F: Figures 52 through 54 present these results. The thrust and chamber pressure trends are very similar to those of Run 7F, which would be expected, because this test displayed the second highest initial oxidizer tank pressure during boost (Figure 43). The slightly lower initial boost O/F ratios delayed the onset of severe nozzle erosion until about 20 seconds. The higher oxidizer flow rates accompanying nozzle erosion tended to maintain thrust level, but reduced system burn time to 170 seconds.

d. Isp and Isp Efficiency Data

(U) The Isp and Isp efficiency data reduced from the certification tests are presented without specific comments for each test, because these parameters were based upon assumed nozzle throat area histories and estimated instantaneous propellant flow rates. Hence, these data are the least accurate of those presented. The Isp trends indicated should be reasonable approximations of engine performance. However, in many cases the Isp efficiency plots very closely approach, and in some cases exceed, theoretical limits. This is due to discrepancies between the assumed nozzle throat area histories used to calculate the theoretical maximum performance for each set of test conditions and the actual (unknown) values which existed. As interpreted from the chamber pressure and thrust data, nozzle throat shrinkage gradually offset by nozzle erosion is evident, but data reduction for Isp efficiency assumed constant nozzle throat area for initial time increments which varied for each test. Obviously, this procedure introduced considerable Isp efficiency errors, but the actual throat area history was impossible to obtain.

e. Nozzle and TCA Case Skin Temperatures

(U) Figure 55 depicts the nozzle and TCA case skin temperatures observed during 70,000-ft mission Run 3F. Similar data was taken for all of the certification tests, but the 70,000-ft mission test data gave the highest readings due to the long duration for this duty cycle. Figure 55 illustrates the maximum temperatures observed during hot firing. Maximum

(This page is unclassified)

THIS DOCUMENT CONTAINS INFORMATION AFFECTING THE NATIONAL DEFENSE OF THE UNITED STATES WITHIN THE MEANING OF THE ESPIONAGE LAWS, TITLE 18, U.S.C., SECTION 793 AND 794, THE TRANSMISSION OR REVELATION OF WHICH IN ANY MANNER TO AN UNAUTHORIZED PERSON IS PROHIBITED BY LAW.

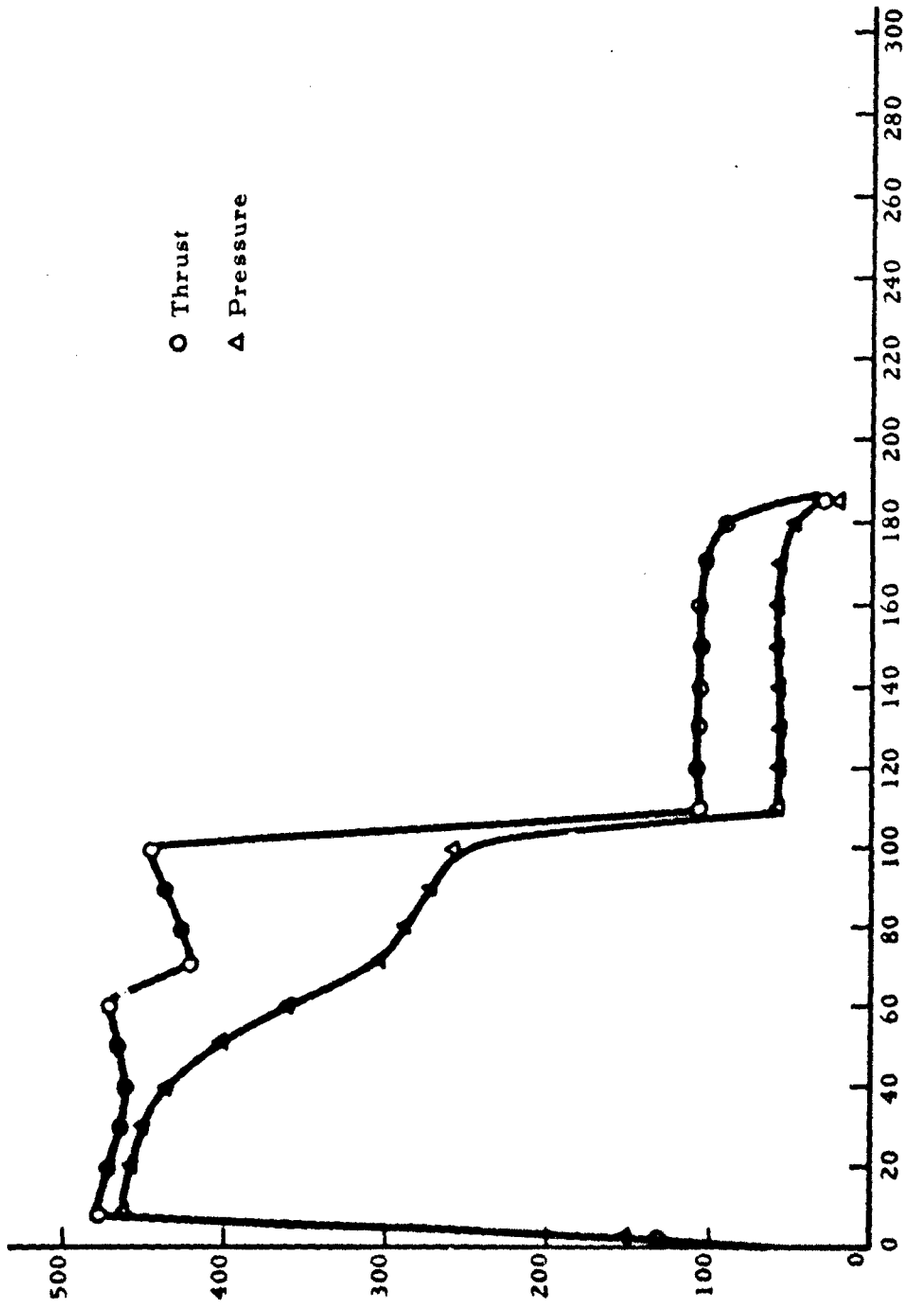

Figure 52. Thrust and Chamber Pressure Versus Time; 80,000-ft Mission, Run 8F

This document contains information affecting the national defense of the United States within the meaning of the Espionage laws Title 18, U.S.C. Section 793 and 794 the transmission of which in any manner to an unauthorized person is prohibited by law

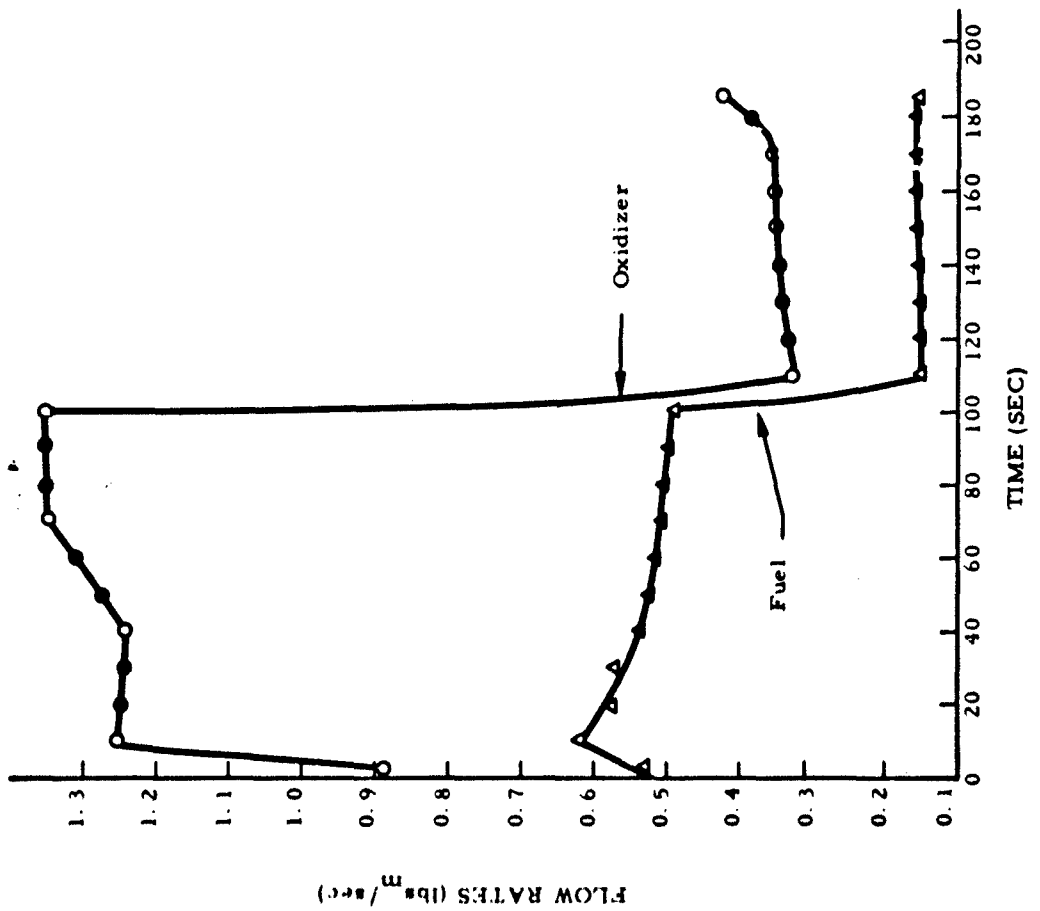

Figure 53. Oxidizer and Fuel Flow Rates; 80,000-ft Mission, Run 8F

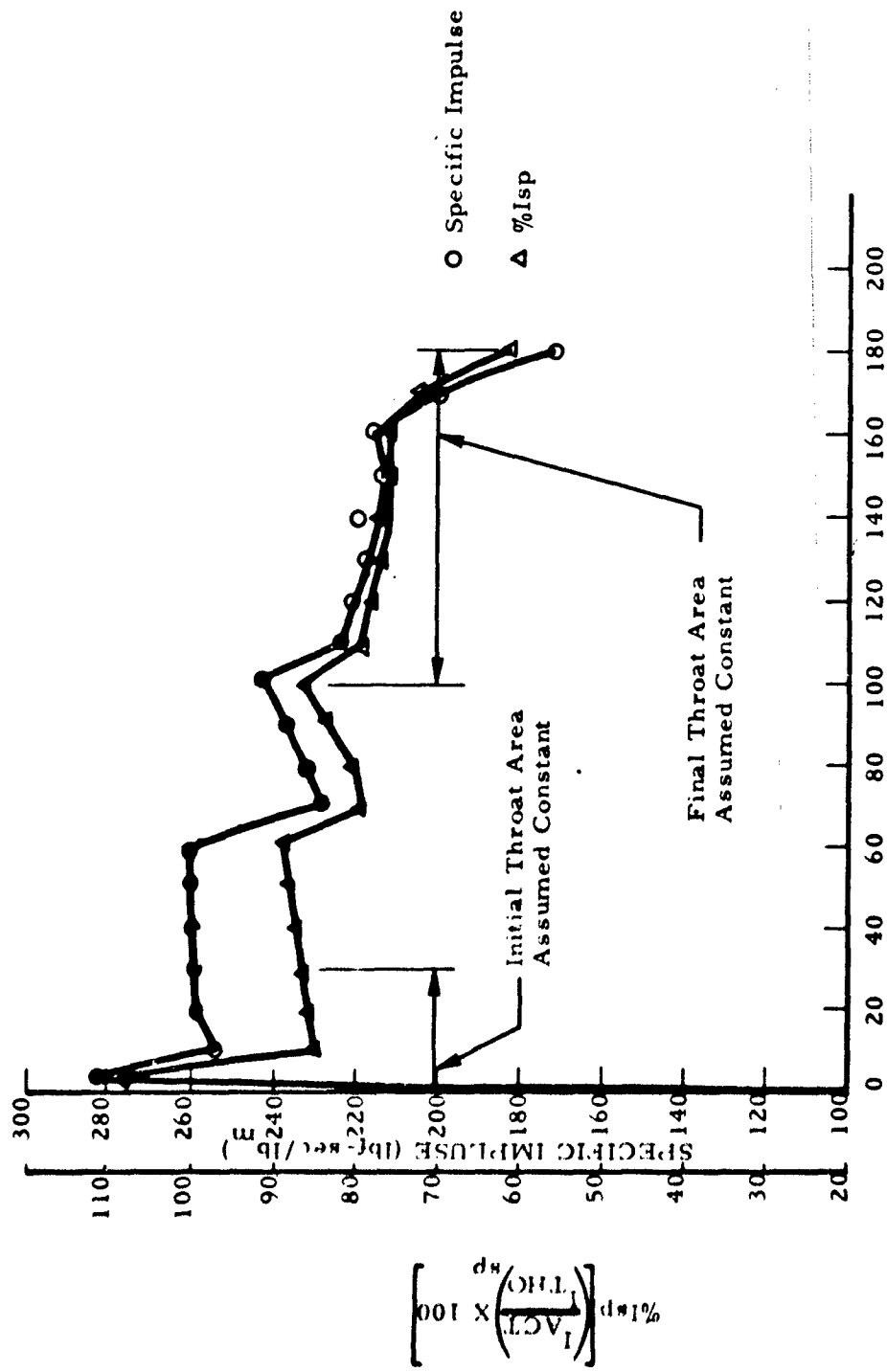

$$\%Isp = \left[\left(\frac{I_{ACT}}{I_{THO}}\right)_{sp} \times 100\right]$$

Figure 54. Isp and Isp Efficiency; 80, 000-ft Mission, Run 8F

THIS DOCUMENT CONTAINS INFORMATION AFFECTING THE NATIONAL DEFENSE OF THE UNITED STATES WITHIN THE MEANING OF THE ESPIONAGE LAWS, TITLE 18, U.S.C., SECTION 793 AND 794, THE TRANSMISSION OF WHICH IN ANY MANNER TO AN UNAUTHORIZED PERSON IS PROHIBITED BY LAW

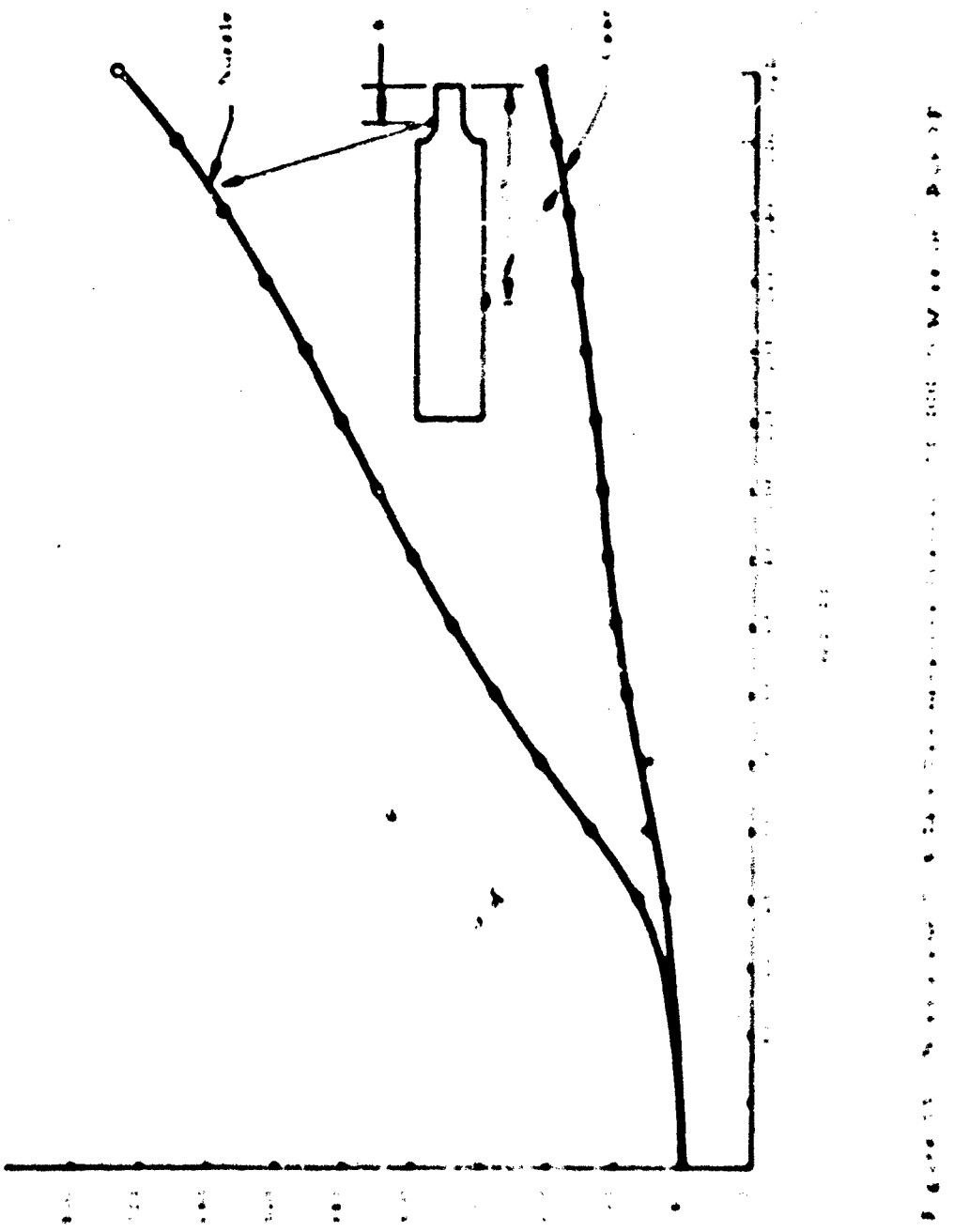

(U) The propulsion system started normally during Flight Number 3, which was intended as a 70,000-ft cruise mission, but missile negative "g" maneuvers induced by the flight programmer during pitchover at cruise altitude resulted in unporting of the oxidizer feed system and extinguishment of the hybrid TCA. Since the gravity-feed-type oxidizer feed system was never intended to operate under zero "g" or negative "g" conditions, unporting of the oxidizer tank outlet would result in shutoff of oxidizer flow and cold GN_2 purge of the hybrid TCA. This sequence of events would be expected to shut down the TCA and prevent reliable reignition of the nonhypergolic propellants. A similar sequence of events with a gravity-fed liquid bipropellant propulsion system might well have resulted in a hard restart and destruction of the TCA. This experience points out the inherent fail-safe nature of this type of hybrid TCA.

(U) Boost thrust and chamber pressure characteristics of the flight propulsion system during Flight Number 3 were very similar to those of Run 2F. The system used in Flight Number 2 operated normally in boost and sustain phases. This system experienced higher initial oxidizer tank pressure and subsequent chamber pressure and thrust levels than any of the certification test systems.

3. Thrust Coefficient Comparison

(U) Delivered thrust coefficients for the flight test systems and selected certification test systems are compared in Table IX. These data were calculated from chamber pressure and thrust data at identical time slices during firing, and assume identical TCA nozzle throat areas for flight and certification systems. Since the flight test thrust data was estimated from the observed missile acceleration, known missile aero-dynamic drag characteristics, and estimated missile weight history, the validity of the flight test thrust estimates is unkown. However, this comparison indicates that about 11 percent greater C_F was delivered during Flights Number 1 and 3 than was observed during comparable certification tests. Since the certification tests were not conducted with a simulated missile boattail

surrounding the TCA nozzle exit, this thrust increase may be due to nozzle or boattail base-pressure effects. Only further well-instrumented flight tests could conclusively evaluate this hypothesis.

TABLE IX. DELIVERED THRUST COEFFICIENT COMPARISON; CERTIFICATION VERSUS FLIGHT TEST

Comparison (Flight Test/ Certification Test)	Time Slice (sec)	$*\frac{C_{f_{mc}}}{C_{f_{flt}}}$
1/4F	20	0.88
**2/7F	20	0.97
3/7F	10	0.89

*Delivered thrust coefficient; $C_f = \frac{F}{P_c A_t}$

$C_{f_{mc}}$ = Delivered certification thrust coefficient based on mission corrected thrust

$C_{f_{flt}}$ = Delivered flight thrust coefficient based on apparent thrust

NOTE: Throat areas assumed equal at comparison time slice

**Noisy TM data casts doubt on estimated flight thrust levels (Reference 3).

SECTION V

SUMMARY AND CONCLUSIONS

(U) A total of 30 heavyweight tests were conducted during Phase I. Twenty-six of these tests were accomplished successfully. Performance was measured at boost and 90,000-ft sustain thrust levels (considered the most critical), over altitudes from ambient (13.2 psia) to 90,000 ft, over magnesium loadings in the fuel of 2%, 10%, and 20%, and over environmental temperature ranges of -65°F to 165°F.

(U) Pyrolytic graphite gave the lowest erosion rate as the nozzle throat material (less than 1 mil/sec) for boost durations up to 97 sec when compared to a Spear Carbon high-density graphite throat with a rate of 3 to 5 mil/sec.

(U) The effect of increased metal loading was increased fuel regression rate and lower combustion efficiency. Temperature conditioning of the fuel only had no noticeable effect on combustion. The stop-start technique used for this phase of the program definitely had its drawbacks. During the cooling processes following shutdown of the engine, an undetermined amount of the volatile fuel binder was vaporized by heat soak into the grain thus changing the fuel composition at the surface. Subsequent tests utilizing such grains may have been significantly influenced by past firing history due to this effect.

(U) Various insulations other than silica phenolic were evaluated. These included graphite tape and asbestos, and no significant improvement was noticed.

(U) Late in the program it was discovered that load cells used to measure thrust were not designed to operate satisfactorily at altitude. A series of tests was made to evaluate thrust accuracies using specially

designed instrumentation. The results showed that abrupt, large-magnitude changes in thrust such as encountered in throttling from boost to sustain temporarily represented the worst condition for instrumentation.

(U) A test was conducted to measure heating of the aft boattail extension designed by the Beech Aircraft Company. Results of this test were used to design an aft heat shield for the airframe.

(U) Various injectors were evaluated and tested. The best performing injector was a swirling hollow-cone injector of wide angle and high momentum. It caused more uniform fuel regression along the length of the fuel grain and less recirculation at the head end. Burning also appeared cleaner with less erosion of head-end insulating material.

(U) A unique procedure for measuring oxidizer flow rates based on cold flow of the injector was developed (Appendix B). This method was used to allow complete data reduction of engine performance during Phase II.

(U) Heavyweight testing demonstrated the safety and reliability of the hybrid system and the propellant combination. There were no accidents of any kind.

(U) The results of the flight-weight certification tests showed considerable dispersion of overall propulsion system performance for any given duty cycle, but this did not preclude adequate performance to meet flight demonstration requirements. The primary factor which determined overall system performance was TCA nozzle response to the oxidizer-rich boost-phase combustion environment as the boost-phase operating time was varied for each mission type. The severity of this environment varied widely for any mission depending upon the performance of the oxidizer tank pressure regulator. Improved TCA nozzle durability and oxidizer tank pressure regulator repeatability should be subjects of future Sandpiper hybrid propulsion system development programs.

(U) One certification test displayed unexplainably high oxidizer flow rates in sustain phase probably attributable to a repeatability problem with the dial-a-thrust valve. This valve should also be the subject of future development to improve repeatability and ease of foolproof adjustment in the field.

(U) Comparison of apparent flight-test thrust levels with those of comparable certification tests indicates that flight-test thrust coefficients are higher by about 11 percent. The validity of this observation and the mechanism, if any, involved should be investigated in future flight tests.

(U) On 12 December 1967, the first hybrid target missile demonstration vehicle was successfully flown over the Eglin AFB test range at an altitude of 50,000 ft. Subsequently, two additional flights (50,000 and 70,000 ft) were successfully accomplished. The demonstration vehicle performed at altitudes up to 78,000 ft and Mach 2.5 and flew under power for durations approaching 5 minutes. Together, these flights demonstrated adequate hybrid propulsion system capability, airframe stability and control, air-launch capability, and maneuverability. The feasibility of a high-performance maneuvering target concept employing a low-cost, dial-a-thrust hybrid rocket engine for propulsion was thus demonstrated by this program.

REFERENCES

1. Required Action Directive, RAD 7-3-(1); (U) "High Performance Target Drone," 20 March 1967, AFRDQRA. SECRET.

2. Major James M. Gafney, "Flight Demonstration of the Sandpiper Rocket Target Missile Test Bed Vehicle," APGC-TR-68-38, April 1968, APGC, Florida. UNCLASSIFIED.

3. M. L. Brubaker, D. E. Wells, "The Sandpiper Target Missile - Exploratory Development and Flight Test," AFATL-TR-68-70, June 1968, Beech Aircraft Corporation, UNCLASSIFIED.

4. R. J. Muzzy, "Demonstration of a High Thrust Hybrid Thrust Chamber Assembly," AFRPL-TR-68-56, Part II. Computer Manual, April 1968, United Technology Center, AD 832444. UNCLASSIFIED.

5. Multi-Stage Ejector-Diffuser, FE-244-3, Final Report Contract AF04(611)-6086, December 1961, The Marquardt Corporation. UNCLASSIFIED.

6. R. A. Jones, "Hybrid Propulsion System for an Advanced Rocket-Powered Target Missile," AFRPL-TR-68-137, August 1968, United Technology Center, AD 392295. CONFIDENTIAL.

APPENDIX A

SUMMARY OF FLIGHT-TEST RESULTS

(U) On 12 December 1967, the first hybrid target missile demonstration vehicle was successfully flown over the AFGC, Eglin AFB test range at the 50,000-ft level. Subsequently, two additional flights (50,000 ft and 70,000 ft) were successfully accomplished on 21 January and 25 February 1968. The demonstration vehicle performed at altitudes up to 77,000 ft at Mach 2.51 and flew under power for durations approaching 5 minutes. A summary of the flight test results is shown in Table A-1. The flight test results have been reported separately and in more detail in References 2 and 3. Although each flight was not entirely successful, the three flights together demonstrated adequate hybrid propulsion system capability.

(U) Flight Test No. 1: Flight test No. 1 was planned for Mach 1.8 sustain (maximum) at 50,000 ft. The hybrid engine was programmed for 5-sec boost and 260 sec of sustain with destruct time set at 277 sec. The dial-a-thrust valve was set for a 50,000-ft mission (7H). The missile was launched at 49,500 ft and Mach 1.5 from an F-4C aircraft. Due to electrical problems, the boost valve was closed during the ignition sequence and the hybrid rocket was ignited in the sustain mode. The target missile flew for 250 sec under powered flight and was destructed aerodynamically by a canard down maneuver at 277 sec. This test demonstrated successful launch and flight of the missile at supersonic speeds. The hybrid engine ignited successfully under uncertified, off-design conditions and performed satisfactorily in the high-altitide supersonic environment.

(U) A comparison between in-flight engine performance and ground certification test performance is made in Figures A-1 and A-2. Figure A-1 presents telemetered and reduced chamber pressure for the flight (Reference 3) and the chamber pressure trace from Run 4F versus time. Certification test 4F was selected for comparison because this was the only

UNCLASSIFIED

TABLE A-I FLIGHT TEST SUMMARY

Flight	Mission	Max/Nominal Mach No.	Max/Nominal Altitude (ft x 10^{-3})	Boost Time (sec)	Sustain Time (sec)	Flight Time (sec)
No. 1	50,000 ft	1.55/1.44	48.7/47.8	0	252	277
No. 2	50,000 ft	1.84/1.72	48.9/48.3	21	196	220
No. 3	70,000 ft*	2.51/1.62	77.7/60.6	80	0	360

*Maneuvered through 2 "S" turns in nonpowered flight;
Negative "g" maneuver extinguished combustion at 80 seconds.

UNCLASSIFIED

APPENDIX A

SUMMARY OF FLIGHT-TEST RESULTS

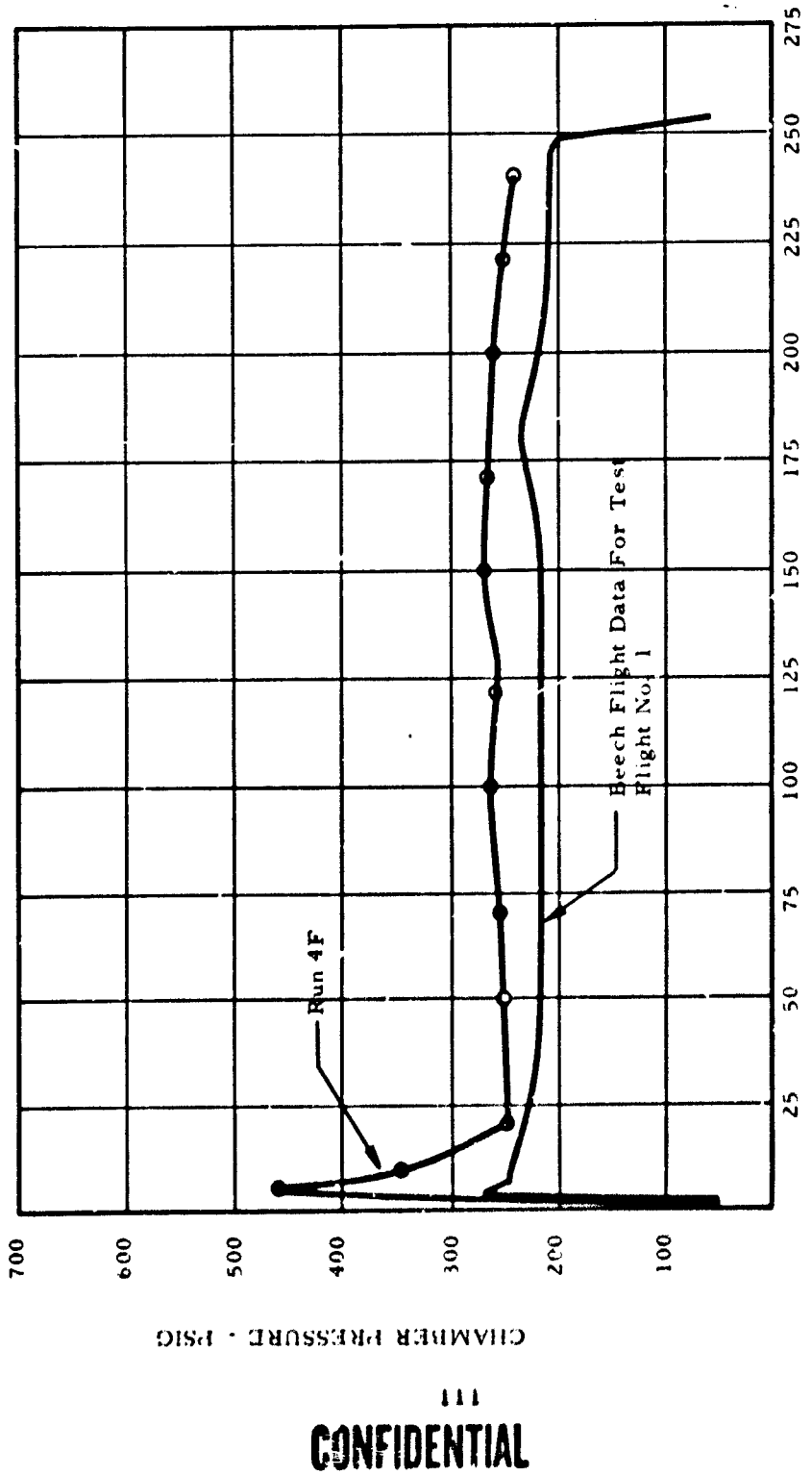

Figure A-1. Comparison of AFRPL Measured Chamber Pressure Data to Actual Flight Data for Flight Number 1

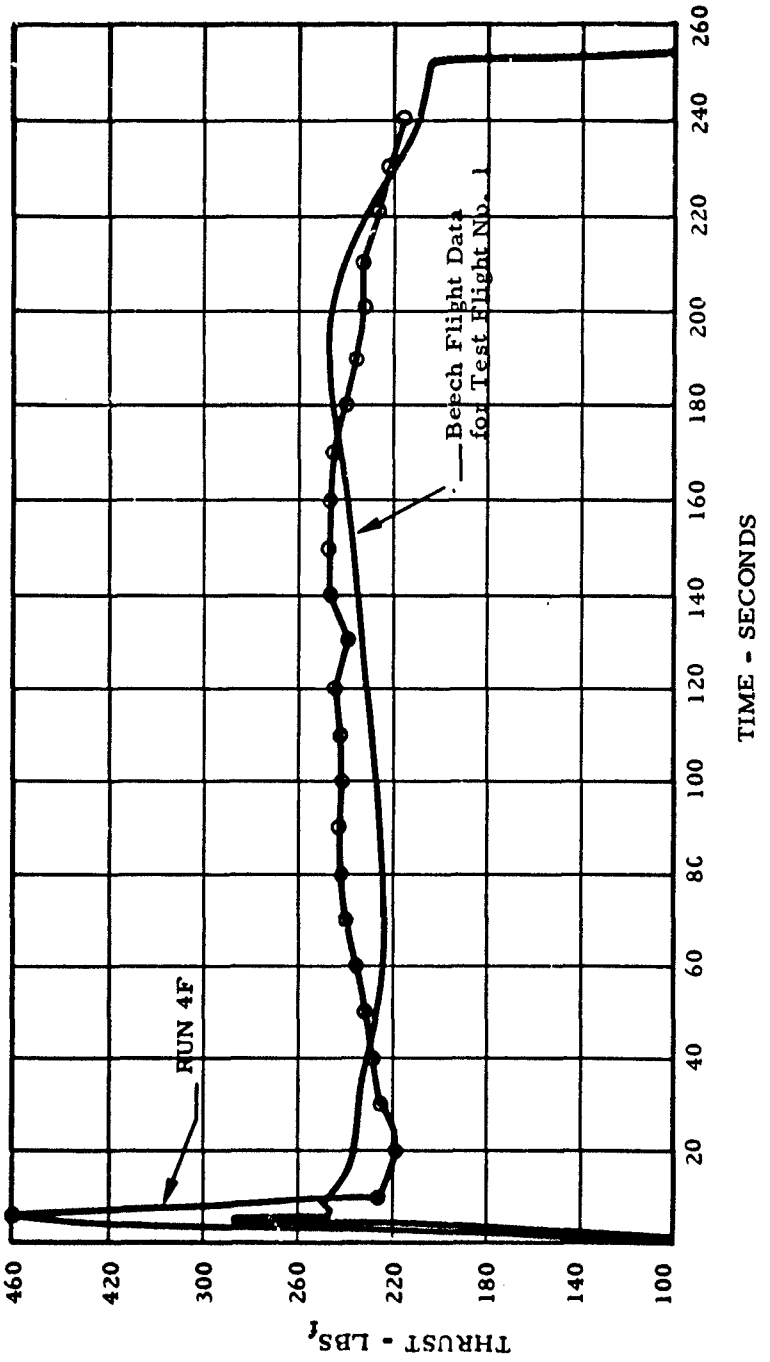

Figure A-2. Comparison of AFRPL Measured Thrust to Beech Computed Thrust Data for Flight Number 1

run at the 50,000-ft mission sustain thrust in which the exhaust nozzle did not incur severe erosion, and resulted in a chamber pressure trace very similar to that observed in the first flight test. It is evident that the flight propulsion system exhibited slightly lower oxidizer tank pressure as evidenced by the lower average level of chamber pressure throughout powered flight. Very little TCA nozzle erosion is indicated by the relative flatness of the chamber pressure trace and the slight rise in thrust with time beginning at 100 seconds.

(U) It must be realized that the indicated thrust data was calculated indirectly from knowledge of the missile axial and normal acceleration and angle-of-attack histories, zero-lift and induced drag characteristics, Mach number and altitude history, and estimated missile weight history. Hence, the estimated thrust levels shown in Figures A-1, A-4 and A-6 should be accurate at the beginning of powered flight but may deviate from actual levels later on as assumed missile weight errors accumulate.

(U) Since the actual TCA nozzle throat areas which existed during certification and flight tests should be almost identical during the first 10 to 20 seconds of run time, the initially indicated flight and certification test thrust and chamber pressure levels can be used to compare delivered thrust coefficients (C_f) for these tests. Comparison of delivered C_f at the 20-second time slice using the above assumptions indicates that 12% greater delivered C_f for flight as compared to Run 4F.

(U) Flight Test No. 2: Flight No. 2 was planned for Mach 2.0 sustain at 50,000 ft. The hybrid engine was programmed for 20 sec of boost and 185 sec of sustain with destruct time set for 223 sec. The dial-a-thrust valve setting was for a 50,000-ft mission (7H). The missile was launched at 49,500 ft and Mach 1.5. The hybrid engine ignited successfully, flew under boost phase power for 21 sec, throttled and flew under sustain phase power for 196 sec.

(U) Since the hybrid propulsion system performance at any time slice was determined by the previous oxidizer tank pressure and TCA nozzle throat erosion histories and no certification test was run with only 21 seconds of boost phase, an exact comparison with certification results cannot be made. However, Figures A-3 and A-4 compare flight number 2 results with those of boost phase for Run 7F. Run 7F was used here because it exhibited the highest boost-phase oxidizer tank pressures and thrust levels observed during certification. It is apparent that the flight propulsion system experienced even higher tank pressure due to the greater boost-phase chamber pressures and thrust levels indicated. Figure A-3 tends to show similar, almost immediate nozzle erosion characteristics. Comparison of the delivered C_f values from these data for the 20-second time slice yield about 3% greater C_f for the flight propulsion system. It should be noted that Reference 3 points out that the telemetered data, including pitot/static pressure (Mach number), were noisy during this flight. This casts doubt on the reliability of the estimated thrust data and the above C_f comparison results.

(U) A comparison of the sustain-phase trace for this flight with that from Flight Number 1 and Run 4F also substantiates higher oxidizer tank pressures for this flight because of the greater average pressure indicated during sustain.

(U) Flight Test No. 3: Flight No. 3 was planned for Mach 3.1 maximum sustain at 70,000 ft. The missile was programmed to achieve Mach 2.2 during an approximately 82-sec boosted climb to altitude followed by 180 sec of sustain phase operation. After powered flight, two "S" turn maneuvers were planned with destruct scheduled for 260 sec. The dial-a-thrust valve was set for 50,000 ft (7H) to insure adequate acceleration during sustain operation. The missile was again launched at 49,500 ft and Mach 1.5. Boost-phase operation lasted 80 sec and terminated when missile pitch-over occurred at an altitude of 78,000 ft. The pitch-over maneuver was violent enough to subject the missile to negative "g" conditions.

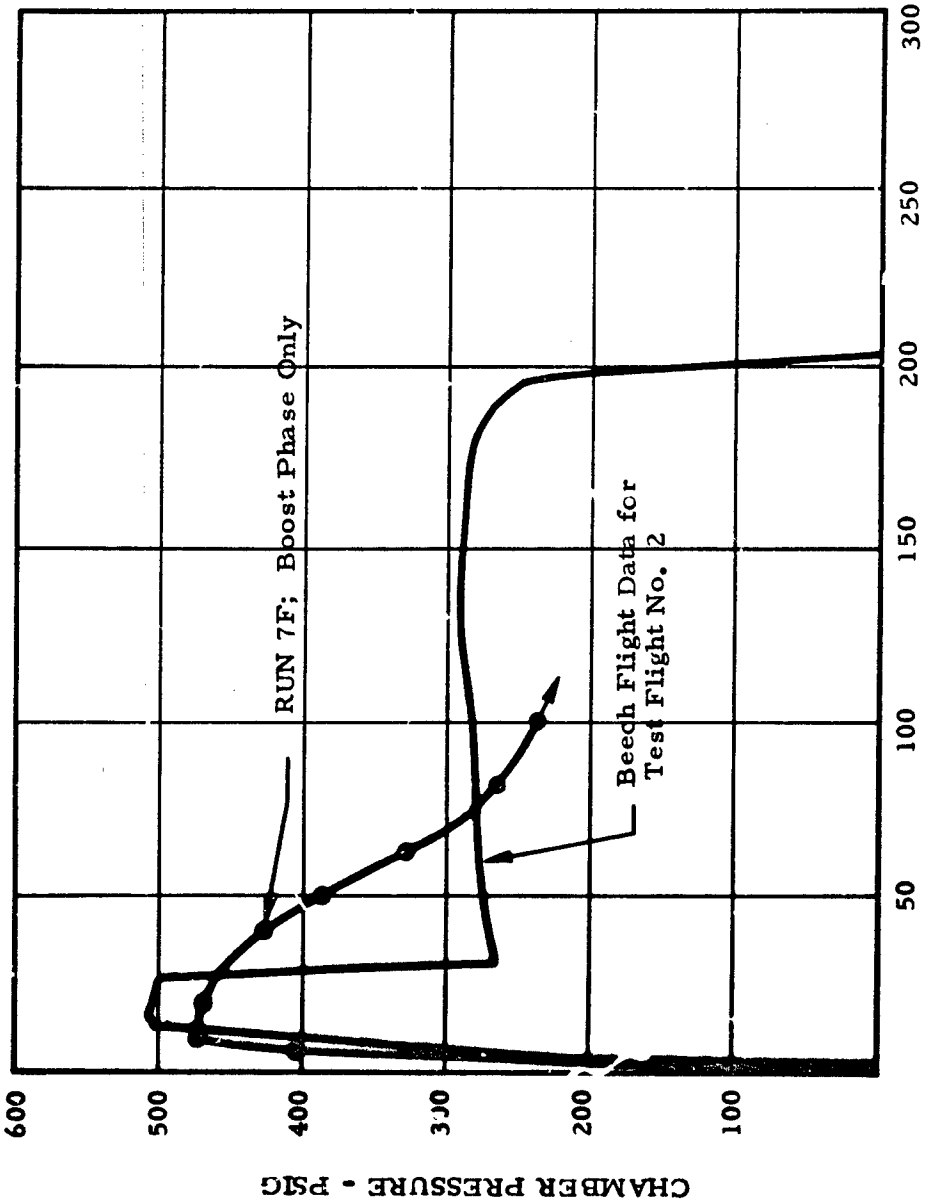

Figure A-3. Comparison of AFRPL Measured Chamber Pressure Data to Actual Flight Data for Flight Number 2

This document contains information affecting the national defense of the United States within the meaning of the Espionage Laws, Title 18, U.S.C., Section 793 and 794, the transmission of which in any manner to an unauthorized person is prohibited by law.

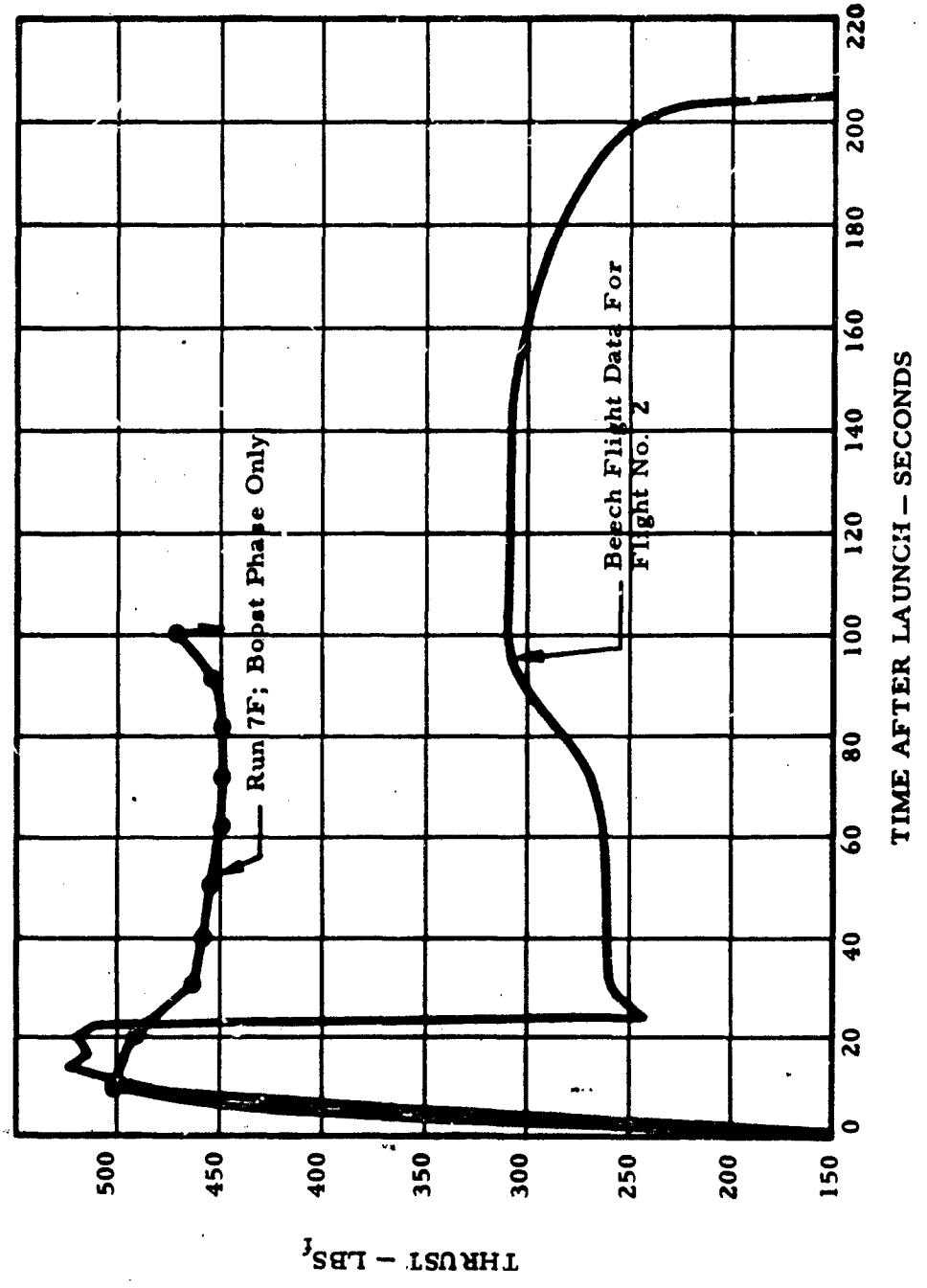

Figure A-4. Comparison of AFRPL Measured Thrust to Beech Computed Thrust Data for Flight Number 2

This document contains information affecting the national defense of the United States within the meaning of the Espionage Laws, Title 18, U.S.C., Sections 793 and 794, the transmission of which in any manner to an unauthorized person is prohibited by law.

Oxidizer flow was temporarily disrupted and engine combustion extinguished because the feed system was not designed to operate under these conditions. Reliable reignition would not be expected because unporting of the oxidizer feedline would cause the cold GN_2 purge of the TCA thus aggravating the nonhypergolic nature of the propellants. The target missile glided for the remaining 4-1/2 minutes. The two "S" turn maneuvers did take place at about 240 sec into the flight.

(U) Figures A-5 and A-6 compare the results of this flight with those of Run 7F. It is apparent that this flight propulsion system experienced initial oxidizer tank pressure levels very similar to those of Run 7F since the maximum boost chamber pressure level (Figure A-5) is almost identical to that for the certification test. However, the flight system tank pressure and TCA nozzle erosion histories apparently were significantly different from Run 7F after ignition, because the pressure and thrust trends diverge. Comparison of these data at the 10-second time slice indicates about 11% greater delivered C_f for the flight system.

(This page is unclassified)

THIS DOCUMENT CONTAINS INFORMATION AFFECTING THE NATIONAL DEFENSE OF THE UNITED STATES WITHIN THE MEANING OF THE ESPIONAGE LAWS, TITLE 18, U.S.C., SECTION 793 AND 794, THE TRANSMISSION OF WHICH IN ANY MANNER TO AN UNAUTHORIZED PERSON IS PROHIBITED BY LAW.

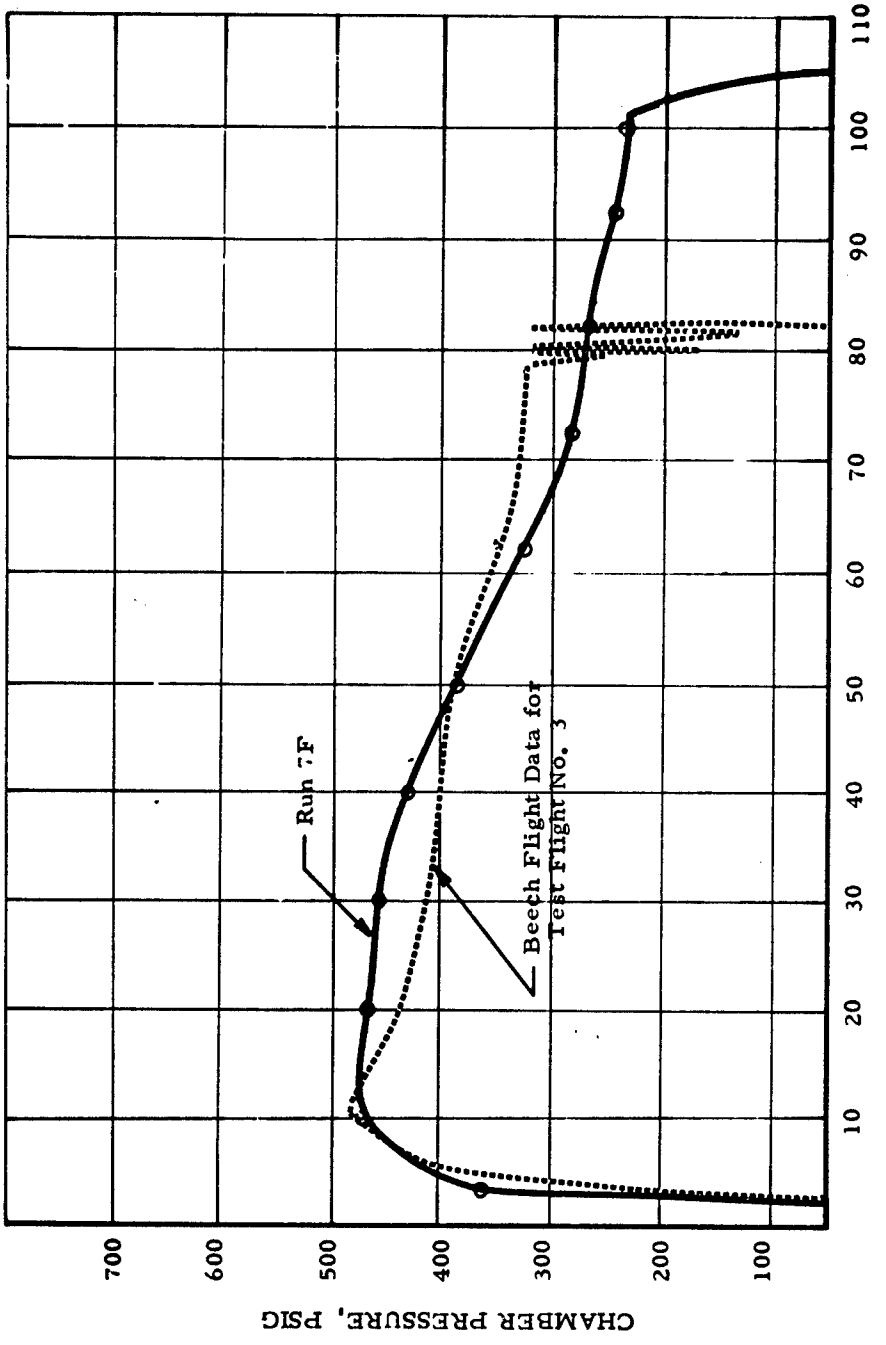

Figure A-5. Comparison of AFRPL Measured Chamber Pressure Data to Actual Fight Data for Flight Number 3

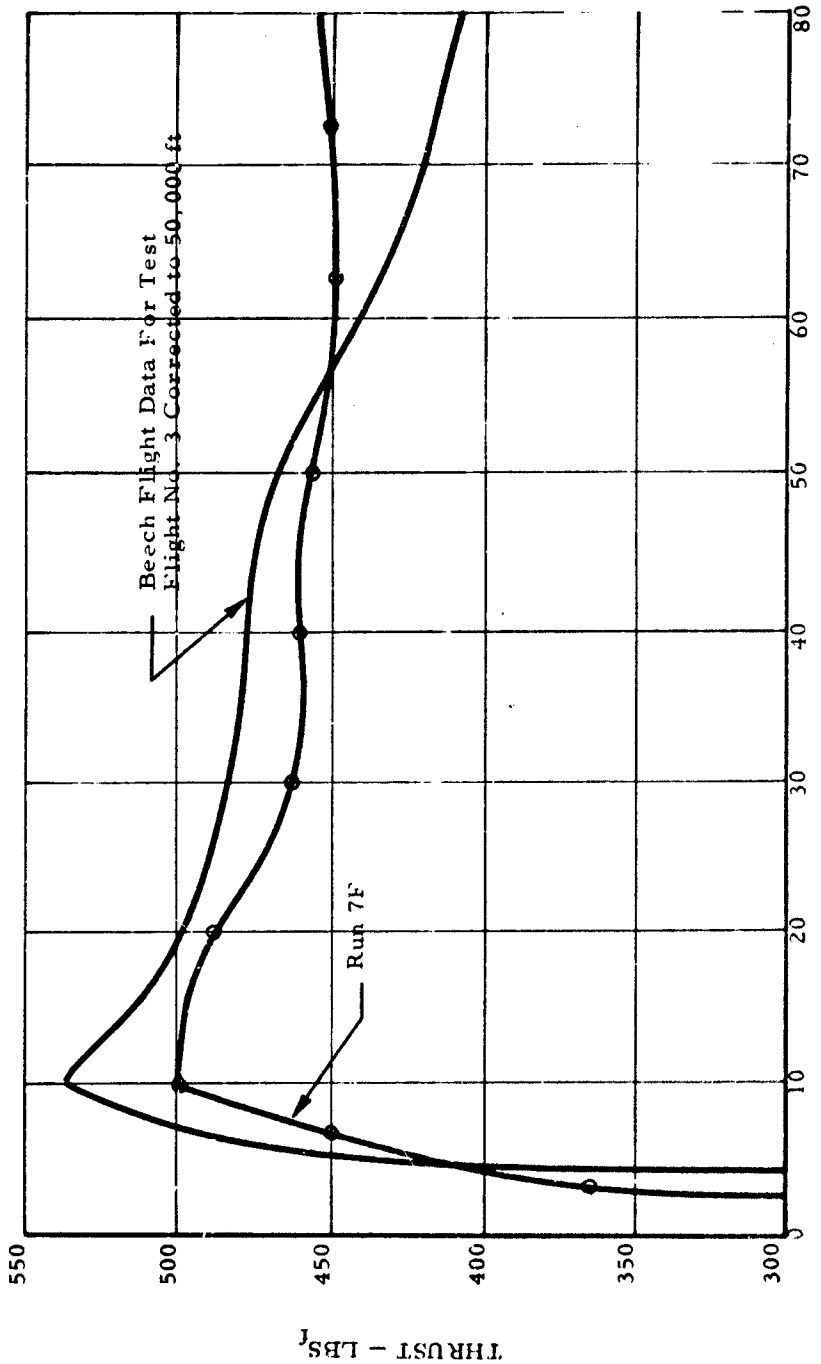

Figure A-6. Compariaon of AFRPL Measured Thrust to Beech Computed Thrust Data for Flight Number 3

PRECEDING PAGE BLANK - NOT FILMED

APPENDIX B

OXIDIZER FLOW ANALYSIS DESCRIPTION

APPENDIX B

OXIDIZER FLOW ANALYSIS DESCRIPTION

(U) Throughout the heavyweight testing phase of this program, no satisfactory technique had been developed to accurately predict oxidizer flow rates from experimental test data. The contractor assumed that during boost-phase operation aeration had little effect and that oxidizer flow rate was purely a function of the injector pressure drop. For sustain-phase operation, the contractor assumed that the oxidizer flow rate was a function of the pressure drop across the dial-a-thrust valve. Calibrations of the injectors (without aeration) and the dial-a-thrust valve with water were used by UTC to predict oxidizer flow rates in the flight-weight hybrid propulsion system. Average or nominal values were the best that the contractor could predict for system flow rates. Tests at the AFRPL, however, had shown that aeration did have a significant effect on oxidizer flow rates during boost phase and that dial-a-thrust valve calibrations were not very accurate because downstream conditions did have a noticeable effect on oxidizer flow rates during sustain. The following technique was developed to accurately predict oxidizer flow rates from test data.

(U) The water-flow calibration facility shown in Figure B-1 was set up in the 1-14 Hydro Laboratory. A heavyweight case with a special flange attached to the aft end was used as the water accumulator tank. The normal head-end closure was used to attach the injector assembly and all other oxidizer lines to simulate as nearly as possible the actual feed system. Pressures were measured as they actually were taken in hot firing tests. Chamber pressure was controlled by the addition of nitrogen through the RTV-11 fill port. The drain valve was operated manually to keep the water level constant. All pressures were recorded on L&N strip charts and the data later reduced. Illustrative tabulated data for certification test injector 6F appears in Table B-1. An aeration pressure upstream of the supersonic orifice was maintained at 750 psia corresponding to the approximate

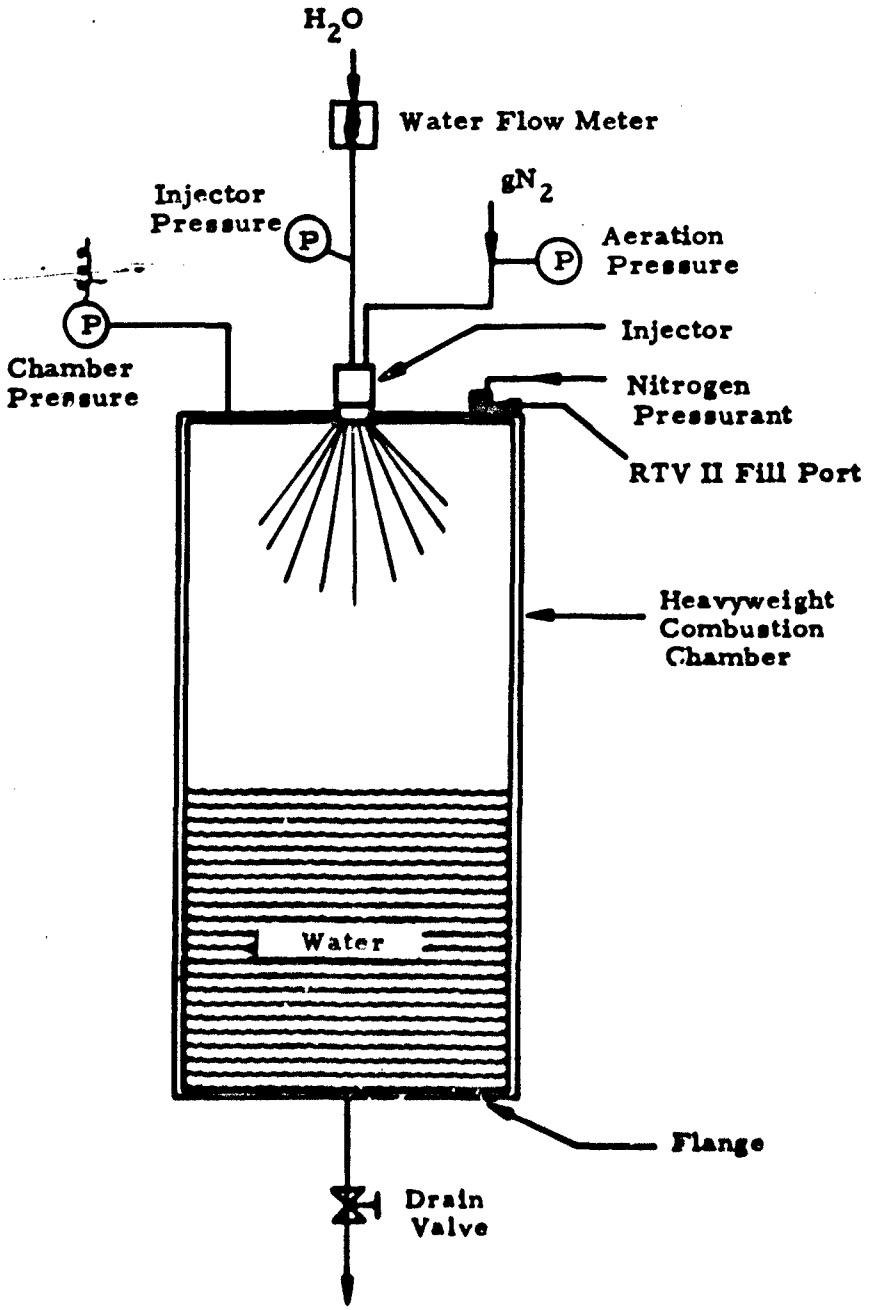

Figure B-1. Injector Water-Flow Calibration Apparatus

TABLE B-I. WATER-FLOW CALIBRATION DATA FOR CERTIFICATION TEST INJECTOR 6F

Aeration Press (psia)	Flow (GPM)	Injector Press (psia)	Chamber Press (psia)	ΔP-Aer (psia)	ΔP-Inj (psia)
750	5.99	740	590	160	150
750	6.23	740	579	171	161
750	6.51	740	563	187	177
750	6.75	740	549	201	191
750	7.01	740	533	217	207
750	7.32	740	513	237	227
750	5.99	720	568	182	152
750	6.25	720	554	196	166
750	6.52	720	541	209	179
750	6.77	720	528	222	192
750	7.01	720	510	240	210
750	7.27	720	492	258	228
750	5.98	700	549	201	151
750	6.27	700	532	218	168
750	6.50	700	522	228	178
750	6.78	700	508	242	192
750	7.02	700	489	261	211
750	7.28	700	474	276	226
750	5.99	650	494	256	156
750	6.23	650	480	270	170
750	6.49	650	468	282	182
750	6.73	650	453	297	197
750	6.99	650	439	311	211
750	7.29	650	414	336	236
750	2.33	350	310		40
750	2.60	350	303		47
750	2.86	350	295		55

TABLE B-I. WATER-FLOW CALIBRATION DATA FOR CERTIFICATION TEST INJECTOR 6F (Cont'd)

Aeration Press (psia)	Flow (GPM)	Injector Press (psia)	Chamber Press (psia)	P-Inj (psia)
750	3.13	349	286	63
750	3.32	349	278	71
750	2.38	300	256	44
750	2.64	300	248	52
750	2.83	300	242	58
750	3.10	300	230	70
750	3.45	300	222	78
750	2.38	249	200	49
750	2.60	251	195	56
750	2.80	250	182	68
750	3.15	250	169	81
750	3.38	249	155	94
750	2.35	199	142	57
750	2.60	200	135	65
750	2.87	201	120	81
750	3.12	199	101	98
750	3.40	200	78	122
750	7.81	720	420	300
750	8.72	720	320	400
750	8.62	700	300	400
750	7.80	700	401	299
750	7.63	648	352	296
750	8.35	650	250	400
748	3.31	350	275	75
748	3.83	350	250	100
750	3.12	300	225	75
748	3.62	300	200	100

regulated pressure during tests. Injector pressure was varied in incremental steps covering a range comparable with actual operation in the engine. Flow rates were selected for each injector pressure to bracket possible flows that might be encountered. Using a specific gravity of 1.385 for MON-25, the boost flow rates covered 1.15 lbm/sec to 1.4 lbm/sec. Chamber pressures resulted from setting all other conditions, flow rate, aeration, and injector pressure. The aeration pressure drop (delta Paer) was the pressure difference between the aeration regulated pressure (750 psia) and the chamber pressure. Chamber pressure was used because the point at which the nitrogen entered the injector was just behind the injector face. The chamber pressure was used as a back pressure rather than injector pressure located in the modified tee because it more realistically approximated the real condition.

(U) Actual computer procedures used a surface mapping routine to determine the volumetric flow rates. The data for each injector was fed into the computer and a statistical plot made. This gave a separate calibration for each injector, and that calibration was used for the test utilizing that particular injector. Figure B-2 illustrates the complex observed relationship of water flow rate to injector pressure drop as influenced by injector pressure, and aeration pressure drop.

(U) Figure B-3 compares the calibrations of five of the eight certification test injectors for fixed injector and aeration pressures. As shown here, deviation from the norm was significant in some cases. In other cases, the data fell almost on top of each other. This scatter of calibration data was the reason for having to calibrate each injector separately. It was assumed that the installation of the injectors in the calibration bench was identical with the installation in the original propulsion system; however, there was no way of telling what differences existed. The effect of engine testing upon the injector must have been small. All injectors showed very little, if any, damage following the tests. They did have to be cleaned because of the deposition of soot in some cases. It was obvious that the

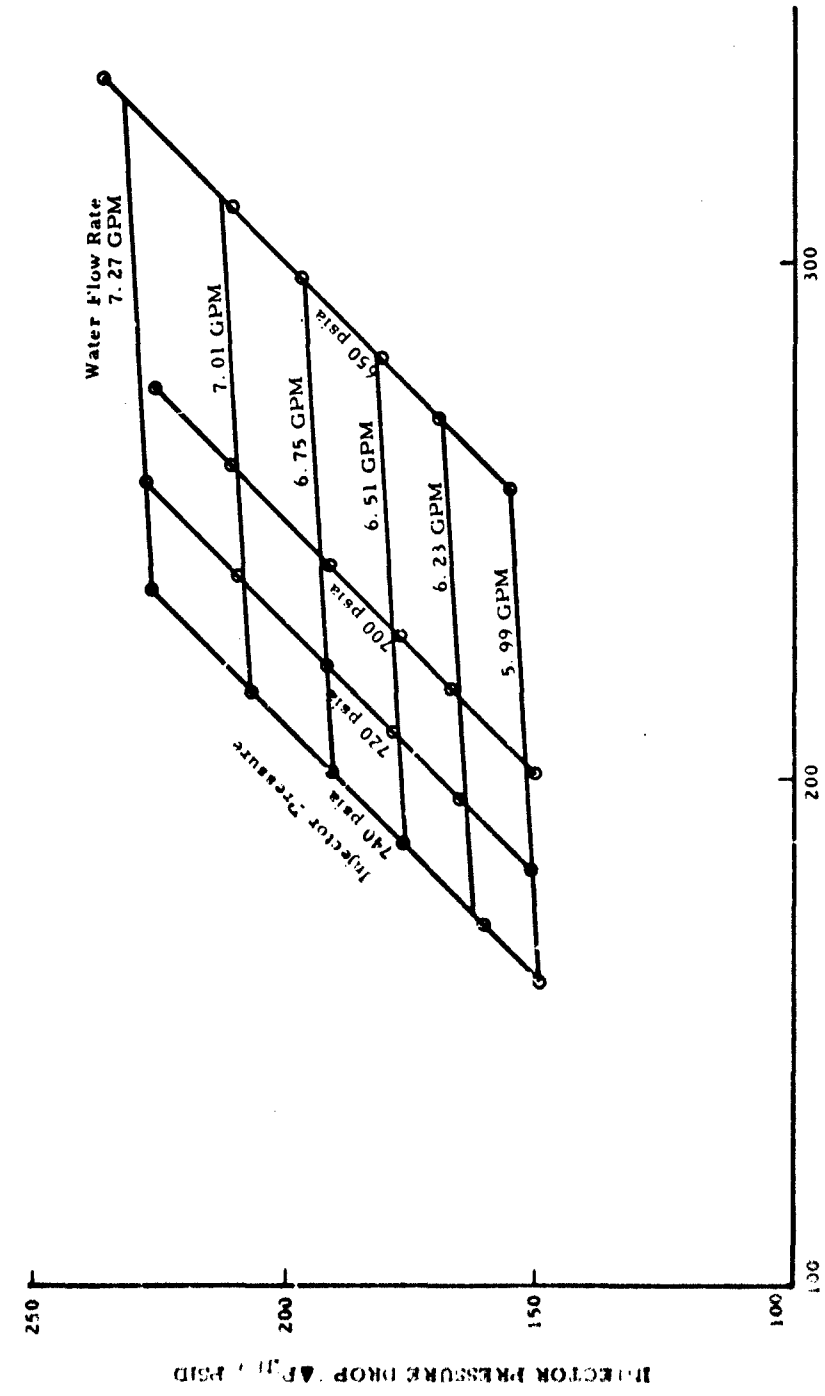

Figure B-2. Water-Flow Calibration Results for Certification Test Injector 6F

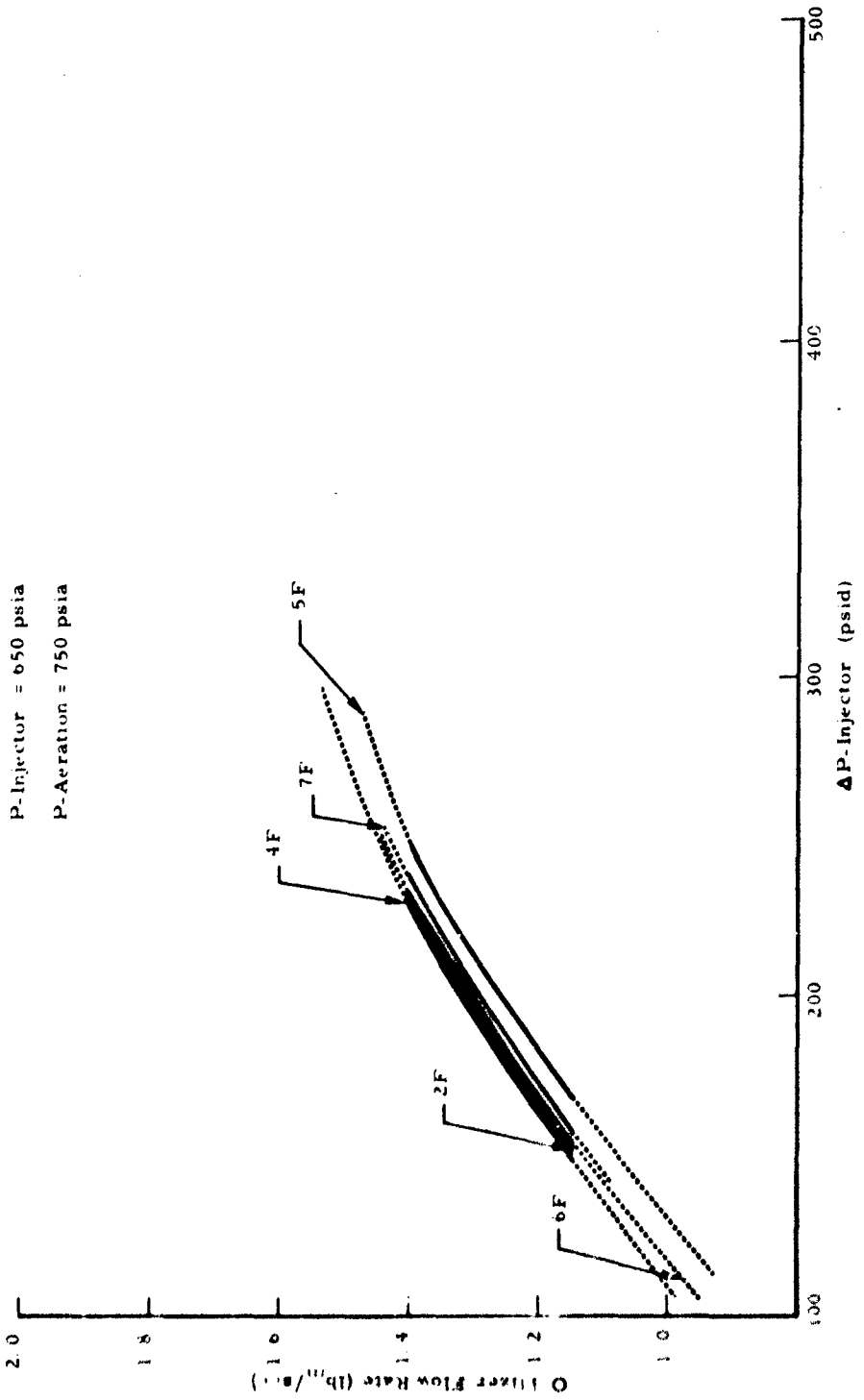

Figure B-3. Injector Calibration Results for Certification Test Injectors 2F, 4F, 5F, 6F and 7F

injectors did get hot, but exactly how this affected the calibration could not be determined.

(U) The end results of this calibration procedure are included in Section IV as plots of estimated oxidizer flow rate as a function of time for each certification test. The data presented are surprisingly close to what would be predicted. These oxidizer flow-rate curves were integrated to determine the oxidizer utilization as a function of time. These data are presented in Figures B-4 through B-11 as compared with the target propellant load of 165 lbs. The exact oxidizer weight for each test was not known. It was assumed that the UTC filling procedures were precise enough to insure close to the 165 lbm, and that this total quantity was expelled during the tests.

(U) The largest single error of the presented technique was caused by aeration. Following the shutdown decay of chamber pressure, nitrogen flow continued through the feed system as the residual nitrogen tank and oxidizer tank pressures dissipated. This nitrogen flow caused the injector pressure to remain significantly high. The computer, when estimating oxidizer flow, would calculate oxidizer flows on the basis of these false pressure readings after the combustion stopped. This result introduced a slight uncertainty into the last 5 seconds of the actual weight-loss predictions. But the closeness of the weight-loss predictions still bore out the accuracy of the presented technique when one considers the very long time period over which error could accumulate. After 200 sec to 300 sec, the maximum predicted error was about 8 lbs. An average flow-rate error of 0.032 lbs/sec would be required to cause this effect. This was about 5% of steady-state predicted flow rate.

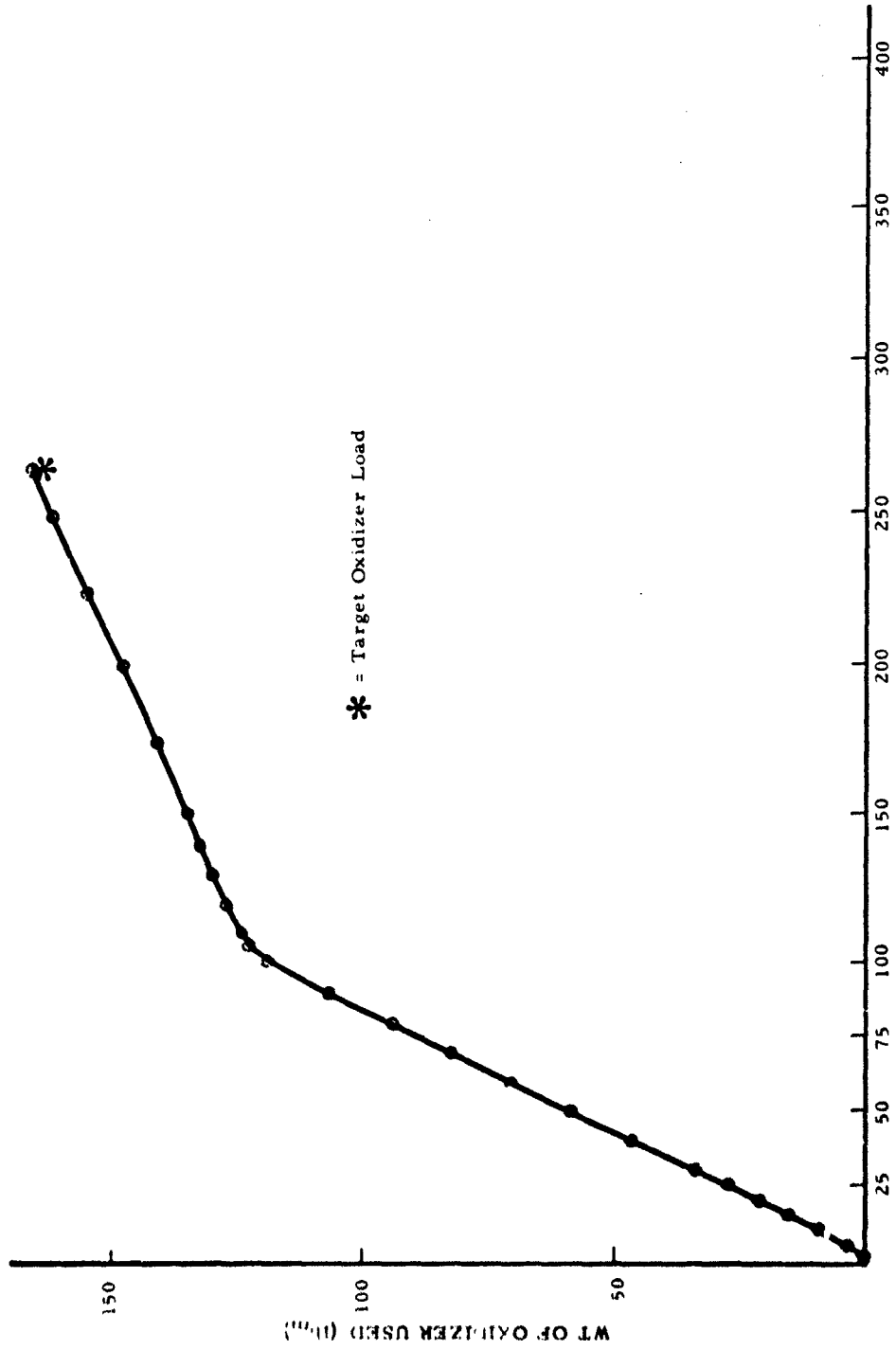

Figure B-4. Estimated Oxidizer Utilization for Certification Test 1F

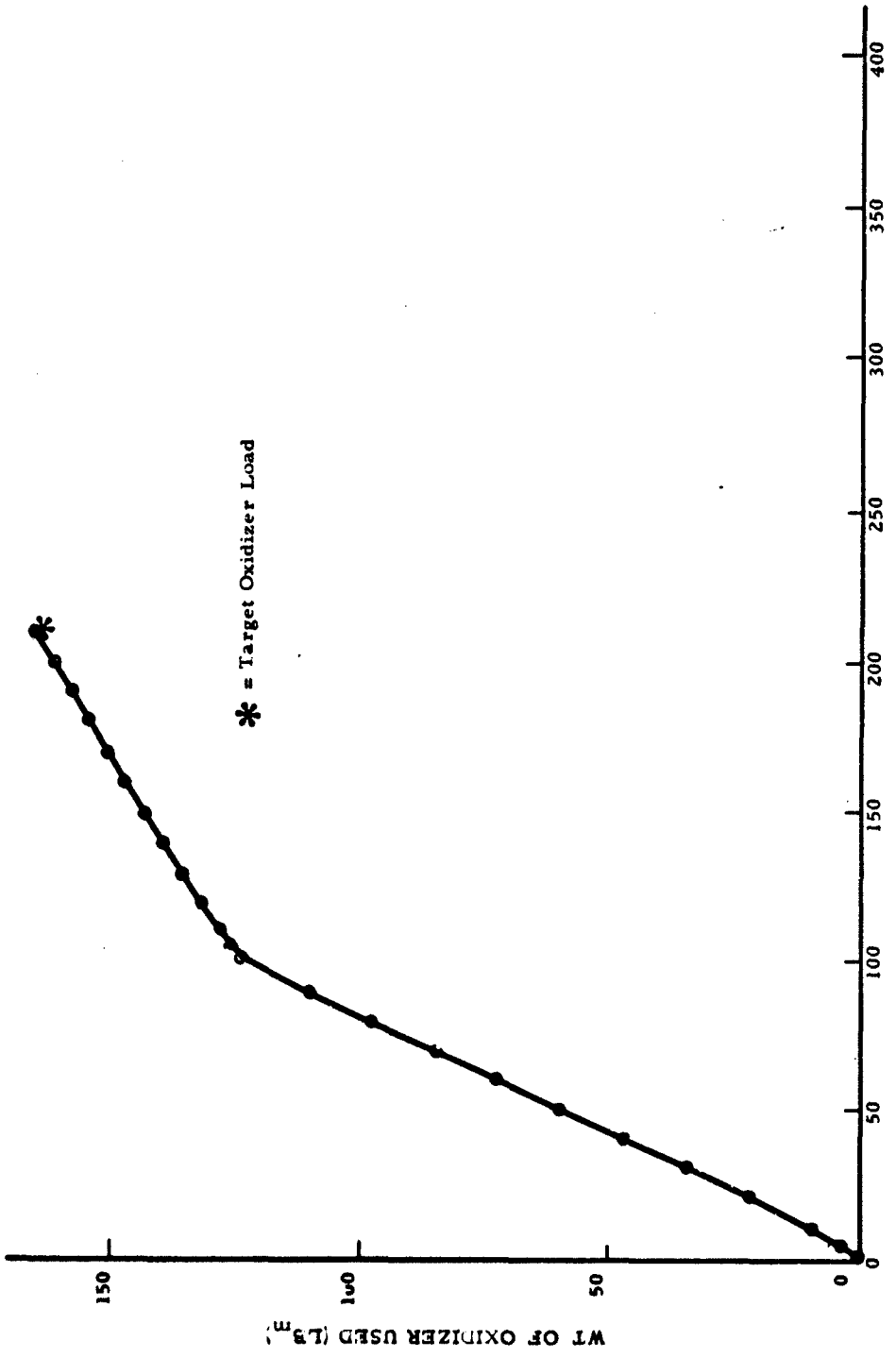

Figure B-5. Estimated Oxidizer Utilization for Certification Test 2F

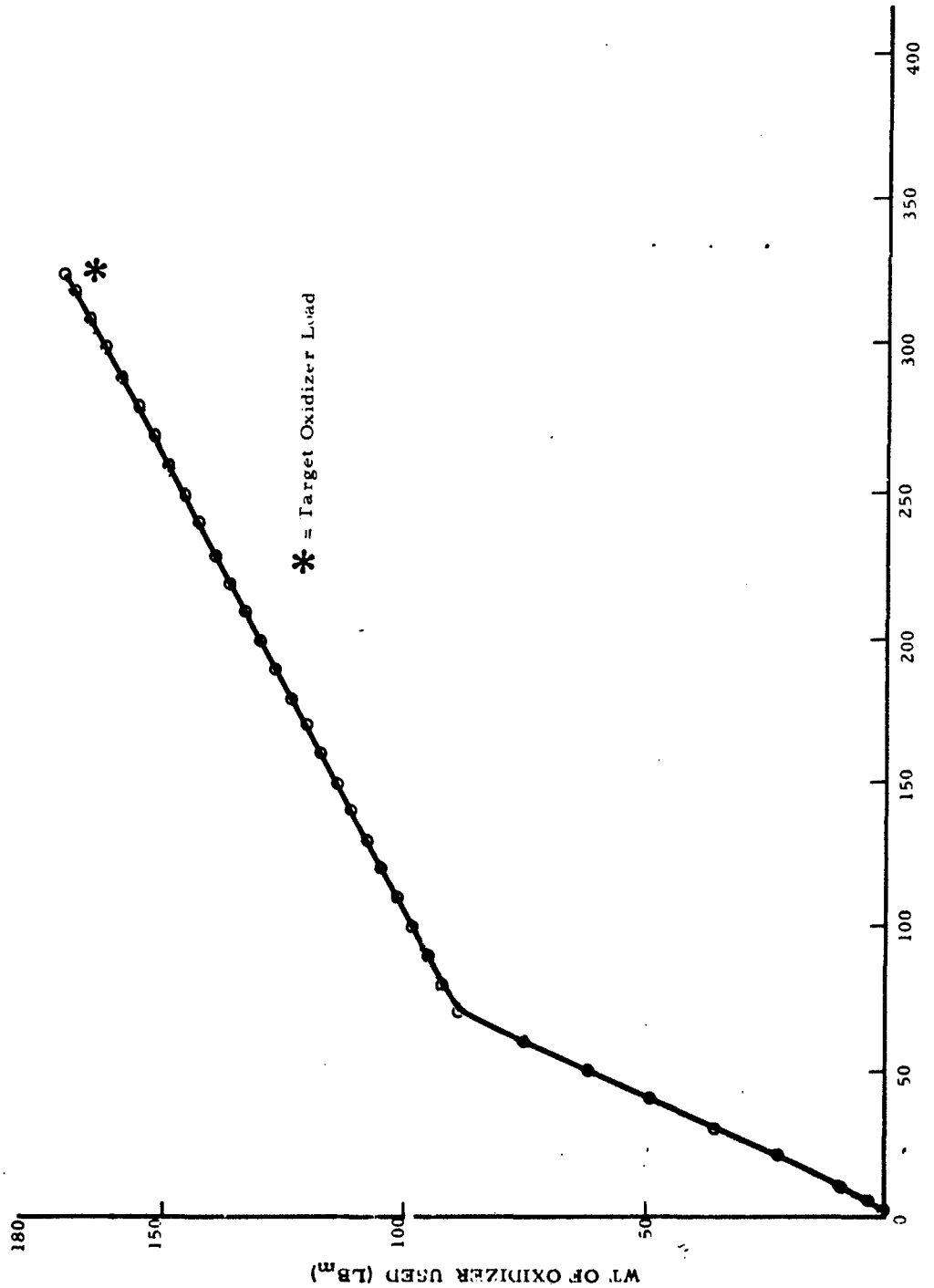

Figure B-6. Estimated Oxidizer Utilization for Certification Test 3F

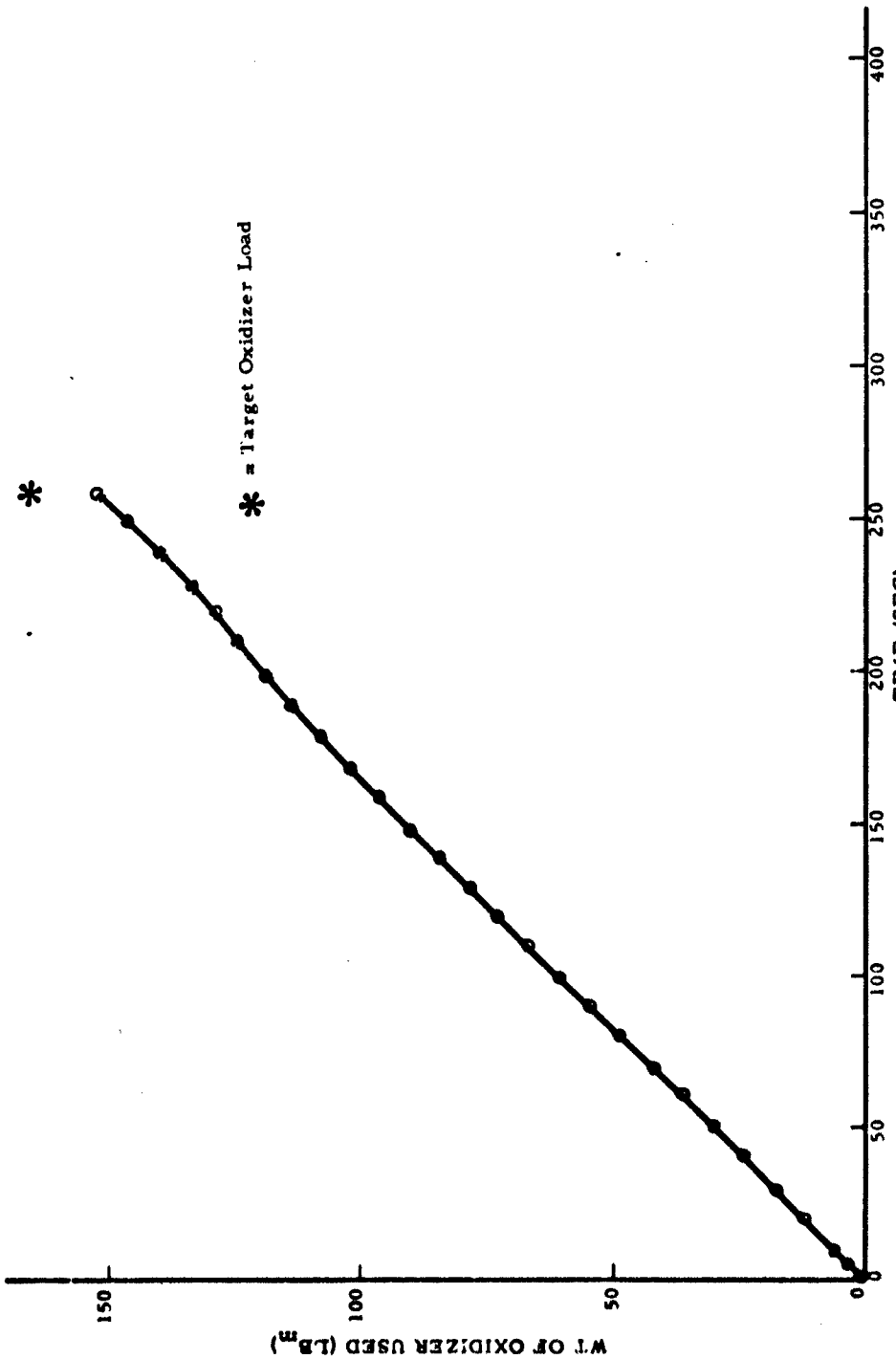

Figure B-7. Estimated Oxidizer Utilization for Certification Test 4F

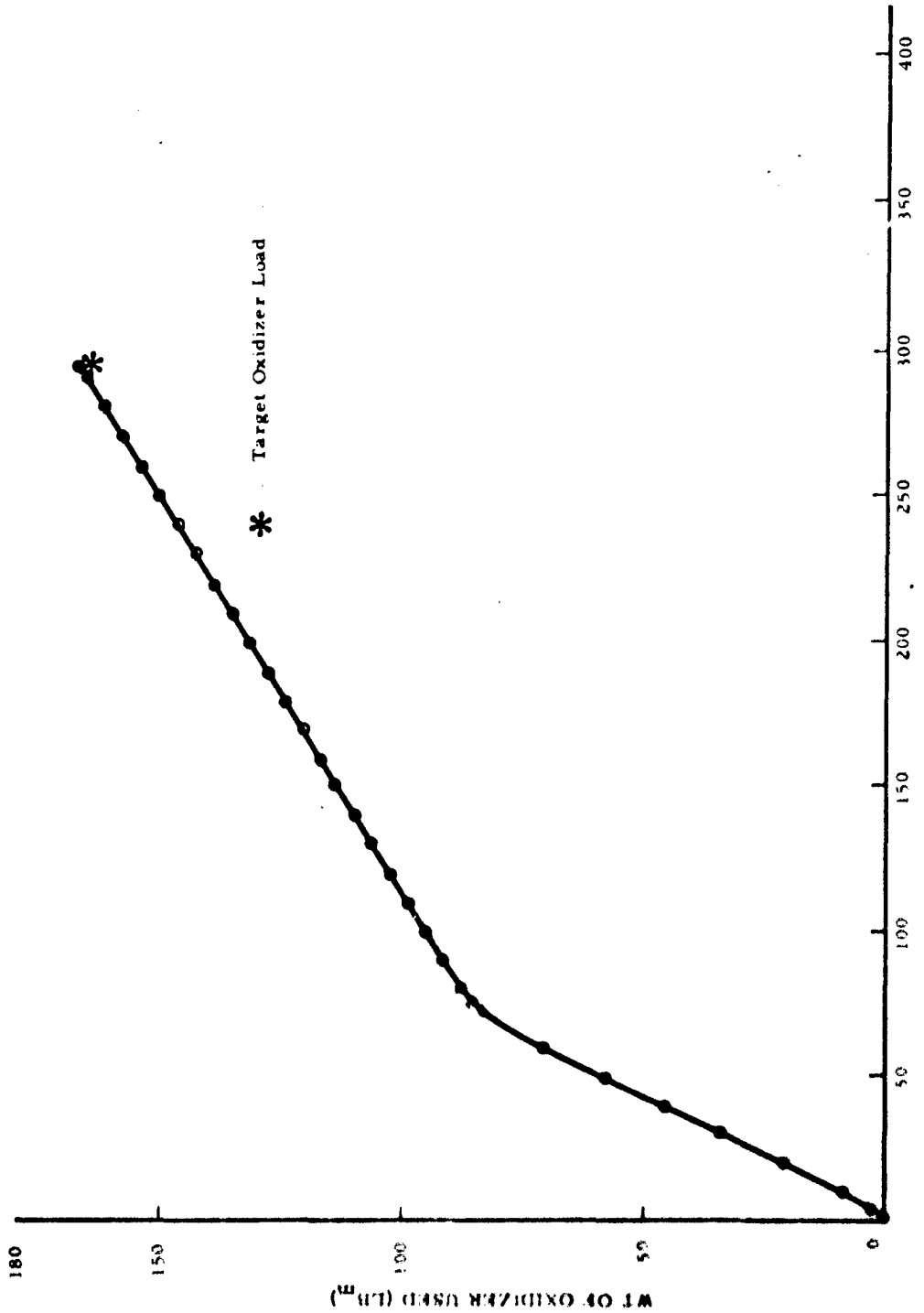

Figure B-8. Estimated Oxidizer Utilization for Certification Test 5F

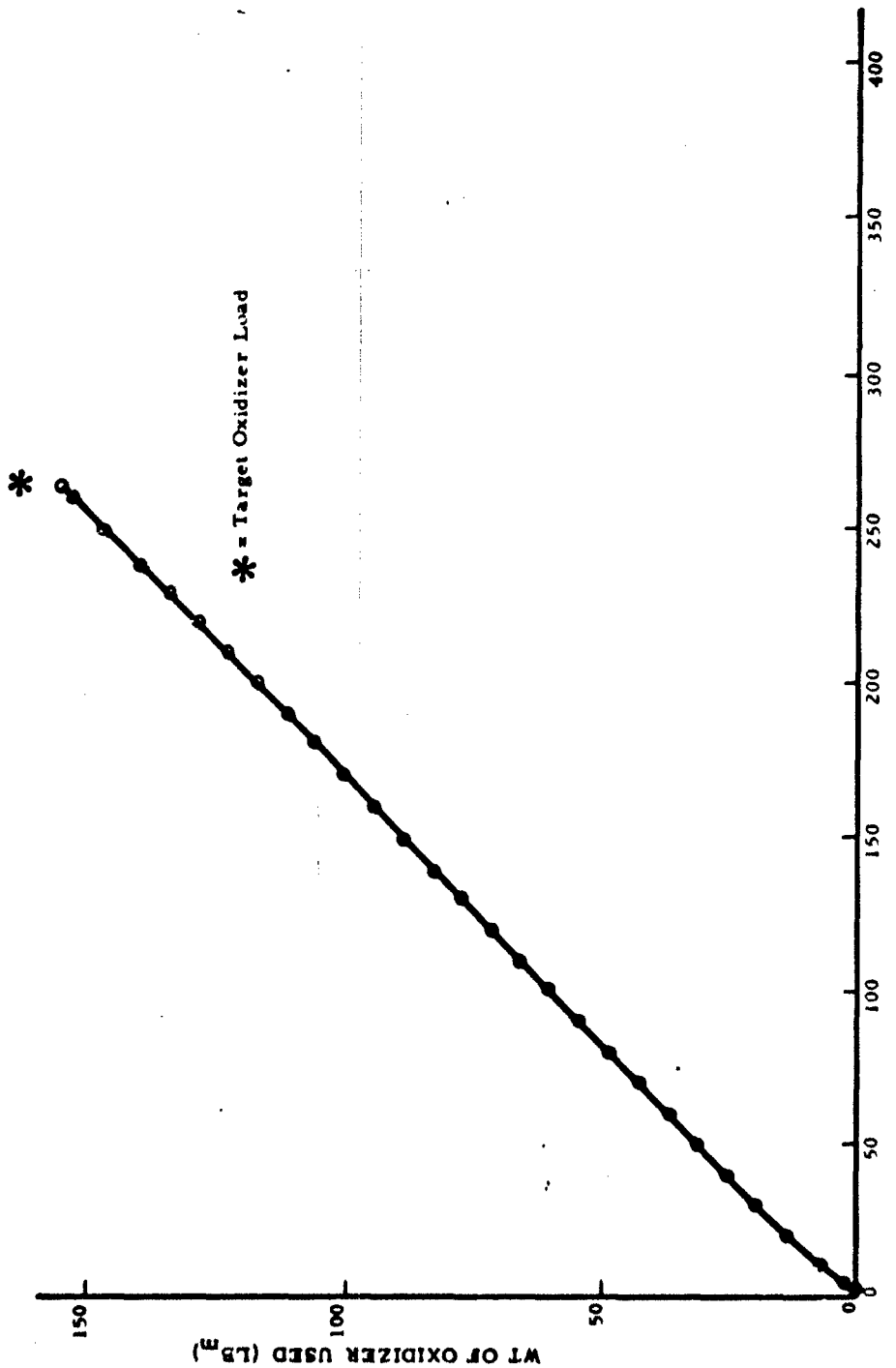

Figure B-9. Estimated Oxidizer Utilization for Certification Test 6F

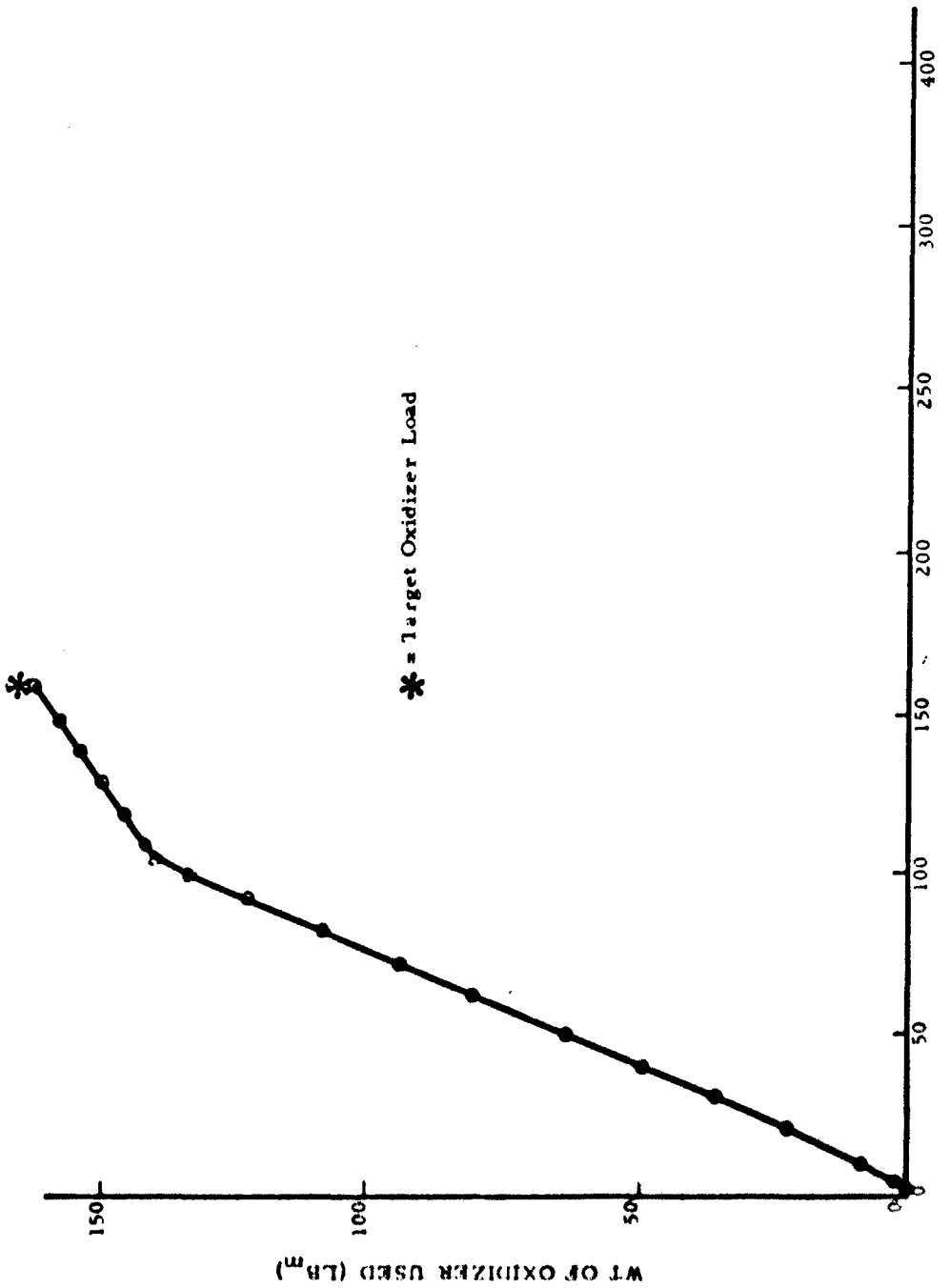

Figure B-10. Estimated Oxidizer Utilization for Certification Test 7F

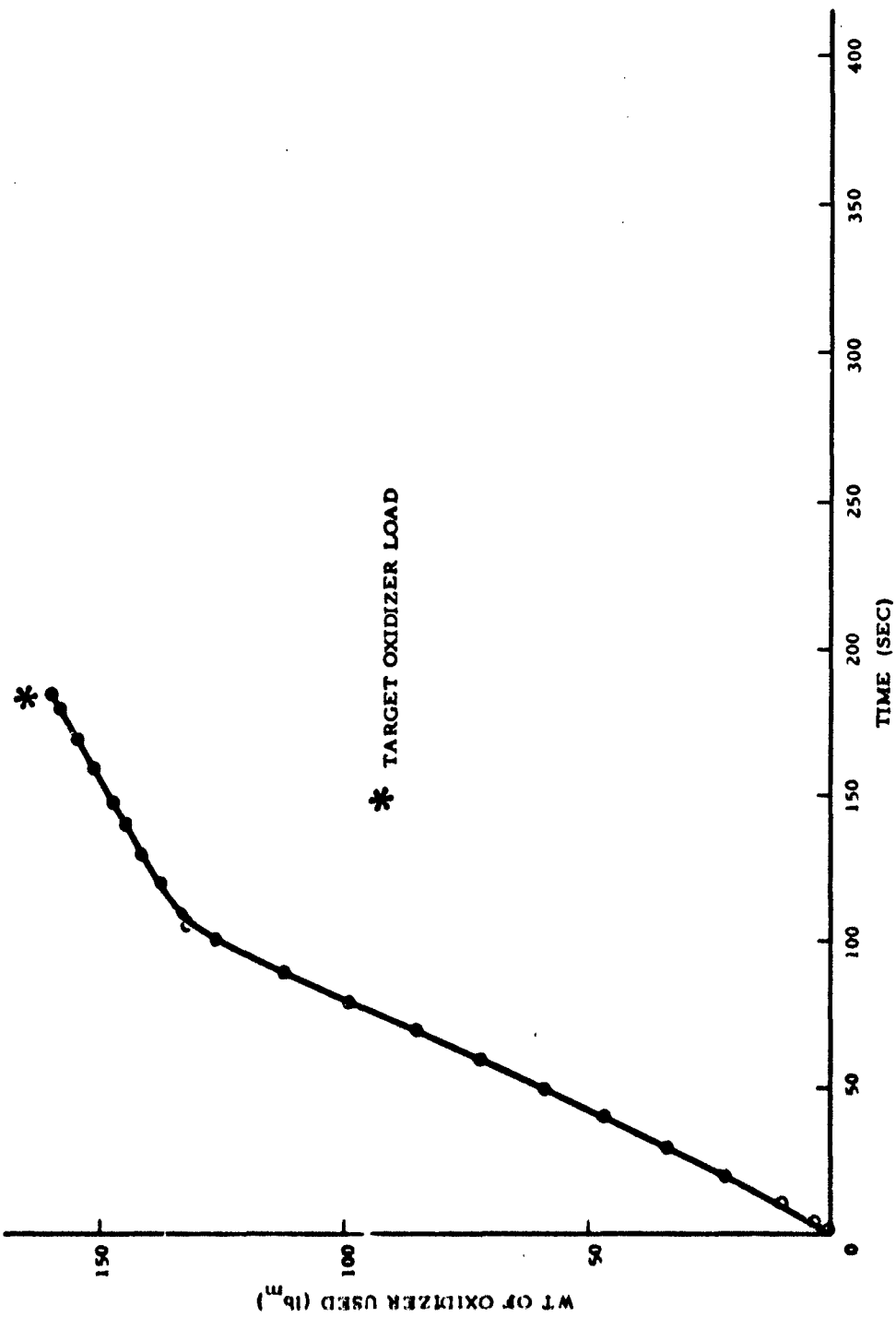

Figure B-11. Estimated Oxidizer Utilization for Certification Test 8F

APPENDIX C

THEORETICAL HYBRID COMPUTER TECHNIQUES

APPENDIX C

THEORECTICAL HYBRID COMPUTER TECHNIQUES

(U) One of the most difficult hybrid parameters to evaluate is the burning rate of the solid fuel. Yet, this parameter must be known as a function of grain length and firing duration to determine fuel utilization, the variation of thrust with time, and the variation of oxidizer-to-fuel ratio with time.

(U) While it is difficult to evaluate this burning rate (sometimes called the regression rate) either experimentally or theoretically, it has been done, with varying degrees of success. Experimentally, an average value of weight loss per total burning time can be found by direct weight or volume displacement measurements of the motor before and after a test. Light probe, thermocouple, and pyrofuse wire techniques have been used to estimate the instantaneous burn rate at particular points along the grain length by indicating physical passage of the fuel surface. They have been found to be difficult to implement and subject to inaccuracy. Theoretically, the instantaneous regression rate can be estimated as a function of both grain length and burning time.

(U) However, any analytical hybrid model is complex. The physical situation for any engine is a two-dimensional, non-isothermal turbulent flow problem complicated by chemical reactions. In a perfectly rigorous mathematical simulation of the hybrid, all of the heat, mass, and momentum transfer processes and chemical kinetic effects must be described and coupled together. Thus, most fundamental investigations, to simplify their theoretical descriptions, have assumed heat transfer to the solid fuel surface and/or kinetic effects to be the controlling mechanisms of combustion. Their work is then limited to describing these phenomena. Spangler has summarized many of these film and boundary layer theories (Reference C-1).

Test data indicate that the theories of Marxman and Muzzy (United Technology Center) and Smoot and Price (Lockheed Propulsion Company) correlate and predict hybrid performance. These two computerized performance programs have been written up in detail in References C-2 and C-3. As the empirical constants required for the UTC analysis had already been evaluated for the MON-25/Mg + Plexiglas propellant system, this heat-transfer theory was used in a modified computer program (WS-275) to calculate fuel flow rates for the Sandpiper.

(U) The detailed derivation and description of the equations used in this model are given in Reference C-2. Thus, this appendix will only describe how they were used on the Sandpiper. Figure C-1 illustrates format and order of input data cards. Figures C-2 and C-3 show general and detailed block diagrams of the computer program. A Fortran listing using the nomenclature shown in Table C-I is provided in Figure C-4. The listing is liberally sprinkled with numbered comment statements to facilitate an understanding of the various parts of the program. The following detailed discussion of the program will be broken up into sections distinguished by these comment cards.

(U) The heat transfer controlled regression rate theory used in this model provides the equation shown below:

$$\dot{r} \sim qc\left(\frac{\dot{m}}{Ap}\right) + qr(Pc)$$

where,

$\dot{r}$ = linear regression rate

qc, qr = convective and radiative heat transfer rates, respectively

$\dot{m}$ = mass flow rate through port

Ap = cross-sectional area of port

Pc = chamber pressure

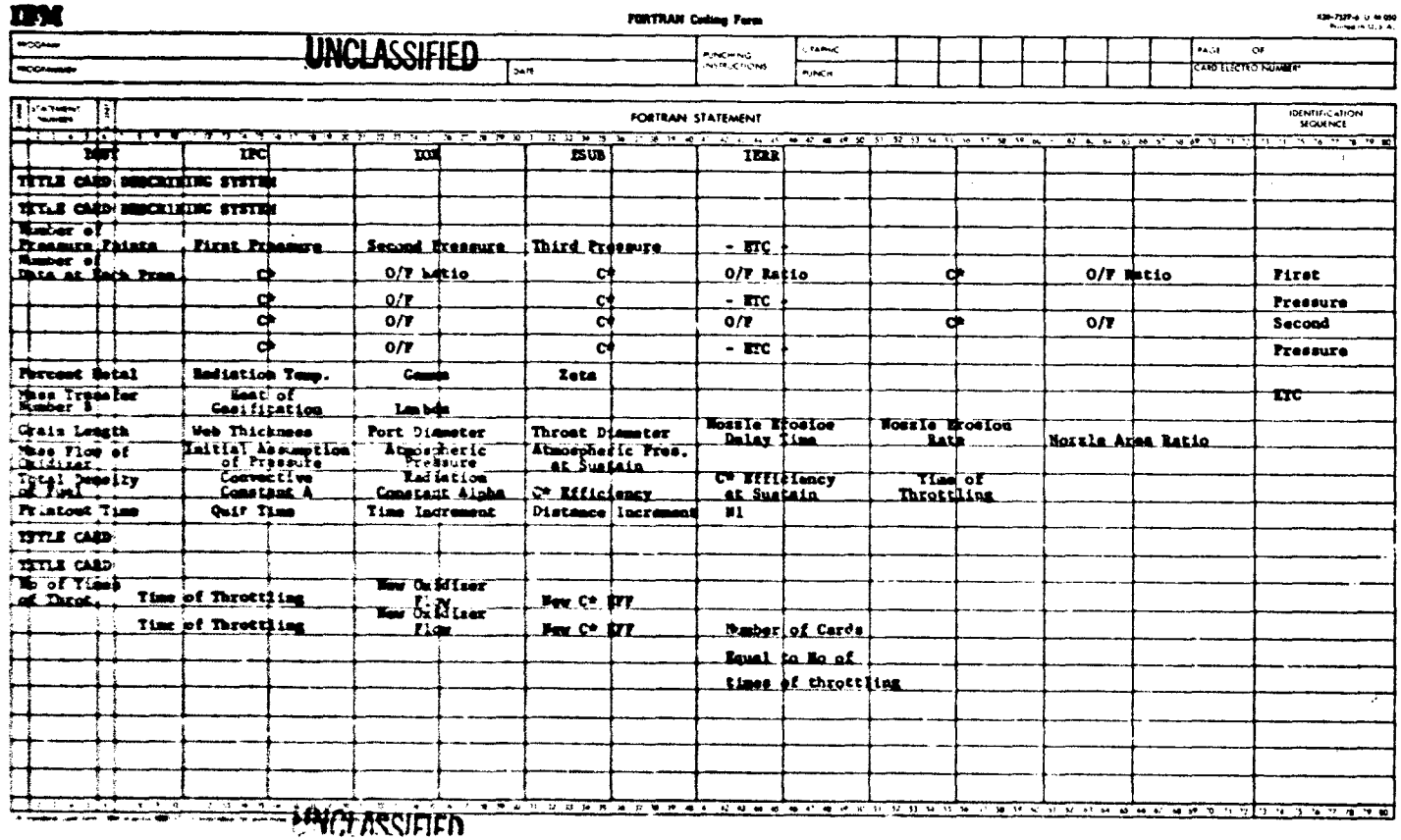

IBM FORTRAN Coding Form

UNCLASSIFIED

	IDENT	IPC	IOB	ESUB	IERR				
TITLE CARD: DESCRIBING SYSTEM									
TITLE CARD: DESCRIBING SYSTEM									
Number of Pressure Points	First Pressure	Second Pressure	Third Pressure	- ETC -					
Number of Data at Each Pres.	C*	O/F Ratio	C*	O/F Ratio	C*		O/F Ratio		First
	C*	O/F	C*	- ETC -					Pressure
	C*	O/F	C*	O/F	C*		O/F		Second
	C*	O/F	C*	- ETC -					Pressure
Percent Metal	Radiation Temp.	Gamma	Zeta						
Mass Transfer Number B	Heat of Gasification	Lambda							ETC
Grain Length	Web Thickness	Port Diameter	Throat Diameter	Nozzle Erosion Delay Time		Nozzle Erosion Rate		Nozzle Area Ratio	
Mass Flow of Oxidizer	Initial Assumption of Pressure	Atmospheric Pressure	Atmospheric Pres. at Sustain						
Total Impulse of Fuel	Convective Constant A	Radiation Constant Alpha	C* Efficiency	C* Efficiency at Sustain		Time of Throttling			
Pressure Time	Quit Time	Time Increment	Distance Increment	N1					
TITLE CARD									
TITLE CARD									
No. of Times of Throt.	Time of Throttling	New Oxidizer Flow	New C* Eff						
	Time of Throttling	New Oxidizer Flow	New C* Eff	Number of Cards Equal to No of times of throttling					

UNCLASSIFIED

Figure C-1. WS-275 Input Data Format

UNCLASSIFIED

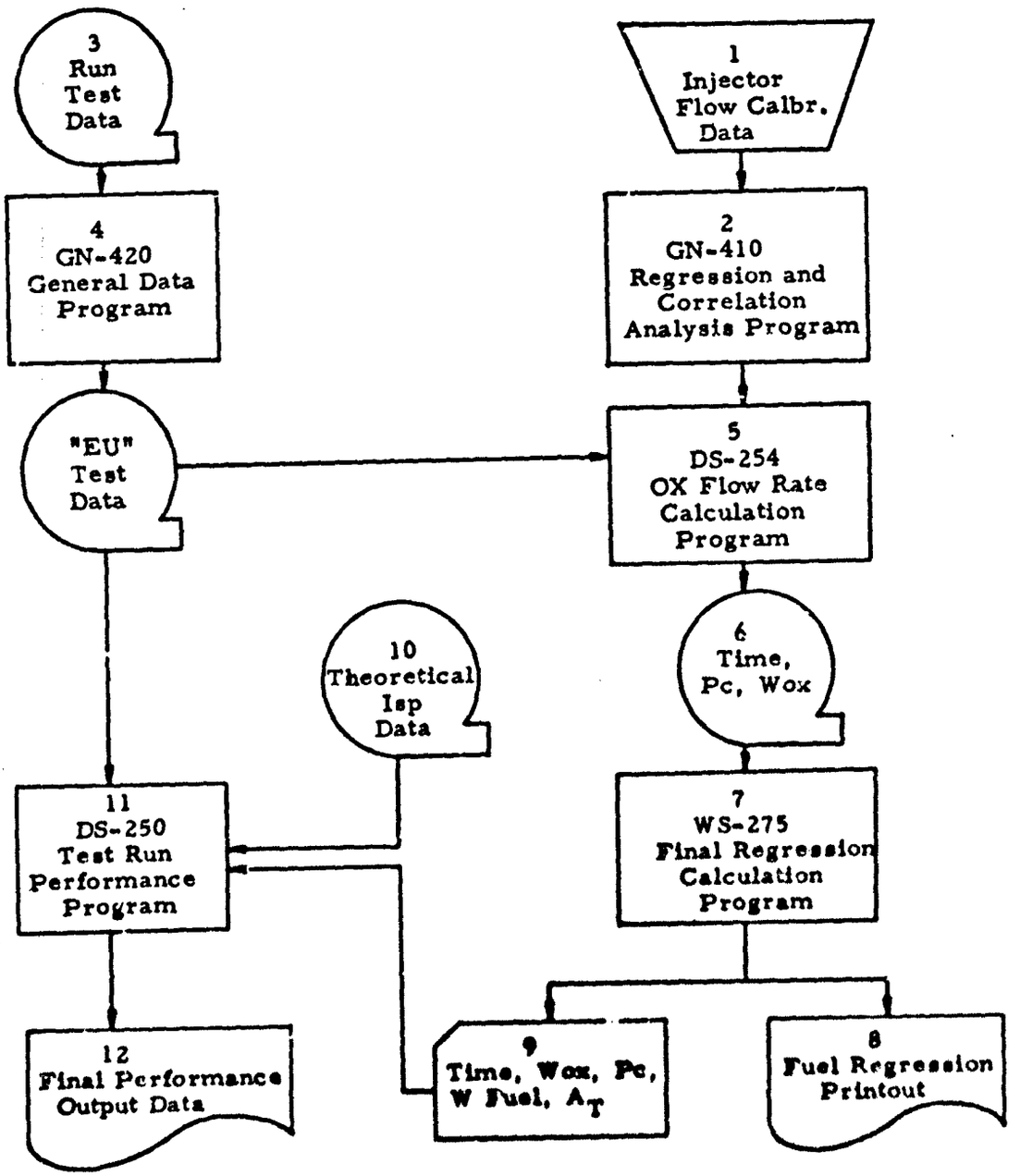

Figure C-2. WS-275 Data Flow Chart

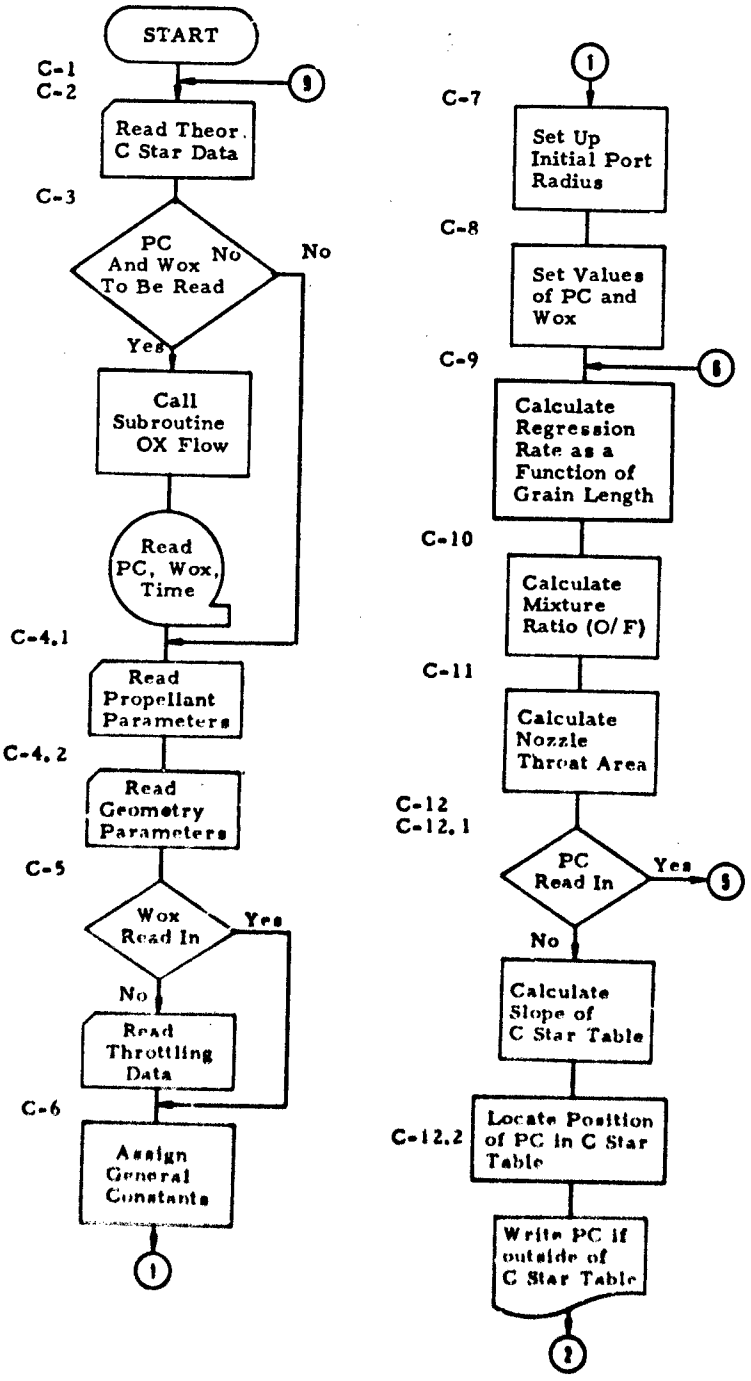

Figure C-3. WS-275 Block Diagram

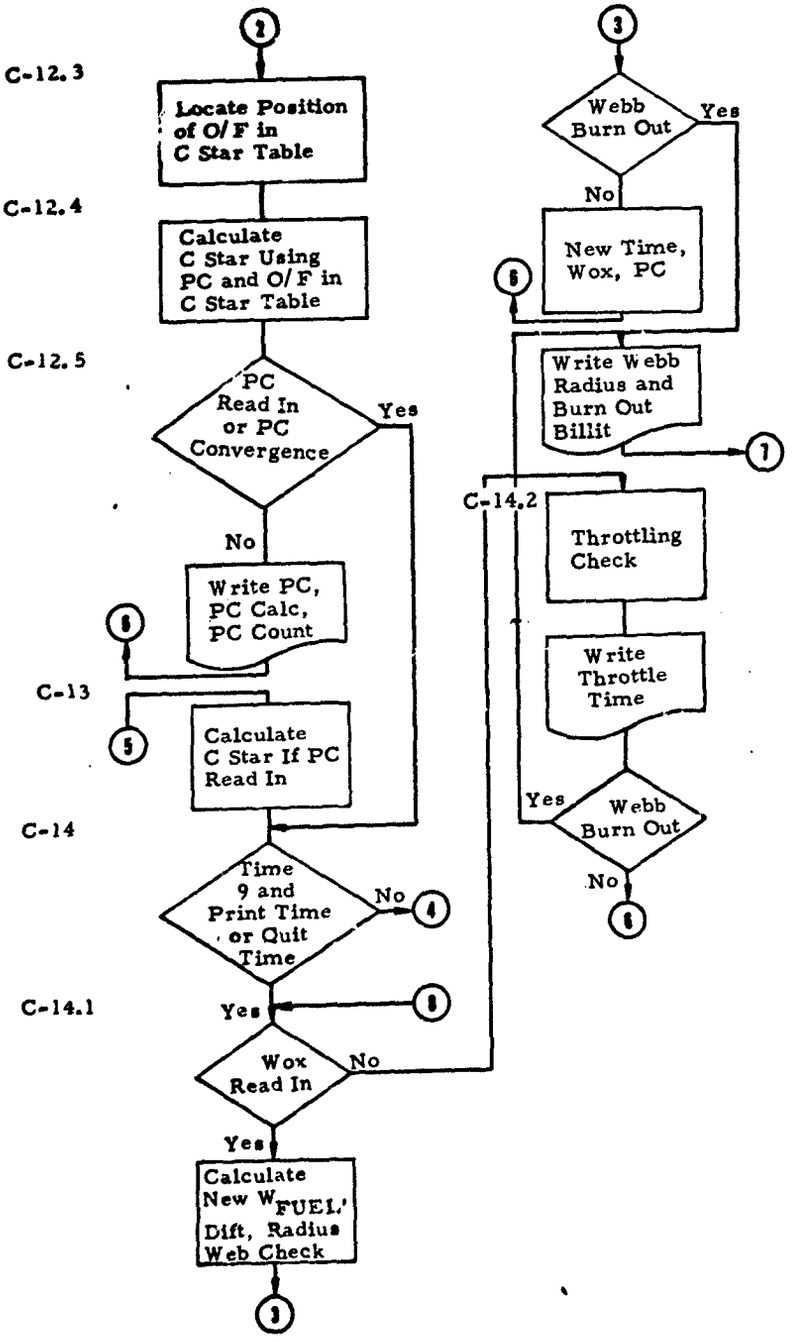

Figure C-3. WS-275 Block Diagram (con't)

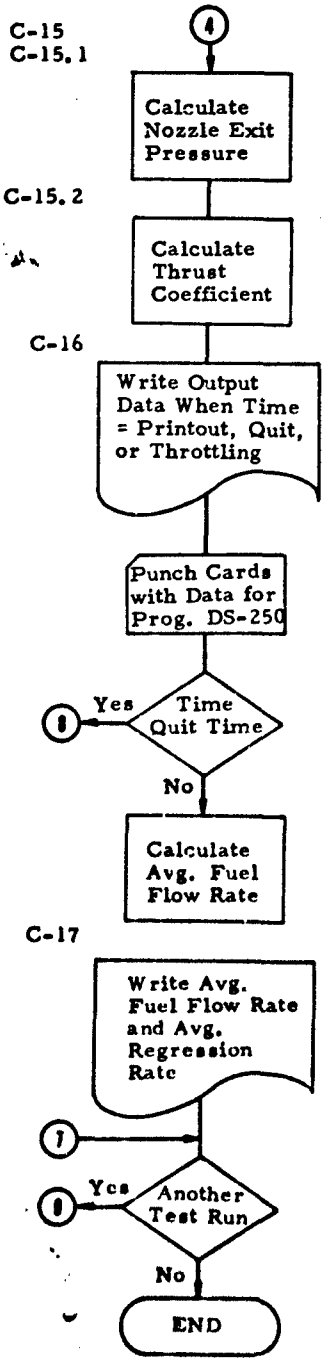

NOTE: C-1 THROUGH C-17 INDICATES COMMENT NUMBERS IN COMPUTER PROGRAM FORTRAN LISTING

Figure C-3. WS-275 Block Diagram (con't)

TABLE C-I. WS-275 PROGRAM NOMENCLATURE

Name	DIM VAL	UTC SYM	Description
A	0.027	a	Convective Constant (K CON)
ALF	24		Header for run information
ALPHA	0.4E12		Radiation Constant
AP		A_p	Port Area
APGEOM	100	A	Geometrical Port Area
AK	21		Area Ratio
ARNEW			
AT			Nozzle Throat Area
AT1			Nozzle Throat Area (Preliminary Value)
AVED			
AVERAD			
B	10	B	Thermochemical mass transfer number
CHGT	10		Time Throttling Occurs
CORR			
CS			C* as calculated from C* Table
CSDIFF			Difference between C* values in C* Table
CSK			
CKSPI			
CST	11,40		C* data for C* Table
CSTAR			C* calculated using Pc from subroutine OXDATA
CSTEFF	90%		C STAR Efficiency
CSTIN			
D	3.1 in	D	Diameter (in.) $(4 A / \pi)^{1/2}$
DELAY	175 sec		Erosion Delay (sec)
DELP			Difference in Pc values in C* Table
DELR			
DELT	1		Time increment (sec)
DELX	1		Distance increment (in.)

TABLE C-I. WS-275 PROGRAM NOMENCLATURE (Cont'd)

Name	DIM VAL	UTC SYM	Description
DIFT			Difference between reduction times
DIN		D	Initial diameter (in.) $(4\ A\ /\pi)^{1/2}$
DISDIA		28*	Boundary-layer displacement thickness *2
DT	0.89 in		Diameter of throat (in.)
EG			
EQ			
EQ1			
ERR	0.000187		Erosion Rate (in/sec)
EW	0.9		
F			Counter for printing C* Table
FRACT			Used for calculation of Pc from C* Table $\left(\frac{P-PCST}{DELP}\right)$
G	100		Mass flux (lb/sec - in^2)
GAMMA	1.2		Specific heat ratio
GASCON	1		Specific heat ratio (Cv/Cp)
GEE	386.4		
GM1			
GP1			
HV	600	Hv	Heat of gasification
I			
ICST	-		Code for C* Table input
IϕX	-		Code for reading WOX from subroutine OXDATA
IPC	-		Code for reading PC from subroutine OXDATA
ISP			
J			Do loop counter
JM1			Subscript term used in calculating data from C* Table

TABLE C-I. PROGRAM NOMENCLATURE (Cont'd)

Name	DIM VAL	UTC SYM	Description
K			Counter for calculating data from C* Table
L			Counter for printing C* Table
LAMBDA	1.666		Mass of particular combustion products formed per unit mass of nonvolatile surface material
LNG	46.7 in	L	Length of fuel grain
MDOT	100	$\dot{m}g$	Total gas flow
MDOTOX	1.27		Head-end ox flow (specified) lb/sec
MOLWT	22		
N			
N1	1		Print out increment for length
NALPHA			Counter for number of different ALPHA's
NCST	40		Number C* + O/F values for each Pc in C* Table
NCSTEF	10		New C* Efficiency
NDP	C-		Number data points from subroutine OXDATA
NEWϕX	10		New ox flow after throttling
NOTIME			Number times motor throttles
NP			Do loop counter for locating Pc in C* Table
NPCST	11		Number Pc inputs to C* Table
NRLIN	C-		Run number from subroutine OXDATA
NT			Subscrip counter for each reduction time
NX			Integer of XN
OF			Mixture ratio for calculating C* in C* Table
OFF	11,40		Mixture ratio (O/F) for C* Table
OX			Ox flow used in calculations for each time

TABLE C-I. WS-275 PROGRAM NOMENCLATURE (Cont'd)

Name	DIM VAL	UTC SYM	Description
OXDATA			Subroutine for inputing Run Pc, WOX, TIME
OXFLOW			Call for subroutine OXDATA
P	-	p	Pc used in calculation for each time
P1			
P2			
PATMOS	1.68		Exit Press (psia)
PC	C400		Chamber press from subroutine OXDATA
PCALC			
PCOUNT			Counter for Pc for each time
PCST	11		Pc for C* Table
PDIFF			
PER		Per	Perimeter of Port
PERM1	0.9		1.-PERME
PERME	0.1	K	Mass fraction of nonvaporizing component in fuel
PERMR			PERME/PERM1
PI	3.14159		Constant
PIA	0.7853975		$\pi/4$ for calculating Area
PMDOT		$\dot{m}g$	MDOT of previous grain billet used in MODT equation
PNEW			
POT	10		Print out time (sec)
PRNT	10		Print time interval
PS	500		Initial Pc (specified) psia
PSTORE		P	Stored value of Pc
QC		$\dot{q}c$	Convective heat transfer in the absence of radiation
QR		$\dot{q}r$	Radiative heat transfer
QRQC		$\frac{\dot{q}r}{\dot{q}c}$	Radiative to convective heat transfer ratio

TABLE C-I. WS-275 PROGRAM NOMENCLATURE (Cont'd)

Name	DIM VAL	UTC SYM	Description
QT	275		Quit time (sec)
R	100	$\dot{r}$	Regression rate (in/sec)
RAD	100		Radius (in.)
RAD134			D/2
RAD2			$\frac{D-1}{2}$
RADCON			
RADN			
RADP	0.59E-4		
RADSUM			
RADTOT			
RATE		$\dot{r}$	Regression rate (in/sec)
RAVE			
RCOUNT			Counter for R for each time
RDEN			
RDIFF			Regression rate difference for each billet
RHO			
RHOOPT			
RHOP	0.137		
RHOT	0.042		Total grain density (lb/in^3)
RHOV			RHOT * PERMI
RHOVR			
RMASS			
SALPHA			Starting ALPHA read in
SIGMA	3.307E-15		Stefan-Boltzman constant
SLOPE	11.40		Slope of C* versus OFF from C* Table
SNGCT			
SUM			Summation of WFuel (SUM = SUM + WF * DIFT)

TABLE C-I. WS-275 PROGRAM NOMENCLATURE (Cont'd)

Name	DIM VAL	UTC SYM	Description
T		t	Time used in calculations
T1			
T2			
TE		Tr	Effective radiation temp used in equation
TEO	800		
TH			
THCOE			
THROT			
TIME	C400		Run time (sec) from subroutine OXDATA
TITLE	24		Heading for C* Table + other information
TR	4000°R	Tr	Effective radiation temp (°R)
TRAD		Tr^4	
UNIT	24		
VISC	0.134E-5		Viscosity
W	3.35 in		Webb thickness (in.)
WEBCHK			Indication of webb burn out (WEBCHK = W + D/2)
WF			Fuel flow
WFUEL	400		Fuel flow (lb/sec) (WFUEL = WF * DIFT)
Wϕ	C400		Ox flow (lb/sec) from subroutine OXDATA
WT			Total flow (ox + wf)
X	100		Distance increment (number)
XA		XA	Value of boundary layer merge point (XA = XBL*2*RAD)
XBL	5		Boundary layer merge point
XCRIT	25		Critical value of X/Diameter
XM	100		Mass flow rate (lb/sec)
XN			LNG/DELX

TABLE C-I. WS-275 PROGRAM NOMENCLATURE (Cont'd)

Name	DIM VAL	UTC SYM	Description
XN1			Real N1
XOD			X/Diameter
XPRNT			
XX			Summation of DELX (XX = XX + DELX)
Z	-	Z	Optical path length
ZETA	0.666		Mass of ox consumed in producing particulate products per unit. Mass of nonvaporizing components in solid fuel.

```
$JOB            WS-275  30  SHIRLEY              RPK             RZ
$ID             WS-275       HYBRID TARGET MISSILE (SANDPIPER) PROGRAM
$**             ONE PART PAPER
$IBJOB          MAP
$FILE           *FTC04.*,U04,U04,BLOCK=3875,SINGLE,REEL,HIGH,LRL=154,
$ETC            RCT=25,EOR=REORX.,ERR=RERRX.,TYPE3,EOF=REOFX.
$IBFTC HYBRID  NODECK,REF
C
C      THIS PROGRAM USES FRANK MEAD'S HYBRID TEST DATA -- CHAMBER PRESSURE
C      VERSUS TIME DATA -- TO CALCULATE OXIDIZER FLOW VERSUS TIME AND FUEL
C      FLOW VERSUS TIME. THE THEORETICAL EXPRESSIONS DEVELOPED BY MR. RAY
C      MUZZY (UTC) ARE USED TO CALCULATE THE REGRESSION RATE.  THE EFFECT
C      OF MASS ADDITION WITH PORT LENGTH AND THE CHANGE OF PORT AREA WITH
C      TIME ARE ACCOUNTED FOR.  HOWEVER, THE OPTION TO ITERATE ON CHAMBER
C      PRESSURE IS AVAILABLE.
C
C
       INTEGER F
       REAL LAMBDA, MDOT, NEWOX, NCSTEF, LNG, MOLWT, ISP, MDOTOX
       LOGICAL THROT
       COMMON/OXDATA/NRUN,NDP,TIME(400),PC(400),WOX(400)
       DIMENSION R(100),  G(100),  XM(100),  RAD(100), UNIT(24), TITLE(24)
      1, NEWOX(10), CHGT(10), NCSTEF(10), PCST(11), CST(11,40), OFF(11,40
      2), SLOPE(11,40),                                ALF(24), X(100),
      3APGECK(100), MDOT(100), WFUEL(400)
C
C       *****COMMENT 1*****
C      INDICATOR VALUES ARE READ.  THESE INDICATORS TELL COMPUTER WHETHE
C      OR NOT TO READ IN C STAR CHARTS8 CALL SUBROUTINE OXFLOW8 OR STOP
C      NOZZLE EROSION AFTER THROTTLING9
C
 1000 READ(5,101) ICST, IPC, IOX, ISUB, IERR
  101 FORMAT (5I10)
C
C      *****COMMENT 2*****
C      IF ICST IS GREATER THAN ZERO8 THE THEORETICAL C STAR DATA IS READ
C      IN AND PRINTED OUT (FOR CHECK PURPOSES) ON INPUT DATA PAGE OF OUTPUT
C
       IF (ICST .EQ. 0 ) GO TO 1060
       READ (5,102) (TITLE(I), I = 1,24)
```

Figure C-4. WS-275 FORTRAN Listing

```
  102 FORMAT (12A6 / 12A6 )
      READ (5, 103) NPCST, ( PCST(I), I = 1,NPCST)
  103 FORMAT (I1[illegible], 6F10.0 / (F20.0, 5F10.0) )
      READ (5, 104) NCST, (( CST(K,J), OFF(K,J), J=1, NCST), K=1,NPCST)
  104 FORMAT(I10, 6F10.0 /(F20.0, 5F10.0) )
      WRITE (6,201)
  201 FORMAT (1H1, 24H THEORETICAL C STAR DATA //)
      WRITE (6,202) (TITLE(I), I = 1, 24 )
  202 FORMAT (1H0, 12A6/ 1X, 12A6 )
      F = 0
 1001 L = F + 1
      F = L + 2
      IF (F .GT. NPCST ) F = NPCST
      WRITE(6,203) (PCST(K), K = L,F )
  203 FORMAT(1H0, 3(F11.0, 5H PSIA, 6X, 6HC STAR, 9X, 3HO/F) /)
      DO 1002  J=1,NCST
 1002 WRITE(6,204) (CST(K,J), OFF(K,J), K = L, F )
  204 FORMAT (1H , 3(16X, 2F12.3))
      IF(F .LT. NPCST) GO TO 1001
C
C     ***** COMMENT 3 *****
C     IF ISUB, IPC, AND IOX ARE GREATER THAN ZERO, THE PROGRAM CALLS FOR
C     SUBROUTINE OXFLOW WHICH PROVIDES PC AND OX FLOW RATE DATA VERSUS
C     BURN TIME.
C     PC IS OBTAINED FROM EXPERIMENTAL TEST RESULTS WHILE THE OXIDIZER
C     FLOW RATE IS CALCULATED FROM INJECTOR DELTA P AND WATER FLOW
C     CALIBRATION TESTS.
C
 1060  IF(IPC.EQ.0.AND.IOX.EQ.0) GO TO 1003
      IF(ISUB.EQ.0) GO TO 1003
      CALL OXFLOW
C
C     ***** COMMENT 4.1 *****
C     READ IN ADDITIONAL PROPELLANT PARAMETERS
C
 1003 READ(5,105)PERME, TR, GAMMA, ZETA
  105 FORMAT (7F10.0)
      READ(5,106) B, MW, LAMDA
      WRITE(6,205)
  205 FORMAT (1H1, 22H PROPELLANT PARAMETERS)
```

Figure C-4. WS-275 FORTRAN Listing (Cont'd)

```
      WRITE(6,205) (TITLE(I), I = 1,24)
  206 FORMAT (1H1, 12A6/ 1X, 12A6 )
      WRITE(6,207) PERME, TR, GAMMA, ZETA
  207 FORMAT(1H0, 30H PERCENT METAL IN THE GRAIN = F10.4, 10X, 25H RADIA
     1TION TEMPERATURE = F10.4, 15H DEGREES RANKIN,//, 1H0, 36H GAMMA (R
     2ATIO OF HEAT CAPACITIES) = F10.4,//, 1H0, 60H ZETA (OXIDIZER CONSU
     3MED PER UNIT MASS OF METAL IN GRAIN) = F10.4 )
      WRITE(6,208) B, HV, LAMBDA
  208 FORMAT(1H0, 36H THERMOCHEMICAL BLOWING PARAMETER B = F10.4,//,1H0,
     134H EFFECTIVE HEAT OF VAPORIZATION = F10.4, 7H BTU/LB,//, 1H0,
     284H LAMBDA (MASS OF PARTICLES FORMED PER UNIT MASS OF NON-VOLATILE
     3 SURFACE MATERIAL) = F10.4 )
C
C     ***** COMMENT 4.2 *****
C     READ IN GEOMETRY PARAMETERS AND OPERATING CONDITIONS OF MOTOR
C
 1004 READ(5,107) LNG, W,D,DT, DELAY, ERR, AR
  107 FORMAT ( 7F10.0 )
      READ(5,107) MOOTOX, PS, PATMOS, PATSUS
      READ(5,114) RHOT, A, ALPHA, CSTEFF,CSTEFS,STIME
  114 FORMAT ( 2F10.0, E10.3,3F10.0 )
      READ(5,113) PUT, UT,DELT, DELX, N1
  113 FORMAT (4F10.0, I5 )
      READ(5,108) ( ALF(I), I = 1,24)
  108 FORMAT ( 12A6 / 12A6 )
      WRITE(6,209) ( ALF(I), I = 1,24)
  209 FORMAT (1H1, 12A6/ 1X, 12A6 )
      WRITE(6,210) ( TITLE(I), I = 1,24 )
  210 FORMAT (1H0, 12A6/ 1X, 12A6 )
      WRITE(6,211) LNG, W, D
  211 FORMAT(1H0, 27H CYLINDRICAL PORT LENGTH = F10.4, 7H INCHES, 5X,
     113H WEB THICKNESS = F10.4, 7H INCHES,/,1H0,17H PORT DIAMETER =
     2F10.4, 7H INCHES )
      WRITE(6,212) DT, DELAY, ERR, AR
  212 FORMAT(1H0, 22H DIAMETER OF THROAT = F10.4, 7H INCHES, 5X, 24H NOZ
     1ZLE EROSION DELAY = F10.4, 6H SECONDS, /, 1H0, 23H NOZZLE EROSION
     2 RATE = F10.6, 13H INCHES / SEC, 14H AREA RATIO = F10.4 )
      WRITE(6,213) MOOTOX,PS
  213 FORMAT(1H0, 32H HEAD END OX FLOW (SPECIFIED) = F10.4, 7H LB/SEC,
     15X, 40H INITIAL CHAMBER PRESSURE (SPECIFIED) = F10.4, 5H PSIA )
```

Figure C-4. WS-275 FORTRAN Listing (Cont'd)

```
      WRITE(6,214) PATMOS,PATSUS
  214 FORMAT(1HO, 24H ATMOSPHERIC PRESSURE = F10.4,13H PSIA (BOOST),
     1F10.4,15H PSIA (SUSTAIN))
      WRITE(6,215) RHOT, CSTEFF,CSTEFS
  215 FORMAT(1HO, 30H TOTAL DENSITY OF THE GRAIN =  F10.4,15H LBS/CUBIC
     1INCH, 5X, 21H C STAR EFFICIENCY =  F10.4 ,8H (BOOST),F10.4,
     210H (SUSTAIN))
      WRITE(6,216) POT, QT, NI
  216 FORMAT(1HO, 24H PRINT OUT TIME (SEC) =  F10.4, 5X, 19H QUIT TIME (
     1SEC) =  F10.4, 5X, 30H DISTANCE INCREMENT (INCHS) =  I5 )
      WRITE(6,217) DELX, DELT
  217 FORMAT(1HO, 29H DISTANCE INCREMENT (INCH) = F15.3, 24H TIME INCREM
     1ENT (SEC) =  F15.3 )
      WRITE(6,218) A, ALPHA
  218 FORMAT(1HO, 25H CONVECTIVE CONSTANT A = F10.4, 5X, 30H RADIATION C
     1ONSTANT (ALPHA) = E15.8 )
C
C     *****  COMMENT 5  *****
C     IF IOX = 0 THEN THROTTLING DATA IS READ IN (NOTE -- IF IOX IS
C     GREATER THAN 0, THIS IS AUTOMATICALLY ACCOUNTED FOR SINCE WOX
C     V.S. TIME IS READ IN DIRECTLY)
C
      IF (IOX .GT. 0) GO TO 112
      READ(5,109) NOTIME, CHGT(1), NEWOX(1), NCSTEF(1)
  109 FORMAT ( I5, F15.0, 2F10.0 )
      IF (NOTIME .LE. 1)  GO TO 111
      READ (5,110) (CHGT(I), NEWOX(I), NCSTEF(I), I = 2, NOTIME)
  110 FORMAT( F20.0, 2F10.0 )
  111 IF( NOTIME .EQ. 0) GO TO 112
      WRITE(6,219) NOTIME
  219 FORMAT( 1HO, 11H THROTTLES  I5, 6H TIMES )
      WRITE(6,220)(CHGT(I), NEWOX(I), NCSTEF(I), I = 1, NOTIME )
  220 FORMAT(1HO, 28H TIME OF THROTTLING (SEC) =  F10.4, 5X, 23H NEW OX
     1FLOW(LB/SEC) =  F10.4, 5X, 14H NEW C STAR = F10.4 )
C
C     *****  COMMENT 6  *****
C     GENERAL CONSTANTS USED IN THIS PROGRAM
C     VALUES SHOULD BE CHECKED EACH TIME PROPELLANT COMBINATION IS
C     CHANGED.
C
```

Figure C-4. WS-275 FORTRAN Listing (Cont'd)

```
  112 RADP = 0.59E-04
      RHOP = 0.137
      VISC = 0.134E-05
      TCC  = 800.0
      EW = 0.9
      PI = 3.14159
      PIA = PI/4.0
      SIGMA = 3.3078-15
      GEC = 386.4
      PERM1 = 1.  - PERME
      RHOV = RHOT * PERM1
      PRNT = 10.0
      XCRIT = 25.0
      XBL = 5.0
      DELR = 0.0
      XN1 = N1
      XN = LNG / DELX
      NX = XN
      PERMR = PERME / PERM1
      GASCON = 1.0
      MOLWT =  28.0
      SUM  = 0.
        F  = 1
      THROT = .FALSE.
C
C     *****  COMMENT 7  *****
C     SET UP INITIAL PORT RADIUS
C     PROGRAM PUTS ORIFICE IN SECOND BILLET (DELX MUST BE
C
      DIN = 1.
      XX = 0.0
      RAD134 = D/2.0
      RAD2 = (D - 1.0) / 2.0
 1005 DO 1007  I = 1, NX
      XX = XX + DELX
      X(I) = XX
      RAD(I) = RAD2
      IF ( I .LE. 10 .OR. I .GE. 22 ) RAD(I) = RAD134
 1007 CONTINUE
C
```

Figure C-4. WS-275 FORTRAN Listing (Cont'd)

```
C      *****  COMMENT 8  *****
C      SET VALUES OF CHAMBER PRESSURE (P) AND OXIDIZER FLOW RATE (OX),
C      DIRECTLY VERSUS TIME FROM SUBR OXFLOW OR WHETHER THE DATA IS
C      CONSTANT WITH TIME.
C      IF ICX = ., P AND OX ARE CONSTANT AND ARE SET EQUAL TO VALUES READ
C      IN FROM INPUT DATA CARDS.
C
       NT = 1
       IF( ICX .GT. 0    ) GO TO 1009
       OX = POCTOX
       P = PS
       T = 0.0
       NT = 1
       GO TO 1022
 1009  OX = WOX(NT)
C
C      WHEN SUBR OXFLOW PROVIDES VALUES OF P AND OX FOR EACH TIME, THE
C      FOLLOWING STATEMENTS ARE USED.
C
       IF (OX .GE. 0.2 ) GO TO 1021
       NT = NT + 1
       GO TO 1009
 1021  P = PC(NT)
       IF(IPC.EQ.0) P=PS
       T = TIME(NT)
 1022  R(1) = 0.1
       RCOUNT = 1.0
       PCOUNT = 1.0
 1010  WF = 0.0
       PHOCT=OX
       RADSUM = 0.0
C
C      *****  COMMENT 9  *****
C      MAIN DO LOOP FOR REGRESSION RATE CALCULATION AS A FUNCTION OF
C      GRAIN LENGTH
C
       DO 1030  I = 1, NX
 1011  XA = XBL * 2.0 * RAD(I)
       IF ( X(I) .GT. XA ) GO TO 1012
       DISDIA = 0.42 * RAD(I) * (X(I)/XA) ** 0.8
```

Figure C-4. WS-275 FORTRAN Listing (Cont'd)

```
      GO TO 1013
 1012 DISDIA = 0.42 * RAD(I)
 1013 AP   = PIA * ( 2.0 * RAD(I) - DISDIA ) ** 2
      APGEOM(I)=PIA * (2.0 * RAD(I)) ** 2
      PER = PI * 2.0 * RAD(I)
 1014 MDOT(I) = PMDOT    * (1.0 - PERME - PERME * ZETA) * RHOT * R(I) *
     1PER * DELX
      G(I) = MDOT(I) / AP
C
C     HEAT TRANSFER FORM CONVECTION IS NOW CALCULATED.
C
      QC = A * HV * B**0.23 * (G(I)**0.8) *  (X(I)/VISC) **(-0.2)
C
C     PREPARATION REQUIRED TO CALCULATE THE RADIATIVE HEAT TRANSFER
C
      XOD = X(I) / (2.0 * RAD(I))
      IF (XOD .LE. XCRIT) GO TO 1015
      TE = TR
      GO TO 1016
 1015 TE = TEC + ((TR - TEC)/XCRIT) * XOD
 1016 RADCON =   3.75 * LAMBDA/PI * PERMR * (1.0 /((RADP**3) * RHOP))
      RDEN =(P   * MOLWT)/(GASCON * TE)
      RADN = RADCON * RDEN * (1.0/ MDOT(I)) * RHOV * R(I) * PER * DELX
      IF (X(I) .GT. XA) GO TO 1017
      RADN = RADN * (XA/X(I)) ** 0.8
 1017 IF ( G(I) .GT. 0.05 ) GO TO 1018
      CORR = (G(I) / 0.05) ** 0.2
      TRAD = CORR * TR ** 4
      GO TO 1019
 1018 TRAD = TR ** 4
 1019 Z = RAD(I)
      RHOOPT =(RADN +  RADSUM)* Z
      EG = 1.0 - EXP( - ALPHA * RHOOPT )
C
C     NOW THE RADIATIVE HEAT TRANSFER IS CALCULATED
C
      QR = SIGMA * EW * TRAD * EG
C
      QROC = QR / QC
      RHOVR = QC/HV * (QROC + EXP( -QROC ))
```

Figure C-4. WS-275 FORTRAN Listing (Cont'd)

UNCLASSIFIED


```
C
C       REGRESSION RATE (INCHES/SEC) SET EQUAL TO RATE
        RATE = RHOVR / RHOV
C
        RDIFF = R(I) - RATE
        IF( ABS(RDIFF) .LE. 0.01* R(I) ) GO TO 1020
        R(I) = ( R(I) + RATE ) / 2.0
        GO TO 1014
 1020 R(I) = RATE
        RADSUM = RADSUM + RADN
        XM(I) = R(I) * RHOT * 6.28 * RAD(I) * OFLX
        WF = WF + XM(I)
        R(I+1) = R(I)
        PPOCT=POCT(I)
 1030 CONTINUE
C
C       ***** COMMENT 10 *****
C
C       NOW THAT FUEL FLOW RATE IS KNOWN, ABLE TO CALCULATE TOTAL WEIGHT
C       FLOW AND O/F RATIO.
C
C
        WT =  OX + WF
        OF = OX / WF
C
C       CHECKS TO MAKE SURE CALCULATED O/F IS WITHIN BOUNDS OF C STAR DATA
C
        IF( OF.LT.OFF(1,1) .OR. OF .GT. OFF(1,NCST)) GO TO 2020
        GO TO 2021
 2020 WRITE(6,253) OF
  253 FORMAT(1HO, 49H STOP -- OF OUTSIDE OF BOUNDARIES OF INPUT DATA ,/,
     1 1HO, 12H OF RATIO = F10.4 )
        OF = 4.0
C
C       ***** COMMENT 11 *****
C       CALCULATE AREA OF NOZZLE THROAT
C
C       WHEN IERR = 0, THE EROSION OF THE THROAT STOPS AFTER THE MOTOR IS
C       THROTTLED AT STIME.  WHEN IERR IS GREATER THAN ZERO EROSION
C       REMAINS CONSTANT DURING SUSTAIN.
```

Figure C-4. WS-275 FORTRAN Listing (Cont'd)

UNCLASSIFIED

```
 2021 IF( IERR .GT. 0 .AND. T .GE. STIME ) GO TO 2026
      AT1 = PIA * ( DT ** 2.0 )
      IF (T .LE. DELAY ) GO TO 2022
      AT = PIA * (( DT + ERR * ( T - DELAY)) ** 2.0 )
      GO TO 2026
 2022 AT = PIA * (DT ** 2.0)
 2026 IF (IPC .GT. 0) GO TO 273
C
C     ***** COMMENT 12 *****
C
C     THIS SECTION IS ON USED TO CALCULATE PC WHEN IT IS NOT
C     AVAILABLE FROM SUBR OXFLOW (IPC = 0). AN ITERATIVE TECHNIQUE IS
C     USED.
C
C
C     ***** COMMENT 12.1 *****
C     THE POSITION OF EITHER THE INITIALLY ASSUMED OR PREVIOUSLY
C     CALCULATED VALUE FOR P IN THE THEORETICAL C STAR TABLE IS
C     DETERMINED.
C
      PSTORE = P
      NP = NPCST - 1
 2000 DO 2002 K = 1, NP
      IF( P  - PCST(K) ) 2004, 2005, 2001
 2001 IF( P  .LT. PCST(K+1) ) GO TO 2005
 2002 CONTINUE
C
C     IF THIS WRITE IS USED, THEN THE PRESSURE EXCEEDS THE LARGEST VALUE
C     IN THE C STAR TABLES.
C
      WRITE(6,251) P
  251 FORMAT(1H0, 80H STOP -- CHAMBER PRESSURE EXCEEDS THE MAXIMUM PRESS
     1URE IN THE C STAR TABLE, PC = F10.4 )
      GO TO 1000
C
C     IF THIS WRITE IS USED, THEN THE PRESSURE IS BELOW THE SMALLEST
C     VALUE IN THE C STAR TABLES.
C
 2004 WRITE(6, 250) P
```

Figure C-4. WS-275 FORTRAN Listing (Cont'd)

```
  253 FORMAT(1H0, 87H STOP -- THE CHAMBER PRESSURE HAS DROPPED BELOW MIN
     1IMUM PRESSURE IN C STAR TABLE, PC = F10.4 )
      GO TO 1000
C
C     *****  COMMENT 12.2  *****
C     CALCULATE SLOPE (USED TO INTEPOLATE BETWEEN C STAR POINTS)
C
 2023 DO 2025 K=1, NPCST
      DO 2024 J=2, NCST
      JM1 = J - 1
 2024 SLOPE(K, JM1) = (CST(K,J) - CST(K,JM1))/(OFF(K,J) - OFF(K,JM1))
 2025 CONTINUE
C
C     *****  COMMENT 12.3  *****
C     PROGRAM HAS LOCATED PC -- IT IS BETWEEN PCST(K) AND PCST(K+1)
C     THE O/F RATIO IS LOCATED IN EACH OF THESE PRESSURE TABLES FOLLOWED
C     BY CALCULATION OF C STAR VALUES USING THE SLOPES DETERMINED IN 12.2
C
 2005 CSDIFF = 0.0
      DO 2015  I = 1,2
      K = K + I -1
      J = 2
 2006 IF( OF - OFF(K,J) ) 2013, 2007, 2008
 2007 CS = CST(K,J)
      GO TO 2014
 2008 IF( J .GT. NCST ) GO TO 3000
      J = J + 1
      GO TO 2006
 2013 JM1 = J - 1
      CS = CST(K, JM1) + SLOPE(K,JM1) * (OF - OFF(K,JM1) )
 2014 CSDIFF = CS - CSDIFF
 2015 CONTINUE
C
C      *****  COMMENT 12.4  *****
C     PROGRAM HAS NOW LOCATED PC BETWEEN PCST(K+1) AND PCST(K),AND
C     OF AND CORRESPONDING C STAR VALUES AT EACH PRESSURE (K+1) AND (K)
C     NOW INTERPOLATES TO FIND C STAR CORRESPONDING TO PC
C
C     SINCE K=K+1 FROM PREVIOUS DO LOOP, MUST SET BACK TO ORIGINAL VALUE
C
```

Figure C-4. WS-275 FORTRAN Listing (Cont'd)

```
      K = K - 1
C
      DELP = PCST(K+1) - PCST(K)
      FRACT = (P  - PCST(K) ) / DELP
      CSKP1 = CS
      CSK   = CS - CSDIFF
      IF(T.GE.STIME) CSTEFF=CSTEFS
      CSTIN = 12.0 * CSTEFF * ( CSDIFF * FRACT + CSK )
C
C     CHAMBER PRESSURE IS NOW CALCULATED
C
      PCALC =(CSTIN * WT)/(GEE * AT)
C
      CSTAR = CSTIN / 12.0
C
C     DIFFERENCE BETWEEN NEW AND OLD CHAMBER PRESSURES
C
      PDIFF = PCALC - P
C
C     PROGRAM EITHER ITERATES UPON PRESSURE OR CONTINUES DEPENDING
C     ON WHETHER OR NOT PCALC - P DIFFERENCE IS WITHIN TOLERANCE.
C
C
C     *****  COMMENT 12.5  *****
C     TEST FOR PRESSURE CONVERGENCE -- IF CRITERIA MET CONTINUE, IF NOT
C     PROGRAM ITERATES UNTIL CONVERGENCE OBTAINED
C
 2016 IF (IPC .GT. 0 ) GO TO 1023
      IF ( ABS(PCALC - P ) .GT. 1.0        ) GO TO 2017
      GO TO 1023
 2017 CONTINUE
C
C     NOT WITHIN TOLERANCE, SO SET NEW VALUE OF P = TO OLD VALUE AND
C     RETURN AND CALCULATE NEW FUEL FLOW AND O/F (ITERATE).
C
      P  =  PCALC
      GO TO 1010
C
C     *****  COMMENT 13  *****
C     WHEN OXFLOW PROVIDES PC DIRECTLY, CSTAR IS CALCULATED DIRECTLY
```

Figure C-4. WS-275 FORTRAN Listing (Cont'd)

```
C
  273 CSTAR = P * AT * 32.2 / WT
C
C     *****  COMMENT 14  *****
C     THE PROGRAM NOW PROVIDES A TIME CHECK
C
C     IF TIME HAS REACHED EITHER PRNT OR OT, THE PROGRAM WRITES
C     OUT ITS RESULTS
C
C     IF TIME IS LESS THAN OT, NEW VALUES FOR THE PORT RADIUS ARE CALCULATED
C     AND, IF APPLICABLE, NEW VALUES FOR PC AND OX FLOW ARE OBTAINED.
C
C     THE REGRESSION RATE CALCULATIONS ARE THEN REPEATED USING THESE
C     NEW VALUES OF RADIUS, FLOW RATE, PC, AND TIME.
C
 1023 IF (T .LE. TC.) GO TO 1036
      IF (T .GE. PRNT .OR. T .GE. OT) GO TO 1035
C
C     *****  COMMENT 14.1  *****
C     IF WOX, PC, AND TIME VALUES ARE AVAILABLE FROM OXFLOW, THIS
C     SECTION IS USED TO INCREMENT T AND PREPARE FOR THE NEXT FUEL
C     FLOW CALCULATION AT THIS NEW TIME.
C
 1031 IF ( ICX .EQ. 0 ) GO TO 1051
      NT = NT + 1
      DIFT = TIME(NT) - TIME(NT - 1)
      SUM = SUM + WF * DIFT
      WFUEL(NT-1) = WF
      DO 1032 I = 1, NX
      RAD(I) = RAD(I) + R(I) * DIFT
      WEBCHK = W + D / 2.0
      IF (RAD(I) .LE. WEBCHK ) GO TO 1032
      GO TO 1033
 1032 CONTINUE
      T = TIME(NT)
      OX = WOX(NT)
      P = PC(NT)
      IF(IPC.EQ.0) P=PS
      GO TO 1015
 1033 WRITE(6,254) T
```

Figure C-4. WS-275 FORTRAN Listing (Cont'd)

```
  254 FORMAT(1H1, 44H TERMINATION DUE TO WEBB BURN-OUT AT TIME = F10.3,
     1 9H SECONDS )
      WRITE(6,272) RAD(I), X(I)
  272 FORMAT (1H0, 2F6.3 )
      GO TO 1003
C
C     ***** COMMENT 14.2 *****
C     PROGRAM NOW PROVIDES A THROTTLING CHECK -- ONLY REQUIRED IF
C      WDX V.S. TIME DATA IS NOT FED IN AS INPUT DATA
C
 1051 T = T + DELT
      IF (T .EQ. CHGT(F)) THROT = .TRUE.
      IF (THROT)  GO TO 1052
      GO TO 1053
 1052 CSTEFF = NCSTEF(F)
      DX = NEWDX(F)
      WRITE( 6, 255)T
  255 FORMAT(1H1, 33H MOTOR HAS THROTTLED AT TIME = , F10.3,  8H SECONDS
     1)
      F = F + 1
      THROT = .FALSE.
 1053 DO 1061 I = 1, NX
      RAD(I) = RAD(I) + R(I) * DELT
      WEBCHK = W + D / 2.0
      IF (RAD(I) .LE. WEBCHK ) GO TO 1061
      GO TO 1033
 1061  CONTINUE
      SUM = SUM + WF * DELT
      WFUEL(NT) = WF
      NT = NT + 1
      GO TO 1013
C
C     ***** COMMENT 14.3 *****
 1035 PRNT = PRNT + POT
C
     ***** COMMENT 15 *****
C     CALCULATION OF THE THRUST COEFFICIENT
C
C     ***** COMMENT 15.1 *****
C     EQUATION 3-25 FROM PAGE  51 OF SUTTON IS USED TO CALCULATE THE
```

Figure C-4. WS-275 FORTRAN Listing (Cont'd)

```
C     NOZZLE EXIT PRESSURE.  THIS MUST BE AN ITERATIVE PROCEDURE DUE TO
C     THE NON - LINEAR NATURE OF THE EQUATION.
C
 1036 ASSIGN 3003 TO N
      GP1 = GAMMA + 1.0
      GM1 = GAMMA - 1.0
      ARNEW = AR * AT1/AT
      P2 = PATMOS
 3001 T1 = (GP1 / 2.0 ) ** (1.0/GM1)
      T2 = (P2/P) ** (1.0/GAMMA)
      T3 = SQRT( GP1/GM1 * (1.0 - (P2/P) ** (GM1/GAMMA)) )
      EQ = ( 1.0/ARNEW ) - T1 * T2 * T3
      IF ( ABS(EQ) - 0.01) 3005, 3005, 3002
 3002 GO TO N, (3003, 3004)
 3003 ASSIGN 3004 TO N
      P1 = P2
      EQ1 = EQ
      P2 = P2 / 2.0
      GO TO 3001
 3004 PNEW = (P1 * EQ - P2 * EQ1) / (EQ - EQ1)
      P1 = P2
      EQ1 = EQ
      P2 = PNEW
      GO TO 3001
 3005 CONTINUE
C
C     *****  COMMENT 15.2  *****
C     THE PROGRAM NOW FINDES THE THRUST COEFFICITNT FROM EQ 3-30 OF
C     SUTTON (PAGE 54).
C
      T1 = ( 2.0 * GAMMA ** 2.0 ) / GM1
      T2 = ( 2.0/GP1) ** (GP1/GM1)
      T3 = 1.0 - (( P2/P ) ** ( GM1/GAMMA ))
      IF (T .GE. STEP2) PATMOS = PATSUS
      THCOE = SQRT( T1 * T2 * T3 ) + (P2 - PATMOS)/ P * ARNEW
      TH = THCOE * AT * P
      ISP = TH / WT
C
C     *****  COMMENT 16  *****
C     PROGRAM PRINTS RESULTS WHEN TIME = POT OR WHEN TIME = QT OR WHEN
```

Figure C-4. WS-275 FORTRAN Listing (Cont'd)

UNCLASSIFIED


```
C      THROTTLING OCCURS
C
       WRITE(6, 260) T,ALPHA,A
  260 FORMAT(1H0, 14H TIME (SEC) = F10.5 ,5X,8HALPHA = ,E11.4,
     15X,4HA = ,F7.4)
       XPRNT = XNI * DELX
       WRITE(6,261) XPRNT
  261 FORMAT(1H0, 23H PRINT OUT INCREMENT = F6.2,  7H INCHES)
       WRITE(6,262)
  262 FORMAT(1H0, 18H DISTANCE (INCHES), 5X, 16H RADIUS (INCHES), 5X,
     122H PORT AREA (SQ INCHES), 5X, 27H REGRESSION RATE (INCH/SEC) 5X,
     225H MASS FLUX (LB/SEC-SQ IN) )
       WRITE(6,263) ( X(I), RAD(I), APGEOM(I), R(I), G(I), I = 1, NX, N1)
  263 FORMAT(1H , 5X, F6.2, 10X, F6.2, 16X, F8.3, 21X, F8.5, 22X, F8.5 )
       WRITE(6,264) P, OX, CSTAR
  264 FORMAT(1H , 27H CHAMBER PRESSURE (PSIA) = F7.2, 5X, 31H OXIDIZER F
     1LOW RATE (LB/SEC) = F6.3, 5X, 19H C STAR (FT/SEC) = F8.3 )
       WRITE(6,265) THCOE, AT, WT
  265 FORMAT(1H0, 22H THRUST COEFFICIENT = F6.3, 34H NOZZLE THROAT AREA
     1(SQ INCHES) = F7.3, 41H TOTAL FLOW RATE (OX + FUEL) IN LBS/SEC =
     2F7.3)
       WRITE(6,266) ISP, TH, OF
  266 FORMAT(1H0, 44H SPECIFIC IMPULSE (THRUST/MASS FLOW RATE) = F8.3,
     116H THRUST (LBS) = F8.3, 27H MIXTURE RATIO (OX/FUEL) = F6.3 )
       WRITE(6,267) SUM, WF
  267 FORMAT(1H0, 43H TOTAL WEIGHT LOSS AT THIS TIME (LBS) = F8.3, 5X,
     1 26HFUEL FLOW RATE (LB/SEC) = F6.3/)
       IF (IPC .EQ. 0) GO TO 1100
       WRITE(7,700) T, OX, WF, P, AT
  700 FORMAT( 5F10.3 )
 1100 IF (T .LT. QT) GO TO 1031
       WRITE(6,268) QT
  268 FORMAT (1H0, 17H MAXIMUM TIME OF F10.5, 17H HAS BEEN REACHED )
C
C      ***** COMMENT 17 *****
C      AT END OF RUN PROGRAM CALCULATES THE AVERAGE FUEL FLOW RATE
C
       RADTOT = 0.0
       DO 1046  I = 1, NX
 1046 RADTOT = RAD(I) + RADTOT
```

Figure C-4. WS-275 FORTRAN Listing (Cont'd)

UNCLASSIFIED

```
      AVERAD = RADTOT/XN
      AVED  = 2.0 * AVERAD
      RMASS = (3.14/4.0) * LNG * RHO * (AVED*AVED - D*D) / (T)
      RAVE  = 12.0 * (AVED - D) / (2.0 * T)
      WRITE(6, 269) RMASS, RAVE
  269 FORMAT(1HO, 30H AVE MASS FLOW RATE OF FUEL = F7.3, 7H LB/SEC,
     123H AVE REGRESSION RATE = F8.5, 7H IN/SEC )
      GO TO 1000
 3000 CALL EXIT
      END
$IBFTC OXCALC
      SUBROUTINE OXFLOW
      COMMON/OXDATA/NRUN,NDP,TIME(400),PC(400),WOX(400)/
     1       TAPE/PINJ(400),DELP(400),WOXGPM(400)
      DIMENSION ITEM(7),NAME(13),DATA(13),KSUB(7),CHTIM1(4),CHTIM2(4)
      DATA ITEM/42HPC    PINJ  DELP  WOXGB WOXPB WOXGS WOXPS /
      EQUIVALENCE (KSUB(1),K1),(KSUB(2),K2),(KSUB(3),K3),(KSUB(4),K4),
     1           (KSUB(5),K5),(KSUB(6),K6),(KSUB(7),K7)
      DOUBLE PRECISION TTIME
      READ(5,80) NCHNG,NRUN,RHO
   80 FORMAT (2I2,F6.0)
      READ(5,82) PTIME,ETIME
   82 FORMAT (2F10.0)
      READ(5,84)(CHTIM1(I),CHTIM2(I),I=1,NCHNG)
   84 FORMAT (8F10.0)
      REWIND 4
      READ(4) (JUNK,I=1,6),NOEU
      READ(4) JUNK
      READ(4)(NAME(I),I=1,NOEU)
      DO 20 J=1,7
      DO 15 K=1,NOEU
      IF(ITEM(J).NE.NAME(K)) GO TO 15
      KSUB(J)=K
      GO TO 20
   15 CONTINUE
      WRITE(6,95)
   95 FORMAT(2X,29HDATA ITEMS DO NOT EQUAL NAMES)
      CALL EXIT
   20 CONTINUE
      DO 25 J=1,15
```

Figure C-4. WS-275 FORTRAN Listing (Cont'd)

```
25 READ(4) JUNK
   RRHO = SQRT(RHO)
   NC=1
   NDP=0
   STIME=PTIME
   ADTIME=1000.
30 READ(4) TTIME,(DATA(I),I=1,NOEU)
   IF(TTIME.LT.STIME) GO TO 30
   NDP=NDP+1
   TIME(NDP)=(TTIME-PTIME)/1000.
   PC(NDP)=DATA(K1)
   PINJ(NDP)=DATA(K2)
   DELP(NDP)=DATA(K3)
   IF(PINJ(NDP).LT.450.) GO TO 32
   WOXGPM(NDP)=DATA(K4)
   WOX(NDP)=DATA(K5)/RRHO
   GO TO 34
32 WOXGPM(NDP)=DATA(K6)
   WOX(NDP)=DATA(K7)/RRHO
34 IF(WOXGPM(NDP).LE.0.) WOXGPM(NDP)=0.
   IF(WOX(NDP).LE.0.) WOX(NDP)=0.
   STIME=STIME+ADTIME
   IF(STIME.GT.ETIME) GO TO 50
   IF(STIME.LT.CHTIM1(NC).OR.NC.GT.NCHNG) GO TO 30
   STIME=CHTIM2(NC)
   IF(ADTIME-5000.) 35,40,40
35 ADTIME=5000.
   GO TO 45
40 ADTIME=1000.
45 NC=NC+1
   GO TO 30
50 CONTINUE
   CALL UNLOAD (4,32,32HIF ANOTHER RUN LOAD NEW WOX TAPE)
   RETURN
   END
```

Figure C-4. WS-275 FORTRAN Listing (Cont'd)

The regression rate is primarily a function of the mass flow through the port, $\dot{m}$; the port cross-sectional area, Ap; the chamber pressure, Pc; and the regression rate itself. An iterative technique must be used to solve this implicit relationship.

(U) An examination of these independent variables helps illustrate the computer program. The mass flow through the port increases with length due to the mass injected from the fuel grain surface. Thus, the regression rate increases with length. The program simulates this increase by dividing the grain into finite increments and assuming the regression rate is constant over each interval. The rate within the first increment is calculated assuming the mass flow to be all oxidizer (input oxidizer flow rate). This regression rate adds a certain amount of mass into the chamber which, when added to the oxidizer flow rate, provides a larger mass flow to calculate the regression rate over the second increment. This additive procedure is continued down the length of the grain to yield a regression rate for each distance increment.

(U) Since the regression rate is inversely proportional to the port cross-sectional area which increases with time, the regression rate tends to decrease with time. To simulate this, the program divides the burning duration into finite time increments. After regression rate values have been determined over each distance increment, they are each multiplied by this time interval to calculate the corresponding change in port radius at each position. Thus, new values of the port area are determined and used to calculate new values of regression rate for this time.

(U) The previous two paragraphs describe in general the computer calculation of regression rate versus grain length and burning duration. When the chamber pressure is not read in versus time as input data from subroutine OXFLOW, it is also calculated. An assumed Pc value is read in to get the program started. Using this assumed value, regression rates are determined to provide the fuel flow rate and O/F ratio. The C-star

corresponding to this O/F and the assumed pressure is found from theoretical C-star data read in as input. Thus, a new chamber pressure can be found from

$$Pc = \frac{(C^*)\ (\dot{w}\ \text{total})}{(gc)\ (A\ \text{throat})}$$

If this new Pc and the initially assumed value do not agree within a specified tolerance, the assumed value is replaced by the new, and the procedure is repeated. This "iteration" process continues until the computer converges on Pc. Since the regression rate calculation is an implicit function, an iterative process is used over each distance increment to converge upon a value which satisfies both sides of the equation.

(U) Figure C-2 ties the above descriptions into a general schematic of the program. The input data are read in first, i.e., $\dot{m}$, Ap, and Pc. Based upon these values, the regression rate is calculated over each distance increment. Once the regression rate is known, values of the fuel flow rate, the total mass flow rate through the port, the O/F ratio, and the throat area are determined. If the Pc is not provided versus time from OXFLOW, an iterative scheme is used to converge upon a chamber pressure. At this point in the program, time is compared with printout time and quit time. If it has reached either a printout time or the end of the run, the computer calculates a thrust coefficient, a thrust, and a specific impulse, and prints out the results of the program. After writing the results, if a printout time was reached, or after calculating Pc, if time was below the printout time, time is incremented by a specified interval. The products of this time interval and the regression rates are added to the old values of port radius to give the new chamber geometry for this new time. If the oxidizer flow rate was not read as input data from OXFLOW, the program checks to see if this new time is equal to a time the motor throttles. If it is, the oxidizer flow rate is replaced by the throttled value. A check is made to make sure the new, enlarged port does not exceed the web thickness. If web burnout occurs, the program stops. Otherwise, the computer returns

and calculates new values of regression rate for this new time (enlarged port area). The program continues in this manner until quit time (end of run) has been reached. A condensed description of this procedure, referenced to the steps shown in Figure C-2, is given below.

(U) Step 1. A series of water-flow calibrations is conduced on each injector to be use. The flow rate is measured as the delta pressure across the injector is varied over the anticipated range.

(U) Step 2. These flow data are surface fit, using regression and correlation analysis program GN-410. This provides a set of coefficients for boost and sustain operating range values of chamber and injector pressures.

(U) Step 3. Run test data are recorded in digital form on magnetic tape.

(U) Step 4. The test data are edited and calibrated with general data program GN-420 and output in engineering units on magnetic tape.

(U) Step 5. Chamber and injector pressures are taken from the test data and used with the flow calibration coefficients to calculate oxidizer flow rate as a function of chamber pressure and injector delta pressure.

(U) Step 6. Chamber pressure (Pc) and oxidizer flow rate (Wox) versus run time are written on magnetic tape to be used with program WS-275.

(U) Step 7. Fuel regression calculation program WS-275 is designed to calculate Pc, Wox, and W FUEL versus time for a purely analytical case or may use actual Pc and Wox as calculated in program DS-254.

(U) Step 8. The data printout from WS-275 includes the various performance parameters as well as the fuel grain profile and regression rate for each desired run time.

(U) Step 9. Data cards are punched by the program to provide run times, Wox, W FUEL, and throat area (At) calculations for program DS-250.

(U) Step 10. Theoretical propellant performance data have been previously calculated and are recorded on magnetic tape to provide theoretical ISP, C star, and Cf.

(U) Step 11. All test data, along with calculated Wox and W FUEL, are compiled in run performance program DS-250. The thrust, pressure, temperature, and flow data are averaged for each time slice and all necessary corrections made. The required performance parameters such as exhaust velocity, expansion ratio, C star, ISP, and Cf are calculated. Calculated C star, ISP, and Cf are compared with the theoretical values to determine engine efficiency.

(U) Step 12. The final performance data are output in a tabulated report format.

(U) Figure C-3, a more detailed block diagram, has its various sections labeled by numbered Comment statements. These Comment statements correspond in number with the more detailed explanation and FORTRAN listing which follow.

(U) Comment 1: In this section, the fixed point indicators used with the program are read. While the significance of these indicators will become apparent as they are used in the program, they can be briefly identified as follows.

(U) ICST: When this indicator is set to zero, the program does not read and write the C-star data (used when multiple cases are run on same propellant combination and C-star values are already stored). When this indicator is any value greater than zero, the C-star data are read and printed out on the first output page.

(U) IPC; IOX; ISUB: When they are set equal to a positive number, these indicators tell the computer to read in subrouting OXFLOW and thus Pc and oxidizer flow rate as a function of time. When set equal to zero, the oxidizer flow rate is specified and held constant (unless motor is step-throttled) with time, and the chamber pressure is calculated via an iteration routine.

(U) IERR: This indicator is used in the routine that calculates the nozzle throat area. When set equal to 0, the nozzle erodes at a specified rate throughout the run (after specified heat-soak time has passed). When set to a positive number, the nozzle will erode up to a specified time, i.e., time of throttling to sustain, and then stop and remain constant at that throat size.

(U) Comment 2: If ICST is greater than zero, this section reads and writes theoretical C star (CST) versus O/F (OFF) data, using chamber pressure (PCST) as a parameter. A title card (TITLE) is also read and printed at this time to show what propellant combination and system these theoretical C-star data represent. The input format and order required for the data cards used in this section is identical with that for its counterpart in Reference C-2.

(U) Comment 3: When IPC, IOX, and ISUB are greater than zero, the program calls for subroutine OXFLOW which provides for storage of the chamber pressure (PC) and oxidizer flow rate (WOX), as a function of time (TIME). These are subscripted variables with as many values as the number of time increments (NT) desired. In other words, TIME (1) would

refer to the first time value (whatever time is picked from the run tape). PC (1) would have stored in its memory slot whatever chamber pressure corresponds to TIME (1). WOX (1) would refer to an oxidizer flow rate calculated (in subroutine OXFLOW) from the injector pressure drops at TIME (1).

(U) Comment 4.1: Additional propellant property parameters are read as follows (specific numerical evaluation of these parameters is discussed in Section IV of Reference C-2):

(U) Format: (7F10.0)

CC	Input	Description
1-10	PERME	Percent by weight metal in the solid fuel grain, %.
11-20	TR	Radiation temperature, ^{o}R. Taken to be 2/3 of stoichiometric flame temperature.
21-30	GAMMA	Ratio of specific heats.
31-40	ZETA	Mass of oxidizer consumed in producing metal oxide products per unit mass of nonvaporizing fuel particles.

(U) Format: (7F10.0)

CC	Input	Description
1-10	B	Thermochemical mass transfer number (commonly called Blowing Parameter).
11-20	HV	Effective heat of gasification of the solid fuel, BTU/lb.
21-30	LAMBDA	Mass of metal oxide product formed per unit mass of elemental metal in the solid fuel.

(U) Comment 4.2: Geometry Parameters and Operating Conditions are read according to the following format:

(U) Format: (7F10.0)

CC	Input	Description
1-10	LNG	Length of the grain, inches.
11-20	W	Web thickness, inches.
21-30	D	Chamber Diameter, inches.
31-40	DT	Nozzle throat diameter, inches.
41-50	DELAY	Delay time before nozzle throat starts eroding, sec.
51-60	ERR	Nozzle throat erosion rate, inches/sec.
61-70	AR	Area ratio.

(U) Format: (7F10.0)

CC	Input	Description
1-10	MDOTOX	Oxidizer flow rate, lb/sec. Used if oxidizer flow versus time is not calculated and made available from OXFLOW subroutine.
11-20	PS	Initial chamber pressure, psia. If Pc versus time not available from OXFLOW subroutine this value is used to start Pc iteration routine.
21-30	PATMOS	Atmospheric pressure, psia, that surrounds nozzle. Subtracted from nozzle exit pressure to calculate thrust coefficient.
31-40	PATSUS	Same as PATMOS if rocket cruises at the same altitude during sustain as in boost. Otherwise, changed accordingly.

(U) Format: (2F10.0, E10.3, 3F10.0)

CC	Input	Description
1-10	RHOT	Total density of the solid fuel grain, lb/in^3
11-20	A	Empirically determined constant (usually called the convective constant).
21-30	ALPHA	Empirically evaluated constant (usually called the radiation constant).
31-40	CSTEFF	C-star efficiency during boost operation.

41-50	CSTEFS	C-star efficiency during sustain.
51-60	STIME	Time at which motor throttles from boost to sustain, seconds.

(U) Format: (4F10.0, I5)

CC	Input	Description
1-10	POT	Printout time, sec. Interval between printouts.
11-20	QT	Quit time, sec. Time signifying end of the run.
21-30	DELT	Interval between time calculations, sec.
31-40	DELX	Interval between distance calculations, inches.
41-45	N	Printout interval for distance.

(U) Format: (12A6/12A6)

CC	Input	Description
1-72	ALF	Two cards that can be used to read and write alphabetic descriptive information.

(U) Comment 5: If the oxidizer flow rate is not available as a function of time from subroutine OXFLOW, the IOX will be equal to zero and the following throttling data will be read:

(U) Format: (I5, F15.0, 2F10.0)

CC	Input	Description
1-5	NOTIME	Number of times that the motor is throttled.
6-20	CHGT	Times at which the motor is throttled, sec.
21-30	NEWOX	New oxidizer flow rate after motor is throttled, lb/sec.
31-40	NSCTEF	New C-star efficiency applicable after motor throttles.

(U) Comment 6: This section sets up general constants that are continually used in the program. They are specified internally rather than read in on data cards each time, since they did not change in all of the

Sandpiper runs. However, when different systems are tested, the following constants should be scrutinized for possible change:

Constant	Description
RADP, RHOP	Radius and density of radiating metal particles.
VISC	Average viscosity of gas in combustion chamber.
TEO	Entering oxidizer temperature.
EW	Emissivity of solid fuel surface.
PRNT	Printout interval. Time between write statements.
XCRIT	Length/diameter ratio beyond which severe main stream dilution of oxidizer concentration causes a drop in regression rate.
XBL	Length/diameter ratio where boundary layers merge.
GASCON	The ideal gas constant was set equal to 1.0 for the MON-Mg + PMM system since UTC included this term in their experimental evaluation of ALPHA (radiation constant).

(U) Comment 7: The initial port radius and distance increments are set up by merely dividing the initial diameter by 2.0 at each point and by starting at zero and incrementing by DELX, respectively. It is pertinent to note that the Sandpiper has an orifice in the second billet. To change to the usually encountered cylindrical chamber, merely set RAD2 equal to RAD134 at internal statement number (ISN) 274. DELX must be equal to 1.0 in the program as it is now set up to obtain the correct orifice length. Measuring from the head end of the grain, the orifice is currently inserted between points 10 and 22 inches down the motor.

(U) Comment 8: Values of chamber pressure (P) and oxidizer flow rate (OX) are set up for each time calculation, depending on whether or not the values are read in from subroutine OXFLOW as a function of time or set constant. When the IOX indicator is zero, P and OX are assumed constant by the computer and set equal to PS and MDOTOX from input data

cards. The only time OX changes values after this is when the motor throttles. P is either kept constant at this value of PD or is changed each time increment through iteration, using the C-star tables. Time (T) is set equal to 0.0 and is evenly incremented by DELT after each time calculation. When IOX is greater than zero, values of WOX, PC, and TIME have been stored in the computer memory from subroutine OXFLOW. These values are redesignated by symbols OX, P, and T, respectively. If OX is below 0.2 lbs/sec, the computer skips up until it is above this value, as the thrust coefficient iteration routine will not converge otherwise (see Section 15.1).

(U) Comment 9: This is one of the most important sections of the program. At this point, the computer has all of the data required to use the Muzzy heat-transfer theory to calculate regression rate. Appendix I of Reference C-2 presents and derives these equations. Only their use will be discussed here. The regression rate is first calculated at the head end of the grain, based upon values of the entering oxidizer flow rate and the initial cross-sectional area of the port. Then this regression rate is assumed constant over a small distance increment, adding mass to the center flow. The regression rate calculated for the next finite increment is based upon a value of mass flow through the port equal to the entering oxidizer flow plus the mass addition over the last distance increment. Thus, the regression rate can be calculated down the length of the grain, increasing the mass flow rate through the port each time by the mass added over the previous increment.

(U) As the equations to calculate the regression rate are implicit (dependent upon this rate), an initial value is assumed at each distance increment and the computer iterates until the whole set of equations are satisfied. Specifically, the iteration process continues at each point until the calculated values of two successive iterations are within a specific tolerance.

(U) Comment 10: Once the regression rate is known for each distance increment down the length of the grain, these values are summed to arrive at the total fuel flow rate. This number, when divided into the oxidizer flow rate yields the O/F ratio. The O/F ratio is compared with the minimum and maximum mixture ratios read in as input C-star data. It it is outside of these boundaries, the panic button is pushed and the computer stops.

(U) Comment 11: During the boilerplate and flight certification tests, it was found that after a finite heat-soak time, the nozzle throat eroded at a fairly constant rate during boost. After the motors were throttled to their sustain level, nozzle throat erosion either continued at the same rate or stopped completely. These characteristics were simulated in this section of the program by calculating an initial throat area based upon the initial throat diameter. This area was kept constant during a DELAY time and then enlarged commensurate with a constant erosion rate, ERR. After throttling at STIME, erosion continued or stopped altogether based upon the value of IERR. After calculating the throat area, the program then proceeds to either Comment 12 and an iteration for pressure or it goes to Comment 13 and direct calculation of C-star, depending upon the IPC indicator value.

(U) Comment 12: This section is used to calculate the chamber pressure when the value of indicator IPC = 0 (Pc not available from OXFLOW). An initial value of the chamber pressure was assumed in order to calculate a fuel flow rate (radiative heat transfer is dependent upon Pc). This fuel flow then provided values of O/F ratio and total weight flow through the por.. Now, based upon the assumed Pc and calculated O/F, and total weight flow rate, a new value of Pc is calculated using the input C star versus O/F and pressure and the equation

$$Pc = \frac{C^* \cdot \dot{w}t}{A_t \cdot gc}$$

The assumed and calculated values of Pc are compared. If not within a specified tolerance, the assumed value is replaced by the calculated pressure and used to determine a new fuel flow, O/F, total weight flow, and pressure. This iterative process is continued until the new and old calculated values of Pc are within tolerance.

(U) Comment 12.1: The position of P within the input C-star table is located. After this section, the computer knows that P is between pressures PCST(K) and PCST(K+1). Checks to determine whether or not P is within bounds of input data are also provided at this point.

(U) Comment 12.2: The slope or ratio of C star to O/F between each input data point is calculated. These values are used to determine C star in Section 12.3.

(U) Comment 12.3: The O/F ratio is located in each of the two pressure tables from 12.1. These O/F ratios are multiplied by the corresponding slopes to provide C-star values at each point.

(U) Comment 12.4: The pressure, P, has now been located between two pressure tables. The O/F has been located within each pressure table and used to calculate corresponding C-star values. Now the slope of C star/pressure is used to calculate C star at P (whole objective of Section 12 really, since a new value of P is readily determined once C star is known).

(U) Comment 12.5: The difference between the newly calculated and old values of Pc is compared with a tolerance. If within tolerance, the program has converged upon a new Pc and continues to Section 14; otherwise, it replaces the old with the new and determines a new fuel flow and O/F (iterates).

(U) Comment 13: When subroutine OXFLOW provides Pc values and the Pc convergence routine is not used, a C-star value is calculated directly from the well-known expression:

$$C^* = (P)\ (AT)\ (gc)/\dot{w}_t$$

(U) Comment 14: The computer has calculated values for fuel flow, O/F, total weight flow, and Pc (if not read directly from OXFLOW). It now checks to see if it has reached either the quit time of the run or a printout time. If so, it prints out the results. If these points have been reached, it also calculates and writes out a thrust coefficient, a thrust, and the specific impulse. If a printout time or the end of the run have not been reached, time is incremented by DELT. Assuming the regression rate is constant over this small time interval, the radius of the port is enlarged by

$$R_{new} = R_{old} + \dot{r}\Delta t$$

Thus, after a new port cross-sectional area is calculated from the new radius, the program returns to Section 9 to repeat regression rate, fuel flow, O/F, etc., calculations for this new time.

(U) If the time, T, is less than 10 secs, the program prints. This can easily be changed (yank out Statement No. 1023), but was used to closely monitor engine characteristics during the first part of the run. If T is equal to printout or quit time, the computer writes out its results. This printout is accomplished by skipping to Sections 15 and 16 to calculate thrust and specific impulse and write, respectively. After printing results in Section 16, the program, depending upon whether or not quit time has been reached, either returns to Section 14 to increment time for another iteration, or continues to Section 17 where it terminates.

(U) Comment 14.1: If subroutine OXFLOW is available, this section is used to increase time and to prepare for the next fuel flow calculation at this new time. Since the run tapes from the actual tests were not marked off in even time increments, the time interval was determined by

subtracting successive values. The total weight loss at this time (called SUM) is calculated by multiplying the fuel flow rate by the time interval and adding this product to the previous value. Thus, the weight loss is accumulated and stored over all of the time intervals in SUM. The fuel flow rate for each time is stored separately and is available as subscripted variable WFUEL (NT), where NT refers to the number of time increments. New radius values are determined down the length of the grain by adding the product of $r\Delta t$ to the old values. If one of the new radius values exceeds the web thickness, the computer stops and prints Termination Due to Web Burn-Out at Time = ———. The value and location of this radius is also written out.

(U) After replacing the old values of T, OX, and P with new ones stored as TIME, WOX, and PC from OXFLOW, the program returns to Section 9 to calculate corresponding values of regression rate, O/F, etc.

(U) Comment 14.2: The only difference between this and the previous section is that a new time is obtained by incrementing with DELT. OX remains unchanged at the input value unless the motor is throttled. P remains unchanged, as it will be calculated in Section 12.

(U) A check is made to see if a throttling time has been reached. If it has, new values of oxidizer flow rate and C-star efficiency are used to replace the ones used previously.

(U) Comment 14.3: Print time is incremented by whatever printout interval was specified in the input data.

(U) Comment 15: The thrust coefficient is calculated using equations 3-25 and 3-30 from Sutton (Reference C-4). After determining the thrust, the specific impulse is found from the thrust/total weight flow ratio.

(U) Comment 15.1: Equation 3-25 from Sutton is used to calculate the nozzle exit pressure.

$$\frac{A_t}{A_e} = \left(\frac{\gamma+1}{2}\right)^{\frac{1}{\gamma-1}} \left(\frac{P_e}{P_c}\right) \left[\frac{\gamma+1}{\gamma-1}\left(1 - \left(\frac{P_e}{P_c}\right)^{\frac{\gamma-1}{\gamma}}\right)\right]^{1/2}$$

As the area ratio of the nozzle, gamma, and Pc are known, the exit pressure can be determined. However, it cannot be determined explicitly due to the nonlinear nature of the above equation. The point-slope convergence technique was utilized, where two initial guesses of the exit pressure, for it should be close to this value if the engine is optimally expanded. The second guess required for the point-slope method was arbitrarily taken as one half of the first guess. This iteration scheme converged very quickly, as long as the chamber pressure was above 10 psi. If a value smaller than 10 was fed in from the first microseconds of the run tape, the program would "blow up". This was caused by ISN 666, where a negative number was being raised by an exponent (illegal FORTRAN procedure).

(U) Comment 15.2: After the exit pressure has been calculated, the thrust coefficient is found explicitly from equation 3-30 of Sutton. The thrust is then determined from the product of the thrust coefficient, the throat area, and the chamber pressure. Dividing this thrust by the total weight flow yields the specific impulse.

(U) Comment 16: This section prints out the results. At each print time, the port radius, port geometrical cross-sectional area, the linear regression rate, and the mass flux (G) through the port are written as a function of distance down the fuel grain. The chamber pressure, oxidizer flow rate, C star, thrust coefficient, nozzle throat area, total flow rate through the port (ox + fuel), specific impulse, thrust, O/F, fuel flow rate, and total weight loss of fuel are also printed out. When Mr. D. Shirley's performance program (DS 250) is going to be used, some of the above results are punched out on cards and used immediately as input data.

(U) Comment 17: At the end of the program, average values of fuel flow rate, and regression rate are calculated over the length of the run.

Fuel Grain Weight Loss Predictions

(U) The above described procedure and computer program were utilized with the instantaneous oxidizer flow-rate estimates developed in Appendix B to predict fuel grain weight loss as a function of time. This was done by integrating the instantaneous fuel flow-rate predictions from the hybrid regression model. Figures C-5 through C-12 present these data. The final fuel grain weight change is compared with an estimate of the total fuel consumed obtained by subtracting the estimated oxidizer expenditure from the total weight loss of each propulsion system.

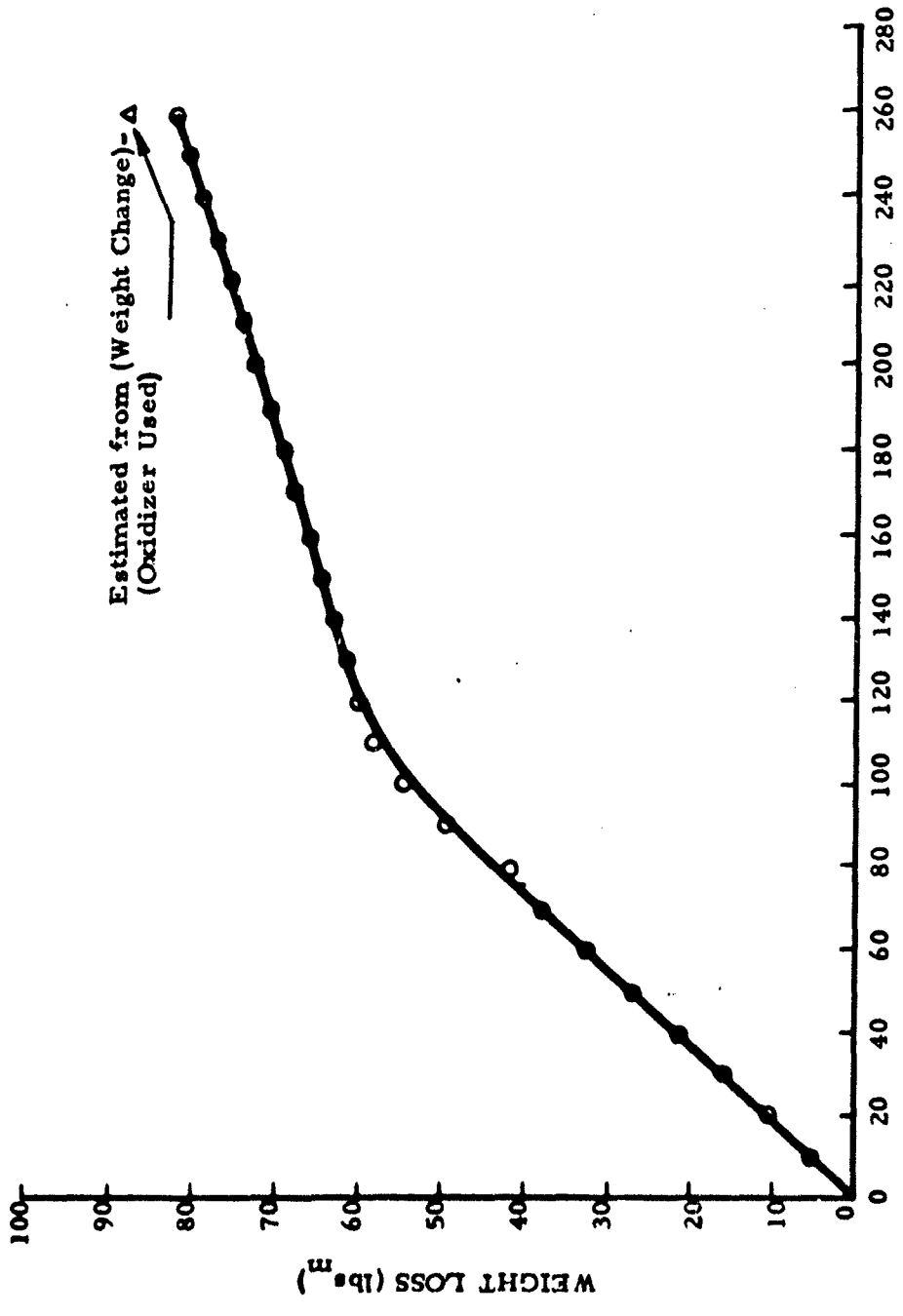

Figure C-5. Fuel Grain Weight Loss, Run 1F

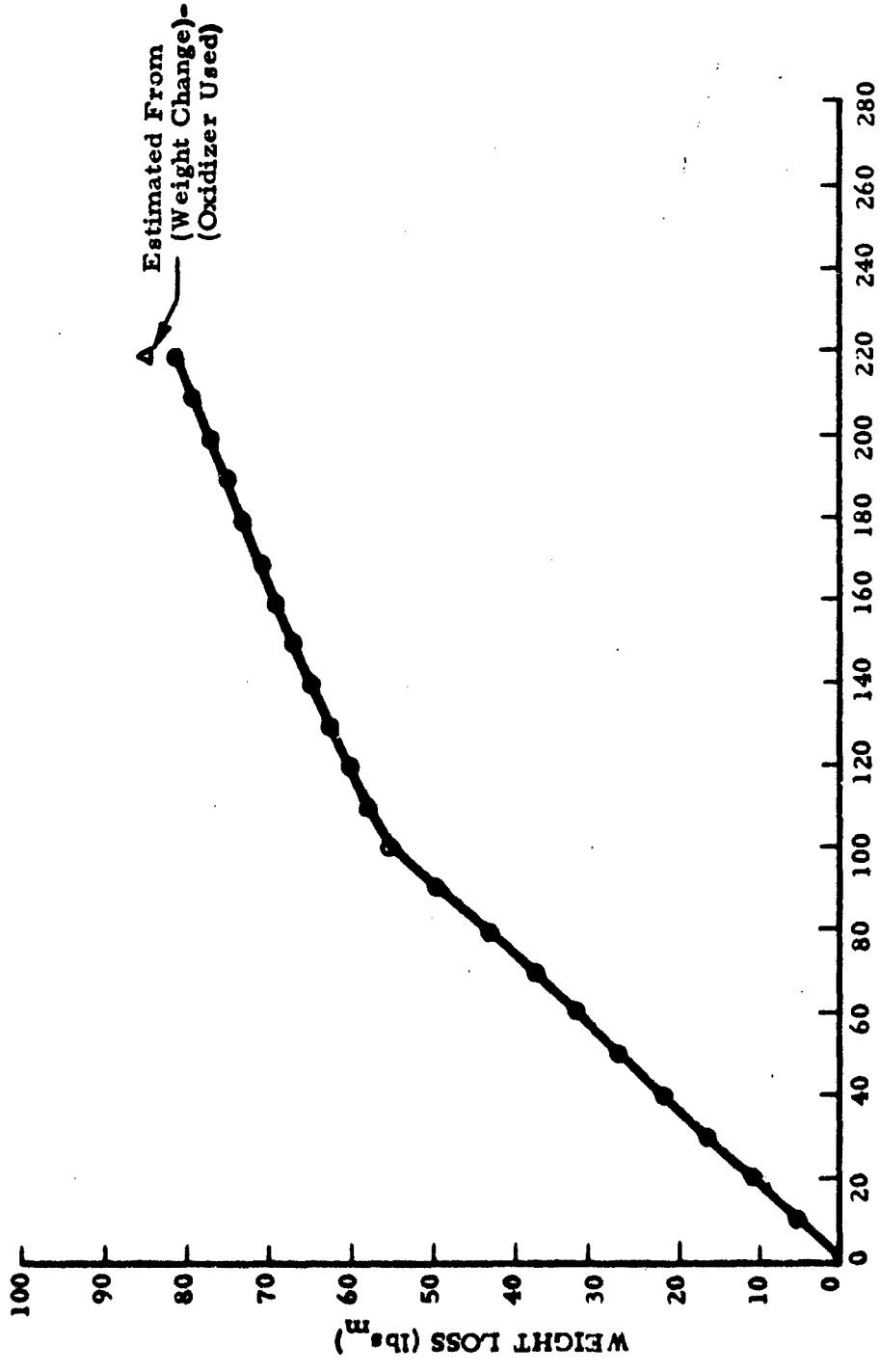

Figure C-6. Fuel Grain Weight Loss, Run 2F

UNCLASSIFIED

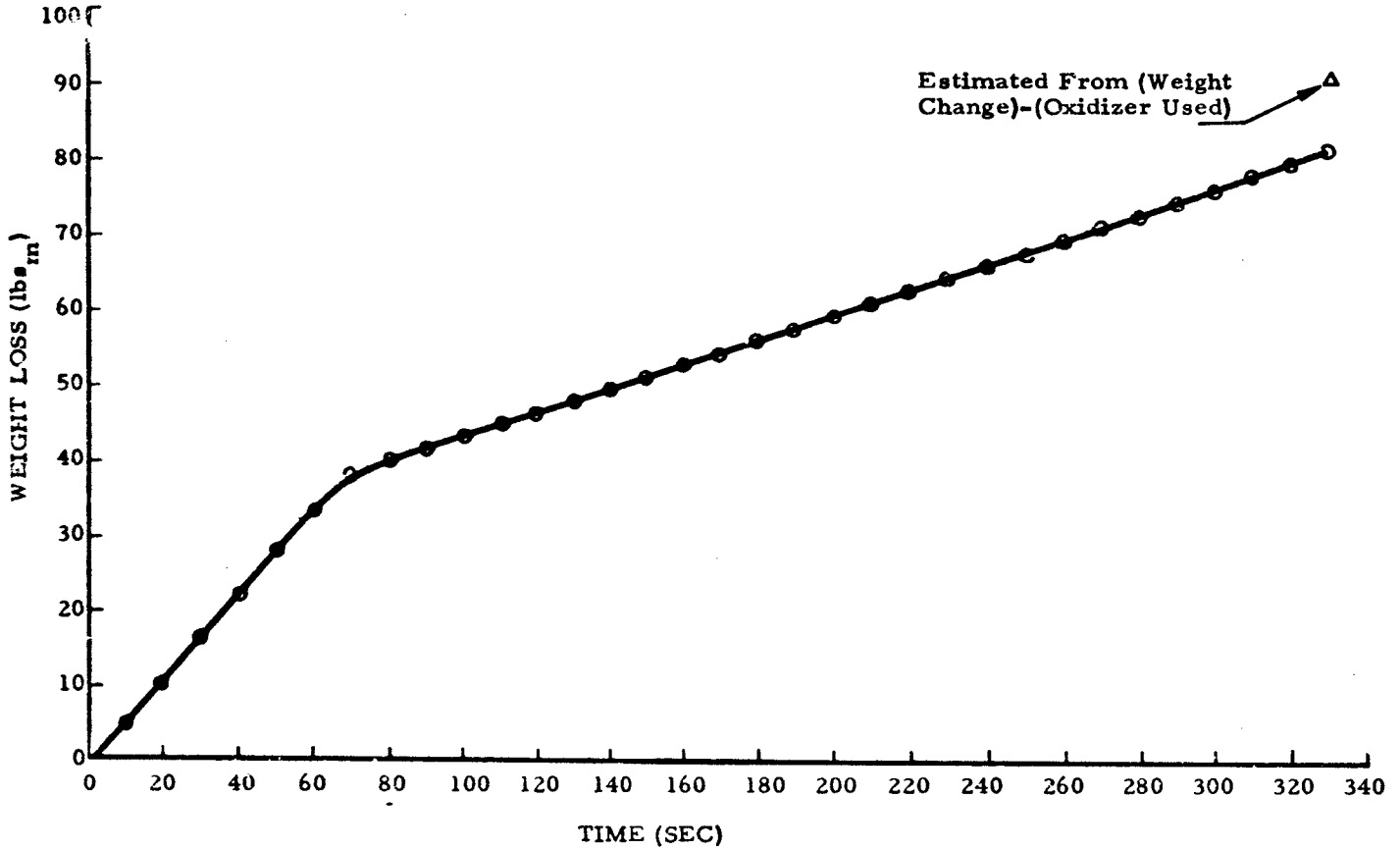

UNCLASSIFIED

Figure C-7. Fuel Grain Weight Loss, Run 3F

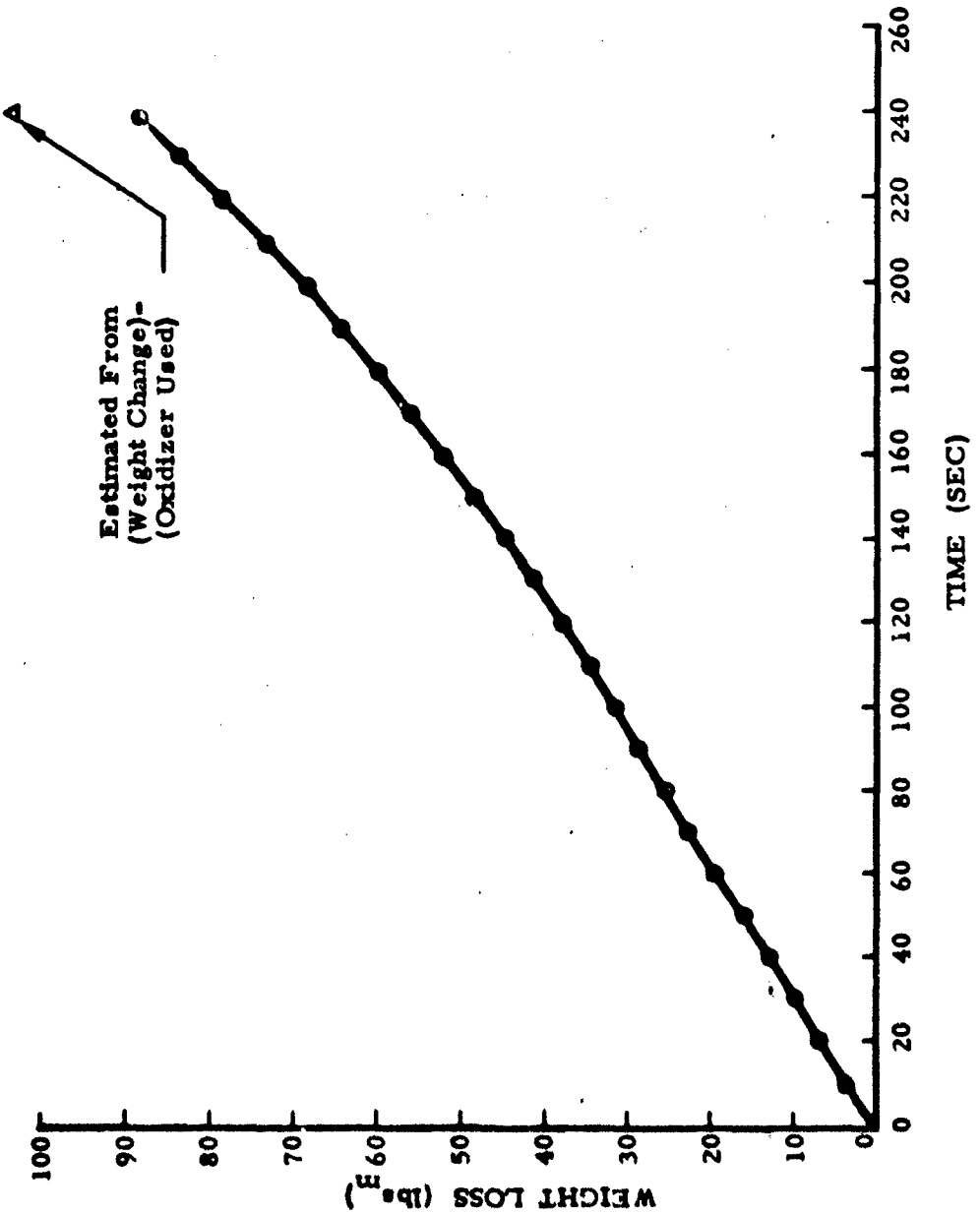
WEIGHT LOSS (lb$_m$)
100
90
80
70
60
50
40
30
20
10
0
0
20
40
60
80
100
120
140
160
180
200
220
240
260
TIME (SEC)
Estimated From
(Weight Change)-
(Oxidizer Used)

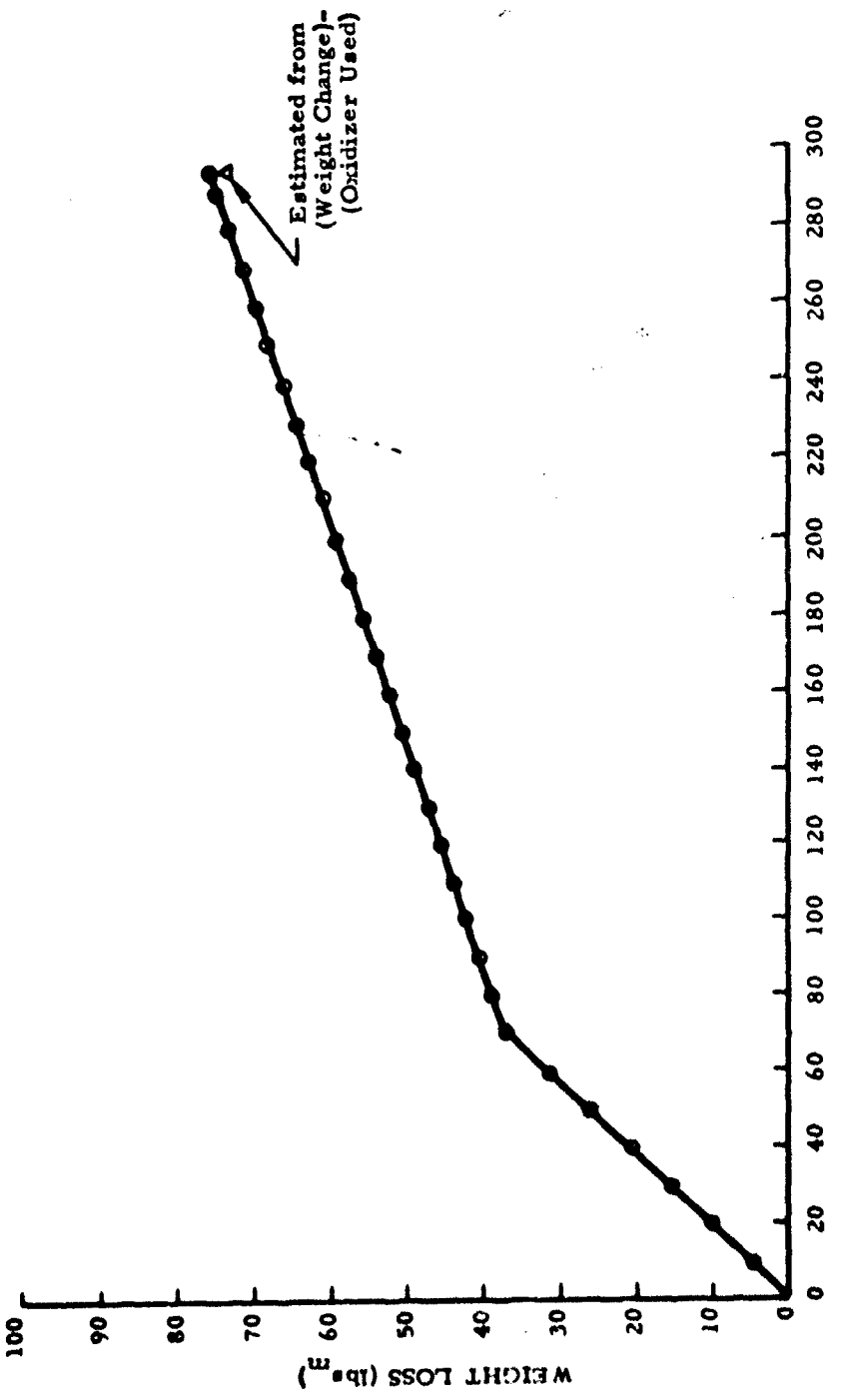

Figure C-9. Fuel Grain Weight Loss, Run 5F

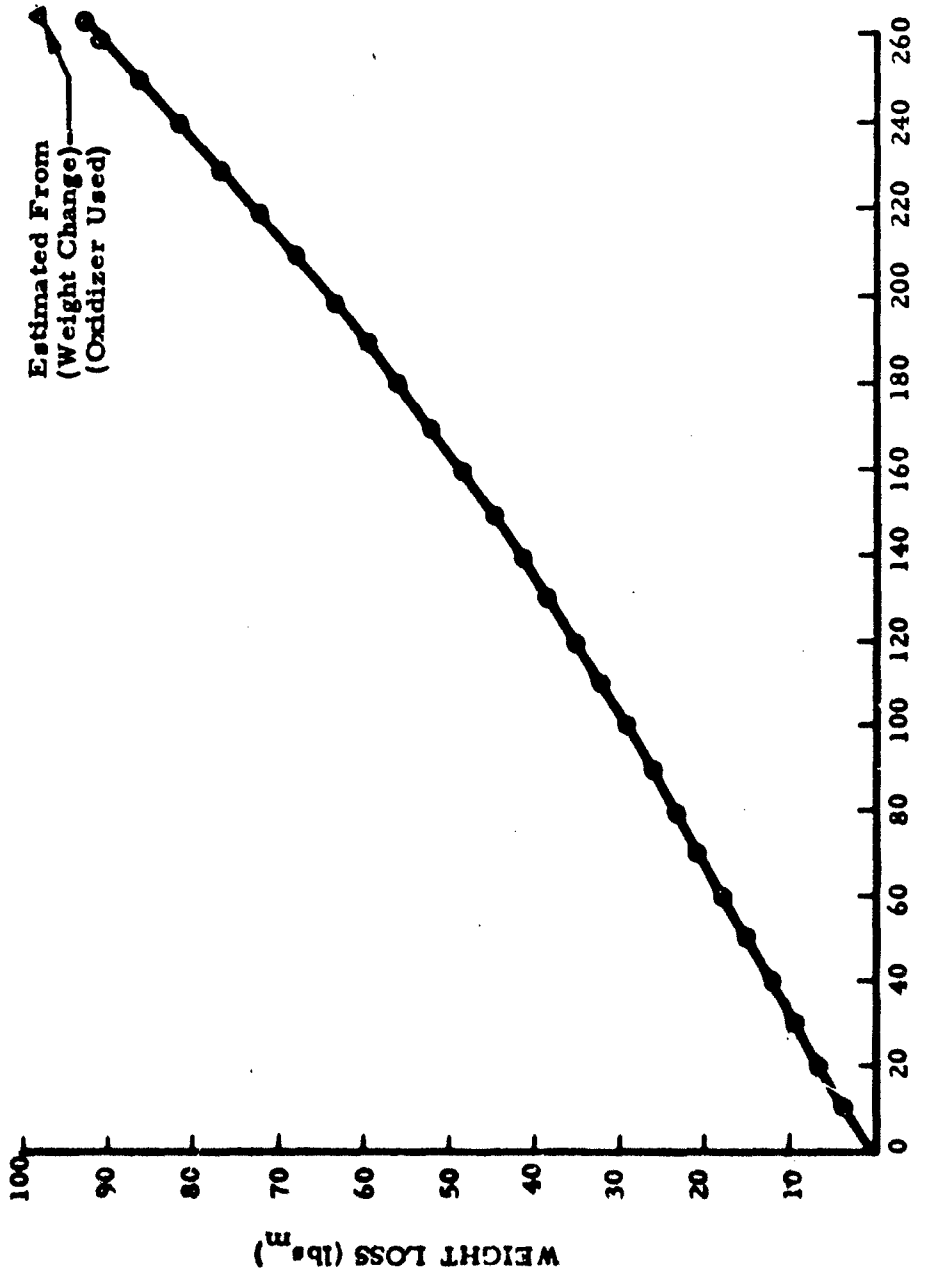

Figure C-10. Fuel Grain Weight Loss, Run 6F

UNCLASSIFIED

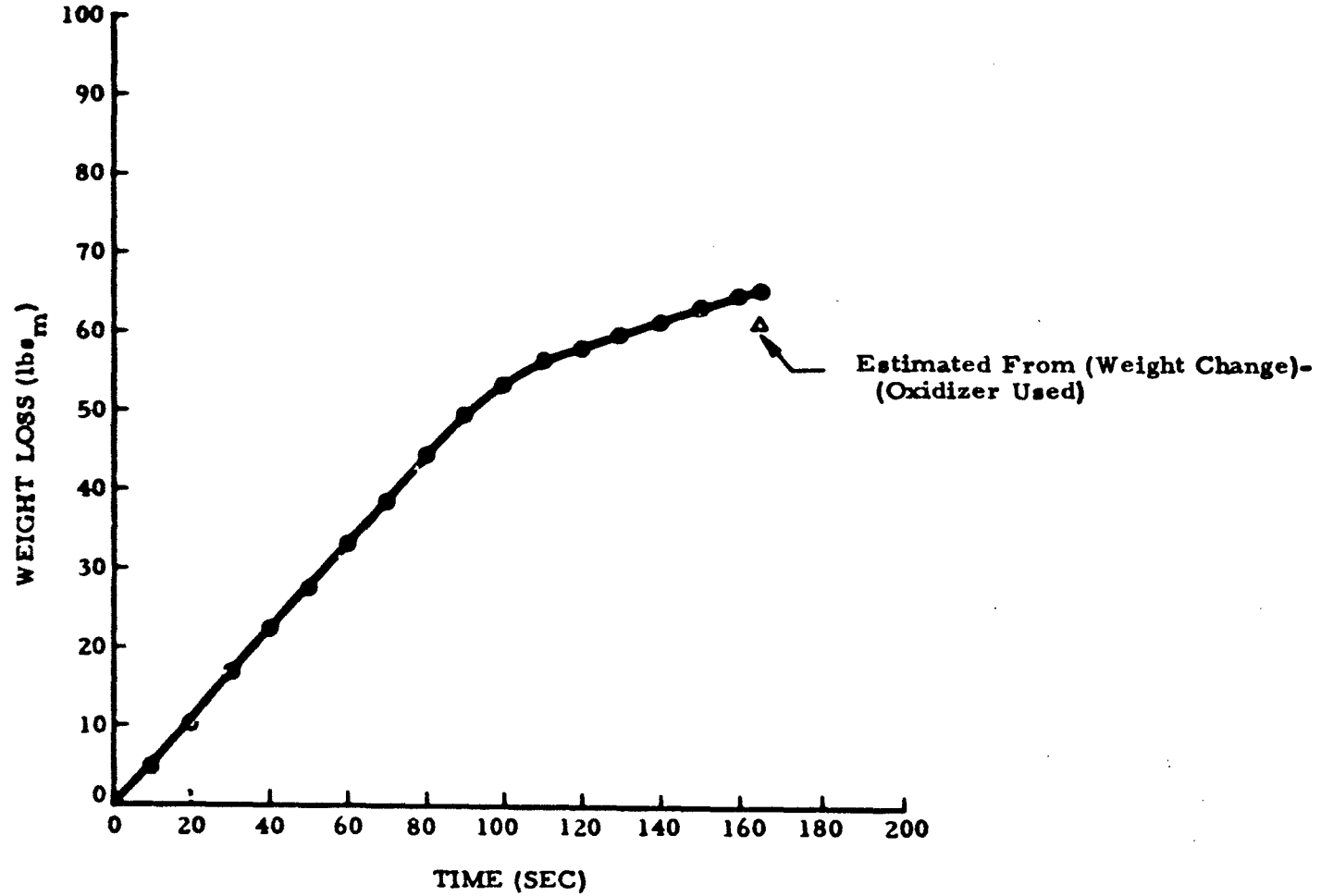

Figure C-11. Fuel Grain Weight Loss, Run 7F

UNCLASSIFIED

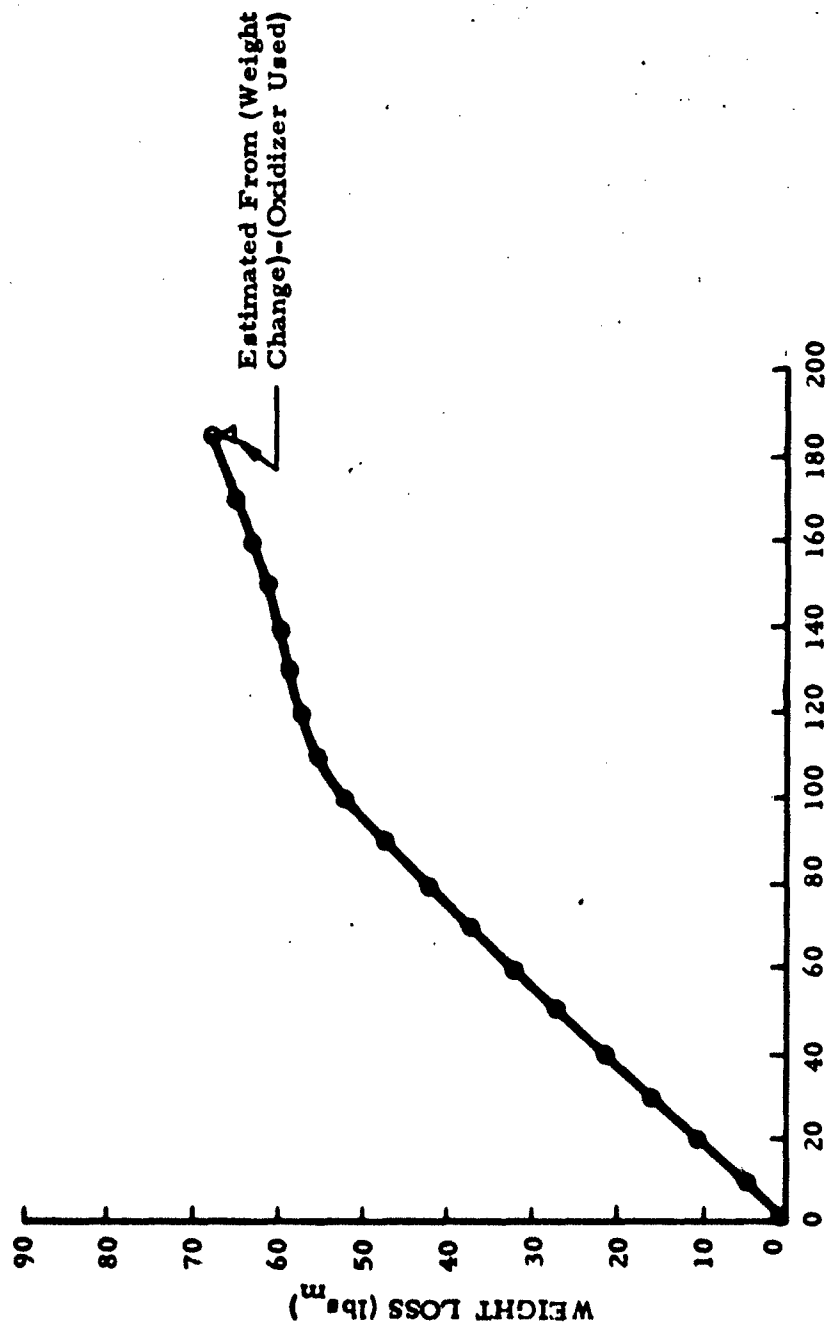

Figure C-12. Fuel Grain Weight Loss, Run 8F

REFERENCES

C-1. Spangler, William E; Ph.D. Dissertation, Tulane University, New Orleans, Louisiana, August 1965; "A Study of the Transport Processes in a Hybrid Rocket Engine."

C-2. Muzzy, R.J.; Final Technical Report (Part II) of Contract AF 04(611)-11618, United Technology Center; "Demonstration of a High Thrust Hybrid Thrust Chamber Assembly," April 1968; AFRPL-TR-68-56, Part II, AD832444. UNCLASSIFIED.

C-3. Smoot, L.D. and Price, C.F.; Final Report of Contracts DA04495, ORD-3577 and DA04495 AMC218(Z), "Hybrid Propulsion Research Program," August 1965; Lockheed Propulsion Company Report No. 640-F.

C-4. Sutton, G.P.; "Rocket Propulsion Elements," 3rd Edition, John Wiley and Sons, 1963. UNCLASSIFIED.

APPENDIX D

JPL VIBRATION TESTS

APPENDIX D

JPL VIBRATION TESTS

(U) Development tests on two Air Force propulsion systems were performed per JPL Procedure TP 503552 dated 1 October 1967, between 20 October and 20 November 1967 at the Northrop Support Operations Department (NSOD) JPL Hazardous Environment Test Facility (ETS) Edwards AFB, California. The Drone tests were given run numbers G-44 and G-45. Two Drone simulated fuel grains were cast and cured by NSOD at ETS. The fuel grains were then assembled to the liquid oxidizer tank, and the oxidizer tank was filled with an equivalent weight of tricloroethylene to simulate the liquid oxidizer. Sinusoidal vibration runs were made on the two shaker test fixtures prior to the actual tests.

Run G-44

(U) Three axis (see Figures D-1, -2, -3) 1 and 2g RMS sine sweeps from 20 to 1200 Hz were made on the first system between 31 October and 7 November 1967. Resonances in excess of 50g RMS on the oxidizer tank with 2g RMS input at fixture were noted. Loose plumbing and valves were secured and padded. The sine sweep was repeated with a marked reduction in resonant levels.

Run G-45

(U) Single axis (z) 1g sine sweeps from 20 to 1200 Hz were made on 15 and 16 November 1967. The runs on 15 November were made to investigate the response of a system with full flight-weight oxidizer plumbing. On 16 November single and two-point control 1g RMS sweeps were made after elastic supports and tape had been added to oxidizer tubing and valves. The last z axis sine sweep was made on 22 November after additional metal brackets and clamps were added to the oxidizer tubing and valves. No significant difference in resonant levels was noted between runs of 16 November and 22 November.

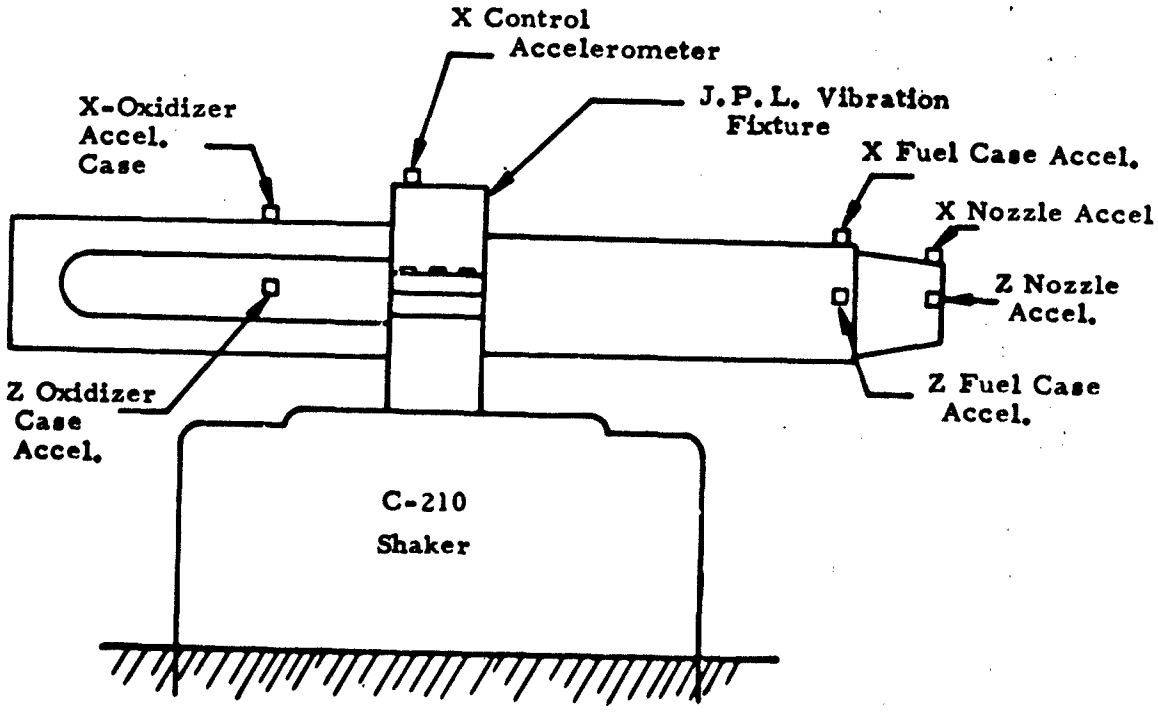

Figure D-1. X-Axis Configuration

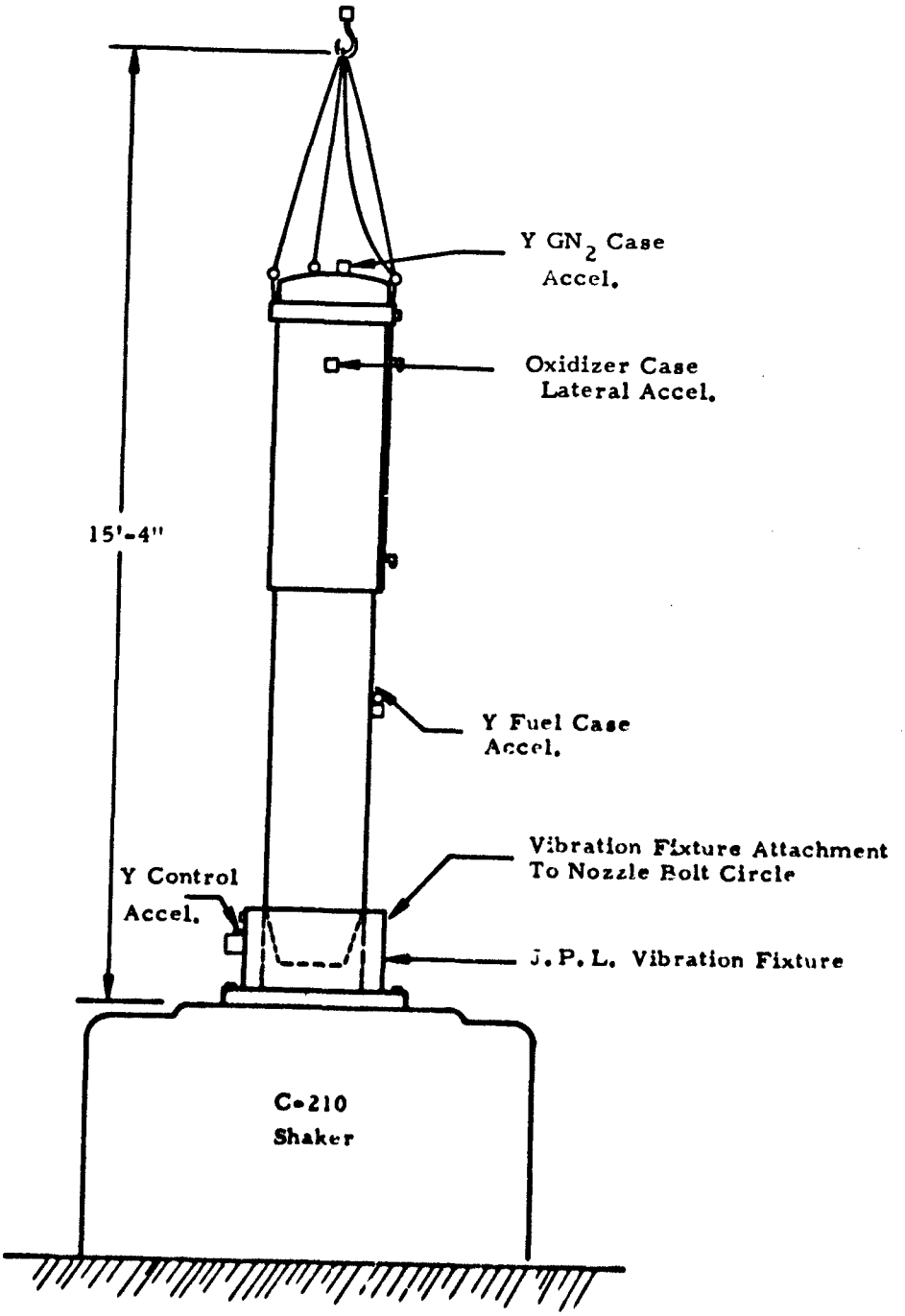

Figure D-2. Y-Axis Configuration

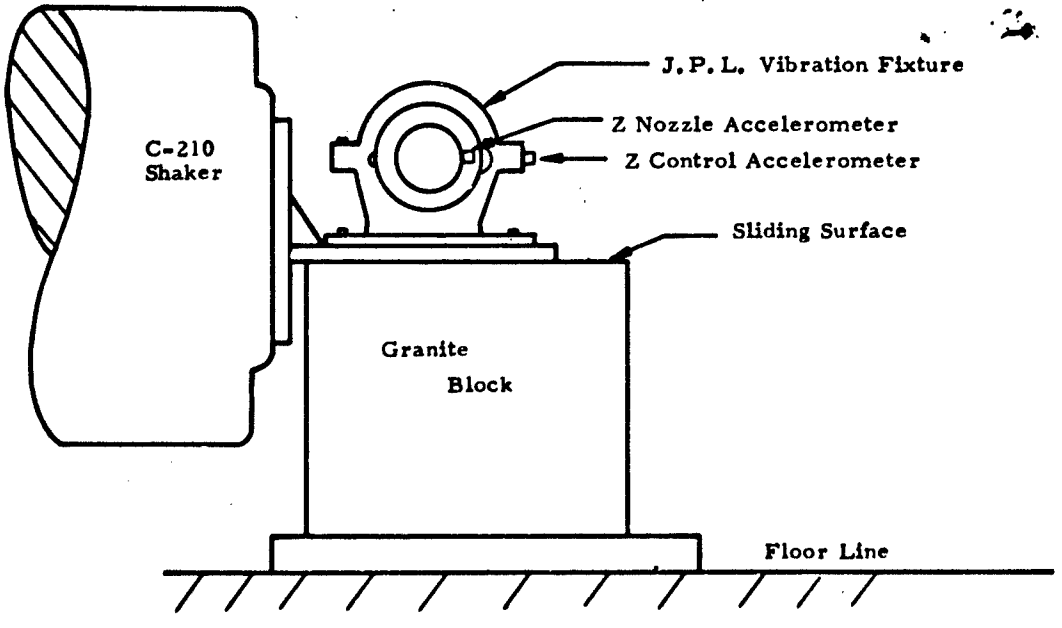

Figure D-3. Z-Axis Configuration

(U) On 23 November 1968 tests were terminated by telecon with Air Force project engineer. It was decided that since the test hybrid drone did not dynamically simulate the aft thrust chamber assembly configuration, as it lacked the airframe structure, further vibration tests would not be fruitful. The identification and development of on-the-spot fixes for the oxidizer feed system successfully achieved the technical objectives of the Hybrid Target Missile Program.

APPENDIX E

CHECKOUT AND SERVICING PROCEDURES

APPENDIX E

CHECKOUT AND SERVICING PROCEDURES

Gaseous Nitrogen Filling Procedure

1. Obtain copy of UTC Drawing No. C01669 Rev. N/C

2. Remove cover from the forward end of raceway by removing retaining screws.

3. Remove nitrogen fill valve protective cap with 9/16-inch wrench backing up stationary part with 11/16-inch wrench; this cap is gray anodized in color and is located in a Tee at station 24E on drawing UTC C01669.

4. Install nitrogen fill adapter, per UTC Drawing No. C04111 (or equivalent) on nitrogen fill valve.

5. Connect gaseous nitrogen source to fill valve. It is recommended that the nitrogen source be capable of maintaining a constant 3500 psig.

6. Open gaseous nitrogen charge valve and slowly charge missile nitrogen tank to 500 psig with nitrogen per MIL Spec MIL-P-27401.

7. Close nitrogen charge valve.

8. Check system for leaks using liquid leak detector. If no leaks are detected, continue to pressurize.

9. Repeat steps 6, 7, and 8 in 500-psig increments until the nitrogen tank is charged to 3,500 psig and no leaks have been detected. If leakage

occurs while performing steps 6, 7, 8, and 9, proceed with the following:

a. Close nitrogen charge valve.

b. Open fill system bleed valve.

c. Loosen "B" nut at nitrogen initiation valve inlet side and bleed tank until all gas has been depleted.

d. Repair leak and proceed from step 6.

10. When nitrogen tank is charged initially to 3,500 psig, it will become very warm. Let nitrogen tank cool to approximately 77°F before recharging to 3500 psig.

11. Close gaseous nitrogen charge valve.

12. Open nitrogen fill line bleed valve and vent fill system to ambient.

13. Disconnect fill line from fill valve on missile.

14. Remove nitrogen fill adapter from nitrogen fill valve.

15. Install cap on missile fill valve.

16. Replace raceway cover, install screws and torque to proper level.

Igniter Assembly Procedure

1. Obtain copy of UTC Drawing No. C01669.

2. Obtain one each of the following parts:

a. Throat Insert, P/N C02123-01-01.

b. Cartridge, P/N C02147-0101.

c. Initiator Assembly, P/N C03118-0101.

d. 2-28 O-ring Compound S418-6.

e. 3-6 O-ring Compound S418-6.

3. Check continuity of initiator assembly using an igniter circuit tester which has a maxium output current of 5 milliamperes DC. An acceptable unit is the Alnico Model 101-5BF. Continuity is checked by shorting pins A and B and recording resistance on balance. Pins C and D are shorted similarly. Short pins A and C, B and D and verify open circuit. Continuity check of all squib valves is performed in this manner.

4. Remove 34 each screws from access door located just aft of the rear launch pin.

5. Remove access door.

6. Locate igniter as illustrated per UTC Drawing No. C01669 location 15F.

7. Remove snap ring from igniter assembly with snap ring pliers.

8. Remove igniter closure from igniter assembly using caution to avoid damaging the closure.

9. Wipe clean interior surfaces of igniter case with cloth lightly dampened with trichlorethylene.

10. Inspect snap ring groove to insure no particles are lodged in groove.

11. Remove O-ring and dust cap from igniter closure.

12. Lubricate 3-5 O-ring with DC-11 silicone grease (or equivalent) and install on initiator assembly, P/N C03118-01-01.

13. Clean igniter boss with a cloth lightly dampened with trichlor-ethylene.

14. Lubricate O-ring surfaces on boss with DC-11 silicone grease.

15. Install initiator assembly into igniter closure and torque to 40 ft-lbs.

16. Install throat insert, P/N C02123-01-01, radius edge first, into igniter case.

17. Lubricate inside of igniter case with DC-11 silicone grease, 1 inch deep.

18. Insert igniter cartridge, P/N C02147-01-01, into igniter case.

19. Lubricate 2-28 O-ring with DC-11 silicone grease and install on igniter closure.

20. Press igniter closure (with initiator assembly installed) into igniter case uniformly using care to not damage the O-ring when passing over the snap ring slot.

21. Install snap ring in slot with snap ring pliers.

22. Replace access door and 34 each screws in door.

Dial-A-Thrust Valve Setting Procedure

1. Remove 34 each screws from access door located just aft of the rear launch pin.

2. Remove access door.

3. Locate adjustable flow control valve, P/N C02817-01-02. This valve is identified in the following manner: The valve is gold anodize in color and has a circular knob with the alphabetic letters "A" through "H" stamped clockwise on the top.

4. Loosen lockscrew on top of valve approximately 1/4 inch with a 5/17-inch wrench.

5. Determine valve setting for mission by obtaining the setting from the calibration tag attached to the side of the valve for the following missions:

Mission No. 1 = 50,000-ft Mission
Mission No. 2 = 70,000-ft Mission
Mission No. 3 = 80,000-ft Mission
Alternate = 90,000-ft Mission (not to be used)

6. The valve settings are interpreted as follows: The valve is set initially at a value of "0A" (zero "A") with the lockscrew being the index. All settings are to be taken with respect to this setting. The numbers are complete counter clockwise turns of 360° from position "A" to "A". The letters are the position to which the knob is turned after the numerical turns have been made. EXAMPLE: 5E is five turns from zero "A" to 5A and then only a portion of a turn to the letter E.

7. Set valve for the mission required.

8. Tighten down lockscrew with 5/16-inch wrench.

APPENDIX F

THRUST MEASUREMENT AND CALIBRATION

APPENDIX F

THRUST MEASUREMENT AND CALIBRATION

(U) Accuracy of measured thrust was of constant concern throughout this program because testing at altitude complicated the prediction of actual delivered thrust due to environmental effects on transducer accuracy.

(U) It is unusual, in the measurement of thrust, to provide a means of applying a calibrated force to the flexurally supported engine cradle prior to actual engine thrust measurements being made. Thus, the thrust stand usually includes a calibration device which is contributory to the overall "end-to-end" error. The evaluation of thrust measurement channels must necessarily include this calibration error as well as those errors attributable to such factors as the manner in which the technicians apply and remove the calibration load. The usual load transducer is a flexurally mounted strain gage "load cell." This cell is placed between the engine cradle and a load takeout abutment. This working cell will produce an output proportional to force, be it from the calibration device or from an actual engine firing load. It is this working cell that is calibrated by the calibration device. Generally, it is not feasible to calibrate the working cell in a laboratory and eliminate stand calibration because only a percentage of the applied load goes through the load cell. A portion of the load is taken out by the flexures, piping, etc.

(U) Before each test firing, the test stand (working cell) was calibrated using the calibration device. The electrical output from the working cell was recorded at each load level. In addition, a precision resistor was placed across one of the bridge resistors in the load cell. This shunt resistor produced an output proportional to the cell excitation voltage. This output was called a "sense step" and was used later in the data reduction process to rationalize differences in system sensitivity between the time of calibration and the time of firings. In some cases, several

different sense steps were recorded, each of which was derived using a different value of shunt resistance. Only one of these values was actually used in the data reduction process. When digital data records were made, the digital value derived at the several calibration loads and the sense step were manually recorded. These data were then sent to the data processing area ahead of, or concurrent with, the tape-recorded test-firing data.

(U) At the data processing facility the calibration data were used to derive a formula or curves suitable for the determination of force from the test-firing records. The sense step became the "common denominator" in the reduction process. From the calibration record, the value of force which the sense step represented could have been determined; however, this this was not usually done because the ratio of the output derived from the recorded force divided by the output from the sense step was more useful.

(U) A typical example of the process was the reduction of data recorded on a digital acquisition device. Starting with the manual calibration record, the number of digital counts recorded at zero pounds force was subtracted from the number of counts at a specific value of calibration force. Also, a difference between counts with and without the sense step applied was computed. The ratio between these differences was then determined. Depending upon the linearity of the system, an analyst chose either a 1st, 2nd, 3rd, or 4th order curve-fit technique to determine a best-fit equation of the form:

$$F = a + bx + cx^2 + dx^3 + ex^4$$

Where:

F = Force in lbs.

a, b, c, d, and e were the derived coefficients using computer routines.

$$x = \text{counts ratio} = \frac{\text{counts at any force - counts at zero force}}{\text{counts with sense step - counts without sense step}}$$

The coefficients determined from the calibration information were stored for further reference when the record from the actual test firing was being processed.

(U) When data from a test firing was processed, pre- and post-run zero values had been recorded. The data analyst had the option of selecting either of these zero values or of computing an average zero value. The denominator of the "counts ratio" was then calculated by subtracting the chosen zero from a similarily chosen or averaged sense-step value. The recorded firing data were a succession of data samples, the count value of which varied with time as a function of the thrust produced by the engine. Each of these samples, or selected ones, was used to derive a value for the numerator of the "counts ratio" expression by subtracting the chosen or computed zero from the data count value. At this point, both the numerator and denominator of the "counts ratio" expression were available and the value of the ratio itself was computed. This value was then used with the coefficients derived from the calibration data to compute a value of force in pounds corresponding to the recorded data count value.

(U) The first step was to calibrate the thrust stand using the calibration equipment associated with the test stand. The results of this calibration were manually recorded.

(U) To evaluate thrust stand accuracy, known forces were applied to the cradle along the axis parallel to the engine. This method of loading the thrust stand did not apply during the stand calibration and was only applicable during the evaluation. The known forces did, however, exert force on the load cell similar to the calibration forces exerted on the same load cell during stand calibration. It was the difference between these two methods that constituted the basis for obtaining data that resulted in the stand accuracy figure.

(U) The force load cell was provided with two strain-gage bridges, Bridge A and Bridge B. Data from each bridge was acquired during stand calibration and evaluation. For evaluation, two channels of a digital record were activated. When any of the known force increments were applied, and held constant, the magnetic tape recorder, associated with the digital recorder, was turned on. The bridge data were thus recorded simultaneously for both channels. This process was continued for each force increment and for three cycles of test.

(U) Data reduction began when the data were placed in the hands of an analyst for evaluation. The first step was to compute the indicated forces using the standard data-reduction programs and techniques peculiar to the particular test area. These computed values were compared with the known applied forces, and using appropriate statistical techniques as indicated below, numbers were derived that reflect the accuracy of the stand.

(U) The accuracy of a calibration test was limited to the accuracy realized when technicians used the available force calibration kit. This force calibration kit was sent to the National Bureau of Standards, and certified to be within the following error limits: $\pm$0.05% of reading down to 1/5 of full scale and to $\pm$0.05% of 1/5 full scale down to zero.

(U) The actual Bureau certification records indicated that these were conservative values. Because these standards were used only by the most competent and meticulous technicians, it was assumed that personnel using the standards do not degrade the accuracy from that actually measured beyond the certified value of 0.05%.

(U) The kit consisted of an indicator and 10 load cells of different capacities, ranging from 120 pounds to 120,000 pounds, full scale.

(U) This thrust stand evaluation did not include a major potential source of thrust measurement error, i.e., error resulting from forces that were caused by propellant line pressurization effects. There were several reasons why this potential error source was not included in this evaluation:

a. It was generally inconvenient to pressure the piping system at the time of evaluation.

b. The engine was not usually in the thrust cradle at the time of the evaluation, and piping errors, if any, would be dependent upon how the piping was twisted and bent to force it into position to torque the mounting bolts in place.

c. Stand and system errors as determined in this evaluation were a constant value plus or minus the piping pressurization errors. Inasmuch as pressurization errors would vary (unless eliminated) with each engine installation, the results of this evaluation would not be consistent or repeatable if piping pressurization effects were included.

d. Piping pressurization errors were, generally speaking, easy to detect as well as eliminate. Good management dictated the necessity to test for and eliminate these errors after each engine change.

(U) The primary standard used in Thrust Stand Calibration was located in Laboratory No. 213.04/185045 of the National Bureau of Standards, Washington, DC. Attesting documentation disclosed that the errors of the applied loads, used in calibrating the Baldwin-Lima-Hamilton secondary standard, did not exceed 0.002%. It was concluded that the accuracy of the primary standard is 99.998%.

(U) The secondary standard was a Baldwin-Lima- Hamilton Force Calibration Kit. The manufacturer guaranteed an accuracy of 0.05% of point when calibrated by the National Bureau of Standards. This was a conservative figure as individual calibration sheets from the Bureau attested. In any event, it was safely concluded that the accuracy of the secondary standard was 99.95%.

(U) The average of pre and post-run sense step sigmas (deviations) were noise check figures. They represented the error band (noise) being recorded. Because the full scale count value was usually $\pm$9,999 counts, the signal to noise ratio was this number divided by 19,998. The average was computed as follows:

a. Fifty data points were recorded for the pre-calibration step value when zero lbs of force was being applied to the stand.

b. These 50 points were averaged.

c. A difference between each of these points and the average value was computed.

d. Squaring each of the differences, summing them, dividing this sum by 49, and taking the square root of this quotient yielded a standard deviation for the step.

e. Repeating the foregoing steps, a through d, for each of the pre and post-sense steps and taking the simple average of the resultant figure yielded the tabulated counts value.

(U) The stand deviation of thrust data channel represented the precision associated with the particular data channel under test. It was calculated from the following equation using data typified by Table F-I.

$$\text{PREC (\%)} = 100 \quad \frac{\frac{Fd_1 + Fd_2 + \ldots Fd33}{32}}{F_{Fs}}$$

Where: The factor of 100 is used to result in a percentage figure.

Fd denotes the difference between the force value in Columns 2, 3 and 4 with Column 1 of Table F-I.

Subscriptions 1 through 33 represent the 33 individual difference.

F_{Fs} denotes the full-scale calibration force.

The data in Column 1 are the forces applied using the Baldwin-Lima-Hamilton Force Calibration Kit. The data in Columns 2, 3, and 4 are the computed forces derived from the tape recording made at the time of test. There are three columns, one for each of three runs. The data in Column 5 are simple arithmetic averages of the values in Columns 2, 3, and 4 subtracted from the corresponding values in Column 1, divided by the value in Column 1 and then multiplied by 100 to result in a percent of point error figure. The figures in Column 6 are derived in the same manner as those in Column 5, except that the difference is divided by the full scale value.

(U) The accuracy of thrust channel was a single number which could be used to represent the entire system accuracy. It was related to the precision derived above and also took into account the uncertainty in the standards. The value was calculated using the following equation:

$$\text{\% Accuracy} = 100 - \text{error}$$

$$= 100 - \sqrt{9\text{PREC}^2 + 9\text{PSD}^2 + 9\,\text{STD}^2}$$

Where: The nines under the radical sign were used to result in three sigma values.

PREC was the precision (%) of the system as determined above.

STD was the precision (%) of the secondary standard.

PSD was the precision (%) of the primary standard.

UNCLASSIFIED

TABLE F-I. TYPICAL LOAD CELL CALIBRATION DATA FOR A SINGLE BRIDGE

TEST STAND 1-14-A TEST NO. 1 19 OCTOBER 1966 BRIDGE A

TRANSDUCER MFG ORMOND TYPE LC MOD WCL-FF35-CC-1K-2193 SER NO. 2111

THRUST		TEST INPUT		PERCENT OF PT	PERCENT OF FS
1	2	3	4	5	6
0.00	1.2970	1.2026	1.3222	******	0.13
200.00	201.8797	201.7979	201.7056	0.90	0.18
400.00	403.1084	403.3370	402.7623	0.77	0.31
600.00	604.9830	605.0544	604.6097	0.81	0.49
800.00	806.8473	807.0613	806.7214	0.86	0.69
1000.00	1009.6134	1009.5337	1009.2904	0.95	0.95
800.00	806.6921	807.0906	806.5914	0.85	0.68
600.00	604.7313	604.9956	604.5866	0.80	0.48
400.00	402.9259	403.0329	402.9070	0.74	0.30
200.00	201.6301	201.7203	201.7371	0.85	0.17
0.00	1.1649	1.4145	1.4837	******	0.14

Accuracy of primary standard = 99.9980 percent.

Accuracy of secondary standard = 99.9400 percent for 3 sigma.

Average of Pre and Post run sense step sigmas = 2.42 counts.

Standard deviation of thrust data channel = 0.4916 percent of full scale.

Accuracy of thrust data channel = 98.5239 percent of full scale for 3 sigma.

UNCLASSIFIED

(U) It should be noted that the foregoing equation is a simple RMS addition, which implies a random error as contrasted to a systematic error.

(U) Table F-II presents the results of thrust stand calibrations using the procedures described above. Load cell S/N 2111 was used during boilerplate tests 1 to 27, and S/N 245372 was used during certification testing.

TABLE F-II. THRUST STAND CALIBRATION RESULTS

	X*	Y**
S/N 2111 (19 Oct 66) Ormond Type LC Model WCL-FF35-CD-1K-2193		
Bridge A	0.4916%	98.523%
Bridge B	0.4637%	98.6077%
Bridge A (7 Feb 67)	0.4985%	98.5033%
S/N 245372 Revere Model U.S.P.2-1-B		
Bridge A (21 Sep 67)	0.2944%	99.1158%
Bridge A (29 Sep 67)	0.2783%	99.1640%

* X = Standard Deviation of Thrust Data Channel in Percent of Full Scale

** Y = Accuracy of Thrust Data Channel in Percent of Full Scale for 3 Sigma

APPENDIX G

THRUST MEASUREMENT CORRECTIONS

APPENDIX G

THRUST MEASUREMENT CORRECTIONS

(U) Heavyweight tests 1 through 27 were conducted with hermetically sealed load cell S/N 2111. Test data from calibration at altitude and ambient pressures are shown in Table VI of Section IV. Tests 28 through 101 were conducted with the second load cell (S/N 4053). This load cell was never evaluated in thrust stand calibration. The second load cell was vented to allow equalization of internal transducer pressure with the altitude chamber pressure. This equalization process was not instantaneous and various transitory effects occurred with temporarily caused large inaccuracies in measured thrust. Figure G-I shows performance of the second (vented) load cell under no-load conditions during typical dynamic test chamber effects that were experienced during engine throttling tests. This second transducer also exhibited significant shifts in calibration points at various simulated loadings between altitude and ambient pressure. Most of the transitory effects are typical of any vented system.

(U) The third load cell (S/N245372) was used for certification tests 1F through 8F. This Revere load cell (Model U. S. P. 2-1-B) was vented similarly to the second load cell. To avoid the start transition deviations, the altitude chamber was allowed to stabilize at a pressure equal to 65,000 ft. If the engine had been allowed to ignite at 50,000 ft, the diffuser would pull down the test cell pressure to the 65,000 ft level. During this period, thrust measurements would obviously be in question because a situation similar to that shown in Figure G-I would exist. No method was devised to avoid the throttling error, but it was fairly small.

(U) Thrust corrections were made to all measured data. Corrections consisted of two types: (1) Corrections for suction pressure forces caused by differential pressures acting on the propulsion system between the diffuser pressure and the altitude test chamber pressure, and (2) altitude

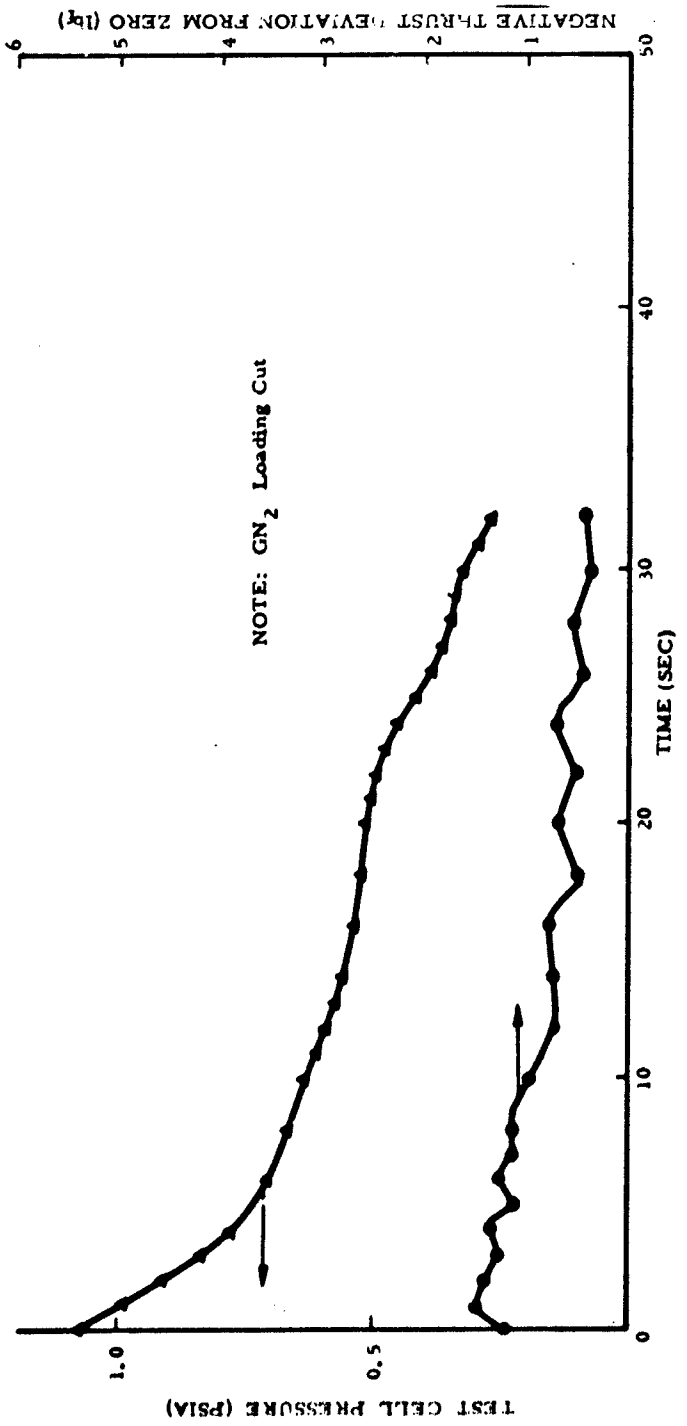

Figure G-1. Typical Thrust Deviation with Test Cell Pressure During Engine Throttling

corrections to predict thrust at standard altitudes different from the actual operating test altitude. The methods are outlined below.

Diffuser/Test Cell Pressure Differential Correction

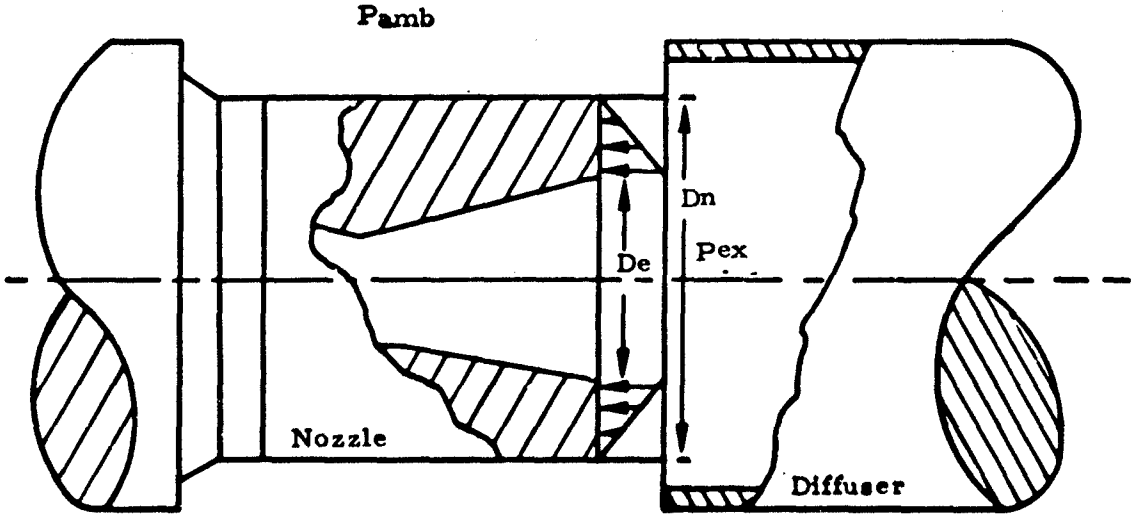

$\Delta P = (Pex - Pamb)$

$w = F - f$

Pex	=	Diffuser pressure
Pamb	=	Test cell pressure
Dn	=	Nozzle O. D. = 7 in.
De	=	Nozzle exit O. D. = 4.09 in.

Where: f = positive force adding to thrust

F = measured thrust

w = actual thrust

$$f = \frac{\pi}{4}(D_n^2 - D_e^2)\frac{\Delta P}{2} = 12.67\ (Pex._1 - Pamb._1)$$

Altitude Correction

$$F_2 = F_1 - A_e\ (Pamb._2 - Pamb._1) = F_1 - 13.14\ (Pamb._2 - Pamb._1)$$

Subscripts: 1 = Test Altitude 2 = Mission Altitude

[redacted]7218

Unclassified
Security Classification

DOCUMENT CONTROL [redacted]
(Security classification of title, body of abstract and indexing annotation [redacted] overall report is classified)

1. ORIGINATING ACTIVITY (Corporate author)
Air Force Rocket Propulsion Laboratory
Edwards, California 93523

2a. REPORT SECURITY CLASSIFICATION
Confidential

2b. GROUP
IV

3. REPORT TITLE
Certification Tests of a Hybrid Propulsion System for the Sandpiper Target Missile (U)

4. DESCRIPTIVE NOTES (Type of report and inclusive dates)
Final August 1966 - March 1968

5. AUTHOR(S) (First name, middle initial, last name)
Franklin B. Mead, Jr.
Bernard R. Bornhorst

6. REPORT DATE	7a. TOTAL NO. OF PAGES	7b. NO. OF REFS
June 1969		

8a. CONTRACT OR GRANT NO.	9a. ORIGINATOR'S REPORT NUMBER(S)
b. PROJECT NO. 573002CRQ	AFRPL-TR-69-73
c.	9b. OTHER REPORT NO(S) (Any other numbers that may be assigned this report)
d.	

10. DISTRIBUTION STATEMENT In addition to security requirements which must be met, this document is subject to special export controls and each transmittal to foreign governments may be made only with prior approval of AFRPL (RPOR-STINFO), Edwards, California 93523.

11. SUPPLEMENTARY NOTES	12. SPONSORING MILITARY ACTIVITY
	Air Force Rocket Propulsion Laboratory Directorate of Laboratories Air Force Systems Command, USAF Edwards, California

13. ABSTRACT

(U) An in-house exploratory development program was accomplished as part of an inter-laboratory team effort to demonstrate the feasibility of hybrid propulsion for the Sandpiper high-performance target missile. The objectives of this program were to: (1) conduct "off-design" tests of a flight type (heavyweight) Hybrid thrust chamber assembly (TCA); (2) conduct flight certification tests on flight weight propulsion systems delivered under a concurrent AFRPL contract; and (3) provide propulsion system field servicing and engineering support during subsequent flight tests of the propulsion system. Thirty heavyweight TCA tests were conducted, and TCA component operating characteristics, TCA component durability, effects of metal fuel grain additives on combustion, effects of fuel grain temperature on combustion, effects of IRFNA oxidizer substitution, and TCA altitude performance were evaluated. MON-25 (75% N_2O_4/25% NO) oxidizer and 90% Plexiglas (polymethylmethacrylate)/10% magnesium metal fuel were the propulsion system propellants. Eight flight weight propulsion systems were tested over simulated mission duty cycles after being subjected to environmental extremes of temperature (-65°F to 165°F) and humidity.

(U) Results of the heavyweight TCA tests and subsequent propulsion system flight tests are summarized. The flight certification test data are presented in detail.

[redacted]

DD FORM 1 NOV 68 1473

Unclassified
Security Classification

14. KEY WORDS	LINK A		LINK B		LINK C	
	ROLE	WT	ROLE	WT	ROLE	WT
Hybrid Rockets						
Hybrid Rocket Combustion						
Altitude Tests						
Sandpiper Target Missile						

UNCLASSIFIED

UNCLASSIFIED